

2018



**School of Engineering
Howard College Campus
Durban**

**HIGH TEMPERATURE FLUE GAS DESULFURIZATION:
EXPERIMENTS AND MODELLING**

By:

Calvin Moodley

**BSc Chemical Engineering
2017**

A dissertation submitted in the School of Engineering
University of KwaZulu-Natal
Durban

In the fulfilment of the requirements of the degree of Master of Science in
Engineering

DECLARATION

The work presented in this dissertation was undertaken at the School of Engineering, University of KwaZulu-Natal, Howard College Campus in Durban, South Africa, from February 2017 until June 2018.

All work presented in this dissertation is original unless otherwise stated. It has neither in whole nor part been submitted previously to any other University or Institute as part of a degree.

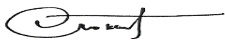
I, Calvin Moodley, declare that

1. The research reported in this thesis, except where otherwise indicated, is my original research.
2. This thesis has not been submitted for any degree or examination at any other university.
3. This thesis does not contain other persons' data, pictures, graphs or other information, unless specifically acknowledged as being sourced from other persons.
4. This thesis does not contain other persons' writing, unless specifically acknowledged as being sourced from other researchers. Where other written sources have been quoted, then:
 - a. Their words have been re-written, but the general information attributed to them has been referenced.
 - b. Where their exact words have been used, then their writing has been placed in italics and inside quotation marks and referenced.
5. This thesis does not contain text, graphics or tables copied and pasted from the Internet, unless specifically acknowledged, and the source being detailed in the thesis and in the References sections.



Calvin Moodley

As the candidate's supervisor(s)/co-supervisor I hereby certify that I find this work to be suitable for submission for the degree of Master of Science in Chemical Engineering.



Dr. David Lokhat

(Supervisor)

ACKNOWLEDGEMENTS

I would like to take this opportunity to acknowledge and show my deepest gratitude to the following people who have all greatly contributed to the completion of this dissertation:

- First and foremost, I would like to thank God, my parents, my brother, my partner: Sheriniya Naidu, and her family, for giving me the strength, motivation and support to pursue my MSc degree and other endeavors in life.
- My supervisors, Doctor David Lokhat and Professor Milan Carsky, for imparting on me their vast knowledge, support and guidance. This includes the opportunity to broaden my horizons to the world of chemical engineering and international exposure via a World Congress visit to Barcelona.
- My co-supervisor, Doctor Suren Moodley, and final year chemical engineering student, Mr. Arshir Narain, for their invaluable input and guidance with regards to developing the Matlab code presented in this thesis.
- The lab technicians: Ms. Xoli Hadebe and Ms. Thobekile Mofokeng as well as the chemical engineering technical staff: Mr. Danny Singh, Mr. Sanjay Deeraj and Mr. Gerald Addieah. Thank you for your valuable assistance throughout my work.
- The ESKOM TESP Program for their greatly appreciated financial support and their dedication to helping scholars pursue their research with these much-needed funds.
- Final year chemical engineering students of 2017: Mr. Arshir Narain and Mr. Rahul Jerrier, for their valued assistance with experimental runs during their laboratory work module.
- Final year vacation work students of 2017: Mr. Devesh Narainpershad and Miss. Janine Govender, for their valued assistance with experimental related work during their vacation work module.

EXECUTIVE SUMMARY

As stringent environmental regulations regarding SO₂ emissions have been enacted in many countries, the removal of SO₂ from flue gas has become a necessity. Conventional methods for flue gas desulfurization (SO₂ removal) involve cooling of the flue gas followed by scrubbing and subsequent reheating of the treated gas. To minimize cooling/heating requirements, thus optimizing energy consumption and related expenses, high temperature flue gas desulfurization technologies utilizing dry sorbent injection have recently been emphasized. Experimental studies reported in literature dictate that possible formation of sulfur trioxide (SO₃) in situ has been largely ignored for the high temperature desulfurization process. Since the performance of desulfurization systems is based on the amount of SO₂ removed, any conversion to SO₃ would result in an overestimated efficiency with respect to SO₂ removal.

This study focused on determining if significant amounts of SO₃ are formed at the excessive temperatures of high temperature flue gas desulfurization and what effect this has on the actual amount of desulfurization achieved. The experiment was designed with one independent variable (desulfurization temperature) and three levels for that variable. The aim of the experimental design was to evaluate the effect of desulfurization temperature (700°C, 800°C and 900°C) on the amount of SO₂ removed using limestone as the solid sorbent – through determination of breakthrough time and sorbent sorption capacity (based on saturation time) – and the amount of SO₃ formed – estimated via the Isopropanol Absorption Bottle Method. Reaction of SO₂ within a packed bed of limestone sorbent particles was modelled by considering two descriptions with regards to the morphological structure of the sorbent surface: a non-porous surface and a porous surface. Solution of the developed model was undertaken utilizing the Method of Lines (MOL).

Experiments were carried out using a bed height of 3 cm and fixing the inlet flowrate of flue gas at $6 \frac{\text{L}}{\text{min}}$, resulting in a residence time within the sorbent bed of 0.3 seconds. A gas chromatograph (GC) was utilized to generate the transient SO₂ concentration profile at the reactor inlet and outlet. This ultimately determines breakthrough time, saturation time and sorbent sorption capacity. The GC was thus required to be calibrated. A third-degree polynomial was found to best fit the calibration curve data. A dead time of three seconds was estimated for flue gas to propagate through the system to the sample extraction point. Sieve tray analysis of the limestone sorbent particles revealed an average particle size of 362.76 μm .

Experimental results for SO₂ removal indicate that breakthrough time, saturation time and SO₂ sorption capacity of limestone sorbent all increase with an increase in operating temperature. This trend is attributed

to formation of larger volume product CaSO₄ layers on active sorbent surfaces effecting a more gradual decline in overall diffusivity (D_z) with increasing operating temperature, as expressed by results of the model analysis. Breakthrough times of 100s, 210s and 240s were achieved for operating temperatures of 700 °C, 800 °C and 900°C respectively; saturation times of 890s, 1060s & 1200s were achieved for operating temperatures of 700 °C, 800 °C and 900°C respectively; SO₂ sorption capacities of 13.50 $\frac{\text{mg of SO}_2}{\text{gram of Sorbent}}$, 16.20 $\frac{\text{mg of SO}_2}{\text{gram of Sorbent}}$ and 18.73 $\frac{\text{mg of SO}_2}{\text{gram of Sorbent}}$ were achieved for operating temperatures of 700 °C, 800 °C and 900°C respectively. The model analysis proves further that the limestone sorbent particles are porous in nature due to a conservative fit between experimental data and the predicted model solution.

Results for SO₃ formation indicate that the generation of SO₃ is predominantly due to the heterogeneous catalytic reaction of SO₂ with the stainless steel walls of the reactor at such elevated temperatures utilized during high temperature flue gas desulfurization. In the absence of stainless steel the mass of sulfur entering the system which is converted to SO₃ was calculated to be 0.251%, 0.249% and 0.247% for the operating temperatures of 700 °C, 800 °C and 900°C respectively. In the presence of stainless steel the mass of sulfur entering the system which is converted to SO₃ was calculated to be 3.24%, 5.60% and 9.30% for operating temperatures of 700 °C, 800 °C and 900°C respectively.

It can thus be concluded that as operating temperature shifts away from 700°C towards 900°C the formation of SO₃ becomes much more significant in the presence of stainless steel. The amount of desulfurization achieved however is similar for the respective operating temperatures. Since stainless steel is a requirement it is recommended to operate at a temperature of 700°C since similar performance is achieved by the limestone sorbent in terms of SO₂ removal, relative to 800°C and 900°C, while SO₃ production is relatively minimal.

TABLE OF CONTENTS

TABLE OF CONTENTS	VI
LIST OF FIGURES	XI
LIST OF TABLES	XIII
NOMENCLATURE	XVII
CHAPTER 1: INTRODUCTION	1
1.1) PROBLEM IDENTIFICATION	1
1.2) RATIONALE AND MOTIVATION	3
1.3) OBJECTIVES OF THE STUDY	5
1.4) SCOPE OF THE STUDY	6
1.5) OUTLINE OF THE DISSERTATION	8
CHAPTER 2: LITERATURE REVIEW	9
2.1) FLUE GAS DESULFURIZATION (FGD)	9
2.1.1) SORBENTS	9
2.1.2) FLUE GAS DESULFURIZATION TECHNOLOGIES: WET SCRUBBING	10
2.1.2.1) Conventional Technique	10
2.1.2.2) Limestone Forced Oxidation (LFSO) Technique	12
2.1.2.3) Magnesium Enhanced Lime (MEL) Technique	13
2.1.3) ADVANTAGES VS DISADVANTAGES OF WET SCRUBBING	15
2.1.3.1) Advantages (Semaru, 1977)	15
2.1.3.2) Disadvantages (Semaru, 1997)	15
2.1.4) FLUE GAS DESULFURIZATION TECHNOLOGIES: SPRAY-DRY SCRUBBING	16
2.1.5) FLUE GAS DESULFURIZATION TECHNOLOGIES: DRY SORBENT INJECTION	18
2.1.6) FLUE GAS DESULFURIZATION TECHNOLOGIES: ADVANCED TECHNOLOGY (WSA & SNOX PROCESSES)	21
2.1.6.1) Wet Sulfuric Acid (WSA) Process	21
2.1.6.2) SNOX Process	24
2.1.7) ADVANTAGES OF THE WSA & SNOX PROCESSES (LAURSEN, 2007)	26
2.2) SULFUR TRIOXIDE (SO_3) MEASUREMENT TECHNIQUES	27
2.2.1) CONTROLLED CONDENSATION METHOD	29
2.2.2) ISOPROPANOL ABSORPTION BOTTLE METHOD	30
2.2.3) SALT METHOD	32
2.2.4) PENTOL SO_3 MONITOR	33
2.3) CONVERSION OF SO_2 TO SO_3 AT ELEVATED TEMPERATURE	34

2.4) LIMESTONE PROPERTIES: THE EFFECT ON DESULFURIZATION	36
2.4.1) SURFACE PROPERTIES	36
2.4.2) IMPURITIES	37
2.5) LIMESTONE SORPTION CAPACITY	38
2.6) BREAKTHROUGH & BREAKTHROUGH TIME; SATURATION TIME; NOMALITY; SO ₃ MOLAR YIELD AND DESULFURIZATION RATIO	39
2.6.1) BREAKTHROUGH & BREAKTHROUGH TIME	39
2.6.2) SATURATION TIME	39
2.6.3) SO ₃ MOLAR YIELD	40
2.6.4) DESULFURIZATION RATIO	40
2.7) STATISTICAL ANALYSIS	41
2.7.1) ABSOLUTE UNCERTAINTY	41
2.7.2) RELATIVE UNCERTAINTY	41
2.7.3) AVERAGE RELATIVE UNCERTAINTY	42
2.7.4) PROPAGATION UNCERTAINTY	42
CHAPTER 3: SO₂ REACTION WITH LIMESTONE - MODEL DEVELOPMENT & SOLUTION APPROACH	44
3.1) NON-POROUS MODEL	45
3.1.1) MASS BALANCE IN PACKED BED REACTOR	45
3.1.2) MASS BALANCE WITHIN PRODUCT LAYER	46
3.1.3) MASS BALANCE AT THE REACTION INTERFACE	47
3.2) POROUS MODEL	48
3.2.1) MASS BALANCE IN PACKED BED REACTOR	49
3.2.2) BALANCE WITHIN PORES OF THE PARTICLE LOCATED AT A DISTANCE 'Z' IN THE REACTOR	49
3.3) REACTION KINETICS	51
3.4) CALCULATED MODEL PARAMETERS	53
3.4.1) FLUE GAS VELOCITY (V _z)	53
3.4.2) LIMESTONE SORBENT AVERAGE PARTICLE RADIUS	54
3.4.3) LIMESTONE SORBENT BED POROSITY (EB)	55
3.4.4) PHYSICAL PROPERTIES	56
3.4.4.1) Flue Gas Density	56
3.4.4.2) Flue Gas Viscosity	58
3.4.5) MASS TRANSFER COEFFICIENT	60
3.4.6) INTRA-PARTICLE POROSITY (A)	63
3.4.7) SURFACE AREA PER UNIT VOLUME	64
3.4.8) PRODUCT LAYER DIFFUSION RESISTANCE	65
3.4.9) EFFECTIVE DIFFUSIVITY (D _E)	65
3.5) NUMERICAL SOLUTION APPROACH	67

3.5.1) NUMERICAL METHOD	67
3.5.2) AXIAL DISCRETIZATION TO ESTABLISH SYSTEM OF TEMPORAL ODE'S	69
3.5.2.1) Non-Porous Model Axial Discretization	69
3.5.2.2) Porous Model Axial Discretization	71
3.5.3) MATLAB CODE: POROUS AND NON-POROUS MODEL SOLUTION ALGORITHM	74
CHAPTER 4: EXPERIMENTAL METHODS	75
4.1) EXPERIMENTAL VARIABLES	75
4.2) EXPERIMENTAL DESIGN	76
4.3) PROCESS DESIGN	77
4.4) EXPERIMENTAL EQUIPMENT	78
4.4.1) DESULFURIZATION REACTOR & FURNACE	79
4.4.2) GAS SAMPLING & ANALYSIS EQUIPMENT	81
4.4.3) SO ₃ ANALYSIS	83
4.4.4) TUBING, VALVES & FITTINGS	84
4.5) REACTOR WASHING	85
4.6) EXPERIMENTAL PROCEDURE	86
4.6.1) SULFUR DIOXIDE (SO ₂) PROCEDURE	86
4.6.2) SULFUR TRIOXIDE (SO ₃) PROCEDURE	87
4.6.2.1) Chemical Preparation	87
4.6.2.2) Barium Perchlorate Standardization	87
4.6.2.3) Titration Procedure	88
CHAPTER 5: RESULTS AND DISCUSSION	89
5.1) GAS CHROMATOGRAPH (GC) CALIBRATION	89
5.2) DEAD TIME RUN	91
5.3) LIMESTONE SORBENT	92
5.3) SULFUR DIOXIDE REMOVAL (DESULFURIZATION)	94
5.3.1) X-RAY DIFFRACTION (XRD) TEST	94
5.3.2) BREAKTHROUGH CURVES: EXPERIMENTAL & MODEL RESULTS	96
5.3.3) SO ₂ SORPTION CAPACITY	106
5.4) SULFUR TRIOXIDE (SO ₃) FORMATION	108
CHAPTER 6: CONCLUSIONS	114
CHAPTER 7: RECOMMENDATIONS	117
REFERENCES	118
APPENDIX A: RAW & CALCULATED DATA	122
A-1.1) CALIBRATION DATA	122

A-1.2) DEADTIME RUN DATA	123
A-1.3) BARIUM PERCHLORATE STANDARDIZATION DATA	123
A-1.4) 700°C DATA	124
A-1.4.1) RUN 1	124
A-1.4.2) RUN 2	134
A-1.4.3) RUN 3	144
A-1.5) 800°C DATA	154
A-1.5.1) RUN 1	154
A-1.5.2) RUN 2	165
A-1.5.3) RUN 3	176
A-1.6) 900°C DATA	187
A-1.6.1) RUN 1	187
A-1.6.2) RUN 2	199
A-1.6.3) RUN 3	211
A-1.7) RESPONSE CURVE DATA AVERAGE RELATIVE UNCERTAINTY CALCULATIONS	223
A-1.7.1) 700°C	223
A-1.7.2) 800°C	227
A-1.7.3) 900°C	231
APPENDIX B: SAMPLE CALCULATIONS	236
B-1.1) CALIBRATION CURVE (REFER TO TABLE A-1)	237
B-1.2) BARIUM PERCHLORATE STANDARDIZATION	238
B-1.3) 700°C - RUN 1 SAMPLE CALCULATIONS	239
B-1.3.1) INLET SULFUR MASS FROM SO ₂	239
B-1.3.1.1) Initial/Inlet SO ₂ Volume Concentration (Refer to Table A-7)	239
B-1.3.1.2) Inlet Mass From SO ₂ (Refer to Table A-12)	240
B-1.3.2) OUTLET SULFUR MASS FROM SO ₂	242
B-1.3.2.1) Reactor Effluent SO ₂ Volume Concentration (Refer to Table A-8)	242
B-1.3.2.2) Outlet Mass From SO ₂ (Refer to Table A-8 & Table A-12)	242
B-1.3.3) OUTLET SULFUR MASS FROM SO ₃ (REFER TO TABLE A-12)	245
B-1.3.4) DESULFURIZATION RATIO	247
B-1.3.5) SO ₃ MOLAR YIELD	248
B-1.3.6) SO ₂ SORPTION CAPACITY OF LIMESTONE	249
B-1.4) STATISTICAL ANALYSIS	251
B-1.4.1) ABSOLUTE UNCERTAINTY (REFER TO TABLE A-2)	251
B-1.4.2) RELATIVE UNCERTAINTY (REFER TO TABLE A-2)	252
B-1.4.3) PROPAGATIONAL UNCERTAINTY (REFER TO TABLE A-9)	253
B-1.4.4) BREAKTHROUGH CURVE DATA AVERAGE RELATIVE UNCERTAINTY	254

APPENDIX C: MATLAB CODE – MODEL SOLUTION FOR REACTION OF SO₂ WITH LIMESTONE	257
C-1.1) NON-POROUS MODEL	257
C-1.1.1) MATLAB SCRIPT: ODE45 SOLVER	257
C-1.1.2) 700°C FUNCTION [DC _B /D _T]: TEMPORAL ODE'S TO BE SOLVED	263
C-1.1.3) 800°C FUNCTION [DC _B /D _T]: TEMPORAL ODE'S TO BE SOLVED	267
C-1.1.4) 900°C FUNCTION [DC _B /D _T]: TEMPORAL ODE'S TO BE SOLVED	271
C-1.2) POROUS MODEL	275
C-1.2.1) MATLAB SCRIPT: ODE45 SOLVER	275
C-1.2.2) 700°C FUNCTION [DC _B /D _T]: TEMPORAL ODE'S TO BE SOLVED	281
C-1.2.3) 800°C FUNCTION [DC _B /D _T]: TEMPORAL ODE'S TO BE SOLVED	284
C-1.2.4) 900°C FUNCTION [DC _B /D _T]: TEMPORAL ODE'S TO BE SOLVED	287
APPENDIX D: HAZOP STUDY	290
APPENDIX E: MATERIAL AND SAFETY DATA SHEETS	297

LIST OF FIGURES

Chapter 2

Figure 2. 1: Conventional wet scrubbing process (Arcor Epoxy Technologies, 1990)	11
Figure 2. 2: Limestone with Forced Oxidation (LFSO) process (Arcor Epoxy Technologies, 1990)	12
Figure 2. 3: Magnesium Enhanced Lime (MEL) process (Anon., 2003)	14
Figure 2. 4: Spray-Dry Scrubbing process (Babcock & Wilcox, 2002)	17
Figure 2. 5: High temperature furnace sorbent injection (Zevenhoven & Kilpinen, 2001)	19
Figure 2. 6: Moderate temperature economizer sorbent injection (Zevenhoven & Kilpinen, 2001)	20
Figure 2. 7: In-Duct sorbent injection at low temperatures (Zevenhoven & Kilpinen, 2001)	20
Figure 2. 8: Process flow diagram for WSA plant (Laursen, 2007)	23
Figure 2. 9: WSA Condenser (Laursen, 2007)	23
Figure 2. 10: Process flow diagram for SNOX plant (Laursen, 2007)	25
Figure 2. 11: Schematic of glass cooler utilized in controlled condensation method (Flied, et al., 2012)	29
Figure 2. 12: Measurement setup of the isopropanol absorption bottle method (Flied, et al., 2012)	31
Figure 2. 13: Measurement setup for the salt method (Flied, et al., 2012)	32
Figure 2. 14: Influence of CO ₂ partial pressure on reaction rate (Khinast, et al., 1996)	37

Chapter 3

Figure 3. 1: Schematic representation of the reaction of SO ₂ with non-porous sorbent (Dasgupta, et al., 2003)	45
Figure 3. 2: Schematic representation of the reaction of SO ₂ with non-porous sorbent (Dasgupta, et al., 2003)	48
Figure 3. 3: Variation of average void fraction of bed with tube size (Rase, 1977)	55
Figure 3. 4: Diffusion volumes of simple molecules (Seader et al., 2011)	62
Figure 3. 5: Reference grid for derivation of finite difference equations	68
Figure 3. 6: Flow diagram of computational algorithm for porous and non-porous model solutions	74

Chapter 4

Figure 4. 1: Process design flow diagram	77
Figure 4. 2: Reactor/Furnace setup	80
Figure 4. 3: Shinko RKS, PID controller	80
Figure 4. 4: Schimadzu gas chromatograph and PC monitoring system	82
Figure 4. 5: Experimental setup for SO ₃ analysis	83
Figure 4. 6: Titrations that have reached endpoint	83

Chapter 5

Figure 5. 1: Calibration curve	89
Figure 5. 2: Dead time run curve	91
Figure 5. 3: Sorbent particle size distribution	92
Figure 5. 4: XRD pattern for fresh sorbent and spent sorbent – run 1	94
Figure 5. 5: XRD pattern for fresh sorbent and spent sorbent at 900°C – run 1	94
Figure 5. 6: SO ₂ Sorption - 700°C run 1	96
Figure 5. 7: SO ₂ Sorption - 800°C run 1	96
Figure 5. 8: SO ₂ Sorption - 900°C run 1	97
Figure 5. 9: Effect of temperature on SO ₂ sorption	97
Figure 5. 10: Effect of temperature on SO ₂ sorption - model results vs run 1 experimental data	100
Figure 5. 11: Model prediction -variation in overall diffusivity during SO ₂ sorption by porous sorbent	100

APPENDIX D

Figure D- 1: HAZOP nodal scheme	290
---------------------------------	-----

LIST OF TABLES

Chapter 2

Table 2. 1: Reaction schemes for WSA & SNOX processes (Laursen, 2007)	21
Table 2. 2: Equilibrium constant and equilibrium conversion at elevated reactor operating temperatures	35

Chapter 3

Table 3. 1: Temperature dependence of kinetic parameters (Orbey et. al. 1981)	52
Table 3. 2: Critical temperature and pressure (Smith et al. 2001)	56
Table 3. 3: Reduced Temperature [T_r] and Pressure [P_r] (operating pressure = 1 bar)	56
Table 3. 4: Flue gas density – [ρ_g] (operating pressure = 1 bar)	57
Table 3. 5: Dynamic viscosity of air and SO_2 (operating pressure = 1 bar)	58
Table 3. 6: Flue gas viscosity – [μg] (operating pressure = 1 bar)	59
Table 3. 7: Mass velocity, Reynolds number & jd factor (operating pressure = 1 bar)	61
Table 3. 8: Binary diffusion coefficient & Scmidt number (operating pressure = 1 bar)	63
Table 3. 9: Average mass transfer coefficient - [k_m] (operating pressure = 1 bar)	63
Table 3. 10: Surface area per unit volume - [a]	64
Table 3. 11: Diffusional resistance through product layer – [D_s]	65
Table 3. 12: Effective diffusivity – [D_e]	66

Chapter 4

Table 4. 1: Summary of experimental design (operating pressure = 1bar)	76
Table 4. 2: Equipment and chemicals utilized in experimental work	78
Table 4. 3: GC operating conditions	81

Chapter 5

Table 5. 1: Flue-Gas tank composition	89
Table 5. 2: Sorbent particle size analysis	92
Table 5. 3: Sorbent composition	93
Table 5. 4: Breakthrough time and saturation time - 700°C	98
Table 5. 5: Breakthrough time and saturation time - 800°C	98
Table 5. 6: Breakthrough time and saturation time - 900°C	98
Table 5. 7: Breakthrough curve data average relative deviation	98
Table 5. 8: SO_2 molar and mass based sulfur analysis - 700°C	99
Table 5. 9: SO_2 molar and mass based sulfur analysis - 800°C	99

Table 5. 10: SO ₂ molar and mass based sulfur analysis - 900°C	99
Table 5. 11: Limestone sorption capacity - 700°C	106
Table 5. 12: Limestone sorption capacity - 800°C	106
Table 5. 13: Limestone sorption capacity - 900°C	106
Table 5. 14: Desulfurization ratio and molar yield of SO ₃ - 700°C	108
Table 5. 15: Desulfurization ratio and molar yield of SO ₃ - 800°C	108
Table 5. 16: Desulfurization ratio and molar yield of SO ₃ - 900°C	108
Table 5. 17: SO ₃ molar yield temperature dependence prior to reactor washing	108
Table 5. 18: SO ₃ molar and mass based sulfur analysis - 700°C	109
Table 5. 19: SO ₃ molar and mass based sulfur analysis - 800°C	109
Table 5. 20: SO ₃ molar and mass based sulfur analysis - 900°C	109
Table 5. 21: Temperature dependence of SO ₃ sulfur profile prior to reactor washing	110

APPENDIX A

Table A- 1: Calibration data	122
Table A- 2: Calibration curve relative uncertainty calculation data	122
Table A- 3: Average relative uncertainty	122
Table A- 4: Deadtime run data	123
Table A- 5: Volumes obtained from sulfuric acid titration	123
Table A- 6: Volumes obtained from water (blank) titration	123
Table A- 7: Initial /inlet SO ₂ concentration - 700°C run 1	124
Table A- 8: Reactor effluent SO ₂ concentration - 700°C run 1	125
Table A- 9: Propagational uncertainty data - 700°C run 1	128
Table A- 10: Volumes obtained from titration for SO ₃ analysis - 700°C run 1	132
Table A- 11: Moles of SO ₃ produced from titrations - 700°C run 1	132
Table A- 12: System sulfur mass balance - 700°C run 1	133
Table A- 13: SO ₂ sorption capacity of limestone sorbent - 700°C run 1	133
Table A- 14: Initial /inlet SO ₂ concentration - 700°C run 2	134
Table A- 15: Reactor effluent SO ₂ concentration - 700°C run 2	135
Table A- 16: Propagational uncertainty data - 700°C run 2	138
Table A- 17: Volumes obtained from titration for SO ₃ analysis - 700°C run 2	142
Table A- 18: Moles of SO ₃ produced from titrations - 700°C run 2	142
Table A- 19: System sulfur mass balance - 700°C run 2	143
Table A- 20: SO ₂ sorption capacity of limestone sorbent - 700°C run 2	143
Table A- 21: Initial /inlet SO ₂ concentration - 700°C run 3	144
Table A- 22: Reactor effluent SO ₂ concentration - 700°C run 3	145
Table A- 23: Propagational uncertainty data - 700°C run 3	148
Table A- 24: Volumes obtained from titration for SO ₃ analysis - 700°C run 3	152
Table A- 25: Moles of SO ₃ produced from titrations - 700°C run 3	152
Table A- 26: System sulfur mass balance - 700°C run 3	153
Table A- 27: SO ₂ sorption capacity of limestone sorbent – 700°C run 3	153
Table A- 28: Initial /inlet SO ₂ concentration - 800°C run 1	154
Table A- 29: Reactor effluent SO ₂ concentration - 800°C run 1	155

Table A- 30: Propagational uncertainty data - 800°C run 1	159
Table A- 31: Volumes obtained from titration for SO ₃ analysis - 800°C run 1	163
Table A- 32: Moles of SO ₃ produced from titrations - 800°C run 1	163
Table A- 33: System sulfur mass balance - 800°C run 1	164
Table A- 34: SO ₂ sorption capacity of limestone sorbent - 800°C run 1	164
Table A- 35: Initial /inlet SO ₂ concentration - 800°C run 2	165
Table A- 36: Reactor effluent SO ₂ concentration - 800°C run 2	166
Table A- 37: Propagational uncertainty data - 800°C run 2	170
Table A- 38: Volumes obtained from titration for SO ₃ analysis - 800°C run 2	174
Table A- 39: Moles of SO ₃ produced from titrations - 800°C run 2	174
Table A- 40: System sulfur mass balance - 800°C run 2	175
Table A- 41: SO ₂ sorption capacity of limestone sorbent - 800°C run 2	175
Table A- 42: Initial /inlet SO ₂ concentration - 800°C run 3	176
Table A- 43: Reactor effluent SO ₂ concentration - 800°C run 3	177
Table A- 44: Propagational uncertainty data - 800°C run 3	181
Table A- 45: Volumes obtained from titration for SO ₃ analysis - 800°C run 3	185
Table A- 46: Moles of SO ₃ produced from titrations - 800°C run 3	185
Table A- 47: System sulfur mass balance - 800°C run 3	186
Table A- 48: SO ₂ sorption capacity of limestone sorbent - 800°C run 3	186
Table A- 49: Initial /inlet SO ₂ concentration - 900°C run 1	187
Table A- 50: Reactor effluent SO ₂ concentration - 900°C run 1	188
Table A- 51: Propagational uncertainty data - 900°C run 1	192
Table A- 52: Volumes obtained from titration for SO ₃ analysis - 900°C run 1	197
Table A- 53: Moles of SO ₃ produced from titrations - 900°C run 1	197
Table A- 54: System sulfur mass balance - 900°C run 1	198
Table A- 55: SO ₂ sorption capacity of limestone sorbent - 900°C run 1	198
Table A- 56: Initial /inlet SO ₂ concentration - 900°C run 2	199
Table A- 57: Reactor effluent SO ₂ concentration - 900°C run 2	200
Table A- 58: Propagational uncertainty data - 900°C run 2	204
Table A- 59: Volumes obtained from titration for SO ₃ analysis - 900°C run 2	209
Table A- 60: Moles of SO ₃ produced from titrations - 900°C run 2	209
Table A- 61: System sulfur mass balance - 900°C run 2	210
Table A- 62: SO ₂ sorption capacity of limestone sorbent - 900° run 2	210
Table A- 63: Initial /inlet SO ₂ concentration - 900°C run 3	211
Table A- 64: Reactor effluent SO ₂ concentration - 900°C run 3	212
Table A- 65: Propagational uncertainty data - 900°C run 3	216
Table A- 66: Volumes obtained from titration for SO ₃ analysis - 900°C run 3	221
Table A- 67: Moles of SO ₃ produced from titrations - 900°C run3	221
Table A- 68: System sulfur mass balance – 900°C run 3	222
Table A- 69: SO ₂ sorption capacity of limestone sorbent – 900°C run 3	222
Table A- 70: Calculation for average relative uncertainty between response curve data - 700°C	223
Table A- 71: Calculation for average relative uncertainty between response curve data - 800°C	227
Table A- 72: Calculation for average relative uncertainty between response curve data - 900°C	231

APPENDIX B

Table B- 1: System operating conditions	236
Table B- 2: Calibration curve equation coefficients	236
Table B- 3: Auxiliary data for subsequent calculations	236

APPENDIX D

Table D- 1: Hazard-And-Operability-Study-Record-Node 1	291
Table D- 2: Hazard-And-Operability-Study-Record-Node 2	292
Table D- 3: Hazard-And-Operability-Study-Record-Node 3	293
Table D- 4: Hazard-And-Operability-Study-Record-Node 4	294
Table D- 5: Hazard-And-Operability-Study-Record-Node 6	295
Table D- 6: Hazard-And-Operability-Study-Record-Nodes - 5, 7 & 8	296

APPENDIX E

Table E- 1: Material Safety Data Sheet - Barium Perchlorate, Anhydrous	297
Table E- 2: Material Safety Data Sheet - Isopropyl Alcohol	299
Table E- 3: Material Safety Data Sheet - Helium	301
Table E- 4: Material Safety Data Sheet - Thoron Indicator	303
Table E- 5: Material Safety Data Sheet - Calcium Carbonate	305
Table E- 6: Material Safety Data Sheet - Sulfuric Acid	307

NOMENCLATURE

Symbol	Description	Unit
a	External surface area per unit volume	m^2/m^3
A_t	Tube cross-sectional area	m^2
BT	Breakthrough time	s
C_b	SO_2 concentration in the bulk gas phase	mol/m^3
\bar{C}_p	Average particle SO_2 concentration	mol/m^3
C_{in}	Average reactor inlet SO_2 concentration	mol/m^3
C_o		
C_{out}	Transient reactor outlet SO_2 concentration	mol/m^3
d_p	Sauter-Mean particle diameter	m
D_{AB}	Binary diffusion coefficient	m^2/s
D_{BA}		
D_e	Effective diffusivity of compound	m^2/s
D_K	Knudsen diffusivity	m^2/s
D_m	Molecular diffusivity	m^2/s
D_s	Product layer diffusion coefficient	m^2/s
D_z	Overall Diffusion coefficient	m^2/s
D	Tube/Reactor diameter	m
D_t		
$fp(r)$	Flux owing to the chemical reaction at reaction surface	$\text{mol}/\text{m}^2 \cdot \text{s}$
G	Mass velocity	$\text{kg}/\text{m}^2 \cdot \text{s}$
j_D	Chilton-Colburn j-factor for mass transfer	-
k	Pre-exponential factor	m/s
k_m	Average mass transfer coefficient	m/s
k_r	Volume based reaction rate constant	m/s
L_{Bed}	Limestone bed length	m
L		
M	Molecular weight	g/mol

MW	Molecular weight	g/mol
n	Number of moles of species	mol
N _r	Molar diffusion flux in the radial direction of grain	mol/m ² .s
P	System operating pressure	bar
P _c	Critical pressure	bar
P _r	Reduced pressure	bar
Q	Flue gas flow rate	m ³ /s
r	Pore radius	m
\bar{r}	Average pore radius	m
r _p	Mean particle radius	m
r _c	Core radius	m
R	Universal Gas constant	m ³ .Pa/mol.k
Re	Reynolds number	-
S _c	Schmidt Number	-
S _g	Specific surface area	m ² /kg
S _{in}	Inlet mass based sulfur content	kg
S _{out}	Outlet mass based sulfur content	kg
t	time	s
t _o	Initial time	s
t _{sat}	Saturation time	s
T	System Operating temperature	°C
T _c	Critical Temperature	°C
T _r	Reduced temperature	°C
T _{sat}	Saturation temperature	s
V	Molar Volume	m ³
V _m	Molar gas volume	cm ³ mmol
V _z	Axial flue gas velocity	m/s
x	Chromatogram area	µV.s
z	Axial position along packed bed	m
($\sum v$)	Summation of atomic and structural diffusion volumes of species	-

Greek Letters		
Symbol	Description	Unit
α	Intra particle porosity	-
β	Temperature dependent empirical parameter	s^{-1}
ϵ_b	Packed bed porosity	-
ρ_B	Limestone bulk density	kg/m^3
ρ_g	Flue gas density	kg/m^3
ρ_p	Sorbent particle density	kg/m^3
ρ_s		
μ_g	Flue gas viscosity	cP
ω	Acentric factor	-
τ	Tortuosity	-
δ	Change in variable	-

CHAPTER 1: INTRODUCTION

1.1) PROBLEM IDENTIFICATION

Fossil fuels such as coal and oil contain many impurities including sulfur. Fossil-fuel power plants generally combust such coal and oil for electricity generation and much of these sulfur impurities are converted to sulfur dioxide (SO_2) which departs with the combustor's exhaust gases (flue gas). As stringent environmental regulations regarding SO_2 emissions have been enacted in many countries, the removal of SO_2 from flue gas has become a necessity. Conventional methods for flue gas desulfurization (SO_2 removal) involve cooling of the flue gas followed by scrubbing and subsequent reheating of the treated gas above its dew point. To minimize cooling/heating requirements, thus optimizing energy consumption and related expenses, high temperature flue gas desulfurization technologies have recently been emphasized. High temperature flue gas desulfurization may however result in the conversion of SO_2 to sulfur trioxide (SO_3) under these excessive temperature conditions thus the degree of desulfurization achieved, from measurement of the SO_2 concentration of both the untreated and treated gas, may be inaccurate since sulfur remains as part of the treated gas in the form of SO_3 . It is thus required to determine if in fact SO_2 is converted to SO_3 at the excessive temperatures of high temperature flue gas desulfurization through use of appropriate techniques for SO_3 measurements since such a task has not been performed over the run-time of this process previously.

This research project aims to answer the following research questions:

1. What *apparent* degree of desulfurization can be achieved using limestone as the solid sorbent within the developed flow-through apparatus (fixed bed reactor)?
2. What amount of SO_3 is produced during high temperature desulfurization of flue gas?
3. What percentage of the total desulfurization is attributed to the conversion of SO_3 i.e.: what is the *actual* degree of desulfurization achievable with limestone used as the solid sorbent?

4. Within what range of operating temperatures should high temperature flue gas desulfurization be undertaken to minimize the conversion of SO₂ to SO₃ and maintain optimal desulfurization of flue gas?

1.2) RATIONALE AND MOTIVATION

Flue gas refers to the combustion exhaust gases produced at power plants as a result of the combustion of fossil fuels such as coal and oil for electricity generation. Its composition depends on what is being burned, but will usually consist of mostly nitrogen (typically more than two-thirds), carbon dioxide, and water vapor as well as excess oxygen. The flue gas further contains a small percentage of a number of pollutants, such as particulate matter (like soot), carbon monoxide, nitrogen oxides, and sulfur oxides which are generated as a consequence of the various impurities contained within fossil fuels. As mentioned previously, stringent environmental regulations regarding sulfur dioxide (SO_2) emissions have been enacted in many countries due to its corrosive and toxic nature, hence the removal of SO_2 from flue gas has become a necessity.

Conventional methods for SO_2 removal involve an initial cooling of the flue gas followed by wet scrubbing and subsequent reheating of the treated gas above its dew point. The treated gas is generally saturated with water and may contain trace amounts of SO_2 resulting in the formation sulfuric acid (H_2SO_4) which may condense if the treated gas is below the requisite dew point temperature, resulting in corrosion of equipment downstream (Nolan, 2000). The treated gas is thus reheated to prevent such an occurrence. These conventional techniques include **Wet Scrubbing** using a slurry of alkaline sorbent, usually limestone, **Spray Dry Scrubbing** using similar sorbent slurries, **The Wet Sulfuric Acid Process** which recovers sulfur in the form of commercial quality sulfuric acid and **The SNOX Process** which removes sulfur dioxide (SO_2) as concentrated sulfuric acid, nitrogen oxides (NO_x) and particulates from flue gases. The issue with cooling and reheating the flue gas as per the conventional techniques mentioned above, is that it requires expensive equipment, increases plant complexity, and lowers overall thermal efficiency, thus making the electricity produced more expensive (Arvanitidis, et al., 2009). An alternative existing approach known as **Dry Sorbent Injection** is now being emphasized to avoid energy losses and the excess costs associated with conventional gas cleaning technologies. This technology is also referred to as **High Temperature Flue Gas Desulfurization** wherein the intermediate heating and cooling steps of the conventional techniques are omitted.

According to Nolan (2000), a conventional technique such as Spray Dry Scrubbing can remove up to 95% of SO_2 from flue gases originating from coal with a maximum sulfur content of 2.5wt% while Krammer & Staudinger (1991) state that high temperature flue gas desulfurization technologies can remove as much as 99% of SO_2 from flue gases originating from coal with a maximum sulfur content of 5wt%. This would dictate that high temperature desulfurization is not only more energy efficient but also may be more suitable for SO_2 removal.

At the excessive temperatures of high temperature desulfurization (700°C to 1100°C) however, it is postulated that conversion of SO₂ to SO₃ occurs. This in turn poses the question:

- Is the desulfurization (SO₂ removal) measured using limestone as the solid sorbent *actual* desulfurization, or is there a considerable amount of SO₂ that is simply converted to SO₃ resulting in a significant *apparent* degree of desulfurization and a reduced *actual* degree of desulfurization?

There are various techniques available for SO₃ measurement. The most significant and commonly used are chemically based including (Flied, et al., 2012):

- Controlled condensation method
- Isopropanol drop method
- Isopropanol absorption bottle method
- Salt method
- Pentol SO₃ monitor

SO₃ behaves very differently to SO₂ as it is highly reactive and quickly forms gaseous H₂SO₄ in the presence of water vapor that is generally present as part of the flue gas. Thus, when SO₃ measurements are discussed, these typically refer to the measurement of H₂SO₄.

The controlled condensation method is based on condensation of H₂SO₄ above the water dew-point and sulfate analysis afterwards. The controlled condensation method is presently the most used SO₃ measurement technique (Flied, et al., 2012). The isopropanol methods are based on absorption of H₂SO₄ in an isopropanol [CH₃CH(OH)CH₃] solution. The main problem with all isopropanol methods is absorption of SO₂ in the isopropanol solution which gives a positive bias if the SO₂ is oxidized to sulfates in the solution (Flied, et al., 2012). This however can be avoided by reducing measurement time and bubbling argon through the solution, rendering the isopropanol methods as viable (Flied, et al., 2012). The salt method is not a commonly used method (Flied, et al., 2012). The method is based on the reaction of H₂SO₄ with sodium chloride (NaCl) and subsequent sulfate analysis.

It should be noted that there is a distinct gap in literature. This is attributed to the fact that no real studies have been performed to determine SO₃ measurements over the run-time of the high temperature desulfurization process with limestone as the solid sorbent, hence it is impossible to draw conclusions about the *actual* degree of desulfurization that takes place. This study aims to fill this gap in the literature by use of an appropriate SO₃ measurement technique throughout the run-time of the high temperature desulfurization process to gain greater insight with respect to the *actual* degree of desulfurization that occurs.

1.3) OBJECTIVES OF THE STUDY

The objectives of this research project are:

Objective 1: To quantitatively determine the *apparent* degree of desulfurization that can be achieved with the use of limestone as the solid sorbent within the developed flow-through apparatus (fixed bed reactor).

Objective 2: To quantitatively determine the amount of SO₃ produced during hot flue gas desulfurization.

Objective 3: To quantitatively determine the percentage of total desulfurization attributed to the conversion of SO₃, and thus the *actual* degree of desulfurization achieved.

Objective 4: To identify the range of operating temperatures under which high temperature flue gas desulfurization should be performed to prevent the conversion of SO₂ to SO₃ and maintain optimal desulfurization of the flue gas.

1.4) SCOPE OF THE STUDY

The primary research method for this study is a quantitative scientific experiment involving the generation of statistically analysable data by systematic manipulation of independent variables. This type of research method allows one to make inferences about the relationship between independent and dependent variables. The system of scientific measurements will be interval based and the intervals will be uniform. The results of the quantitative experimental work will be used to test the hypotheses of the research. The primary research method will be supported by a literature review. The latter will guide the selection of the test limits of the experimental designs employed.

In order to meet the four objectives associated with the fulfilment of the aims of the project, the following tasks need to be carried out:

1. An extensive literature review will be performed to understand the conventional technologies available for flue gas desulfurization and their performance. Thereafter high temperature flue gas desulfurization will be reviewed to determine the performance achieved in similar studies using limestone as the solid sorbent, as well as the review of various SO₃ measurement techniques available. Research will also be undertaken into the kinetics involved for the reaction of SO₂ to SO₃, modelling of the reaction of limestone with SO₂, the effect of limestone properties on the rate of desulfurization and the SO₂ sorption capacity of limestone.

2. The fixed bed reactor apparatus required for the performance of experiments will be designed and commissioned. This will include the performance of a preliminary control experiment whereby flue gas will pass through the apparatus with no limestone present. This will provide insight on the performance of the limestone. An initial deadtime run will also be performed and factored into subsequent experimental results.

3. The *apparent* degree of desulfurization achieved will be determined by measuring the amount of SO₂ available at the inlet and outlet of the fixed bed apparatus. This is accomplished through use of a GC analyzer which detects the SO₂ concentration at each respective end and displays this information in terms of chromatogram areas. The flue gas used will be moist and contain 2073 ppmv SO₂ content entering the fixed bed.

-
-
-
4. SO₃ generation will be determined by use of an appropriate SO₃ measurement technique as established by the literature review. This measurement technique will be employed to determine the amount of SO₃ produced hence providing an indication of the *actual* degree of desulfurization achieved.
5. Experimental runs will be performed at different operating temperatures to determine an acceptable range of temperature within which to operate to optimize the *actual* degree of desulfurization. This temperature range, if such a range exists, shall be determined by SO₂ measurements at the inlet and outlet of the apparatus together with measurement of the amount of SO₃ generated at the outlet.

1.5) OUTLINE OF THE DISSERTATION

This dissertation was divided into four phases:

- The theoretical background of this research topic: covered in chapter 2.
- The gas-solid reactor modelling for this process: covered in chapter 3.
- The experimental methodology for the process design, and equipment used: covered in chapter 4.
- A discussion of results as well as conclusions and recommendations: covered in chapters 5-7.

The main hypothesis is that there is a certain degree of conversion of SO_2 to SO_3 during high temperature desulfurization of flue gas, over a certain temperature range, that leads to an *apparent* degree of desulfurization that is greater than the *actual* desulfurization which occurs.

With the aid of the results presented in this dissertation, insight into the production of SO_3 , and thus the *apparent* and *actual* rate of desulfurization achieved at elevated temperatures of high temperature flue gas desulfurization is envisaged.

CHAPTER 2: LITERATURE REVIEW

2.1) FLUE GAS DESULFURIZATION (FGD)

Many techniques have been developed to facilitate the removal of SO₂. Discussed below is the process description and performance of conventional techniques employed, together with some advanced technologies that have been implemented in industry due to the advantage of lower capital investment associated with these technologies over that of conventional techniques. Prior to discussion of these various techniques however, a brief explanation on the various sorbents used in these processes will be discussed as many of the techniques that follow are based on scrubbing utilizing sorbent slurries, as well as direct sorbent injection to effect SO₂ removal.

2.1.1) SORBENTS

SO₂ is an acid gas, therefore the typical sorbents and sorbent slurries used to remove SO₂ from flue gases are alkaline in nature. Depending on the application, the most important are lime, limestone and sodium hydroxide (also known as caustic soda). Lime and limestone is typically used on large coal or oil-fired boilers as found in power plants, since it is very much less expensive than caustic soda and more readily available. The problem is that it results in a slurry being circulated through the scrubber instead of a solution. This results in reduced abrasion resistance thus life expectancy of equipment is adversely affected (Nolan, 2000). Caustic soda is limited to smaller combustion units because it is more expensive than limestone, but it has the advantage that it forms a solution rather than a slurry. This makes it easier to operate (Nolan, 2000). Other less common sorbents include the use of a magnesium hydroxide Mg(OH)₂ slurry. A natural alkaline that is also used to absorb SO₂ is seawater. SO₂ is absorbed in the water, and when oxygen is added, reacts to form sulfate ions SO₄⁻ and free H⁺. The surplus of H⁺ is offset by the carbonates in seawater pushing the carbonate equilibrium to release carbon dioxide (CO₂) gas (Zevenhoven & Kilpinen, 2001).

2.1.2) FLUE GAS DESULFURIZATION TECHNOLOGIES: WET SCRUBBING

2.1.2.1) CONVENTIONAL TECHNIQUE

This conventional system employs two stages: An initial stage for fly ash removal using an electrostatic precipitator (ESP) or baghouse and a second stage for SO₂ removal. A simplified process flow diagram of a conventional wet scrubber is shown in Figure 2.1. After leaving the particulate removal device - ESP or a fabric filter/baghouse (top left) - the gas enters a spray tower or absorber (top center), where it is sprayed with a water slurry (approximately 10 percent lime or limestone). To provide good contact between the waste gas and the sorbent, the nozzles and injection locations are designed to optimize the size and density of the slurry droplets formed by the system. A portion of the water in the slurry is evaporated and the waste gas stream becomes saturated with water vapor. Sulfur dioxide dissolves into the slurry droplets where it reacts with the alkaline particulates to form calcium sulfite (CaSO₃). The slurry falls into the bottom of the absorber where it is collected. The treated flue gas passes through a mist eliminator before exiting the absorber which removes any entrained slurry droplets. The absorber effluent is sent to a reaction tank to which fresh slurry is also added.

A portion of the spent slurry from the reaction tank is recycled while the rest is pumped into the thickener, where the solids settle before going to a filter for final dewatering to about 50% solids (Arcor Epoxy Technologies, 1990). The waste product is usually mixed with fly ash (approximately 1:1) and fixative lime (approximately 5%) and disposed of in landfills (Arcor Epoxy Technologies, 1990).

Typical sorbent material used in this process is limestone or lime. Limestone is inexpensive but control efficiencies for limestone systems are limited to approximately 90% (Cooper & Alley, 2002). Lime on the other hand is easier to manage on-site and has control efficiencies up to 95% but it is more costly (Cooper & Alley, 2002).

Scale formation in the early systems tended to occur as the result of uncontrolled crystallization of the naturally oxidized product CaSO₄ (gypsum), from CaSO₃ recirculated to the absorber. This collects on the surfaces in the absorber and causes plugging of pipes and nozzles. It ultimately resulted in the use of redundant columns to overcome the scale formation. The net effect was that the costs of these first-generation systems tended to be higher than they otherwise might have been.

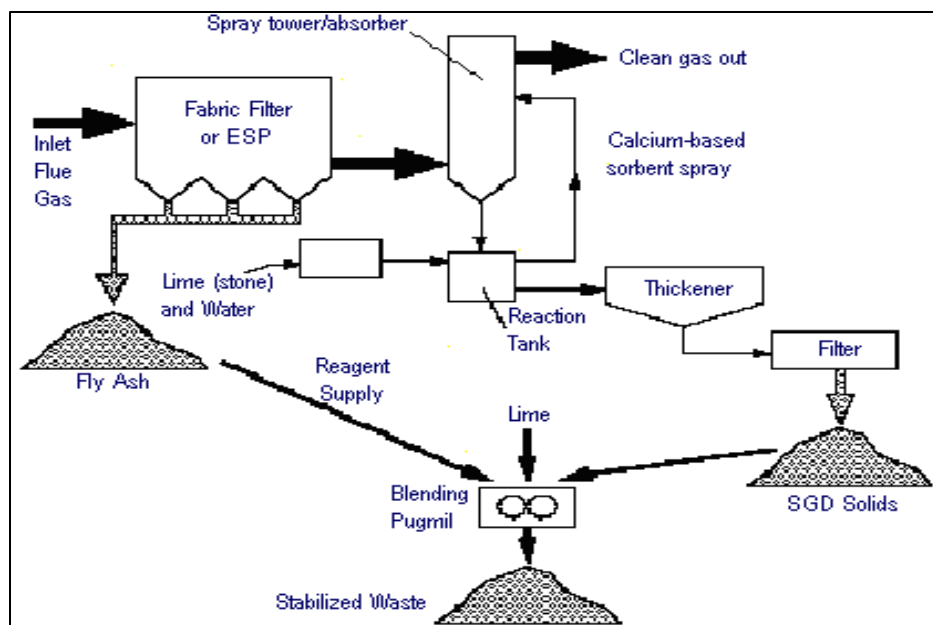


Figure 2. 1: Conventional wet scrubbing process (Arcor Epoxy Technologies, 1990)

2.1.2.2) LIMESTONE FORCED OXIDATION (LFSO) TECHNIQUE

Limestone with forced oxidation (LSFO) is a slight variation of the conventional wet scrubber system discussed above in that it utilizes limestone instead of lime, and the CaSO_3 initially formed in the spray tower absorber is nearly 100 percent oxidized to form gypsum by bubbling compressed air through the spent slurry in the reaction tank. This minimizes tendency for CaSO_4 to precipitate on surfaces in the absorber and cause plugging of pipes and nozzles since majority of CaSO_3 is oxidized prior to recirculation. This is achieved by maintaining a gypsum concentration in the absorber slurry liquid at 80-90% of the concentration at which scale would form (Anon., 2003).

The high gypsum content permits disposal of the dewatered waste without fixation (Srivastava, 2002). Gypsum also has a commercial value; by controlling the gypsum quality in the dewatering step, a wallboard-grade gypsum can be produced.

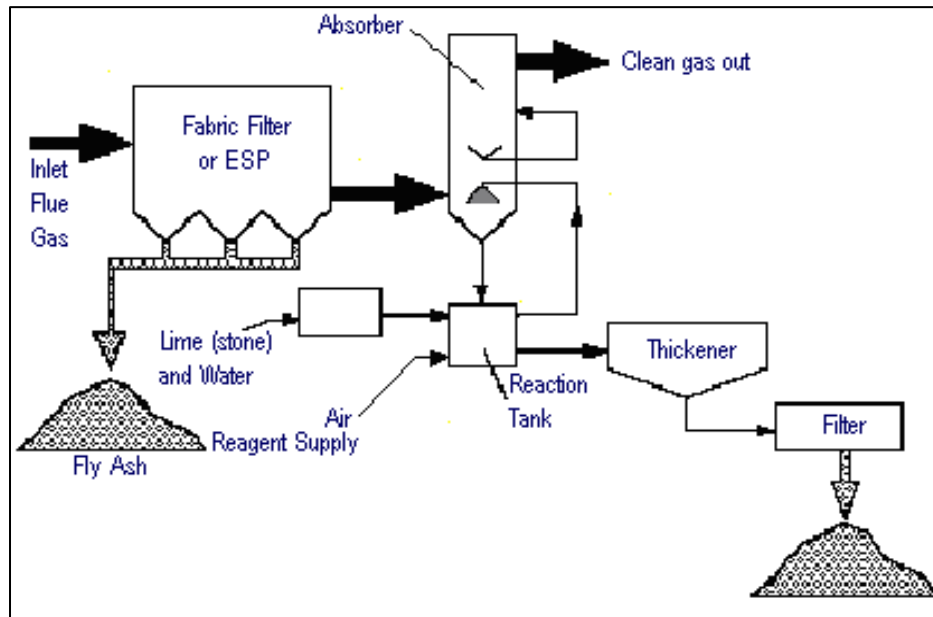


Figure 2. 2: Limestone with Forced Oxidation (LFSO) process (Arcor Epoxy Technologies, 1990)

2.1.2.3) MAGNESIUM ENHANCED LIME (MEL) TECHNIQUE

In the MEL process, slaked lime, containing calcium hydroxide [$\text{Ca}(\text{OH})_2$] and a portion of magnesium hydroxide [$\text{Mg}(\text{OH})_2$], is used to react with SO_2 resulting in the formation of calcium sulfite. As with the LSFO process, the slurry is aerated causing gypsum formation to prevent crystal deposition within the scrubber thus avoiding pipe and nozzle blockage. In this process however, aeration occurs in a separate tank. The slurry is still added to a reaction tank at the bottom of the absorber under pH control to replenish reagent consumed. Overall, SO_2 , which is a strong acid, reacts with and is neutralized by slaked lime.

The soluble magnesium salts greatly increase SO_2 capture and allow reduction in power consumption and equipment costs (Anon., 2003). When $\text{Mg}(\text{OH})_2$ is present in slurry which is in contact with the flue gas, it buffers (prevents from falling sharply) the pH of the slurry as it absorbs acidic SO_2 . This improves absorber performance by increasing solubility of SO_2 in the slurry, which allows operation at a lower L/G ratio. It also allows operation at a lower slurry pH, near 6.0, which improves reagent utilization to near 100% (Anon., 2003). $\text{Mg}(\text{OH})_2$ is not consumed by the absorption process but is replenished by addition of fresh lime slurry to the reaction tank. This provides the MEL flue gas desulfurization processes with a greater capacity to absorb SO_2 , than LSFO.

The magnesium salts also prevent formation of build-ups on surfaces in the absorber. The salts suppress solubility of hard-scale-forming substances like calcium sulfate (Anon., 2003). This further reduces the tendency for calcium sulfate to precipitate on surfaces in the absorber and cause plugging of pipes and nozzles by maintaining the concentration of calcium sulfate in absorber slurry liquid at about 10% of the concentration at which scale would form (Anon., 2003).

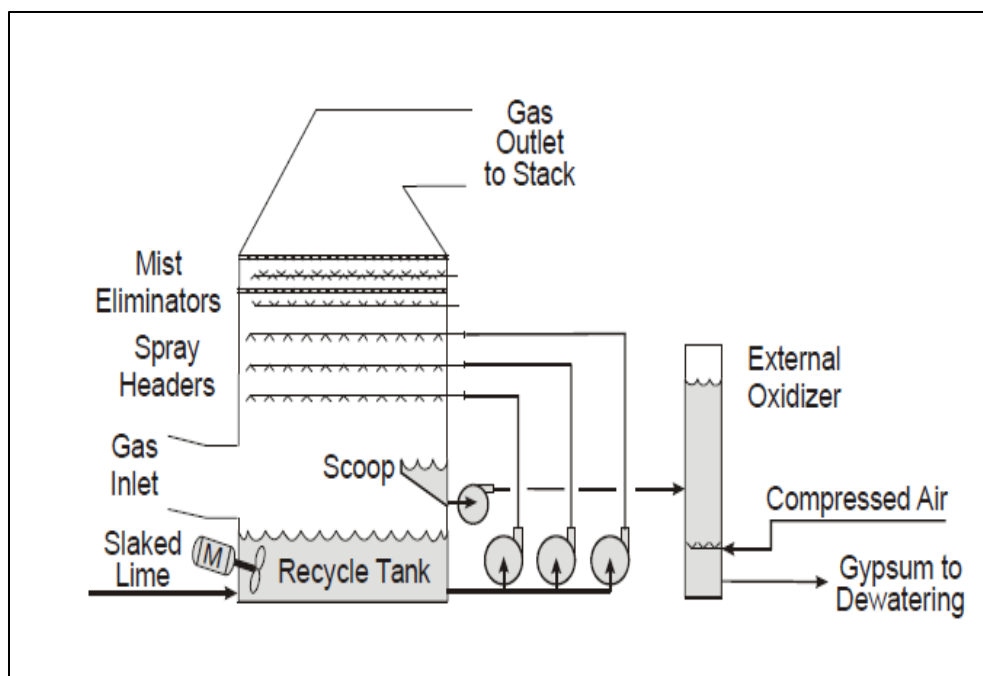


Figure 2. 3: Magnesium Enhanced Lime (MEL) process (Anon., 2003)

2.1.3) ADVANTAGES VS DISADVANTAGES OF WET SCRUBBING

2.1.3.1) ADVANTAGES (SEMARU, 1977)

- Relatively high removal efficiency (90-95%)
- Low cost of operation
- Minimal safety hazards (explosions, fires)
- Collects both gas and particulate matter

2.1.3.2) DISADVANTAGES (SEMARU, 1997)

- Wet waste production (contaminated scrubber liquid)
- Formation of highly corrosive acids
- High capital and operating cost due to the handling of liquid reagent, waste, and high-power requirements

2.1.4) FLUE GAS DESULFURIZATION TECHNOLOGIES: SPRAY-DRY SCRUBBING

Semi-dry systems, or spray dryers, inject an aqueous sorbent slurry, similar to a wet system, however, the slurry in this instance has a higher sorbent concentration. The flue gas may initially pass through an ESP for fly ash pre-collection. This is optional and usually not implemented. The heart of the spray dry system is the rotary atomizer. A Niro rotary atomizer is used to atomize the fresh and recycle feed slurry into a finer (atomized) spray than in wet scrubbing systems (Srivastava & Josewicz, 2001). As the hot untreated flue gas counter-currently mixes with the ‘atomized’ slurry solution, a chemical reaction occurs resulting in the removal of SO₂ together with evaporation of water from the slurry. The water that remains on the solid sorbent enhances the reaction with SO₂. This process forms a dry waste product which is collected with a standard particulate matter collection device such as a baghouse or ESP. The waste product can be disposed, sold as by-product, or alternatively an optional solids recycle system can be implemented to recycle slurry to the absorber. The latter of the three waste treatment methods aids in the reduction of fresh reagent consumption (Babcock & Wilcox, 2002).

Various calcium and sodium-based reagents can be utilized as sorbent. Spray dry scrubbers typically inject lime since it is more reactive than limestone and less expensive than sodium-based reagents. The performance of a lime spray dry scrubber however, is more sensitive to operating conditions. A close approach to adiabatic saturation temperature is required to maximize the removal of SO₂. However, excess moisture causes the wet solids to deposit onto the absorber and downstream equipment hence, fouling of equipment is caused (Srivastava & Josewicz, 2001). The optimum temperature approach is 10°C to 15°C below saturation temperature (Srivastava & Josewicz, 2001). Lower L/G ratios, approximately 1:3, must be utilized due to the limitation on flue gas moisture (Schenelle & Brown, 2002). Flue gas with high SO₂ concentrations or temperatures tend to reduce the performance of the scrubber (Schenelle & Brown, 2002). The ratio of fresh lime slurry to recycle slurry must be controlled to maintain the required level of alkalinity in the feed slurry to achieve the desired level of SO₂ removal. The total amount of slurry fed to the atomizer is also controlled to maintain the desired outlet temperature. SO₂ control efficiencies for spray dry scrubbers are slightly lower than wet systems, between 80% and 90% due to its lower reactivity and L/G ratios (Schenelle & Brown, 2002).

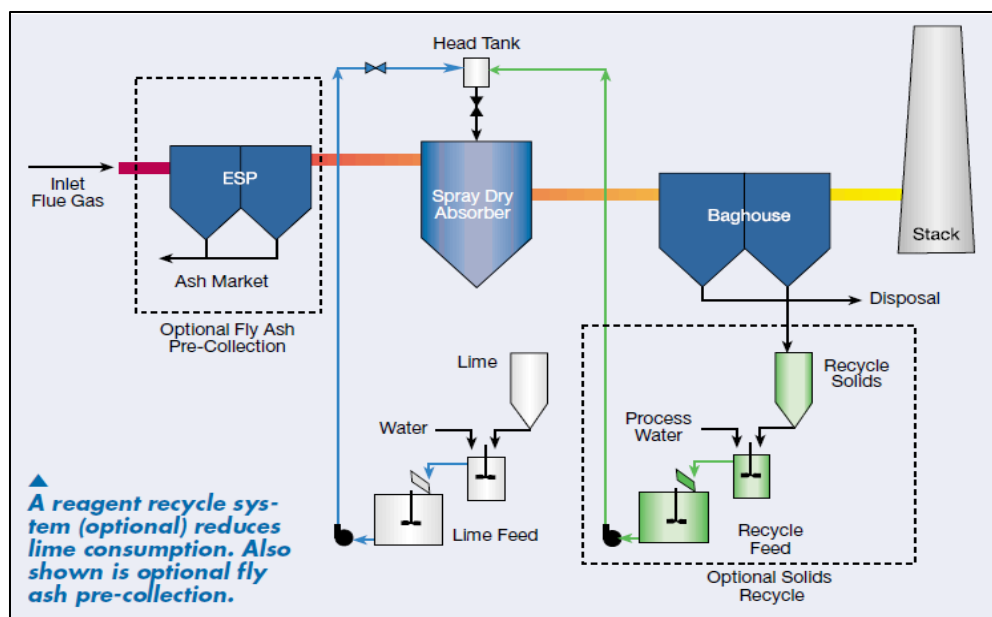


Figure 2. 4: Spray-Dry Scrubbing process (Babcock & Wilcox, 2002)

2.1.5) FLUE GAS DESULFURIZATION TECHNOLOGIES: DRY SORBENT INJECTION

Dry sorbent injection systems pneumatically inject powdered sorbent directly into the furnace, the economizer or downstream ductwork as can be seen in Figures 2.5, 2.6 and 2.7 respectively. The dry waste product is removed using particulate control equipment such as a baghouse or ESP. The flue gas is generally cooled prior to entering the particulate matter control device through use of an air heater. Having removed the dry waste product, the treated gas is sent to stack. The dry waste product may either be disposed of or sent to a reactivation unit for use as recycle sorbent to either the downstream duct (Figure 2.5), upstream furnace (Figure 2.6) or economizer (Figure 2.7).

Furnace injection requires flue gas temperatures between 750°C and 1000°C to decompose the solid sorbent thus promoting increases surface area for reaction (Srivastava & Josewicz, 2001). Injection into the economizer requires temperatures of 500°C and 570°C (Srivastava & Josewicz, 2001). Duct injection requires the dispersion of a fine sorbent spray into the flue gas downstream of the air preheater. The injection must occur at flue gas temperatures between 150°C to 180°C (Joseph & Beachler, 1998).

Dry sorbent systems typically use calcium and sodium based alkaline reagents. In general, the sorbent used is limestone (CaCO_3) which needs additional humidification that is not required when a (more reactive) sodium-based sorbent is used, such as sodium bicarbonate (NaHCO_3) and sodium sesquicarbonate (trona) (Anon., 2002). Limestone is preferred due to its availability and cheap cost price (Nolan, 2000). Improved activation of the limestone sorbent however can be obtained by feeding water into the duct downstream of the point where the actual sorbent is fed (which reactivates the unreacted sorbent that is still in the flue gas) (Zevenhoven & Kilpinen, 2001). This can be seen in Figures 2.5, 2.6 and 2.7. The unreacted limestone will be converted to calcium hydroxide $\text{Ca}(\text{OH})_2$ which is known to be more reactive to SO_2 (Srivastava & Josewicz, 2001).

An even distribution of sorbent across the reactor and adequate residence time at the proper temperature are critical for high SO_2 removal rates (Srivastava & Josewicz, 2001). Another important process parameter is the so-called approach temperature, which is how far the gas temperature is above the saturation temperature for the water in the gas. With a lower approach temperature, more time is needed for water evaporation, resulting in a higher sulfur uptake by the sorbent (Ciemat, 1998). The optimal flue gas temperature range of 10°C to 15°C below its saturation temperature is to be maintained for optimal sulfur uptake while minimizing deposits on the absorber and downstream equipment by condensation (Srivastava & Josewicz, 2001).

Dry sorbent systems have significantly lower capital and annual costs than wet systems because they are simpler, demand less water and waste disposal is less complex (Anon., 2002). Dry injection systems also install easily and use less space; therefore, they are good candidates for retrofit applications (Anon., 2002). SO₂ removal efficiencies however are significantly lower than wet systems, between 50% and 70% for calcium-based sorbents (Srivastava & Josewicz, 2001). Sodium based dry sorbent injection into the duct however can achieve up to 80% removal efficiency (Srivastava & Josewicz, 2001). It should also be noted that low temperature in-duct sorbent injection achieves a lower removal efficiency (50% -60%) as compared to the higher temperature furnace and economizer sorbent injection systems (65% - 75%) (Srivastava & Josewicz, 2001).

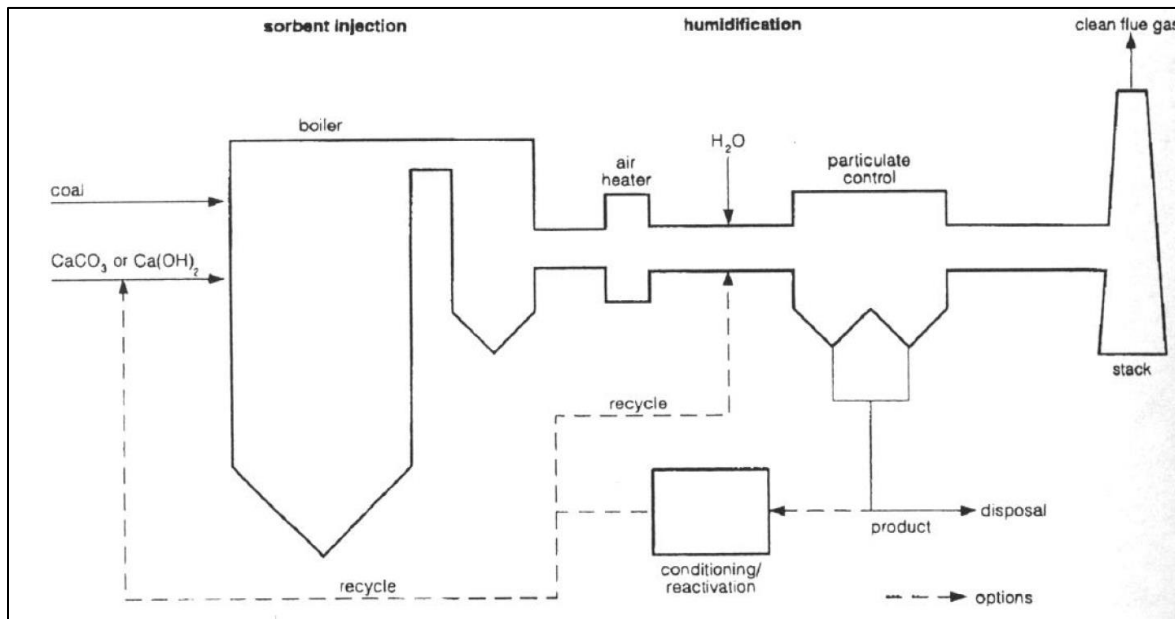


Figure 2. 5: High temperature furnace sorbent injection (Zevenhoven & Kilpinen, 2001)

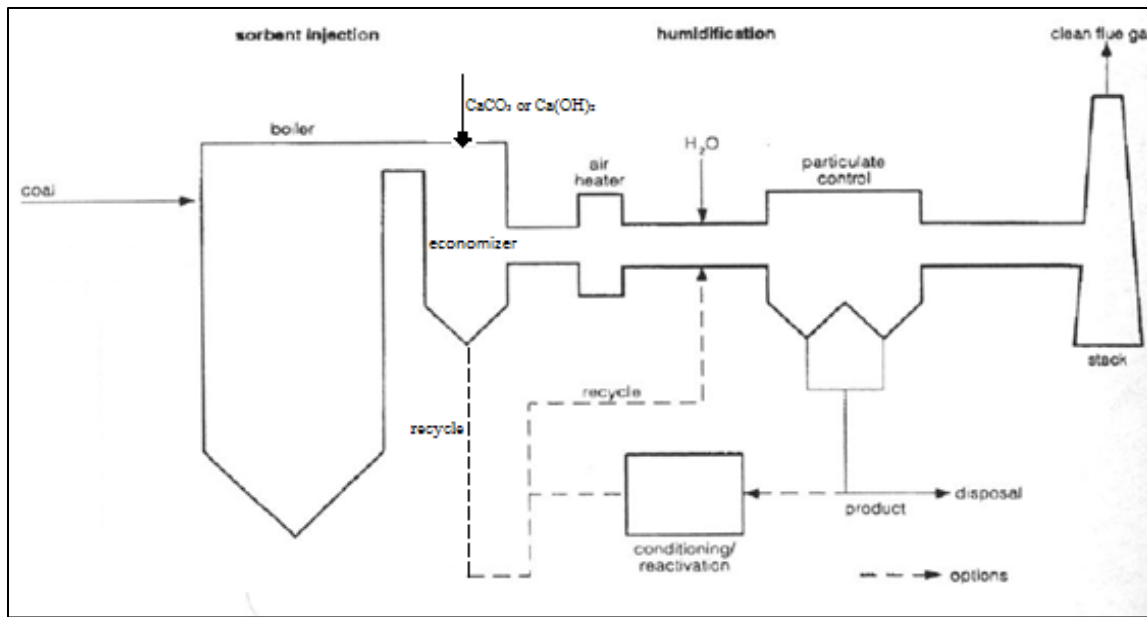


Figure 2. 6: Moderate temperature economizer sorbent injection (Zevenhoven & Kilpinen, 2001)

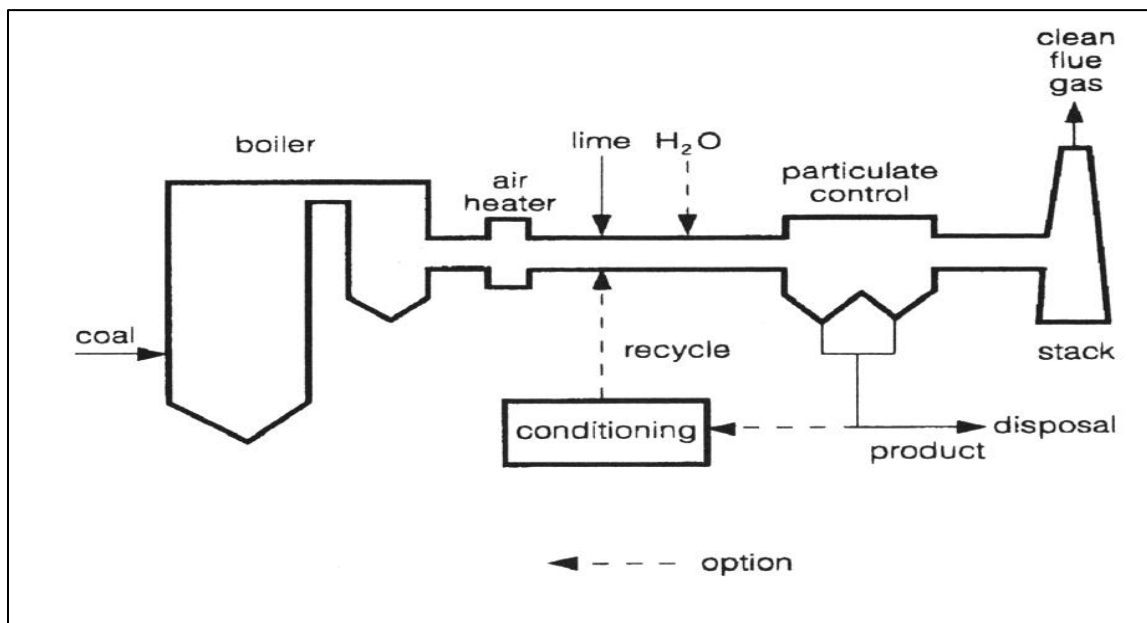


Figure 2. 7: In-Duct sorbent injection at low temperatures (Zevenhoven & Kilpinen, 2001)

2.1.6) FLUE GAS DESULFURIZATION TECHNOLOGIES: ADVANCED TECHNOLOGY (WSA & SNOX PROCESSES)

Table 2. 1: Reaction schemes for WSA & SNOX processes (Laursen, 2007)

Combustion	$\text{H}_2\text{S} + \frac{3}{2}\text{O}_2 \rightarrow \text{H}_2\text{O} + \text{SO}_2 + 518 \text{ kJ/mole}$
Oxidation	$\text{SO}_2 + \frac{1}{2}\text{O}_2 \rightarrow \text{SO}_3 + 99 \text{ kJ/mole}$
Hydration	$\text{SO}_3 + \text{H}_2\text{O} \rightarrow \text{H}_2\text{SO}_4(\text{gas}) + 101 \text{ kJ/mole}$
Condensation	$\text{H}_2\text{SO}_4(\text{gas}) + 0.17\text{H}_2\text{O}(\text{gas}) \rightarrow \text{H}_2\text{SO}_4(\text{liq.}) + 69 \text{ kJ/mole}$
DENOX	$\text{NO} + \text{NH}_3 + \frac{1}{4}\text{O}_2 \rightarrow \text{N}_2 + \frac{3}{2}\text{H}_2\text{O} + 410 \text{ kJ/mole}$

2.1.6.1) WET SULFURIC ACID (WSA) PROCESS

The WSA process is a proprietary development by Haldor Topsoe A/S. Since its introduction in the 1980s, it has been recognized as an efficient process for recovering sulfur from various process gases in the form of commercial quality sulfuric acid (H_2SO_4). The WSA process has found widespread application in the metallurgical, steel (coking plants), power and cellulose industries, however majority of applications are within the refinery and petrochemical industry.

The process principal involves four major processes. These processes remain the same for the various feed gases that are applicable to the WSA technique (Figure 2.8):

- 1) Heating/Cooling of gas to reactor temperature
- 2) Conversion of SO_2 to SO_3
- 3) Hydration of SO_3 to H_2SO_4
- 4) Condensation to liquid H_2SO_4 in the WSA condenser

The feed gas is incinerated to SO_2 in a burner ('Combustion' reaction in Table 2.1) followed by a waste heat boiler. The incinerated gas typically contains 5 to 6% SO_2 (Laursen, 2007). The gas leaving the waste heat boiler will have a temperature of approximately 400°C (Laursen, 2007). The gas then enters the SO_2 reactor, which will contain one, two or three catalytic beds, depending on the process conditions and actual degree of conversion ('Oxidation' reaction in Table 2.1). Since the reaction is exothermal, the gas is cooled between the beds to optimize the SO_3/SO_2 equilibrium. After the last conversion stage, the gas is cooled

and the SO₃ will react with the water vapor present from combustion to form gas phase sulfuric acid ('Hydration' reaction in Table 2.1). The process gas then goes to the WSA condenser, where final hydration and condensation of the acid takes place ('Condensation' reaction in Table 2.1).

The WSA condenser (Figure 2.9) is a vertical shell and tube type falling film condenser/concentrator with tubes made of shock and acid resistant boron silicate glass. The process gas flows inside the tubes, which are cooled on the outside by ambient air in crosscurrent flow pattern. Sulfuric acid condenses in the tubes and flows downwards while being concentrated in countercurrent contact with the hot process gas. The sulfuric acid is collected in the acid resistant brick lined bottoms part and is cooled to 30°C - 40°C in a water-cooled plate type heat exchanger and then pumped to storage (Laursen, 2007). The cleaned process gas leaves the WSA at approximately 100°C and can be sent directly to stack (Laursen, 2007). The cooling air will leave the WSA condenser at approximately 200°C - 250°C (Laursen, 2007). Part of the hot air is used as combustion air in the incinerator, and the remaining part can be mixed into the stack or used for boiler feed water preheating.

The heat of reaction is recovered in the form of steam. Saturated steam at approximately 50-60 bar gauge is generated in the waste heat boiler and in the gas cooler downstream of the SO₂ reactor (Laursen, 2007). Saturated steam drawn from the steam drum is then used for cooling between the catalytic reactor stages and is exported as superheated steam at > 440°C, or it can be conditioned to other properties. The required steam pressure is determined by the content of sulfur and water in the process gas so that all surface temperatures are well above the acid dewpoint.

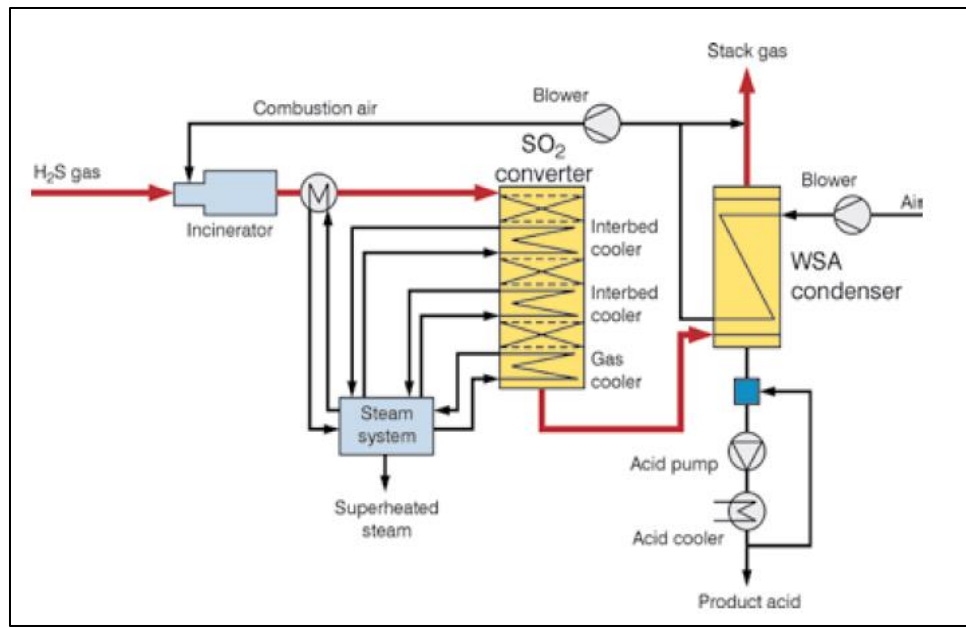


Figure 2. 8: Process flow diagram for WSA plant (Laursen, 2007)

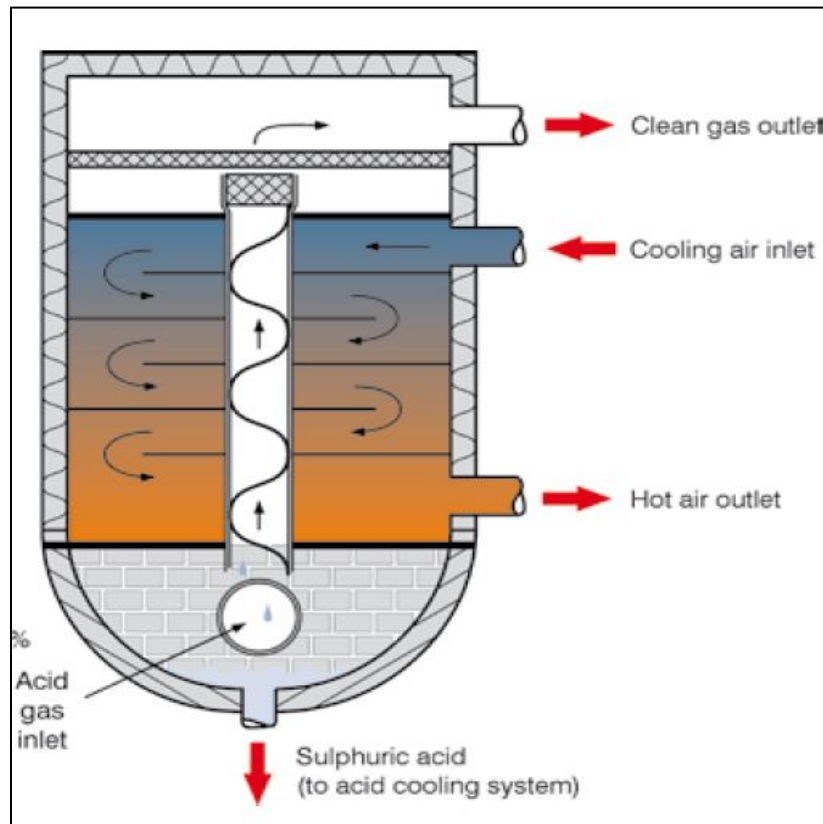


Figure 2. 9: WSA Condenser (Laursen, 2007)

2.1.6.2) SNOX PROCESS

The SNOX process is a process which removes sulfur dioxide (SO_2), nitrogen oxides (NO_x) and particulates from flue gases. The sulfur is recovered as concentrated sulfuric acid (H_2SO_4) and the nitrogen oxides are reduced to free nitrogen (N_2). When the feed gas contains appreciable amounts of ammonia (NH_3), hydrogen cyanide (HCN) or other nitrogen compounds, or if the incineration takes place at elevated temperatures, nitrogen oxides will be formed. To comply with statutory requirements, it is necessary to remove these nitrogen oxides.

The SNOX process is nearly identical to the WSA process discussed above with the addition of a selective catalytic reduction (SCR) stage upstream of the SO_2 reactor. The process principal thus involves the four major processes mentioned above for the WSA technique, in addition to the SCR reduction stage. Like the WSA technique, these processes remain the same irrespective of various feed gases implemented:

- 1) Heating/Cooling of gas to reactor temperature
- 2) Catalytic reduction of NO_x by adding NH_3 to the gas upstream the SCR DeNO_x reactor
- 3) Conversion of SO_2 to SO_3
- 4) Hydration of SO_3 to H_2SO_4
- 5) Condensation to liquid H_2SO_4 in the WSA condenser

With processes one, three, four and five being identical to the WSA technique, process two is the defining process which separates the SNOX technique from that of the WSA technique. The SCR stage is located upstream of the SO_2 reactor. Ammonia in stoichiometric amounts relative to the nitrogen oxide content is injected into the process gas, which passes over the SCR catalyst (usually vanadium oxide) whereby the nitrogen oxides are reduced to water and nitrogen ('DENOX' reaction in Table 2.1.). A particulate matter collection device such as a baghouse may also be located upstream of the SCR stage for removal of such particles.

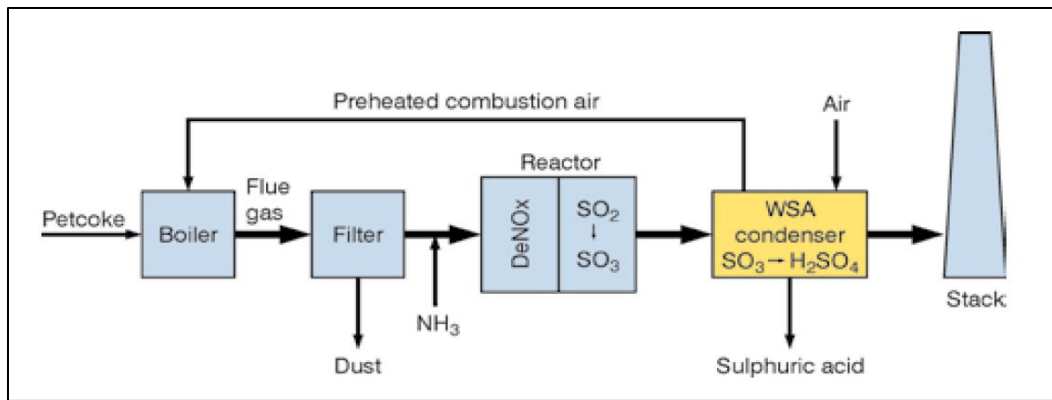


Figure 2. 10: Process flow diagram for SNOX plant (Laursen, 2007)

2.1.7) ADVANTAGES OF THE WSA & SNOX PROCESSES (LAURSEN, 2007)

- More than 99% recovery of the total sulfur content, always in compliance with environmental legislation
- Product is clean, concentrated sulfuric acid of commercial quality, also in turn down situations
- Heat of reaction is recovered as superheated or saturated steam
- Optional DeNO_x for gases with high content of NH₃ and HCN
- Gases containing hydrocarbons and with very high CO₂ content are accepted
- No consumption of chemical reagents
- Very low consumption of cooling water
- No consumption of process water
- No liquid or solid waste effluents
- Simple layout, simple operation, overall attractive economy
- Recycling of hot combustion air to the boilers in combination with high pressure steam production in the WSA & SNOX plants increase the thermal efficiency and output of the boilers, resulting in a proportional reduction in CO₂ emission

Of significant importance above is the > 99% recovery of sulfur from the untreated gas. This surpasses the removal efficiency of all the other techniques previously discussed rendering the WSA and SNOX processes as the most efficient in terms of SO₂ removal. While these processes may require lower capital investment, they are significantly more expensive to operate and maintain in comparison to those that have been previously discussed hence they are not as commonly employed in industry for flue gas desulfurization in power plants, which is the focus of this study (Nolan, 2000).

2.2) SULFUR TRIOXIDE (SO_3) MEASUREMENT TECHNIQUES

Combustion sources which contain sulfur impurities tend to produce sulfur compounds such as SO_2 , which further oxidizes to SO_3 , as these fuels are burned (Jaworowski & Mack, 1979). The SO_3 in turn reacts with water vapor present in the flue gas, according to Equation 2.1.



Thus, when SO_3 measurements are discussed, these typically refer to the measurement of H_2SO_4 . The formation of H_2SO_4 can have detrimental effects when the gas reaches its dew point. Condensation of H_2SO_4 which can be highly concentrated results in severe corrosion of operating equipment (Jaworowski & Mack, 1979).

It is expected that preventing the condensation of H_2SO_4 by maintaining a temperature above that of the flue gas dew point temperature will relieve the process of such adverse effects related to corrosion. The issue with predicting the dew point of flue gases however is that the dew point depends on both the partial pressure of water vapor and the partial pressure of H_2SO_4 (IAPWS , 2012). The major problems with respect to current prediction methods on the dew points of flue gas have been summarised by the IAPWS (2012) as follows:

- Dew-point equations with experimental data for several flue gas compositions exist, but there are significant discrepancies among the results.
- Concentration of H_2SO_4 depends on the SO_3 conversion rate and on the surface temperature of the wall. Therefore, it is important to attempt to control SO_3 content and to predict precisely local surface temperatures.
- Reliability of dew-point estimation depends not only on the equation but also on the temperature measurement uncertainty such as an accuracy of duct surface temperature distribution. A precise measuring method is necessary.

Therefore, the above considerations must be accounted for when measuring SO_3 concentrations from measured flue gas acid-dew point temperatures.

There are however several other techniques available to measure SO₃ concentrations, that are currently in use. According to Flieg, et al. (2012) however, these methods do have limitations due to the highly reactive nature of SO₃ and various other hindering factors. These hindering factors include (Flied, et al., 2012):

- Comparatively low concentrations of SO₃ under typical conditions.
- High SO₂ concentrations constituting an interference factor.
- Surface reactions in the sampling line.
- Condensing H₂SO₄ at temperatures below saturation.
- Losses of gaseous SO₃/H₂SO₄ by surface reactions before the measurement.

The main techniques used to measure SO₃ which are based on adsorption and absorption of SO₃, followed by sulfate analysis, include:

- Controlled condensation method
- Isopropanol absorption bottle method
- Salt method
- Pentol SO₃ monitor

2.2.1) CONTROLLED CONDENSATION METHOD

The controlled condensation method (CCM) is based on the condensation of sulfuric acid in the flue gas by cooling the flue gas between the acid dew point and water dew point. The condensation of sulfuric acid takes place on the walls of the condenser and the capillary glass filter. Thereafter a sulfate analysis can be conducted using ion chromatography. CCM is a widely accepted method for SO₃ analysis. (Flied, et al., 2012).

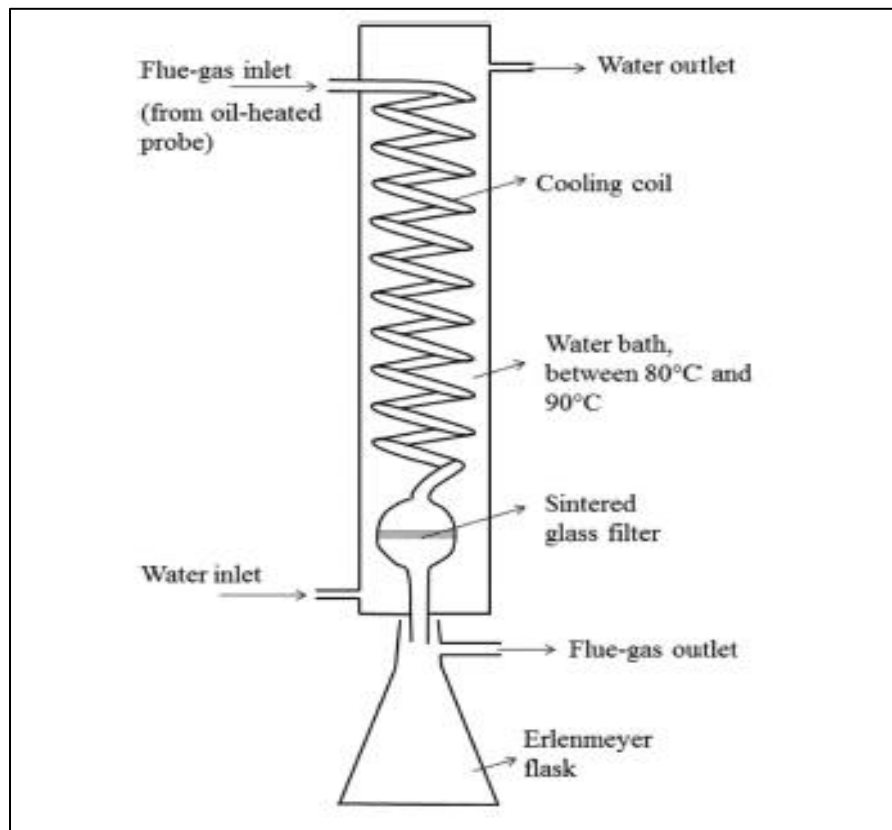


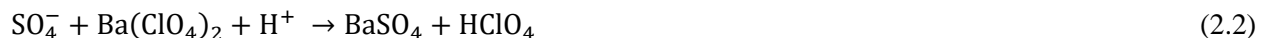
Figure 2. 11: Schematic of glass cooler utilized in controlled condensation method (Flied, et al., 2012)

2.2.2) ISOPROPANOL ABSORPTION BOTTLE METHOD

The isopropanol absorption method is based on the absorption of sulfate ions in solution. A train of interconnected dreschel bottles are set in series through which the flue gas bubbles. From Figure 2.12, the initial dreschel bottle is filled with approximately 100ml of 80% (vol) isopropanol (IPA) solution to absorb SO₃, in the form of H₂SO₄ (Jaworowski & Mack, 1979). Thereafter the flue gas passes through two more dreschel bottles filled with 100 mL of 3% (vol) H₂O₂ solution to absorb the remaining SO₂, and, finally, through a bottle with silica gel for gas drying (Jaworowski & Mack, 1979). The bottles are submerged in an ice bath to ensure that sulfuric acid vapor condenses into the IPA solution (Jaworowski & Mack, 1979). Lastly, argon (Ar) is bubbled through the IPA solution to remove possible SO₂ that may have absorbed into solution (Frieg, et al., 2012). Following this a sulfate analysis is conducted through titration.

The IPA solution is titrated against a barium perchlorate solution and thoron is used as an indicator. As the flue gas is bubbled through the IPA solution, the sulfuric acid condensate immediately dissociates into sulfate ions. These sulfate ions react with the barium ions during the titration to from barium sulfate. Hence by using appropriate molar ratios, the amount of sulfate ions can be determined and as a result, the amount of sulfur in the solution can be calculated (Jaworowski & Mack, 1979).

The following reaction governs the titration (Jaworowski & Mack, 1979):



The main problem with all isopropanol methods is the absorption of SO₂ into solution which gives a positive bias if the SO₂ is oxidized to sulfate ions in the IPA solution. This however can be avoided by reducing measurement time and bubbling an inert gas such as argon through the solution to avoid SO₂ oxidation as mentioned above (Frieg, et al., 2012).

A typical experimental set up is shown in Figure 2.12, however modifications to this set up are possible depending on the type of system used.

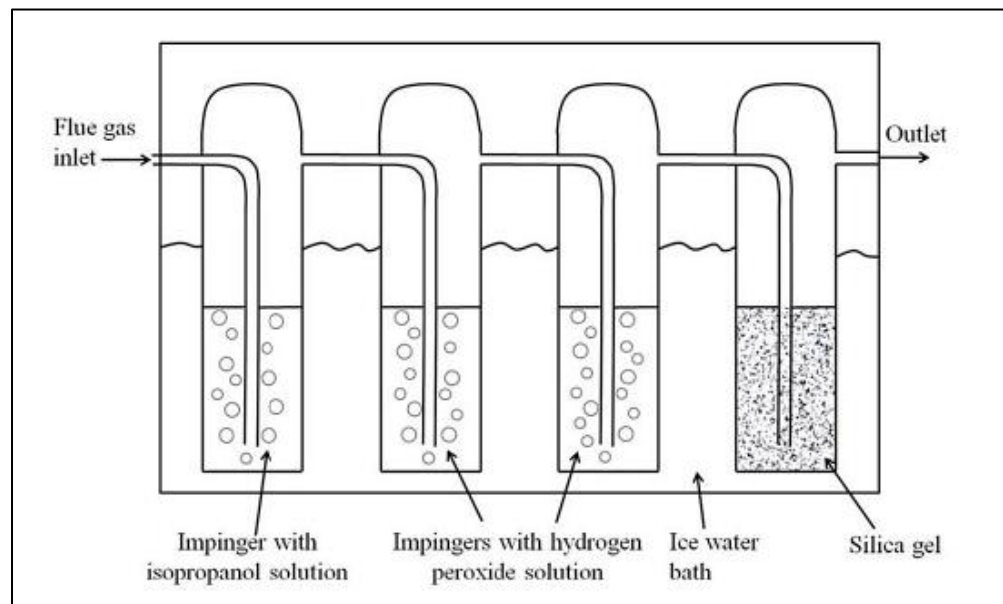


Figure 2. 12: Measurement setup of the isopropanol absorption bottle method (Flied, et al., 2012)

2.2.3) SALT METHOD

The salt method is conducted by allowing the flue gas to pass through a bed of sodium chloride (NaCl). It must be noted that as the flue gas passes through the salt bed, the temperature of the flue gas is kept above its acid dew point. Thereafter the sulfuric acid vapor within the flue gas reacts with the sodium chloride to form sodium bisulfate (NaHSO_4) and sodium sulfate (Na_2SO_4) according to Equations 2.3 & 2.4. (Frieg, et al., 2012).



The formed salts are dissolved in deionized water and the sulfate ion content is analyzed through ion chromatography or by titration.

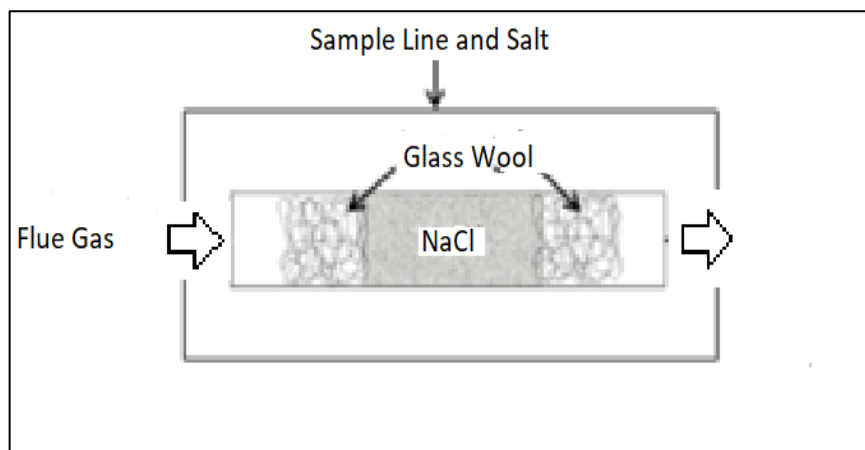


Figure 2. 13: Measurement setup for the salt method (Frieg, et al., 2012)

2.2.4) PENTOL SO₃ MONITOR

The pentol SO₃ method is used for continuous measurement of SO₃ concentration in flue gas. The pentol SO₃ monitor uses an automatized set up analysis. An IPA solution is used and is continuously treated with barium chloranilate. Thereafter a photometer is used to continuously measure the absorption of the light absorbed by the acid chloranilate ions. The higher the absorption reading on the photometer, the higher the amount of sulfate ions absorbed. Hence the amount of SO₃ can be determined since the amount of sulfate in the solution is proportional to the SO₃ concentration in the flue gas. (Frieg, et al., 2012).

2.3) CONVERSION OF SO₂ TO SO₃ AT ELEVATED TEMPERATURE

The conversion of sulfur dioxide (SO₂) to sulfur trioxide (SO₃) has significant environmental implications associated with the combustion of fossil fuels such as coal. The presence of such sulfur emissions (SO_x) in the air results in the formation of photochemical smog and acid rain.

The general formation of SO₂ occurs as a result of simultaneous decomposition and oxidation of inorganic sulfur found in combustion fuels. Thereafter, SO₂ is converted to SO₃ through either homogenous gas-phase reactions or heterogeneous catalytic reactions (Belo, et al., 2014).

The governing homogenous reaction is represented by Equation 2.5.



There is very limited data available on high temperature kinetics for the homogenous reaction of SO₂ to SO₃ in the presence of oxygen (in-bed reaction) since the reaction mechanisms and kinetics associated with the conversion are not fully understood (Smith, et al., 1982). However, the major factors which effect the homogenous conversion of SO₂ to SO₃ at elevated temperatures can be summarized as follows (Belo, et al., 2014):

- SO₂ partial pressure
- O₂ partial pressure
- Moisture content
- Presence of catalytically active components
- Temperature-residence time profile of the plant

According to Belo, et al. (2014), for uncatalyzed (homogenous) conversions of SO₂ to SO₃:

- The effect of O₂ concentration on the conversion of SO₂ to SO₃ only has an influence for concentrations of 3–10% (vol)
- The oxidation of SO₂ is independent of the water vapor content in the flue gas
- Temperatures of at least 900°C are required to see a significant conversion of SO₂ to SO₃.

Belo, et al. (2014) developed Equation 2.6 which accounts for the temperature dependence of the pressure-based equilibrium constant that limits conversion of SO₂ to SO₃, as per Equation 2.5.

$$K_p = 1.53 \times 10^{-5} \exp\left(\frac{11760}{T}\right) \quad (2.6)$$

Where: K_p = Pressure-based equilibrium constant [atm^{-0.5}]

T = Reaction temperature [K]

Based on derivation from first principals, the pressure-based equilibrium constant can further be related to equilibrium conversion (a function of gas phase partial pressures) by Equation 2.7 (Lokhat, 2015).

$$K_p = K_{eq} = \frac{4 X_{eq} (1.5 - 0.5 X_{eq})^{0.5}}{(1 - X_{eq})^{1.5} P^{0.5}} \quad (2.7)$$

Where: K_p = Pressure-based equilibrium constant [atm^{-0.5}]

X_{eq} = Equilibrium conversion [Dimensionless]

P = System pressure [atm]

Table 2. 2: Equilibrium constant and equilibrium conversion at elevated reactor operating temperatures

Operating Temperature - [T] (K)	Operating Pressure - [P] (atm)	K _{eq} (atm ^{-0.5})	X _{eq}
973.15	1	2.71	0.32
1073.15	1	0.88	0.15
1173.15	1	0.35	0.07

As seen from Table 2.2, practically attainable conversions are limited to 32% and 7% at operating temperatures of 700°C and 900°C respectively. Additionally, an increase in operating temperature promotes the reverse reaction, as per Equation 2.5, thus further inhibiting SO₃ formation.

Hamer (1986) performed experiments investigating the formation of SO₃ in a stainless-steel reactor utilized as a bubbling Fluidized Bed Combustor (FBC). For an inlet SO₂ concentration of 2800 ppmv, it was found that 300 ppmv of SO₃ was present at the reactor outlet however, the formation of SO₃ in the bed itself (regardless of the sorbent utilized) is negligible. This indicates that SO₂, in the presence of stainless steel, is heterogeneously catalyzed to form SO₃.

2.4) LIMESTONE PROPERTIES: THE EFFECT ON DESULFURIZATION

2.4.1) SURFACE PROPERTIES

Desulfurization technologies at high temperatures are receiving attention owing to their higher thermal efficiency and major reduction in capital costs. Calcium-based sorbents, such as limestone, are prime candidates for in bed capture of sulfur from flue gas at such high temperatures (Nolan, 2000). As a desulfurization agent, calcium-based sorbents have been traditionally used in coal combustion processes, even at lower to moderate temperatures. Calcium carbonate (limestone) is very common in nature and used in the building industry as well as the chemical industry. It has been used as the cheapest sorbent in flue gas desulfurization processes since the mid-20th century. Being the main component of limestone, calcium carbonate can be used in a dry powered form (dry desulfurization) or as a wet slurry.

For high temperature flue gas desulfurization, limestone is used in the form of crushed white powder that is irregular in shape. Chan, et al. (1970) states that limestone particles between the size range of 79 μm -149 μm ensures that the sulfur contained in the fuel is effectively oxidized and subsequently absorbed by the limestone in a high temperature dry-state reaction.

According to Dasgupta, et al. (2003), the SO₂ sorption by limestone sorbent at high temperatures (700⁰C-1100⁰C) takes place through two reaction steps: 1) calcination (decomposition) of the sorbent calcium carbonate (CaCO₃) having small surface area to produce porous calcium oxide (CaO) having significantly larger surface area and porosity; and 2) reaction of SO₂ with CaO in the presence of oxygen to form the higher molar volume solid product, calcium sulfate (CaSO₄).



The formation of CaSO₄ reduces the available internal surface area of CaO thus hindering the reaction represented in Equation 2.9 until the limestone is spent. The CaSO₄ produced effects the reaction in two ways. Firstly, CaSO₄ covers the fresh CaO surface and blocks the passage between CaO and the gas; secondly, volumetric expansion upon conversion results in plugging of the pores in the CaO. As a result, the passages between the sorbent and the flue gas becomes blocked. Hence, pore-plugging and the consequent loss of porosity of the particle are the dominant causes of premature termination and incomplete utilization of the sorbent (Dasgupta, et al., 2003).

As mentioned, Equation 2.8 represents the limestone decomposition reaction. This reaction is influenced not only by temperature but also the equilibrium CO₂ partial pressure. Figure 2.14 represents the change in limestone decomposition rate with varying CO₂ partial pressures.

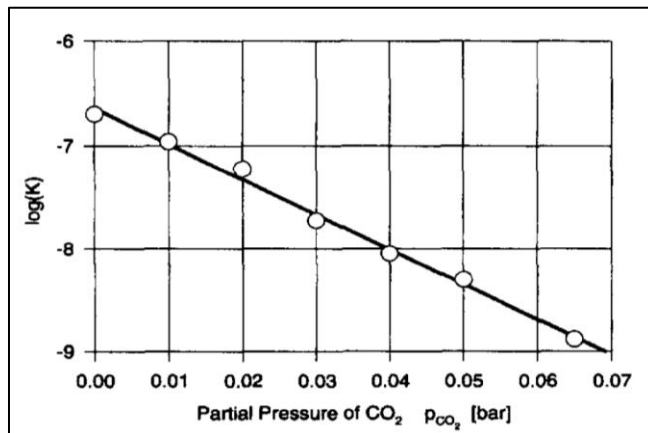


Figure 2. 14: Influence of CO₂ partial pressure on reaction rate (Khinast, et al., 1996)

Figure 2.14 indicates that greater CO₂ partial pressures tend to inhibit the limestone decomposition rate (calcination rate). This in turn affects the temperature at which limestone decomposition occurs since the decomposition rate is inherently related to reaction temperature through an Arrhenius type rate expression (Khinast, et al., 1996). According to Khinast et. al. (1996), greater CO₂ partial pressures demand a higher reaction temperature to promote limestone decomposition, as per Equation 2.8.

2.4.2) IMPURITIES

According to Chang, et al.(1998), mineral components of coal and impurities of limestone can affect the capacity of sulfur capture during combustion. The effect of limestone accompanying impurities such as Al₂O₃, SiO₂, Fe₂O₃ and MgCO₃ on limestone desulfurization during coal gasification is promotive while MgCl₂ and NaOH is negative. The promotive roles of impurities at higher temperatures are important and can often have a positive influence on attainable conversions of CaO to CaSO₄ as well as affect the decomposition temperatures of CaCO₃ or CaSO₄. The negative role of impurities in sulfur capture can change the limestone decomposition course and form compounds of unknown structure which can restrain CaO and CaSO₄ decomposition (Chang, et al., 1998)

2.5) LIMESTONE SORPTION CAPACITY

Montes, et al. (2012) defines the sorption capacity of limestone sorbent as the mass of SO₂ removed in milligrams, per gram of sorbent (X/M) and is calculated by integration of the area below the breakthrough curve, from the SO₂ concentration in the inlet gas, the flue gas flow rate and the saturation time.

$$\frac{X}{M} = \frac{Q \times MW_{SO_2}}{W \times V_m} (C_0 t_{sat} - \int_0^{t_{sat}} C(t) dt) \quad (2.10)$$

Where:

Q - Inlet flow rate ($\frac{m^3}{s}$)

MW - Molecular weight of SO₂ ($\frac{g}{mol}$)

W - Mass of sorbent used (g)

V_m - Molar gas volume ($\frac{cm^3}{mmol}$)

C₀ - Inlet concentration of SO₂ (ppmv)

C(t) - Outlet concentration of SO₂ (ppmv)

t_{sat} - Saturation time (s)

$\int_0^{t_{sat}} C(t) dt$ - A definite integral of the area below the breakthrough curve with a range between the initial time (t = 0s) and the saturation time (t_{sat}).

2.6) BREAKTHROUGH & BREAKTHROUGH TIME; SATURATION TIME; NOMALITY; SO₃ MOLAR YIELD AND DESULFURIZATION RATIO

2.6.1) BREAKTHROUGH & BREAKTHROUGH TIME

Breakthrough refers to the response of an initially clean bed (i.e. free of reacting species) to an influent containing reacting species (Dasgupta, et al., 2003).

For a typical experiment in this study, the reactor bed initially consisting of limestone sorbent is heated to the experimental reaction temperature. A gaseous mixture containing the reactive gas (SO₂ in this instance) of a specific concentration, is fed at a constant flow rate. During the initial stage of the sorption reaction, most of the SO₂ entering the bed is removed by chemical reaction. At this stage, no SO₂ or a very small concentration of SO₂ is observed in the reactor outlet. A product layer of CaSO₄ is expected to gradually form, which offers resistance to the diffusion of SO₂ through the pores, thereby preventing it from reacting with the limestone sorbent. This resistance progressively increases until diffusion of SO₂ terminates, implying that the overall sorption process is completed. Under the prevailing condition, the concentration of SO₂ at the reactor outlet becomes equal to that at the inlet. This transient behaviour in concentration is called ‘breakthrough’ and the corresponding concentration vs. time response is called a ‘breakthrough curve’ (Dasgupta, et al., 2003).

According to EU Communities (2001), a maximum concentration limit of $50 \frac{\text{mg}}{\text{Nm}^3}$ SO₂ is to be satisfied for any gas stream containing SO₂, which is intended to be vented to atmosphere. This is considered as environmentally acceptable.

‘Breakthrough Time’ in this study is therefore defined as the time taken to observe a $50 \frac{\text{mg}}{\text{Nm}^3}$ SO₂ concentration at the reactor outlet.

2.6.2) SATURATION TIME

Saturation time refers time taken for the outlet concentration of SO₂ to reach the initial inlet concentration of SO₂ i.e. the time taken for the sorbent-gas reaction to reach completion (Dasgupta, et al., 2003).

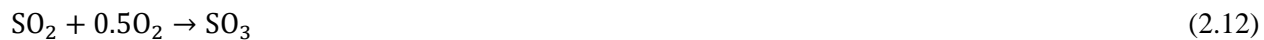
For experiments performed in this study, an average inlet concentration was quantified. The saturation time is therefore represented as the time taken for the outlet concentration of SO₂ to reach the initial average inlet concentration of SO₂.

2.6.3) SO₃ MOLAR YIELD

According to (Felder & Rousseau, 2005), Molar yield is defined as:

$$\text{Molar Yield} = \frac{\text{Moles of Desired Product Formed}}{\text{moles of desired product that would have been formed with no side reactions and the limiting reactant reacting completely}} \quad (2.11)$$

In this study, conversion of SO₂ to SO₃ is the desired reaction:



Thus, the SO₃ Molar yield is defined as:

$$\text{SO}_3 \text{ Molar Yield} = \frac{\text{Moles SO}_3 \text{ Produced}}{\text{Moles SO}_2 \text{ Entering system}} \quad (2.13)$$

2.6.4) DESULFURIZATION RATIO

The Desulfurization Ratio is defined by the author as the ratio of the actual degree of desulfurization to the apparent degree of desulfurization that occurs. It is used to numerically inspect the amount of sulfur entering the system that is converted to SO₃, on a **mass basis**.

$$\text{Desulfurization Ratio} = \frac{S_{\text{in}} - S_{2\text{out}}}{S_{\text{in}} - S_{1\text{out}}} \quad (2.14)$$

Where:

S_{in} = Inlet/Initial Sulfur mass from SO₂+SO₃ (grams)

S_{1out} = Outlet Sulfur mass from SO₂ (grams)

S_{2out} = Outlet Sulfur mass from SO₂+SO₃ (grams)

2.7) STATISTICAL ANALYSIS

2.7.1) ABSOLUTE UNCERTAINTY

The absolute uncertainty, usually called absolute error, is the size of the range of values in which the ‘true value’ of the measurement most likely lies (Harris, 2015). Absolute uncertainty is calculated utilizing the following equation:

$$\text{Absolute Uncertainty} = |\text{Measured/Observed Value} - \text{Predicted Value}| \quad (2.15)$$

The unit of measurement is equivalent to measured/observed value.

2.7.2) RELATIVE UNCERTAINTY

Relative uncertainty is the ratio of the absolute uncertainty of a measurement to the actual measured/observed value i.e.: it expresses the relative size of the absolute uncertainty of a measurement (Harris, 2015).

$$\text{Relative Uncertainty} = \frac{|\text{Measured/Observed Value} - \text{Predicted Value}|}{\text{Measured/Observed Value}} \quad (2.16)$$

The unit of measurement is dimensionless.

Symbolically, if ΔX is the absolute uncertainty in a measurement X , then the relative uncertainty in X , S_x , is:

$$S_x = \frac{\Delta X}{X} \quad (2.17)$$

The percentage in relative uncertainty is calculated as:

$$\% \text{ Relative Uncertainty} = \frac{|\text{Measured}/\text{Observed Value} - \text{Predicted Value}|}{\text{Measured}/\text{Observed Value}} \times 100 \quad (2.18)$$

2.7.3) AVERAGE RELATIVE UNCERTAINTY

An average of relative uncertainties can be calculated as (Harris, 2015):

$$\text{Average relative uncertainty} = \frac{\sum(\text{relative uncertainty})}{n} \quad (2.19)$$

Where: n = number of data points/measured-values

2.7.4) PROPAGATION UNCERTAINTY

The variable of interest in an experiment is rarely obtained by measurement of that variable directly. It is often dependent on the measurement of other variables which have associated with them a certain degree of error. This degree of error or uncertainty consequently propagates due to further calculation in an attempt to evaluate the variable of interest.

According to Harris (2015), if variables (a, b, c, ..., z) are measured directly, for which uncertainties (δa , δb , δc , ..., δz) have been determined, and the variable of interest, F, depends on multiples or quotients of (a, b, c, ..., z):

$$F = \frac{ab...c}{xy...z} \quad (2.20)$$

Then the uncertainty, δF , which propagates due to further calculation in the determination of desired variable, F, is calculated as:

$$\frac{\delta F}{|F|} = \sqrt{\left(\frac{\delta a}{a}\right)^2 + \left(\frac{\delta b}{b}\right)^2 + \dots + \left(\frac{\delta c}{c}\right)^2 + \left(\frac{\delta x}{x}\right)^2 + \left(\frac{\delta y}{y}\right)^2 + \dots + \left(\frac{\delta z}{z}\right)^2} \quad (2.21)$$

Where:

$$\left(\frac{\delta a}{a}\right)^2 + \left(\frac{\delta b}{b}\right)^2 + \dots + \left(\frac{\delta c}{c}\right)^2 + \left(\frac{\delta x}{x}\right)^2 + \left(\frac{\delta y}{y}\right)^2 + \dots + \left(\frac{\delta z}{z}\right)^2 = \text{Average relative uncertainty associated with } (a, b, c, \dots, z).$$

The unit of measurement is equivalent to units of desired variable, F.

CHAPTER 3: SO₂ REACTION WITH LIMESTONE - MODEL DEVELOPMENT & SOLUTION APPROACH

The model development below was adapted from work by (Dasgupta, et al., 2003). As mentioned previously, SO₂ sorption by limestone takes place through two reaction steps:

- a) Calcination of relatively non-porous CaCO₃ having small surface area to produce CaO having significantly larger surface area.



- b) Reaction of SO₂ with CaO in the presence of oxygen to form CaSO₄ (sulfation reaction)



Munoz et al. (1995) have experimentally demonstrated that the CaO-SO₂ reaction at temperatures below 673 K proceeds primarily through the formation of CaSO₃ as a key intermediate stage, regardless of the presence or absence of O₂. It was observed by the authors that, above this temperature, the behavior however differs due to the participation of O₂, in which case the CaSO₃ formation is masked by the presence of O₂ and the subsequent CaSO₄ formation. In the present work, all sorption reactions were carried out at temperatures between 973 K and 1173 K, thus the sulfation reaction is correctly represented by Equation 3.2.

In modelling the reaction of SO₂ with CaO, two descriptions of the morphological structure of the sorbent surface were considered in this study: A Non-Porous Model and a Porous Model.

3.1) NON-POROUS MODEL

An individual non-porous particle of CaO is assumed to be a single grain. The reacting species, SO₂, reacts first at the periphery of the non-porous grain to give high molar volume porous product layer, CaSO₄. As reaction proceeds, the reaction interface moves inward. This is schematically depicted in Figure 3.1. The model considers particle swelling due to formation of larger volume product CaSO₄ layers. This poses a resistance to diffusion of SO₂ within the product layers and often becomes a limiting factor in complete utilization of the sorbent. The conversion for such type of sorbents is typically low.

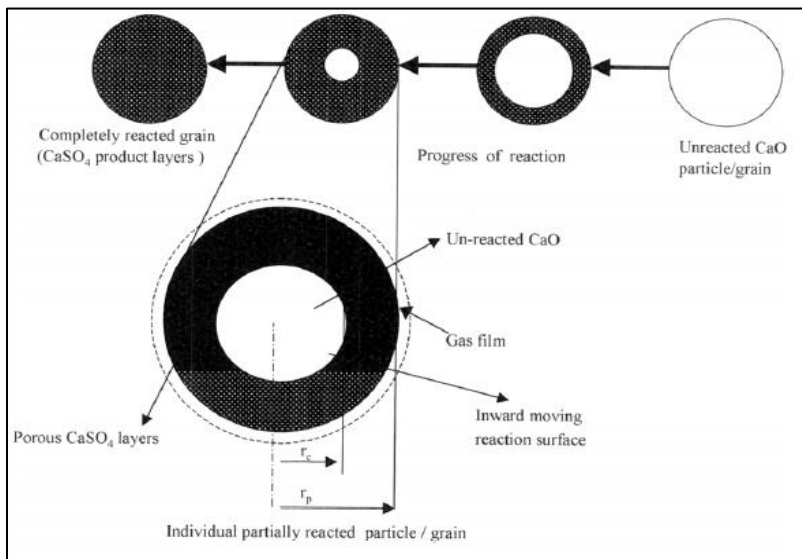


Figure 3. 1: Schematic representation of the reaction of SO₂ with non-porous sorbent (Dasgupta, et al., 2003)

3.1.1) MASS BALANCE IN PACKED BED REACTOR

An isothermal plug flow system in a packed bed of spherical grains, in which pressure drop is negligible and there is no variation in fluid velocity along the bed length, is assumed. This yields a species balance in the gaseous phase of the following form:

$$\frac{\partial C_b}{\partial t} + \frac{V_z}{\varepsilon_b} \frac{\partial C_b}{\partial z} = D_z \frac{\partial^2 C_b}{\partial z^2} - \frac{1-\varepsilon_b}{\varepsilon_b} k_m a (C_b - C_p|_{r=r_p}) \quad (3.3)$$

subject to the boundary conditions:

$$C_b|_{z=0} = C_{b(\text{initial})} \quad (3.4)$$

$$\frac{\partial C_p}{\partial z}|_{z=L} = 0 \quad (3.5)$$

and initial condition:

$$C_b|_{t_0} = 0 \text{ ppm} \quad (3.6)$$

The terms on the left-hand side of Equation 3.3 are unsteady-state and convection, respectively, while those on the right-hand side are axial dispersion and flux, respectively.

3.1.2) MASS BALANCE WITHIN PRODUCT LAYER

The transport of SO₂ within the CaSO₄ product layers is described by a diffusion equation:

$$\frac{\partial C_p}{\partial t} = \frac{D_s}{r^2} \frac{\partial}{\partial r} \left(r^2 \frac{\partial C_p}{\partial r} \right) \quad (3.7)$$

Assuming a pseudo-steady-state, i.e. $\frac{\partial C_p}{\partial t} = 0$, with the following boundary conditions (one at the inward moving reacting interface and the other at the outer surface of the grain or particle):

- Inward moving reacting interface:

$$-D_s \left(\frac{\partial C_p}{\partial r} \right) = -k_r C_p, \text{ at } r = r_c \quad (3.8)$$

- Outer surface of the particle:

$$-D_s \left(\frac{\partial C_p}{\partial r} \right) = -k_m (C_b - C_p), \text{ at } r = r_p \quad (3.9)$$

Integration of Equation 3.7, subject to the pseudo steady state condition, together with the above boundary conditions (Equation 3.8 & 3.9), yields:

$$C_p|_{r=r_p} = C_b \left(\frac{B}{A} - \frac{1}{Ar_p} \right) \quad (3.10)$$

Where:

$$A = \frac{D_s}{r_p^2 k_m} + \frac{D_s}{r_c^2 k_r} - \frac{1}{r_p} + \frac{1}{r_c} \quad (3.11)$$

$$B = \frac{1}{r_c} + \frac{D_s}{r_c^2 k_r} \quad (3.12)$$

Substituting the value of C_p from Equation 3.10 into Equation 3.3, the following governing equation is obtained:

$$\frac{\partial C_b}{\partial t} + \frac{V_z}{\varepsilon_b} \frac{\partial C_b}{\partial z} = D_z \frac{\partial^2 C_b}{\partial z^2} - \frac{3(1-\varepsilon_b)k_m C_b}{r_p \varepsilon_b} \left(1 + \frac{1}{Ar_p} - \frac{B}{A} \right) \quad (3.13)$$

3.1.3 MASS BALANCE AT THE REACTION INTERFACE

The rate at which the reaction interface at $r = r_c$ moves inward due to reaction of SO_2 with CaO , of original radius r_p , is expressed as (Levenspiel, 1999):

$$\frac{\partial r_c}{\partial t} = - \frac{k_r}{\rho_s} C_p|_{r=r_c} \quad (3.14)$$

Substituting C_p from Equation 3.10 into Equation 3.14, the following governing equation is obtained:

$$\frac{\partial r_c}{\partial t} = - \frac{k_r C_b}{\rho_s} \left(\frac{B}{A} - \frac{1}{Ar_c} \right) \quad (3.15)$$

Subject to the initial condition:

$$r_c|_{t_0} = r_p \quad (3.16)$$

Governing Equations 3.13 & 3.15 are solved simultaneously as the solution to this non-porous model. The solution approach is presented in section 3.5.

3.2) POROUS MODEL

In this model, a particle or grain is assumed to consist of spherical sub-grains of uniform size separated by pores through which the reacting gases diffuses. As the reaction proceeds, a shell of the reaction product is formed on the surface of the sub-grains. Figure 3.2 is the schematic representation of such a type of sorption process in a porous material. As shown in the schematic, the CaO sub-grains at the periphery within the grains are consumed prior to those at the core of the grains. As the reaction continues, the diffusion of SO_2 through the pores is hindered by the formation of the larger volume product, CaSO_4 , within the pores. Since the volume of CaSO_4 is about three times that of CaO , swelling of the grains takes place (Hartman & Coughlin, 1976). Therefore, the transport of SO_2 to the core of the grain is prematurely terminated.

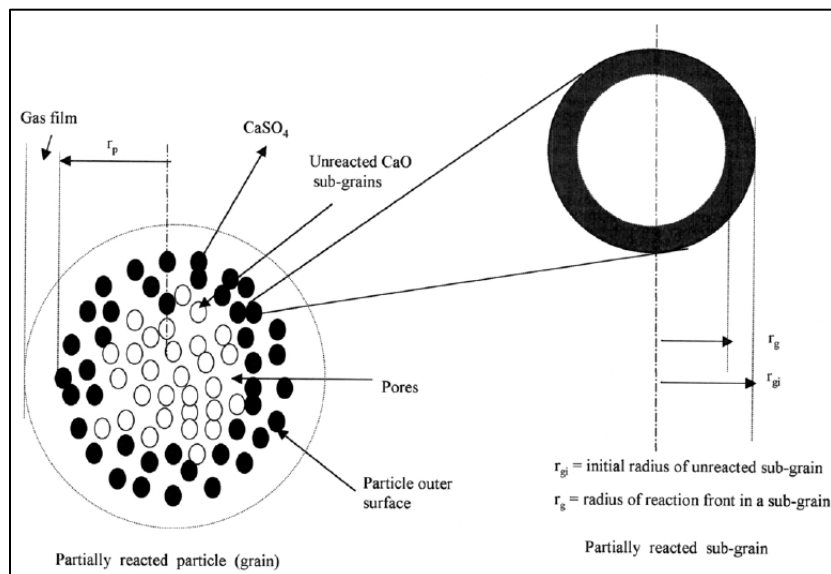


Figure 3. 2: Schematic representation of the reaction of SO_2 with non-porous sorbent (Dasgupta, et al., 2003)

The mathematical model developed for the reaction of SO_2 within the porous spherical particle of CaO comprising of sub-grains consists of the following steps:

3.2.1) MASS BALANCE IN PACKED BED REACTOR

The required governing equation for mass balance remains the same as that established for the non-porous model (refer to Equation 3.3).

3.2.2) BALANCE WITHIN PORES OF THE PARTICLE LOCATED AT A DISTANCE ‘Z’ IN THE REACTOR

The mass balance of diffusing gas, SO_2 , inside the pores of the spherical grain at an axial location z in the bed is given as:

$$\alpha \frac{\partial C_p}{\partial t} + \frac{1}{r^2} \frac{\partial}{\partial r} (r^2 N_r) + a f_p(r) = 0 \quad (3.17)$$

where, N_r is the molar diffusion flux in the radial direction of the grain and $f_p(r)$ is the flux owing to the chemical reaction at the reaction surface.

The governing Equations 3.3 & 3.17 form the basis of the model developed for predicting the performance of porous sorbents under different conditions. As Equations 3.3 & 3.17 are coupled partial differential equations (time, axial and radial directions being independent variables), an approach was adopted to simplify numerical computations and significantly reduce the CPU time. Essentially, in this approach radial concentration profiles within the solid pores were averaged and the average surface and gas phase concentrations within the pores of the pellet are determined as follows (Gupta & Verma, 2002):

$$\frac{\partial \bar{C}_p}{\partial t} - \frac{3}{r_p} K_m \left(C_b - C_p|_{r=r_p} \right) + \frac{3(1-\alpha)}{r_p \alpha} k_r \bar{C}_p = 0 \quad (3.18)$$

Subject to the initial condition:

$$\bar{C}_p|_{t_0} = 0 \text{ ppm} \quad (3.19)$$

where the value of C_p at the periphery of the spherical particle is determined as:

$$C_{p|_{r=r_p}} = \frac{(K_m C_b + \frac{5D_e}{r_p} \bar{C}_p)}{(K_m + \frac{5D_e}{r_p})} \quad (3.20)$$

Thus, the original partial differential equation, 3.17, is reduced to partial differential equation, 3.18, with only temporal (t) and axial (z) dependence. Equation 3.18 & 3.3 describe the behavior of SO_2 sorption in a packed bed of solid porous sorbents in gas flow under isothermal conditions. These two partial differential equations, containing dependent variables C_b and \bar{C}_p (both functions of time and axial location), are solved simultaneously as the solution to the porous model. The solution approach is presented in section 3.5.

3.3) REACTION KINETICS

According to Orbey, et al. (1981), significant structural changes occur within the CaO sorbent during conversion of CaO to CaSO₄ for high temperature desulfurization and these variations must be accounted for when considering the kinetics involved for the desulfurization process. Reaction kinetics which account for structural changes, the effect of film mass transfer and pore diffusion on the observed reaction rate have been presented by Orbey, et al. (1981). The results observed from the experiments conducted by Orbey, et al. (1981) have shown that the predicted reaction kinetics agree well with the observed experimental results. The reaction kinetics developed by Orbey, et al. (1981) cover a wide temperature range, inclusive of the temperatures utilized in this study, thus the reaction kinetics can be implemented here.

According to Orbey, et al. (1981), the volume based reaction rate constant, k_r , of solid CaO sorbent changes during reaction due to the formation of solid product, CaSO₄, on the active CaO surface. The active surface area per unit mass, S_g , and particle density, ρ_p , are expected to vary with time during reaction. Additional diffusion resistance caused by formation of product layer on active surfaces may also lead to a change in the apparent reaction rate constant. While proposing different models and writing another equation for diffusion of reactant gas through the product layer is possible, an alternative and simpler empirical expression is implemented for the reaction rate constant (Orbey, et al., 1981):

$$k_r = k \exp(-\beta t) \quad (3.21)$$

With such an expression, all the aforementioned factors which could change the value of the rate constant are lumped into one empirical parameter, β , which has a temperature dependence. It has also been shown by Dogu (1981) and Candan (1979) that an exponential decrease in k_r provides a good fit with many of the experimental results reported in the literature.

While the reaction rate constant is expected to vary with both time and radial position, for mathematical simplicity, radial variations of the reaction rate constant and diffusivity are neglected in comparison to the time dependence of k_r . This assumption is quite reasonable for small particles where diffusion resistance is not very high. It has however been shown by Dogu (1981) that even for very large particles in which diffusion limitations are important, experimental findings and the proposed model agree well. Based on the negligible diffusional resistances calculated in section 3.4, such an assumption is acceptable.

The temperature dependence of the kinetic parameters k & β are listed in Table 3.1.

Table 3. 1: Temperature dependence of kinetic parameters (Orbey et. Al. 1981)

Temperature ($^{\circ}\text{C}$)	$\beta \times 10^4 (\text{s}^{-1})$	$k (\text{s}^{-1})$
720	2.67	87
800	4.19	142
860	5.55	199
900	7.50	260
950	10.12	294

Based on regression analysis, the temperature dependence of k was found to best fit an exponential function of the form:

$$K = K_o \exp(\alpha_k/T) \quad (3.22)$$

Where:

$$K_o = 7.08E+04 [\text{s}^{-1}]$$

$$\alpha_k = -2889.27 [\text{K}^{-1}]$$

$$T = \text{Temperature [K]}$$

Similarly, regression analysis proved the temperature dependence of β to take the form:

$$\beta = \beta_o \exp(\alpha_\beta/T) \quad (3.23)$$

where:

$$\beta_o = 2.76E-01 [\text{s}^{-1}]$$

$$\alpha_\beta = -6938.82 [\text{K}^{-1}]$$

$$T = \text{Temperature [K]}$$

Since the system is isothermal, the temperature dependence of k & β is specified, for a certain operating temperature, according to the aforementioned expressions. This in turn specifies the temperature dependence of k_r .

3.4) CALCULATED MODEL PARAMETERS

3.4.1) FLUE GAS VELOCITY (V_z)

$$\begin{aligned}\text{Flue Gas Flowrate (Q)} &= 6 \frac{\text{L}}{\text{min}} \\ &= 0.0001 \frac{\text{m}^3}{\text{sec}}\end{aligned}$$

$$\text{Tube Diameter (D}_t\text{)} = 3.5\text{cm}$$

$$= 0.035\text{m}$$

$$\begin{aligned}\text{Tube Cross Sectional Area (CSA)} &= \pi \times \frac{(\text{Tube Diameter})^2}{4} \\ &= \pi \times \frac{(0.035)^2}{4} \\ &= 0.000962 \text{ m}^2\end{aligned}\tag{3.24}$$

$$\begin{aligned}\text{Flue Gas Velocity (V}_z\text{)} &= \frac{\text{Flue Gas Flowrate}}{\text{Tube Cross Sectional Area}} \\ &= \frac{0.0001}{0.02} \\ &= 0.104 \frac{\text{m}}{\text{s}}\end{aligned}\tag{3.25}$$

3.4.2) LIMESTONE SORBENT AVERAGE PARTICLE RADIUS

Particle size analysis of the limestone sorbent utilized was undertaken by means of a sieve tray analysis. The results obtained are presented in Table 5.2. The analysis proves that more than 70wt% of particles lie within the relatively narrow range +250 µm to +500 µm . A Sauter-Mean Particle Diameter (d_p) corresponding to 50% of accumulated mass retained was determined from this data. The mean particle radius (r_p) was thus calculated as:

$$\begin{aligned}\text{Mean Particle Radius } (r_p) &= \frac{\text{Sauter-Mean Particle Diameter } (d_p)}{2} \\ &= \frac{362.76}{2} \\ &= 181.38\mu\text{m}\end{aligned}\tag{3.26}$$

3.4.3) LIMESTONE SORBENT BED POROSITY (ε_b)

In a randomly packed bed, a variation in the void fraction (porosity) is extant. The average void fraction has been shown to be a function of the ratio of tube diameter to particle diameter - $\frac{D}{d_p}$, particle sphericity and particle size distribution. Packing different sized tubes with identical particles has revealed that above a $\frac{D}{d_p}$ ratio of 10, the average void fraction is constant, whereas below 10, the variation of average void fraction with $\frac{D}{d_p}$ is dramatic (Rase, 1977). This empirical relation can be viewed in Figure 3.3. According to Dogu (1981), sphericity of limestone particles typically ranges between 0.6 to 0.9. A particle sphericity of 0.7 is assumed.

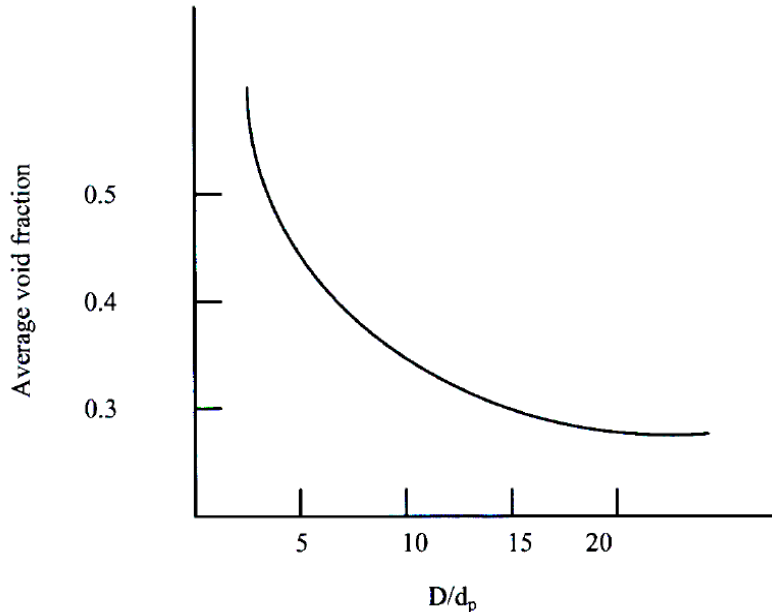


Figure 3. 3: Variation of average void fraction of bed with tube size (Rase, 1977)

For the current study:

$$\frac{D}{d_p} = \frac{3.5 \times 10^{-2} m}{181.38 \times 10^{-6} m} = 193 \quad (3.27)$$

Thus, the average void fraction is constant: $\varepsilon_b = 0.28$

3.4.4) PHYSICAL PROPERTIES

Table 3. 2: Critical temperature and pressure (SMITH, ET AL., 2001)

	MW $(\frac{g}{mol})$	T_c (K)	P_c (bar)	ω
Air	28.85	132.2	37.45	0.035
SO₂	64.07	430.8	78.84	0.245

Table 3. 3: Reduced Temperature [T_r] and Pressure [P_r] (operating pressure = 1 bar)

	Operating Temperature - [T] (K)	$\frac{T}{T_c} = T_r$ (Dimensionless)	$\frac{P}{P_c} = P_r$ (Dimensionless)
Air	973.15	7.361	0.027
	1073.15	8.118	
	1173.15	8.874	
SO₂	973.15	2.259	0.013
	1073.15	2.491	
	1173.15	2.723	

3.4.4.1) FLUE GAS DENSITY

A myriad of methods exists for prediction of vapor density as a function of temperature and pressure. For simple molecules at temperatures above the critical and at pressures no more than a few atmospheres (P_r < 0.4), as is the case in this study, the ideal gas law, Equation 3.28, may be used to estimate vapor density (Perry, 2008).

$$PV = nRT \quad (3.28)$$

Re-arrangement of Equation 3.28 yields Equation 3.29, to evaluate a molar gas density:

$$\rho_g = \frac{n}{V} = \frac{P}{RT} \quad (3.29)$$

Where: ρ = Molar vapor density $[\frac{mol}{m^3}]$

P = Operating Pressure [Pa]

R = Gas constant $[\frac{m^3 \cdot Pa}{mol \cdot K}]$

T = Operating Temperature [K]

To determine a mass-based gas density, the following conversion is applied:

$$\rho_g \left[\frac{\text{kg}}{\text{m}^3} \right] = \frac{\rho \left[\frac{\text{mol}}{\text{m}^3} \right] \times M_m \left[\frac{\text{g}}{\text{mol}} \right]}{1000} \quad (3.30)$$

Since the flue gas is a mixture of sulfur dioxide and air, a weighted average molar mass is calculated to determine the mass-based density of Equation 3.30. According to Perry (2008), Equation 3.31 is utilized to determine a weighted average molar mass.

$$M_m = \sum y_i M_i \quad (3.31)$$

Where: M_m = Molar mass of gas mixture $\left[\frac{\text{g}}{\text{mol}} \right]$

y_i = Mole fraction of component i in mixture [Dimensionless]

M_i = Molar mass of component i in mixture $\left[\frac{\text{g}}{\text{mol}} \right]$

From Table 5.1 the flue gas composition is 98% air and 2% sulfur dioxide. The weighted average molar mass is thus calculated as:

$$\begin{aligned} M_m &= y_{\text{air}} M_{\text{air}} + y_{\text{SO}_2} M_{\text{SO}_2} \\ &= (0.98)(28.85) + (0.02)(64.07) \\ &= 29.55 \frac{\text{g}}{\text{mol}} \end{aligned}$$

Table 3. 4: Flue gas density – $[\rho_g]$ (operating pressure = 1 bar)

Operating Temperature - [T] (K)	R $\left(\frac{\text{m}^3 \cdot \text{Pa}}{\text{mol} \cdot \text{K}} \right)$	ρ_g $\left[\frac{\text{mol}}{\text{m}^3} \right]$	M_m $\left(\frac{\text{g}}{\text{mol}} \right)$	ρ_g $\left[\frac{\text{kg}}{\text{m}^3} \right]$
973.15	8.314	12.52	29.55	0.425
1073.15	8.314	11.36	29.55	0.384
1173.15	8.314	10.39	29.55	0.352

3.4.4.2) FLUE GAS VISCOSITY

According to Perry (2008), for prediction of the vapor viscosity of pure hydrocarbons and light non-hydrocarbons as a function of temperature and at low pressure ($\text{Pr} < 0.6$), Equation 3.32 developed by Stiel and Thodos is the most accurate. Only the molecular weight, the critical temperature, and the critical pressure are required.

$$\mu_i = 4.6 \times 10^{-4} \frac{NM^{1/2}P_c^{2/3}}{T_c^{1/6}} \quad (3.32)$$

Where: μ_i = Dynamic viscosity of pure component i [cP]

M = Molar Mass [$\frac{\text{g}}{\text{mol}}$]

T_c = Critical Temperature [K]

P_c = Critical Pressure [Pa]

$N = 0.0003400T_r^{0.94}$ for $T_r \leq 1.5$ [Dimensionless]

$N = 0.0001778(4.58T_r - 1.67)^{0.625}$ for $T_r > 1.5$ [Dimensionless]

Table 3. 5: Dynamic viscosity of air and SO_2 (operating pressure = 1 bar)

	Operating Temperature – [T]	$M \left(\frac{\text{g}}{\text{mol}} \right)$	$T_c \text{ (K)}$	$\frac{T}{T_c} = T_r$	$P_c \text{ (Pa)}$	$N (T_r > 1.5)$	$\mu_i \text{ (cP)}$
Air	973.15	28.85	132.2	7.361	3745000	1.55×10^{-3}	0.041
	1073.15			8.118		1.65×10^{-3}	0.044
	1173.15			8.874		1.75×10^{-3}	0.046
SO_2	973.15	64.07	430.8	2.259	7884000	6.86×10^{-4}	0.036
	1073.15			2.491		7.37×10^{-4}	0.039
	1173.15			2.723		7.87×10^{-4}	0.042

The above data represents viscosities of the individual components which constitute the flue gas mixture. The flue gas mixture viscosity is thus required to be determined. According to Perry (2008), for prediction of the vapor viscosity of gaseous mixtures at low pressures ($\text{Pr} < 0.6$), Equation 3.33 developed by Bromley and Wilke is recommended.

$$\mu_g = \sum_{i=1}^n \frac{\mu_i}{1 + \sum_{\substack{j=1 \\ j \neq i}}^n (Q_{ij} \frac{y_j}{y_i})^{1/4}} \quad (3.33)$$

Where: μ_g = Dynamic viscosity of gas mixture [cP]

$$Q_{ij} = \frac{1 + \left[\left(\frac{\mu_j}{\mu_i} \right)^{1/2} \left(\frac{M_j}{M_i} \right)^{1/4} \right]^2}{\sqrt{8} \left[1 + \frac{M_i}{M_j} \right]^{1/2}} \quad [\text{Dimensionless}]$$

μ_i, μ_j = Dynamic viscosity of pure component i, j in gas mixture[cP]

y_i, y_j = Mole fraction of pure component i, j in gas mixture [Dimensionless]

M_i, M_j = Molar mass of pure component i, j in gas mixture [$\frac{\text{g}}{\text{mol}}$]

Table 3. 6: Flue gas viscosity – [μ_g] (operating pressure = 1 bar)

Operating Temperature [K]	M_{AIR} [$\frac{\text{g}}{\text{mol}}$]	M_{SO_2} [$\frac{\text{g}}{\text{mol}}$]	y_{AIR}	y_{SO_2}	μ_{AIR} [cP]	μ_{SO_2} [cP]	$Q_{\text{AIR}, \text{SO}_2}$	$Q_{\text{SO}_2, \text{AIR}}$	μ_g [cP]
973.15	28.85	64.07	0.98	0.02	0.041	0.036	0.791	0.313	0.041
1073.15					0.044	0.039	0.787	0.314	0.044
1173.15					0.046	0.042	0.773	0.318	0.046

3.4.5) MASS TRANSFER COEFFICIENT

Average mass transfer coefficients were estimated using the Colburn analogy from (Seader, et al., 2011), applicable between a gaseous mixture and the particles of a packed bed:

$$j_D = \frac{k_m \rho_g}{G} Sc^{2/3} \quad (3.34)$$

Upon re-arrangement of Equation 3.34, gas phase mass transfer coefficients were estimated as:

$$k_m = \frac{j_D G}{\rho_g Sc^{2/3}} \quad (3.35)$$

Where: k_m = Average mass transfer coefficient [$\frac{m}{s}$]

j_D = Chilton-Colburn j -factor for mass transfer [Dimensionless]

G = Mass velocity [$\frac{kg}{m^2 \cdot s}$]

ρ_g = Density of gaseous mixture [$\frac{kg}{m^3}$]

$Sc^{2/3}$ = Schmidt number [Dimensionless]

The j_D factor is a function of Reynolds number. For flow through beds packed with spherical particles, the Chilton-Colburn correlation given by Seader et al. (2011), for Reynolds numbers between 10 and 2500, was utilized:

$$j_D = 1.17(Re)^{-0.415} \quad (3.36)$$

$$Re = \frac{d_p G}{\mu_g} \quad (3.37)$$

$$G = \frac{Q \rho_g}{A_t} \quad (3.38)$$

$$A_t = \frac{\pi (D_t)^2}{4} \quad (3.39)$$

Where: $j_D = j_D$ Factor [Dimensionless]

Re = Reynolds number [Dimensionless]

d_p = Particle diameter [m]

μ_g = Viscosity of flue gas mixture [Pa.s]

G = Mass velocity [$\frac{\text{kg}}{\text{m}^2 \cdot \text{s}}$]

ρ_g = Density of flue gas mixture [$\frac{\text{kg}}{\text{m}^3}$]

Q = Flue gas volumetric flow rate [$\frac{\text{m}^3}{\text{s}}$]

A_t = Tube cross-sectional area [m²]

D_t = Reactor tube diameter [m]

Table 3. 7: Mass velocity, Reynolds number & jd factor (operating pressure = 1 bar)

Operating Temperature – [T] (K)	D _t (m)	A _t (m ²)	Q (m ³ /s)	ρ_g (kg/m ³)	G (kg/m ² .s)	d _p (m)	μ_g (Pa.s)	Re	j _D
973.15	0.035	0.002	0.0001	0.425	0.0442	1.81 × 10 ⁻⁴	4.1 × 10 ⁻⁵	29.31	0.288
1073.15				0.384	0.0399		4.4 × 10 ⁻⁵	24.67	0.309
1173.15				0.352	0.0366		4.6 × 10 ⁻⁵	21.64	0.327

According to Seader et al. (2011), the Schmidt number, for a binary gas mixture, may be calculated as follows:

$$Sc = \frac{\mu_g}{\rho_g D_{AB}} \quad (3.40)$$

Where: Sc = Schmidt number [Dimensionless]

μ_g = Viscosity of mixture [Pa.s]

ρ_g = Density of mixture [$\frac{\text{kg}}{\text{m}^3}$]

D_{AB} = Binary diffusion coefficient of components A and B [$\frac{\text{m}^2}{\text{s}}$]

According to Seader et al. (2011), the binary diffusion coefficients are equivalent (i.e.: $D_{AB} = D_{BA}$) and may be estimated using the following empirical equation of (Fuller, et al., 1966):

$$D_{AB} = D_{BA} = \frac{0.00143T^{1.75}}{PM_{AB}^{0.5}[(\Sigma v)_A^{\frac{1}{3}} + (\Sigma v)_B^{\frac{1}{3}}]^2} \quad (3.41)$$

$$M_{AB} = \frac{2}{(1/M_A) + (1/M_B)} \quad (3.42)$$

Where: D_{AB} = Binary diffusion coefficient of components A and B [$\frac{cm^2}{s}$]

P = Pressure [atmosphere]

T = Temperature [K]

M_A, M_B = Molar mass of components A, B [$\frac{g}{mol}$]

M_{AB} = Mean molar mass [$\frac{g}{mol}$]

$(\Sigma v)_A, (\Sigma v)_B$ = Summation of atomic and structural diffusion volumes for components A, B

[Dimensionless]

Diffusion Volumes of Simple Molecules			
He	2.67	CO	18.0
Ne	5.98	CO ₂	26.7
Ar	16.2	N ₂ O	35.9
Kr	24.5	NH ₃	20.7
Xe	32.7	H ₂ O	13.1
H ₂	6.12	SF ₆	71.3
D ₂	6.84	Cl ₂	38.4
N ₂	18.5	Br ₂	69.0
O ₂	16.3	SO ₂	41.8
Air	19.7		

Figure 3. 4: Diffusion volumes of simple molecules (Seader et al., 2011)

Table 3. 8: Binary diffusion coefficient & Schmidt number (operating pressure = 1 bar)

A - SO₂

B - Air

Operating Temperature – [T] (K)	M _A (g/mol)	M _B (g/mol)	M _{AB} (g/mol)	($\sum v$) _A	($\sum v$) _B	D _{AB} (cm ² /s)	D _{AB} (m ² /s)	ρ_g (kg/m ³)	μ_g (Pa.s)	Sc
973.15	64.07	28.85	39.79	41.8	19.7	1.010	1.01×10^{-4}	0.425	4.1×10^{-5}	0.956
1073.15						1.198	1.20×10^{-4}	0.384	4.4×10^{-5}	0.957
1173.15						1.400	1.40×10^{-4}	0.352	4.6×10^{-5}	0.934

Table 3. 9: Average mass transfer coefficient - [k_m] (operating pressure = 1 bar)

Operating Temperature – [T] (K)	j _D	G (kg/m ² .s)	ρ_g (kg/m ³)	$(Sc)^{\frac{2}{3}}$	k _m (m/s)
973.15	0.288	0.0442	0.425	0.970	0.313
1073.15	0.309	0.0399	0.384	0.971	0.336
1173.15	0.327	0.0366	0.352	0.955	0.367

3.4.6) INTRA-PARTICLE POROSITY (α)

In this study the reaction of SO₂ with limestone is modelled based on a non-porous particle approach as well as a porous particle approach. Irrespective of the approach, the initial limestone sorbent is calcined to produce larger surface area CaO (Equation 3.1) when exposed to elevated operating temperatures. This CaO will subsequently react with SO₂ according to the reaction represented by Equation 3.2 (sulfation reaction).

For the porous model approach, the CaO particles were considered as porous. The particles thus possess an associated internal porosity referred to as the intra-particle porosity (α). To model the porous approach, this intra-particle porosity was required to be known.

(Newton, et al., 1998) executed such experiments to determine the intra-particle porosity of porous CaO, derived from both calcium carbonate (CaCO₃) and calcium hydroxide [Ca(OH)₂]. For CaO derived from CaCO₃, over a temperature range of 700°C – 900°C, the measured intra-particle porosity was found to be maintained at an approximately constant value of 0.2 (i.e.: $\alpha = 0.2$), with minimal variation.

3.4.7) SURFACE AREA PER UNIT VOLUME

For chemical reactions involving a solid material, the surface area to volume ratio is an important factor in terms of reactivity, i.e.: the rate at which the chemical reaction will proceed. Larger area to volume ratios promote increased reactivity while the converse is expected for reduced area to volume ratios. According to Seader (2011), Equation 3.43 may be used to determine the area to volume ratio for a fixed bed of sorbent particles.

$$a = S_g \times \rho_s \quad (3.43)$$

Where: a = Surface area per unit volume $\left[\frac{m^2}{m^3}\right]$

S_g = Specific surface area $\left[\frac{m^2}{kg}\right]$

ρ_s = Density of sorbent particle $\left[\frac{kg}{m^3}\right]$

(Milne, 1998) developed a correlation relating intra-particle porosity to specific surface area, as per Equation 3.44 below. This correlation is suitable for CaO derived from both calcium carbonate ($CaCO_3$) or calcium hydroxide [$Ca(OH)_2$], over the temperature range $700^\circ C - 1200^\circ C$.

$$S_g = 84.94 \frac{\alpha}{1-\alpha} \quad (3.44)$$

Where: S_g = Specific surface area $\left[\frac{m^2}{g}\right]$

α = Intra-particle porosity [Dimensionless]

Table 3. 10: Surface area per unit volume - [a]

Operating Temperature - [T] (K)	α	S_g ($\frac{m^2}{g}$)	S_g ($\frac{m^2}{kg}$)	ρ_s ($\frac{kg}{m^3}$)	a ($\frac{m^2}{m^3}$)
973.15					
1073.15	0.2	21.24	21240	1441	3.1×10^7
1173.15					

3.4.8) PRODUCT LAYER DIFFUSION RESISTANCE

In the model analysis for a non-porous sorbent particle assumption, diffusion of SO₂ through the larger volume product CaSO₄ layers and to active sorbent particle surface may affect the degree of SO₂ removal. This is dependent upon the extent of the inhibiting effect associated with the diffusional resistance through the CaSO₄ layer. Agnihotri et. al. (1999) performed experiments, at elevated operating temperatures utilized in this study, to quantify the resistance to diffusion of SO₂ within the CaSO₄ product layer. This diffusional resistance is represented by diffusion coefficient, D_s. The results of these experiments are displayed in Table 3.11.

Table 3. 11: Diffusional resistance through product layer – [D_s]

Operating Temperature – [T] (K)	D _s ($\frac{m^2}{s}$)
973.15	1.2×10^{-6}
1073.15	4.9×10^{-6}
1173.15	1.5×10^{-7}

3.4.9) EFFECTIVE DIFFUSIVITY (D_e)

In the model analysis for a porous sorbent particle assumption, an effective diffusivity, D_e, was defined. This diffusion coefficient accounts not only for the diffusional resistance of SO₂ through product CaSO₄ layers, but also for resistance associated with the diffusion of SO₂ through the pores within the porous sorbent particle, to the active site. According to Satterfield (1991), the effective diffusivity with respect to reacting species A, of a binary gas mixture, may be estimated as:

$$D_{e,A} = \frac{\alpha}{\tau} D_{m,A} \quad (3.45)$$

Where: D_{e,A} = Effective diffusivity [$\frac{m^2}{s}$]

α = Intra-particle porosity [Dimensionless]

$\tau = \frac{1}{\alpha}$ = Tortuosity [Dimensionless]

D_{m,A} = Molecular diffusivity [$\frac{m^2}{s}$]

A = Reacting species A

$$\frac{1}{D_{m,A}} = \frac{1}{D_{AB}} + \frac{1}{D_{K,A}} \quad (3.46)$$

Where: D_{AB} = Binary diffusion coefficient $\left[\frac{m^2}{s}\right]$

$D_{K,A}$ = Knudsen Diffusivity $\left[\frac{m^2}{s}\right]$

$$D_{K,A} = \frac{4}{3} \bar{r} \left(\frac{2}{\pi} \frac{RT}{M_A} \right)^{0.5} \quad (3.47)$$

Where: R = Universal gas constant $\left[\frac{\text{Pa.m}^3}{\text{K.kmol}}\right]$

T = Operating temperature [K]

M_A = Molecular weight of reacting species A $\left[\frac{\text{kg}}{\text{kmol}}\right]$

\bar{r} = average pore radius [m]

Table 3. 12: Effective diffusivity – $[D_e]$

A - SO_2

B - Air

Operating Temperature (K)	\bar{r} (m)	M_A ($\frac{\text{kg}}{\text{kmol}}$)	R ($\frac{\text{Pa.m}^3}{\text{K.kmol}}$)	D_{KA} ($\frac{m^2}{s}$)	D_{AB} ($\frac{m^2}{s}$)	$D_{m,A}$ ($\frac{m^2}{s}$)	τ	α	$D_{e,A}$ ($\frac{m^2}{s}$)
973.15	2.70×10^{-8}	64.07	8314	1.02×10^{-5}	1.01×10^{-4}	9.27×10^{-6}	5	$\frac{1}{5}$	3.71×10^{-7}
1073.15				1.07×10^{-5}	1.20×10^{-4}	9.84×10^{-6}			3.94×10^{-7}
1173.15				1.12×10^{-5}	1.40×10^{-4}	1.04×10^{-5}			4.15×10^{-7}

3.5) NUMERICAL SOLUTION APPROACH

3.5.1) NUMERICAL METHOD

The physical system for both the porous and non-porous models are convection-diffusion-reaction systems modelled in cylindrical co-ordinates (with only two variables: axial, z and radial, r). Both models contain parabolic partial differential equations (PDE's) that are inherently coupled.

A numerical solution approach capable of handling such coupled PDE's thus had to be implemented. Initially the Crank-Nicolson numerical solution method was considered. The non-porous model equation, 3.15, is nonlinear due to the term containing the core particle radius, ' r_c '. One of the criteria for the Crank-Nicolson method is the linearization of any non-linearities present. Linearization of Equation 3.15 proved to be complicated. An alternative numerical solution method for the respective porous and non-porous models was therefore implemented. The technique utilized was the Method of Lines (MOL). This technique was selected since it accommodates such non-linearities in differential equations (no linearization required) (Scheissser & Griffiths, 2009). This enabled ease of incorporation of the non-linearity associated with Equation 3.15 into the solution approach.

The MOL is based on finite difference approximations for the partial derivatives (Scheissser & Griffiths, 2009). It entails the use of orthogonal collocation (discretization), usually in the spatial dimension, to reduce a system of PDE's to a system of temporal ODE's; this is coupled with an implicit, linear, multi-step solution algorithm for integration in the temporal (t) dimension (Hopkins & Golding, 1993). In this study the orthogonal collocation occurs in the axial (z) spatial dimension and integration in the temporal dimension was performed through use of a built in implicit Matlab solver, ODE45, based on Runge-Kutta 4th order numerical solution equations. Axial discretization was accomplished using difference formulas to yield the ODE's required for the temporal integrators. Figure 3.5 displays the reference grid that was used for the derivation of the difference equations.

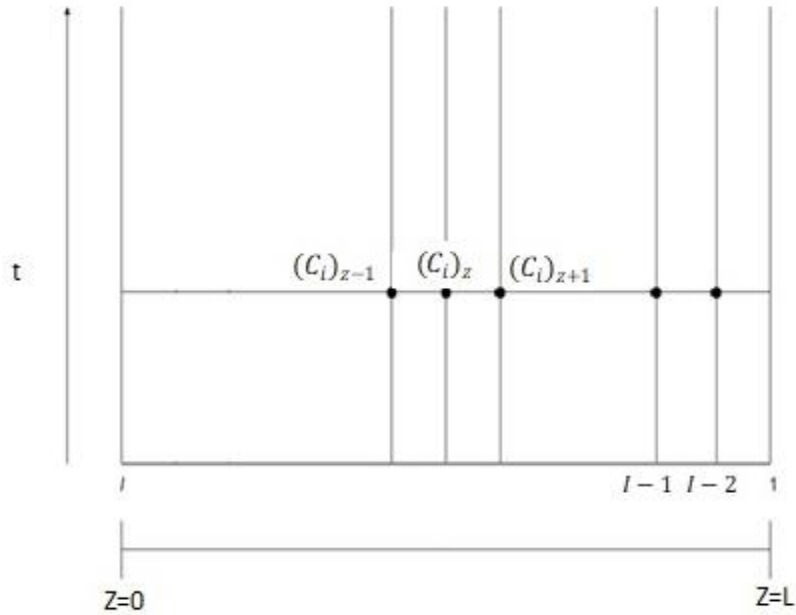


Figure 3.5: Reference grid for derivation of finite difference equations

The fixed sorbent bed is divided into several equally sized increments, $\Delta z = L/I$. Programming of the temporal ODE's begins with discretization of the first axial derivative. For reasons of convergence, a second order central difference approximation for the first partial derivative is utilized (Nauman, 2002):

$$\frac{\partial C_i}{\partial z} = \frac{(C_i)_{z+1} - (C_i)_{z-1}}{2\Delta z} \quad (3.48)$$

Similarly, for the second axial derivative, the following approximation is employed:

$$\frac{\partial^2 C_i}{\partial z^2} = \frac{(C_i)_{z+1} - 2(C_i)_z + (C_i)_{z-1}}{\Delta z^2} \quad (3.49)$$

For the boundary condition represented by Equation 3.5, at $z = L$, the first derivative is approximated as:

$$\frac{\partial C_i}{\partial z} = \frac{(C_i)_{z+1} - (C_i)_{z-1}}{2\Delta z} = 0 \quad (3.50)$$

Thus,

$$(C_i)_{z+1} = (C_i)_{z-1} \quad (3.51)$$

The above expression is used to eliminate the fictitious value $(C_i)_{z+1}$ at the boundary where $z = L$

3.5.2) AXIAL DISCRETIZATION TO ESTABLISH SYSTEM OF TEMPORAL ODE's

3.5.2.1) NON-POROUS MODEL AXIAL DISCRETIZATION

Governing Equation 3.13:

$$\frac{\partial C_b}{\partial t} + \frac{V_z}{\varepsilon_b} \frac{\partial C_z}{\partial t} = D_z \frac{\partial^2 C_b}{\partial z^2} - \frac{3(1-\varepsilon_b)k_m C_b}{r_p \varepsilon_b} \left[1 + \frac{1}{Ar_p} - \frac{B}{A} \right]$$

Step 1 - Substitute Equations 3.11 & 3.12 in Governing Equation 3.13:

$$\frac{\partial C_b}{\partial t} + \frac{V_z}{\varepsilon_b} \frac{\partial C_z}{\partial t} = D_z \frac{\partial^2 C_b}{\partial z^2} - \left\{ \frac{3(1-\varepsilon_b)k_m C_b}{r_p \varepsilon_b} \left[1 + \frac{1}{r_p \left(\frac{D_s}{r_p^2 k_m} + \frac{D_s}{r_c^2 k_r} - \frac{1}{r_p} + \frac{1}{r_c} \right)} - \frac{\left(\frac{1}{r_c} + \frac{D_s}{r_c^2 k_r} \right)}{\left(\frac{D_s}{r_p^2 k_m} + \frac{D_s}{r_c^2 k_r} - \frac{1}{r_p} + \frac{1}{r_c} \right)} \right] \right\} \quad (3.52)$$

Step 2 - Discretize in axial (z) dimension by substituting Equations 3.48 & 3.49 in Equation 3.52:

$$\frac{\partial C_b}{\partial t} + \frac{V_z}{\varepsilon_b} \left[\frac{(C_b)_{z+1} - (C_b)_{z-1}}{2\Delta z} \right] = D_z \left[\frac{(C_b)_{z+1} - 2(C_b)_z + (C_b)_{z-1}}{\Delta z^2} \right] - \left[1 + \frac{1}{r_p \left(\frac{D_s}{r_p^2 k_m} + \frac{D_s}{r_c^2 k_r} - \frac{1}{r_p} + \frac{1}{r_c} \right)} - \frac{\left(\frac{1}{r_c} + \frac{D_s}{r_c^2 k_r} \right)}{\left(\frac{D_s}{r_p^2 k_m} + \frac{D_s}{r_c^2 k_r} - \frac{1}{r_p} + \frac{1}{r_c} \right)} \right] \quad (3.53)$$

Step 3 - Express Equation 3.53 in terms of the temporal derivative $\frac{\partial C_b}{\partial t}$:

$$\frac{\partial C_b}{\partial t} = D_z \left[\frac{(C_b)_{z+1} - 2(C_b)_z + (C_b)_{z-1}}{\Delta z^2} \right] - \left[1 + \frac{1}{r_p \left(\frac{D_s}{r_p^2 k_m} + \frac{D_s}{r_c^2 k_r} - \frac{1}{r_p} + \frac{1}{r_c} \right)} - \frac{\left(\frac{1}{r_c} + \frac{D_s}{r_c^2 k_r} \right)}{\left(\frac{D_s}{r_p^2 k_m} + \frac{D_s}{r_c^2 k_r} - \frac{1}{r_p} + \frac{1}{r_c} \right)} \right] - \frac{V_z}{\varepsilon_b} \left[\frac{(C_b)_{z+1} - (C_b)_{z-1}}{2\Delta z} \right] \quad (3.54)$$

Governing Equation 3.15:

$$\frac{\partial r_c}{\partial t} = \frac{-k_r C_b}{\rho_s} \left(\frac{B}{A} - \frac{1}{A r_c} \right)$$

Step 1 - Substitute Equations 3.11 & 3.12 in Governing Equation 3.13:

$$\frac{\partial r_c}{\partial t} = \frac{-k_r C_b}{\rho_s} \left[\frac{\left(\frac{1}{r_c} + \frac{D_s}{r_c^2 k_r} \right)}{\left(\frac{D_s}{r_p^2 k_m} + \frac{D_s}{r_c^2 k_r} - \frac{1}{r_p} + \frac{1}{r_c} \right)} - \frac{1}{r_c \left(\frac{D_s}{r_p^2 k_m} + \frac{D_s}{r_c^2 k_r} - \frac{1}{r_p} + \frac{1}{r_c} \right)} \right] \quad (3.55)$$

Since equation 3.55 contains no axial derivatives, discretization is complete. Equation 3.55 is also expressed in terms of the temporal derivative $\frac{\partial r_c}{\partial t}$.

3.5.2.2) POROUS MODEL AXIAL DISCRETIZATION

Governing Equation 3.3:

$$\frac{\partial C_b}{\partial t} + \frac{V_z}{\varepsilon_b} \frac{\partial C_b}{\partial z} = D_z \frac{\partial^2 C_b}{\partial z^2} - \frac{1-\varepsilon_b}{\varepsilon_b} K_m a (C_b - C_p|_{r=r_p})$$

Step 1 - Substitute Equation 3.20 in Governing Equation 3.3:

$$\frac{\partial C_b}{\partial t} + \frac{V_z}{\varepsilon_b} \frac{\partial C_b}{\partial t} = D_z \frac{\partial^2 C_b}{\partial z^2} - \left\{ \frac{(1-\varepsilon_b)}{\varepsilon_b} K_m a \left[C_b - \frac{(k_m C_b + \frac{5D_e}{r_p} C_p)}{(k_m + \frac{5D_e}{r_p})} \right] \right\} \quad (3.56)$$

Step 2 - Discretize in axial (z) dimension by substituting Equations 3.48 & 3.49 in Equation 3.56:

$$\frac{\partial C_b}{\partial t} + \frac{V_z}{\varepsilon_b} \left[\frac{(C_b)_{z+1} - (C_b)_{z-1}}{2\Delta z} \right] = D_z \left[\frac{(C_b)_{z+1} - 2(C_b)_z + (C_b)_{z-1}}{\Delta z^2} \right] - \left\{ \frac{(1-\varepsilon_b)}{\varepsilon_b} K_m a \left[C_b - \frac{(k_m C_b + \frac{5D_e}{r_p} C_p)}{(k_m + \frac{5D_e}{r_p})} \right] \right\} \quad (3.57)$$

Step 3 - Express Equation 3.57 in terms of the temporal derivative $\frac{\partial C_b}{\partial t}$:

$$\frac{\partial C_b}{\partial t} = D_z \left[\frac{(C_b)_{z+1} - 2(C_b)_z + (C_b)_{z-1}}{\Delta z^2} \right] - \left\{ \frac{(1-\varepsilon_b)}{\varepsilon_b} k_m a \left[C_b - \frac{(k_m C_b + \frac{sD_e}{r_p} \bar{C}_p)}{(k_m + \frac{sD_e}{r_p})} \right] \right\} - \frac{V_z}{\varepsilon_b} \left[\frac{(C_b)_{z+1} - (C_b)_{z-1}}{2\Delta z} \right] \quad (3.58)$$

Governing Equation 3.18

$$\frac{\partial \bar{C}_p}{\partial t} - \frac{3}{r_p} K_m \left(C_b - C_p |_{r=r_p} \right) + \frac{3(1-\alpha)}{r_p \alpha} k_r \bar{C}_p = 0$$

Step 1 - Substitute Equation 3.20 in Governing Equation 3.18:

$$\frac{\partial \bar{C}_p}{\partial t} - \frac{3}{r_p} k_m \left(C_b - \frac{(k_m C_b + \frac{sD_e}{r_p} \bar{C}_p)}{(k_m + \frac{sD_e}{r_p})} \right) + \frac{3(1-\alpha)}{r_p \alpha} k_r \bar{C}_p = 0 \quad (3.59)$$

Since Equation 3.59 contains no axial derivatives, discretization is complete

Step 2 - Express equation 3.59 in terms of the temporal derivative $\frac{\partial \bar{C}_p}{\partial t}$:

$$\frac{\partial \bar{C}_p}{\partial t} = \frac{3}{r_p} k_m \left(C_b - \frac{(k_m C_b + \frac{5D_e}{r_p} \bar{C}_p)}{(k_m + \frac{5D_e}{r_p})} \right) - \frac{3(1-\alpha)}{r_p^\alpha} k_r \bar{C}_p \quad (3.60)$$

3.5.3) MATLAB CODE: POROUS AND NON-POROUS MODEL SOLUTION ALGORITHM

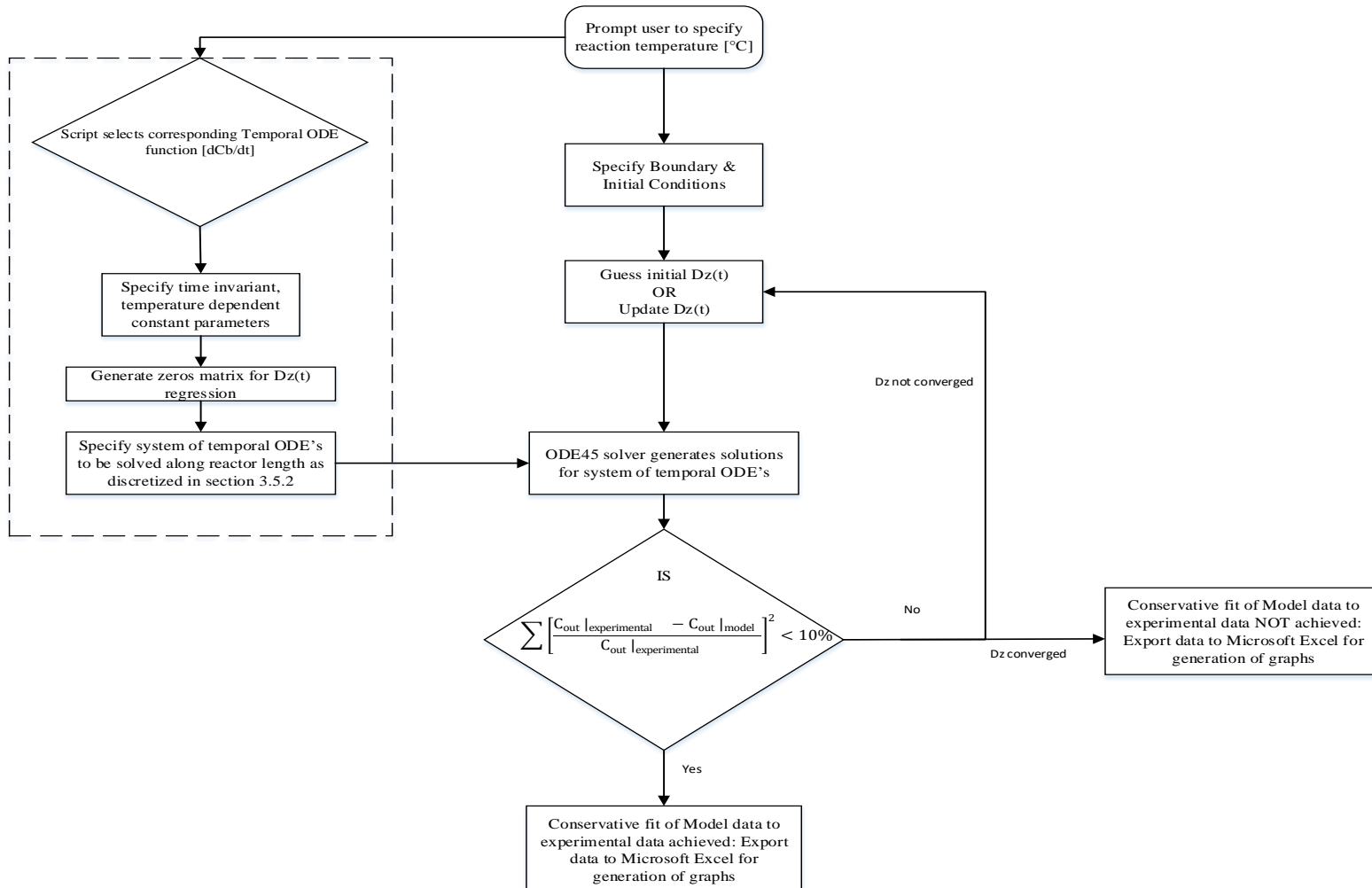


Figure 3. 6: Flow diagram of computational algorithm for porous and non-porous model solution

CHAPTER 4: EXPERIMENTAL METHODS

Before experimental runs were conducted, the experiment was planned. This was done to determine exactly what data was desired from an experiment, how it was going to be obtained from the apparatus and how it realizes the goals of the study.

4.1) EXPERIMENTAL VARIABLES

The independent variables for this experiment should remain constant during each run. These variables are listed below:

- Pressure of gas mixture through the system (101.3 kPa discharge from tank)
- Flue Gas composition (SO₂ 2073 ppmv, O₂ 20 vol %, remainder N₂)
- Flue Gas flowrate
- Desulfurization temperature of the reactor.
- Sorbent
 - Type
 - Volume of sorbent loaded into reactor
- Space velocity in reactor: determined by flowrate and the volume of sorbent in the bed
- Barium Perchlorate concentration
- Mass of Thoron indicator
- Volume of isopropanol used to generate respective solutions

The dependent variables depend on the values of the independent variables previously mentioned:

- Breakthrough time
- Sorbent sorption capacity (based on saturation time)
- Amount of SO₃ generated

4.2) EXPERIMENTAL DESIGN

The experiment was designed with one independent variable and three levels for that variable. The aim of the experimental design is to evaluate the effect of temperature on:

- Breakthrough & Saturation time (via measurement of SO₂ concentration at the reactor inlet and outlet)
- The amount of SO₃ generated.

For each level of the independent temperature variable, three runs will be performed as a means of testing for repeatability, resulting in a total of nine experimental runs performed for this study. The following general set up will be used:

Table 4. 1: Summary of experimental design (operating pressure = 1bar)

Temperature	Breakthrough time & Saturation time			
	700 °C	Run 1	Run 2	Run 3
	800 °C	Run 1	Run 2	Run 3
	900 °C	Run 1	Run 2	Run 3
SO ₃ generated				

4.3) PROCESS DESIGN

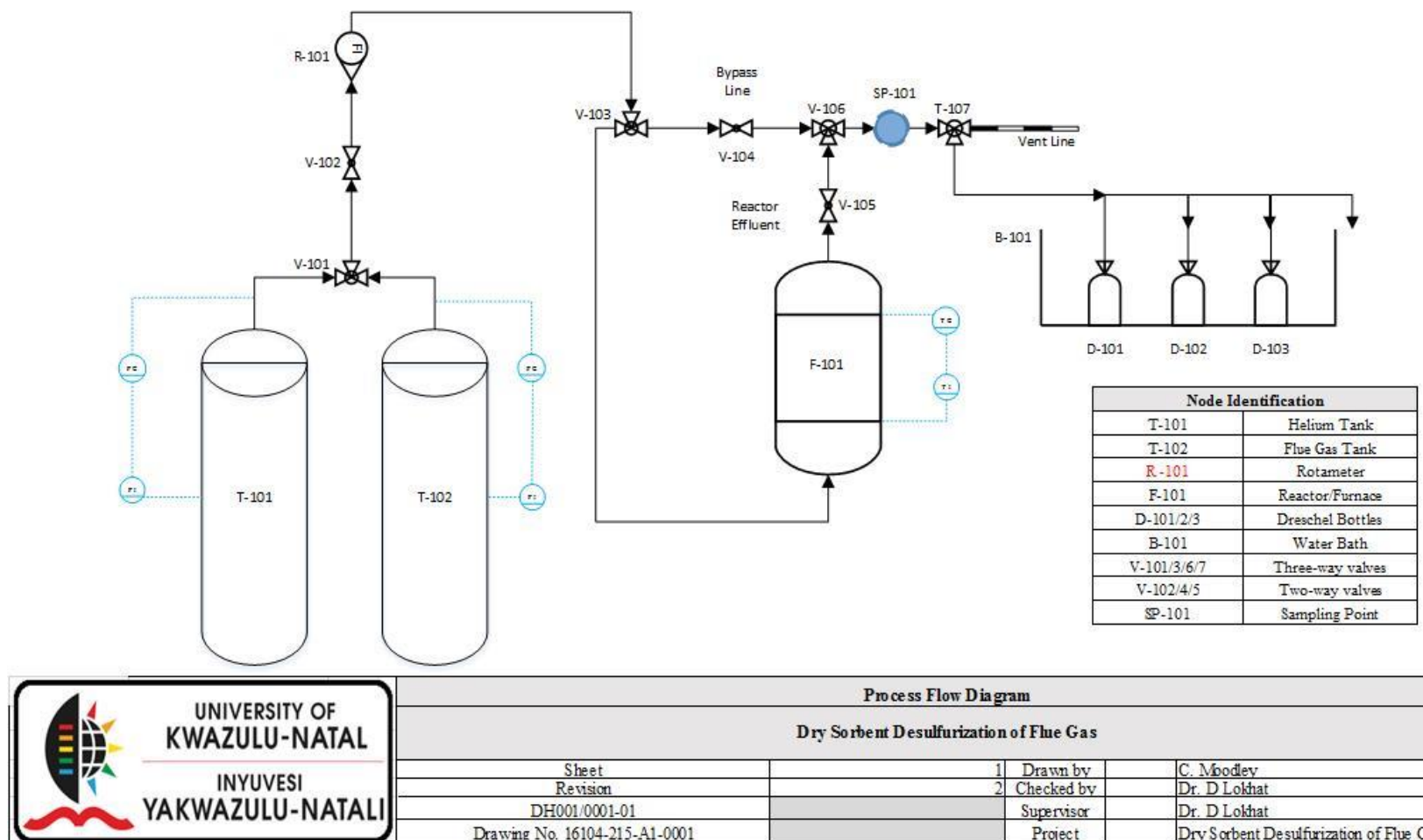


Figure 4. 1: Process design flow diagram

4.4) EXPERIMENTAL EQUIPMENT

The following equipment and chemicals were utilized to carry out experimental work:

Table 4. 2: Equipment and chemicals utilized in experimental work

General Equipment	Chemicals
Furnace/Reactor	Sulphuric Acid
Valves, Tubing & Fittings	Nitric Acid
Inert Quartz Glass Bead Packing Material	Hydrofluoric acid
Temperature Probe	Limestone
Temperature Controller	Thoron Indicator
Thermometer	Helium
Rotameter	Isopropyl Alcohol
Gas Chromatograph (GC) Unit	Barium Perchlorate
Gas Syringes	Flue Gas
Ice Bath	
3× Dreschel Bottles	
Acid Gloves	
3× Steel Water Bath with Temperature Control	
Glass-ware for Solution Preparation & Titration	

Major equipment used in the experimental set up can be divided into four important sections:

4.4.1) DESULFURIZATION REACTOR & FURNACE

A Carbolite (UK) manufactured tubular furnace served the purpose of heating the desulfurization reactor. The furnace tube is 400mm long with an I.D of 40mm. The furnace tube is housed within a square metal box and insulated with vermiculite. The furnace is under temperature control via a K-type thermocouple, inserted co-axially to the reactor tube, which is connected to a Shinko RKS PID controller, to set the furnace temperature at a desired operating set point of either 700°C, 800°C or 900°C. The reactor is manufactured using stainless steel 316 to withstand the corrosive nature of H₂SO₄ (a result of SO₂ present in the moist flue gas). It contains a 450mm long tube with an I.D. of 35mm and is inserted vertically into the tubular furnace.

The sorbent loaded in the reactor had to form a fixed bed to prevent the channelling of the gas flow and to provide a well-defined reaction front. The sorbent was held in place with two stainless steel mesh grids located 30mm apart (as per the requisite bed length), midway through the reactor, and is surrounded by inert quartz glass packing beads on either side for the remaining reactor length. The packing on the inlet side serves as the preheating zone while packing on the outlet section serves the purpose of maintaining packing of the sorbent bed.

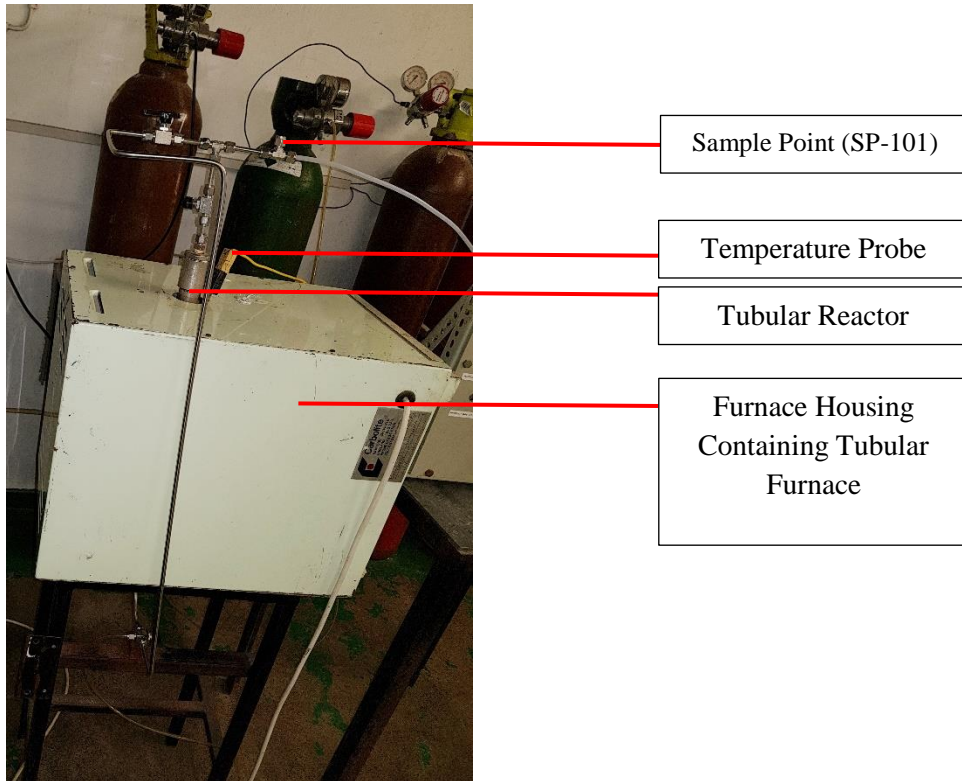


Figure 4. 2: Reactor/Furnace setup

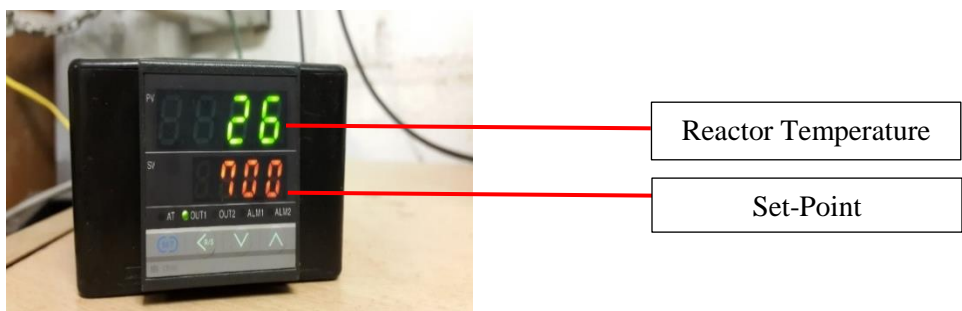


Figure 4. 3: Shinko RKS, PID controller

4.4.2) GAS SAMPLING & ANALYSIS EQUIPMENT

1ml SGE type gas syringes were utilized to extract samples at the reactor sampling point, SP-101, for injection into the gas chromatograph (GC) sample point (see Figure 4.4).

A Shimadzu GC 2014; equipped with a flame photometric detector (FPD) was used to determine the composition of SO₂ in the inlet and exit gas. The FPD is sensitive to sulfur and phosphorus containing compounds only. This makes it applicable to this experiment.

The GC contained an Inertcap 5MS/NP capillary column of length of 30m, I.D. of 0.25mm with a wall thickness of 0.25µm. The carrier gas selected was helium, whereas the reference gases were zero air and hydrogen. These gases had to be pure to ensure no reactions take place with the column's stationary phase, which would inhibit the separation process. For optimum separation, the pressure for zero air and hydrogen on the GC gauges were set at 40 and 100 kPa respectively. Helium also serves as a make-up gas to increase the flow of gas across the detector; the pressure gauge was set at 20 kPa. The function of a split ratio is to prevent the formation of broad and tailing peaks due to high concentrations of SO₂ in the gas mixture. The split ratio operates in such a way that the hot sample is mixed with the carrier gas and divided up into two streams depending on the specified ratio. The carrier gas flow enters the column and the split flow is vented. A split ratio of 11.8:1 was chosen as this was the maximum value that could be used to maintain the desired gas velocities required by the GC setup.

Table 4. 3: GC operating conditions

Parameter	Set-point	Units
Detector Temperature	250	°C
Column Temperature	130	°C
Injection Temperature	250	°C
Total Flow	15,7	ml/min
Column Flow	1	m/s
Purge flow	3	m/s
Split Ratio	11.8:1	
Linear Velocity	27,4	m/s

The GC is connected to the PC via a 'GC solution' program. Subject to the GC operating conditions above (Table 4.4), the GC will output the SO₂ concentration of a desired sample in the form of a chromatogram with an associated area that is representative of the SO₂ concentration within that sample. These areas are collected from the 'GC solution' program on the PC.

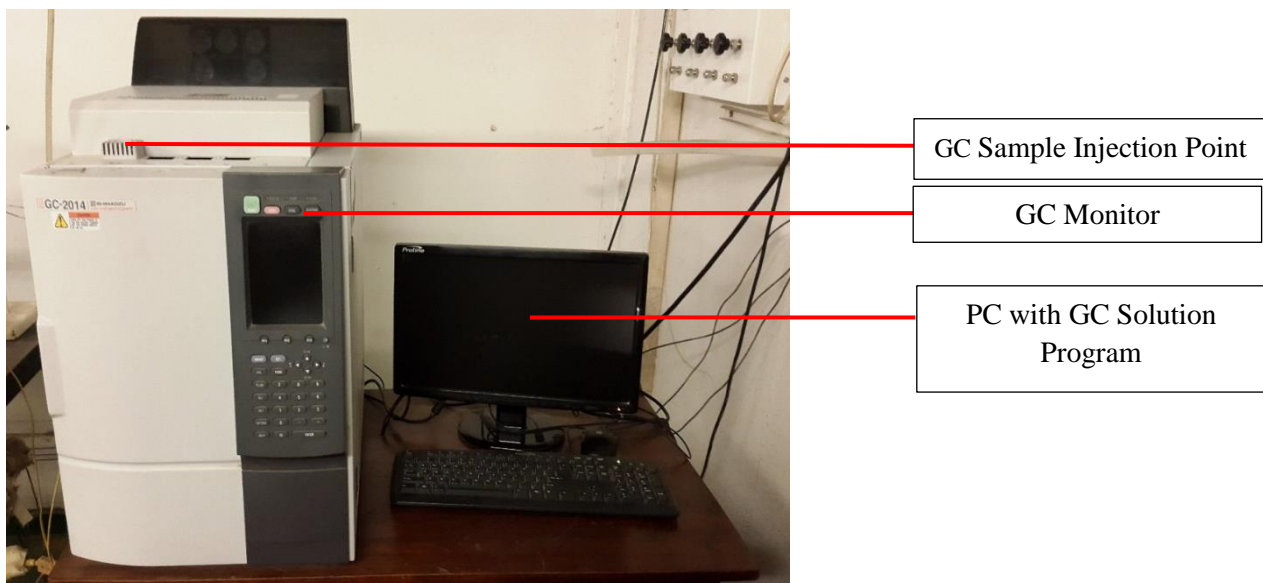


Figure 4. 4: Shimadzu gas chromatograph and PC monitoring system

4.4.3) SO₃ ANALYSIS

In this section the reactor effluent gas is passed through a series of 3 interconnected dreschel bottles. Each bottle is maintained in an ice bath and filled with 100ml of an 80% isopropanol solution. The effluent gas bubbles through each bottle for the total desulfurization reaction run time. Inert helium gas is thereafter allowed to pass through the system to remove trace amounts of SO₂ and prevent absorption of SO₂ into the isopropanol solutions which would result in calculation of over-estimated SO₃ production after titration. The isopropanol solutions are analyzed by the titration procedure (section 4.6.2.3) to determine the amount of SO₃ produced.

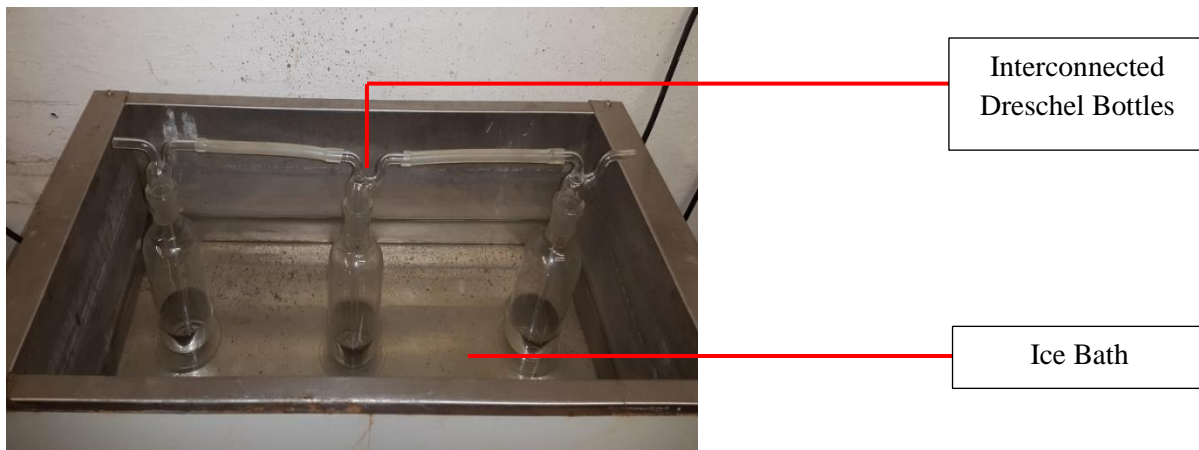


Figure 4. 5: Experimental setup for SO₃ analysis



Figure 4. 6: Titrations that have reached endpoint

4.4.4) TUBING, VALVES & FITTINGS

All tubing (excluding the vent line), valves and fittings are composed of stainless steel 316. The Tubing used to commission the equipment is of $\frac{1}{4}$ inch I.D.

Valve V-101 is adjusted to allow either helium from tank T-101 or flue gas from tank T-102 to flow through the system. The tanks are both pressurized, and pressure is controlled via pressure regulators fitted onto the respective tanks. The flow of gas from either tank is controlled via a rotameter. Valve V-103 is adjusted to allow flow of the required gas either through the reactor or to by-pass the reactor while valve V-106 passes either the reactor effluent, or fresh feed from the respective gas tanks, through to the sampling point (SP-101) for the desired purpose of determining the SO₂ concentration at either the reactor inlet or exit.

Valves V102, V-104 & V-105 are non-return valves that are utilized to prevent back flow of the gas on the respective lines. This will prevent a scenario of pressure build-up, contamination of the feed gas tanks, as well as flow of treated gas back into the reactor thus affecting the desulfurization reaction. Valve V-107 directs the flow of process gas to either atmosphere via the vent line during determination of the inlet SO₂ concentration or to the dreschel bottles (D-101/2/3) in the water bath (B-101) during the desulfurization reaction, for subsequent SO₃ analysis.

4.5) REACTOR WASHING

With respect to the cleaning of stainless steel, the term ‘pickling’ refers to the removal of a surface contaminant (scale) with the use of an appropriate acidic cleaning agent. The most commonly utilized acids for the pickling process are nitric acid (HNO_3), hydrofluoric acid (HF), sulfuric acid (H_2SO_4) and hydrochloric acid (HCl) (Institute, 1998). HNO_3 is known to display corrosion resistant qualities but it does not effectively remove scale from a stainless-steel surface. HF, H_2SO_4 and HCl conversely, are capable of effectively removing scale deposit however, render the underlying metal surface prone to corrosive attack (Institute, 1998). For this reason, a combination of HNO_3 and either HF, H_2SO_4 or HCl is used in solution as the acidic pickling agent since it not only removes scale deposit but also provides the exposed metal surface with corrosion resistant properties. The most commonly utilized acidic agent is a combination of HNO_3 and HF ((Institute, 1998)).

A dilute aqueous solution of H_2SO_4 is also commonly implemented in the pickling process. This serves as a preliminary descaling step by initiating a quick initial attack on the scale deposit leading to ease in the removal of scale during implementation of the subsequent HNO_3 -HF solution.

For low carbon based stainless steel, such as stainless steel 316L utilized in this study, the following washing procedure is usually implemented (Institute, 1998):

1. A steel water bath under temperature control is filled with an 8.5% (vol) H_2SO_4 aqueous solution and the temperature of the bath set to 70°C. The tubular reactor is submersed in the solution for approximately 5 minutes. This serves as the preliminary wash.
2. Once this is completed the reactor is removed from solution and submersed in a second steel water bath (pure H_2O), maintained at 70°C via temperature control, for 5 minutes. This serves as an intermediate rinsing step for removal of loose scale deposit present on the reactor stainless steel surface, from the preliminary wash.
3. A third steel water bath is filled with a combination of 10% (vol) HNO_3 and 4% (vol) HF aqueous solution. This solution is utilized at room temperature. Following the intermediate rinse, the reactor is placed into this solution for approximately 20 minutes. Whilst in solution the reactor is scrubbed with a brush to aid in the removal of remaining scale deposit.
4. Once this is completed the reactor is removed from solution and again submersed in the water bath (pure H_2O), maintained at 70°C via temperature control, for 5 minutes. This serves as a final rinse for the removal of any remaining loose scale deposits present on the reactor stainless steel surface.

4.6) EXPERIMENTAL PROCEDURE

The experimental procedure can be separated into 2 phases: 1) Sulfur Dioxide (SO_2) Phase & 2) Sulfur Trioxide (SO_3) Phase.

4.6.1) SULFUR DIOXIDE (SO_2) PROCEDURE

1. The furnace, under temperature control, heats the reactor tube to the desired operating temperature (700°C-900°C). Heating of furnace takes approximately 2 hours since this is the time it takes the controller to stabilize to the desired set point temperature (response time of the controller).
2. Once set point is reached the flue gas, which contains approximately 2073 ppmv SO_2 , is allowed to flow through the bypass line through to the sampling point, SP-101, by adjusting valves V-101, V-103 & V-106 accordingly. Thereafter inlet concentration is measured every 10 seconds for 5 minutes by extracting 1ml samples from the sample point, SP-101, and injecting this into the GC sample injection point, to obtain an average SO_2 inlet concentration. A suitable flue gas inlet flowrate of 6L/min was chosen based on the residence time through the furnace bed.
3. Thereafter the flue gas flows through the limestone sorbent packed bed by appropriately adjusting the valve V-103, allowing desulfurization to occur. The reactor effluent (treated gas) then proceeds to the SO_2 sampling point, SP-101, by re-directing valve V-106 to the reactor effluent line. Readings are recorded every 10 seconds by extracting 1ml samples from the sample point, SP-101, and injecting this into the GC sample injection point, to obtain the reactor effluent SO_2 concentration. Sample extraction is terminated when the sorbent is 100% spent (i.e.: sorbent saturation is achieved).
4. Following desulfurization, inert helium gas is allowed to pass through the system via adjustment of valve V-101. This action is performed to purge the system and flush out any traces of SO_2/SO_3 within the system. The inert helium will also bubble through the isopropanol solution to remove trace amounts of SO_2 that may have absorbed into the isopropanol solution which may cause bias results during the SO_3 titration analysis.
5. Lastly, the treated reactor effluent gas proceeds into a series of 3 interconnected dreschel bottles (D-101/2/3) set up to prepare samples for SO_3 analysis (via titration). This occurs for the entire run time of the experiment. The dreschel bottles are submerged in an ice bath (B-101) to allow any SO_3 (in the form of H_2SO_4) to condense and absorb into the isopropanol solution. The dreschel bottle solutions are then collected for further analysis to determine the amount of SO_3 produced (see Chapter 4.6.2.3 for titration procedure).

4.6.2) SULFUR TRIOXIDE (SO_3) PROCEDURE

This procedure was adapted from (Jaworowski & Mack, 1979). Quantities utilized for titrations and to generate the respective solutions required were scaled accordingly for this study.

4.6.2.1) CHEMICAL PREPARATION

- **Preparation of solutions for analysis**

- An 80% isopropanol (IPA) solution was prepared by mixing 800ml IPA with 200ml water.
- A 50% isopropanol (IPA) solution was prepared by mixing 500ml IPA with 500ml water.
- 100ml of the 80% IPA was deposited into each of the 3 dreschel bottles.

- **Preparation of Thorin indicator**

- Approximately 0.2g of thoron powder was dissolved in 100ml of water.

- **Preparation of $\text{Ba}(\text{ClO}_4)_2$ solution -0.01N (Nomality)**

- Approximately 1.95g of $\text{Ba}(\text{ClO}_4)_2$ powder was dissolved in 200ml of water and diluted to 1 litre with IPA.

4.6.2.2) BARIUM PERCHLORATE STANDARDIZATION

- The standardization of $\text{Ba}(\text{ClO}_4)_2$ was carried out against a standard solution of 0.02N H_2SO_4 .
- 10ml of H_2SO_4 was added into a 250ml Erlenmeyer flask.
- 40ml of 100% IPA was added with approximately 2-4 drops of thoron indicator.
- Thereafter the solution was titrated using the $\text{Ba}(\text{ClO}_4)_2$ solution prepared until the pink end-point was reached.
- The titration was repeated using another aliquot of 0.02N H_2SO_4 and an average of the titration values was determined.
- A blank titration was also undertaken by replacing the 10ml of H_2SO_4 with 10 ml of water. The 10 ml of water was deposited into a 250ml Erlenmeyer flask.
- 40ml of 100% IPA was added with approximately 2-4 drops of thoron indicator.

- Thereafter the solution was titrated using the Ba(ClO₄)₂ solution prepared until the light/rose pink end-point was reached.
- The blank titration was repeated, and an average of the titration values was determined. All replicate values agreed to within 1%.
- Calculate the normality of Ba(ClO₄)₂ as follows (see Appendix B-1.2):

$$\text{BaClO}_4 \text{ Molarity} = \frac{\text{Vol.H}_2\text{SO}_4 \times \text{Molarity H}_2\text{SO}_4}{[\text{Avg. Vol.from H}_2\text{SO}_4 \text{ Titration} - \text{Avg.Vol.from H}_2\text{O Titration}]} \quad (4.1)$$

- If the normality achieved was not 0.01N of Ba(ClO₄)₂, a new Ba(ClO₄)₂ solution must be prepared with a smaller or larger mass of Ba(ClO₄)₂. 3H₂O depending on whether the normality calculated is larger or smaller than 0.01N.

4.6.2.3) TITRATION PROCEDURE

The following reaction governs the titration (Frieg, et al., 2012):



- The contents of each dreschel bottle was transferred into a 250ml volumetric flask.
- The glassware was rinsed with 50% IPA into the volumetric flask. This was done 3 times.
- The sample was thereafter diluted to 250ml with 50% IPA, stopped and mixed well.
- 25ml aliquots of the IPA samples were transferred from the volumetric flasks into a 100ml Erlenmeyer flask.
- 32.5ml of 100% IPA was added to each aliquot and mixed thoroughly.
- Approximately 2-4 drops of thoron indicator were added to the sample.
- The solution was titrated against the standardized 0.01M Ba(ClO₄)₂ until the light/rose pink end-point was reached.
- All volumes were recorded to the nearest 0.02ml.
- The titration was repeated with a second and third sample of aliquot and an average value was determined. The replicate titrations agreed to within 1%.

CHAPTER 5: RESULTS AND DISCUSSION

5.1) GAS CHROMATOGRAPH (GC) CALIBRATION

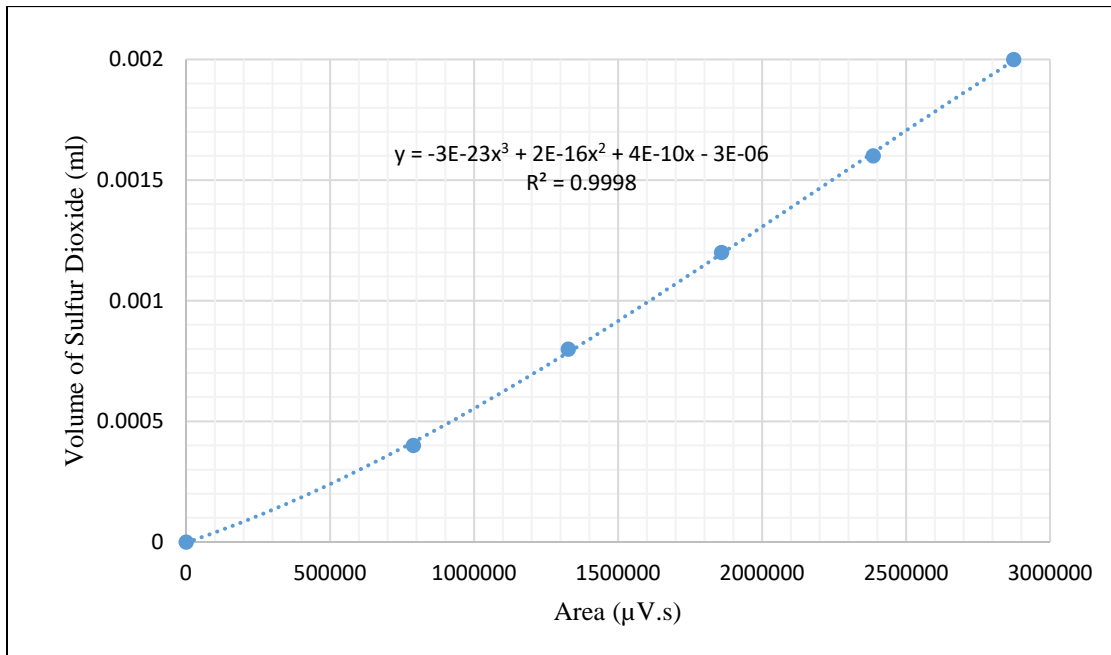


Figure 5. 1: Calibration curve

Table 5. 1: Flue-Gas tank composition

Flue Gas Tank	
Chemical Component	Certified Amount
Sulphur Dioxide	2073 ppm
Oxygen	20.0%
Nitrogen	Balance

To assess the amount of desulfurization that had taken place for subsequent experimental runs, the concentration of sulfur dioxide (SO_2) had to be determined at the reactor inlet and reactor outlet. The concentration of SO_2 was analyzed using the gas chromatograph (GC) unit. Calibration of the GC was thus required to enable quantification of the SO_2 concentration profile at the requisite reactor locations, i.e.: inlet & outlet.

The calibration plot was constructed by injecting increasing volumes of a 2073 ppmv SO_2 flue gas (Table 5.1), utilizing a 1 milliliter SGE type gas syringe, into the GC. The samples injected ranged from 0.2ml to 1ml and were extracted from the sampling point, SP-101 (Figure 4.2). For each sample injected the GC outputs a chromatogram with an associated area, representative of the SO_2 concentration. The area underneath the chromatograms were read off directly from the ‘GC solution’ program, installed on the computer (PC) attached to the GC (Figure 4.4), and recorded. Three areas, each from a separate calibration run, were recorded for each sample volume injected.

A plot of average chromatogram area ($\mu\text{V} \cdot \text{s}$) vs SO_2 gas volume (ppmv) was then constructed to obtain the calibration curve displayed in Figure 5.1. Upon non-linear regression utilizing the Microsoft Excel function, a third-degree polynomial was found to best fit the data of this plot. The calibration data utilized to generate Figure 5.1 is tabulated in Table A-1.

It is mentioned above that an ‘average’ chromatogram area was utilized to generate the calibration curve. Since calibration samples were extracted from sampling point SP-101 and injected into the GC manually, the presence of human error must be considered. To this end, three samples were extracted for each gas volume utilized to generate the calibration curve; a consequence of three separate calibration runs being performed. This resulted in three chromatogram areas for each respective gas volume. An average chromatogram area was thereafter calculated. This average area was subsequently utilized to generate the calibration curve thus accounting for any variances due to human error. These areas are displayed in Table A-1.

The calibration plot is represented by five data points. To evaluate intermediate SO_2 gas volumes, a third-degree polynomial was determined. The R^2 correlation co-efficient was calculated to be 0.9998. Since this value is very close to unity, it implies that the fitted curve will accurately determine SO_2 volumes within the specified data range. To ascertain this implication, absolute uncertainties were calculated for the respective data points utilized to generate the third order polynomial. From Table A-1, it can be seen that these absolute uncertainties are of the order of 10^{-5} ml. This further indicates that there is a minute difference between observed SO_2 gas volume data and that predicted by the third-degree polynomial; this in turn corresponds with a correlation co-efficient close to unity. The absolute uncertainty was incorporated into

the calibration plot as error bars however, due to its negligible order of magnitude (10^{-5} ml), the error bars cannot be viewed.

5.2) DEAD TIME RUN

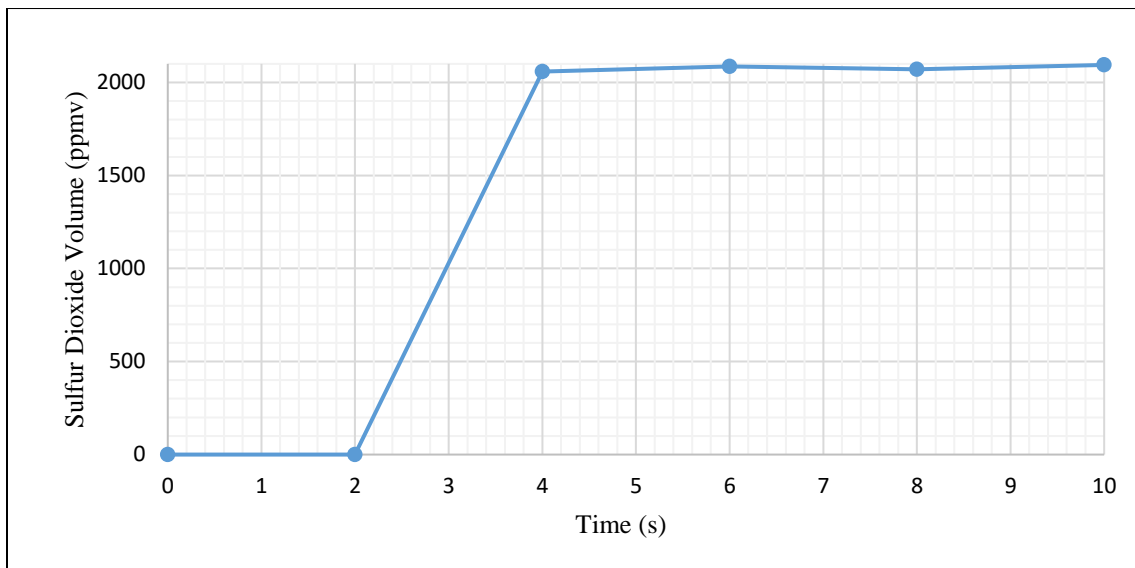


Figure 5. 2: Dead time run curve

A dead time run was performed to determine the time taken for the flue gas to propagate from the flue gas tank exit, V-101, to the sampling point, SP-101. The reactor was packed with limestone however the temperature was not raised to that at which desulfurization could take place in the presence of limestone thus the delay was due only to the flow of gas through the system.

1ml samples were extracted and injected into the GC every two seconds and the outputted chromatogram areas recorded. Utilizing the calibration curve, SO₂ concentrations were further calculated. The time at which the SO₂ concentration at the sampling point is approximately equal to the SO₂ concentration of the flue gas tank, was taken to be the dead time. From Figure 5.2 it can be seen that the dead time resides between two and four seconds.

Due to a two second restriction on the minimum time required to withdraw successive samples from the sampling point, SP-101, a higher time resolution could not be achieved. An average dead time of three seconds was thus selected.

For subsequent experiments, the dead time was incorporated in order to determine the most accurate SO₂ concentration at time t = 0 seconds.

5.3) LIMESTONE SORBENT

Table 5. 2: Sorbent particle size analysis

Sieve Size (μm)	Mass Retained (g)	Retained percent (%)	Cumulative Mass Retained (g)	Cumulative percent (%)	Pass Percentage (%)
750	0,00 \pm 0,01	0,00 \pm 0,07	0,00 \pm 0,01	0,00 \pm 0,07	100,00 \pm 0,07
+500-750	4,80 \pm 0,01	32,00 \pm 0,07	4,80 \pm 0,01	32,00 \pm 0,07	68,00 \pm 0,07
+355-500	2,86 \pm 0,01	19,07 \pm 0,07	7,66 \pm 0,01	51,07 \pm 0,07	48,93 \pm 0,07
+250-355	2,70 \pm 0,01	18,00 \pm 0,07	10,36 \pm 0,01	69,07 \pm 0,07	30,93 \pm 0,07
+212-250	1,04 \pm 0,01	6,93 \pm 0,07	11,40 \pm 0,01	76,00 \pm 0,07	24,00 \pm 0,07
+180-212	0,80 \pm 0,01	5,33 \pm 0,07	12,20 \pm 0,01	81,33 \pm 0,07	18,67 \pm 0,07
+45-180	2,80 \pm 0,01	18,67 \pm 0,07	15,00 \pm 0,01	100,00 \pm 0,07	0,00 \pm 0,07
-45	0,00 \pm 0,01	0,00 \pm 0,07	15,00 \pm 0,01	100,00 \pm 0,07	0,00 \pm 0,07

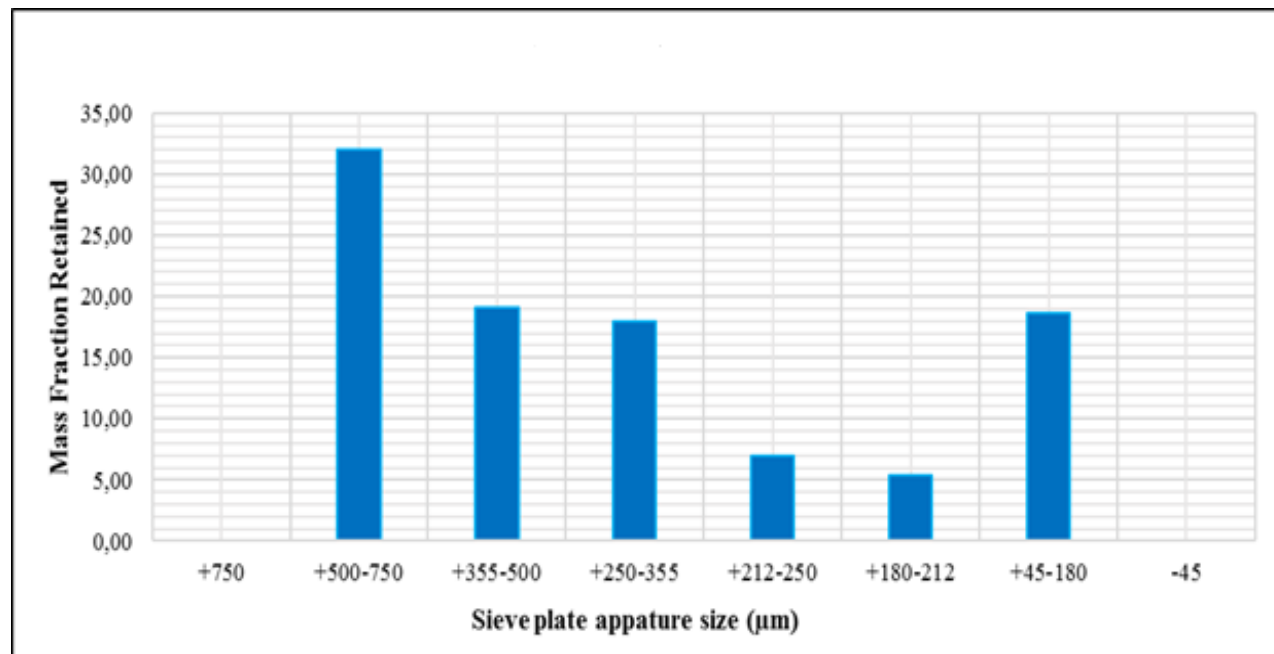


Figure 5. 3: Sorbent particle size distribution

Table 5. 3: Sorbent composition

Chemical Reagent	Composition (wt%)
White Powder Assay	99.5
Ca(OH) ₂	0.01
HCl- insoluble matter	0.005
NH ₄ OH	0.005
Chloride (Cl)	0.001
Nitrate (NO ₃)	0.005
Sulphate (SO ₄)	0.005
Heavy Metals (Pb)	0.0005
Arsenic (As)	0.0005
Iron (Fe)	0.001

Characterization of the limestone sorbent became pertinent since factors such as particle size and the presence of impurities are known to affect the capacity of sulfur capture by limestone sorbent during flue gas desulfurization (Chan, et al., 1970).

- Impurities

Table 5.3 displays a breakdown of the comoposition of limstone sorbent used, as provided by the manufacturer. It can be seen that the total concentration of impurities amount to 0.5%. This is substantially low when compared to the concentration of white poweder assay (99.5%). Therefore the effect of impurites on the desulfurization capacity of the sorbent can be considered neglegible.

- Particle Size Analysis

Particle size analysis of the limestone sorbent utilized was undertaken by means of a sieve tray analysis. The results obtained are presented in Table 5.2. It can be seen that the limestone particle size ranges from +45μm to +500μm. Figure 5.3 illustrates the particle size distribution that was achieved. It is observed that a large mass fraction (32wt%) of particles is retained within the +500μm screen. Particle mass fractions decrease gradually until the +45μm screen where it was observed that a considerable amount (18.67wt%) of finely ground particles (almost powder like) had deposited. Due to the presence of larger particle sizes (+500μm fraction) other analysis techniques such Laser Diffraction particle sizing proved difficult. A mean particle size of 362.76μm was calculated.

5.3) SULFUR DIOXIDE REMOVAL (DESULFURIZATION)

5.3.1) X-RAY DIFFRACTION (XRD) TEST

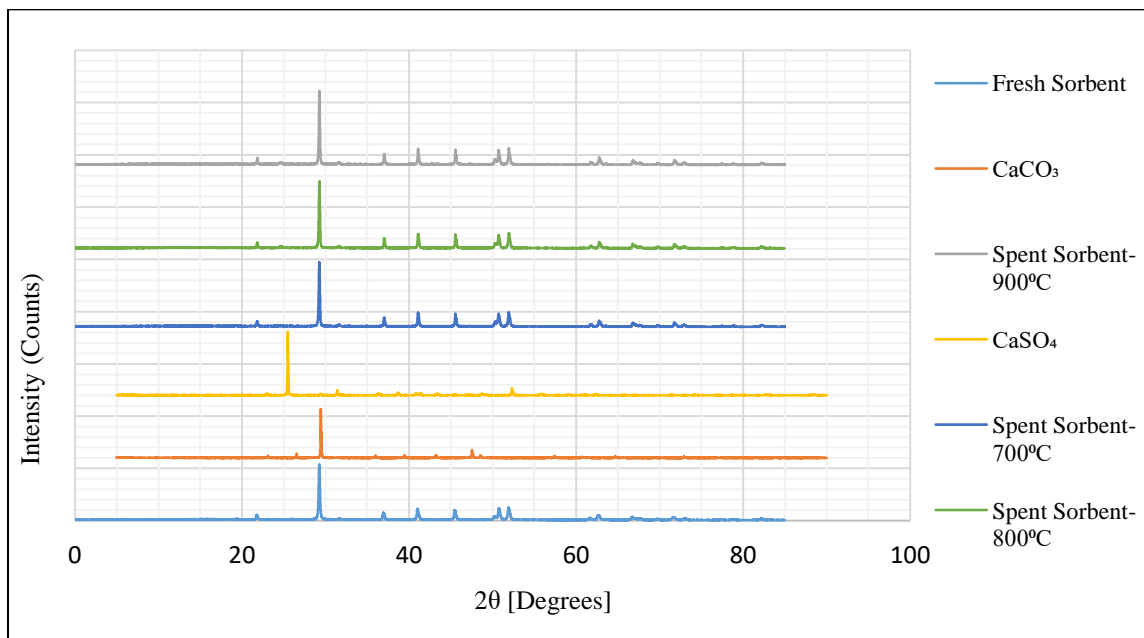


Figure 5. 4: XRD pattern for fresh sorbent and spent sorbent – run 1

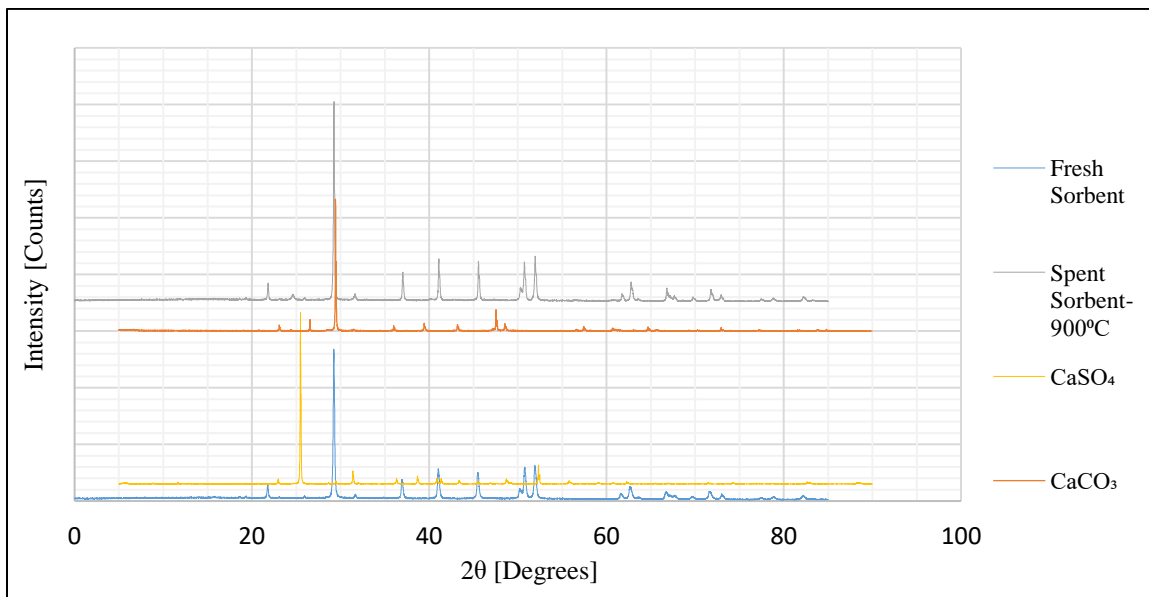


Figure 5. 5: XRD pattern for fresh sorbent and spent sorbent at 900°C – run 1

An XRD test provides an assessment of the mineralogical content of a sample. Such a test was performed on fresh sorbent (prior to reaction), calcium carbonate (CaCO_3), calcium sulfate (CaSO_4) and spent sorbent (post-reaction), for the experimental operating temperature range of 700°C to 900°C. Samples of spent sorbent were collected after completion of the respective runs.

According to Figure 5.4, fresh sorbent and CaCO_3 share common peaks at 29, 32, 37, 63 and 67 degrees 2 theta. This indicates that the ‘white powder assay’ component constituting 99.5wt% of the fresh sorbent makeup, as displayed in Table 5.3, is essentially calcium carbonate (limestone).

From Figure 5.4 it can also be seen that the spent sorbent (for all temperatures) and calcium sulfate share a peak at 31 and 52 degrees 2 theta. This confirms that there is in fact formation of a calcium sulfate product as per the desulfurization reaction represented by Equation 3.2.

Due to the large number of samples tested, resulting in a broad intensity scale, it may be difficult to view the identical peaks between fresh sorbent/calcium carbonate and spent sorbent/calcium sulfate displayed in Figure 5.4. Figure 5.5 excludes spent sorbent patterns at 800°C and 900°C to minimize the range of the intensity scale and thus better view these similar peaks.

It should be noted that the XRD test was performed for all runs (run 1, run 2 and run 3) however, only run 1 test results are displayed. This is because XRD test results for run 2 and run 3 are nearly identical to that of run 1. The reason for this can be attributed to the great similarity in desulfurization data (response curve data) of run 1, run 2 and run 3; such similar transient data, between the respective runs, is indicative of a nearly identical reaction of the fresh sorbent with SO_2 . This similarity was quantified in terms of an ‘average relative uncertainty’ which indicates that there is a minimal deviation between desulfurization data of run 1 and the subsequent repeatable runs i.e.: run 2 and run 3. The quantitative analysis is further discussed in section 5.3.2.

5.3.2) BREAKTHROUGH CURVES: EXPERIMENTAL & MODEL RESULTS

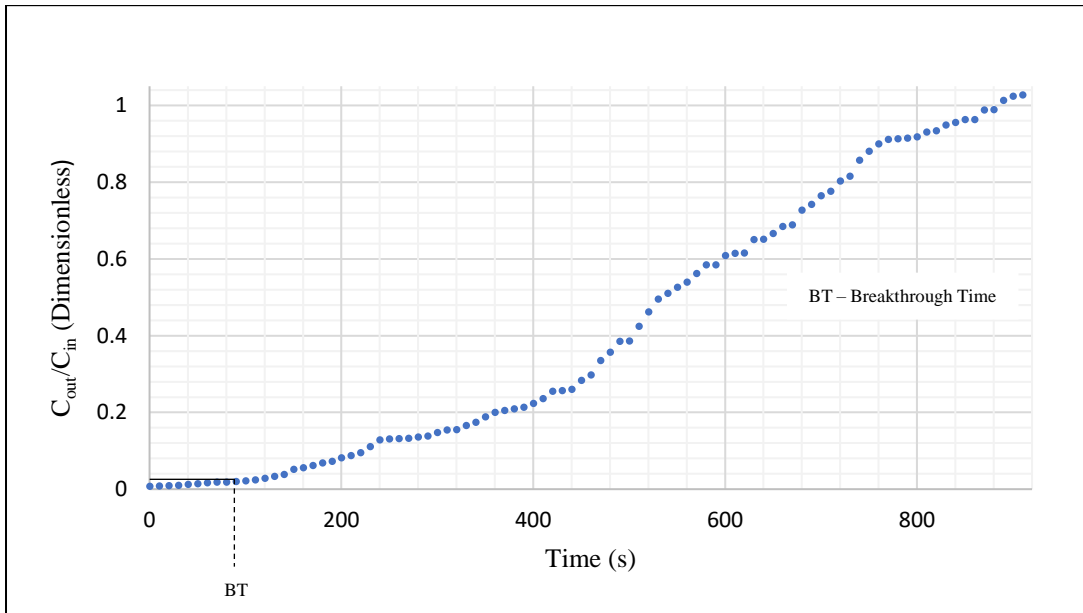


Figure 5. 6: Breakthrough curve representative of SO_2 sorption - 700°C run 1

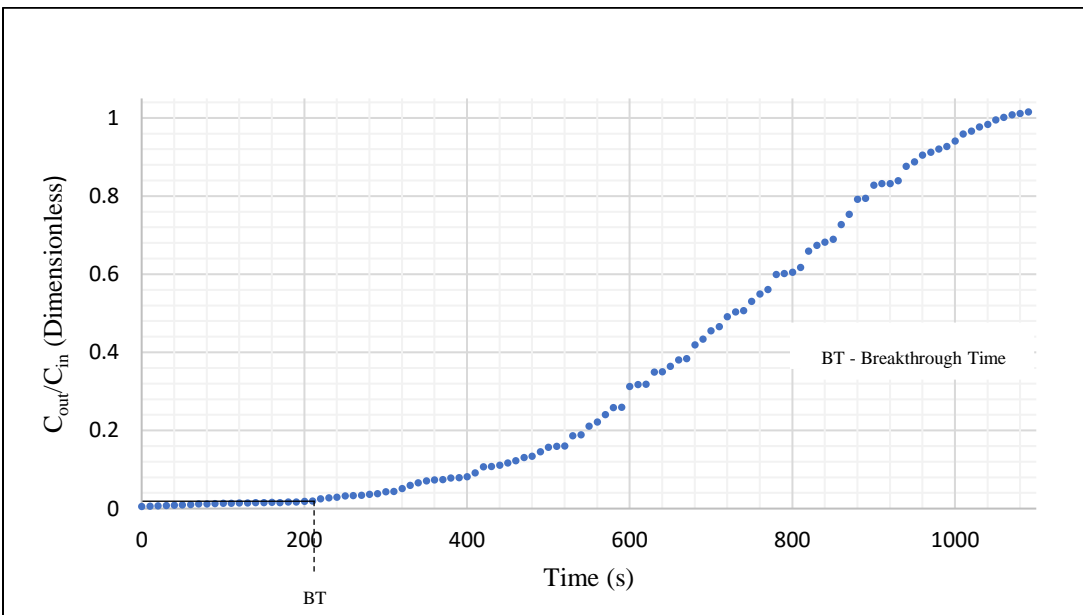


Figure 5. 7: Breakthrough curve representative of SO_2 sorption - 800°C run 1

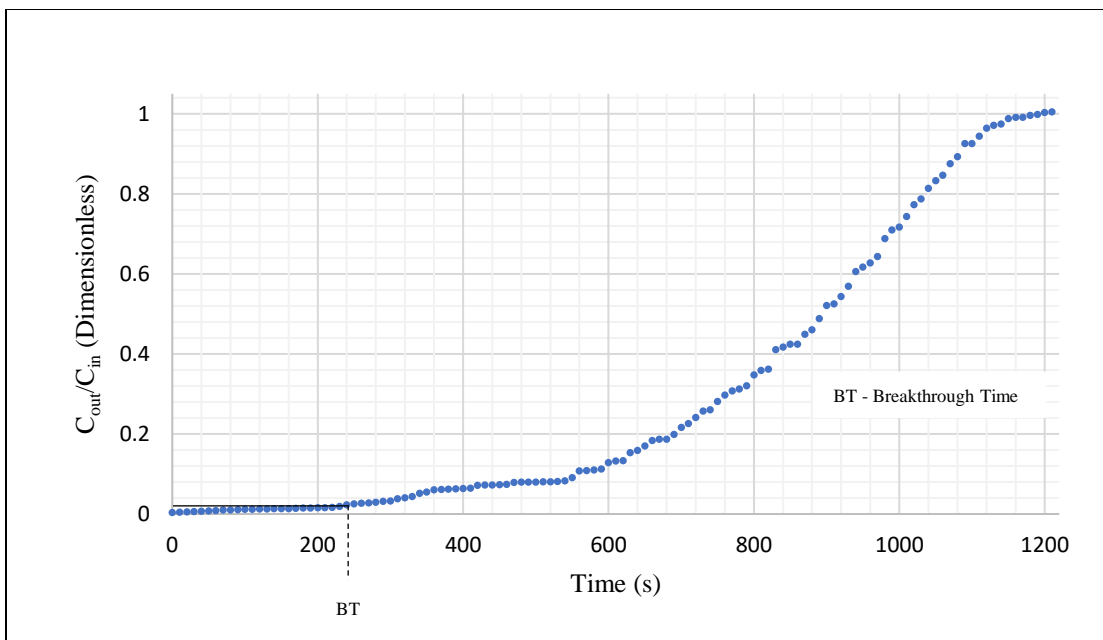


Figure 5.8: Breakthrough curve representative of SO_2 sorption - 900°C run 1

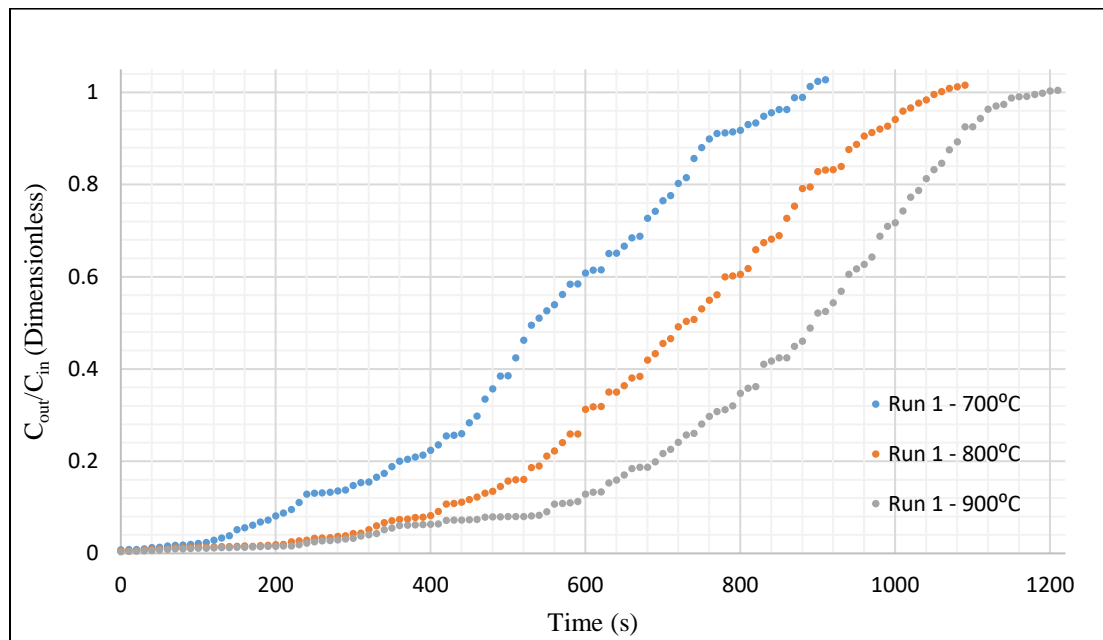


Figure 5.9: Effect of temperature on Breakthrough

Table 5. 4: Breakthrough time and saturation time - 700°C

	Breakthrough Time (sec)	Saturation Time (sec)
Run 1	100	890
Run 2	90	900
Run 3	90	890

Table 5. 5: Breakthrough time and saturation time - 800°C

	Breakthrough Time (sec)	Saturation Time (sec)
Run 1	210	1060
Run 2	210	1060
Run 3	210	1070

Table 5. 6: Breakthrough time and saturation time - 900°C

	Breakthrough Time (sec)	Saturation Time (sec)
Run 1	240	1200
Run 2	240	1190
Run 3	240	1180

Table 5. 7: Breakthrough curve data average relative deviation

	$\frac{\sum_{k=1}^n (\frac{y_{1,k} - y_{2,k}}{y_{1,k}})_{\ell} }{n}$	$\frac{\sum_{k=1}^n (\frac{y_{1,k} - y_{3,k}}{y_{3,k}})_{\ell} }{n}$
Run 1/Run 2 Avg. Relative Deviation		Run1/Run 3 Avg. Relative Deviation
700°C	2.56%	2.47%
800°C	3.41%	3.21%
900°C	3.71%	3.93%

Table 5. 8: SO₂ molar and mass based sulfur analysis - 700°C

	Inlet Moles SO ₂ (mols)	Inlet Mass of Sulfur from SO ₂ (grams)	Outlet Moles SO ₂ (mols)	Outlet Mass of Sulfur from SO ₂ (grams)	Mass of Inlet Sulfur Desulfurized [%]	Mass of Inlet Sulfur Unreacted [%]
Run 1	0,00271	0,08677	0,00106	0,03404	57.53	39.23
Run 2	0,00272	0,08709	0,00107	0,03430	57.39	39.38
Run 3	0,00271	0,08698	0,00107	0,03435	57.25	39.49

Table 5. 9: SO₂ molar and mass based sulfur analysis - 800°C

	Inlet Moles SO ₂ (mols)	Inlet Mass of Sulfur from SO ₂ (grams)	Outlet Moles SO ₂ (mols)	Outlet Mass of Sulfur from SO ₂ (grams)	Mass of Inlet Sulfur Desulfurized [%]	Mass of Inlet Sulfur Unreacted [%]
Run 1	0,00275	0,08809	0,00099	0,03177	58.32	36.07
Run 2	0,00276	0,08835	0,00100	0,03209	58.11	36.32
Run 3	0,00277	0,08870	0,00100	0,03210	58.24	36.19

Table 5. 10: SO₂ molar and mass based sulfur analysis - 900°C

	Inlet Moles SO ₂ (mols)	Inlet Mass of Sulfur from SO ₂ (grams)	Outlet Moles SO ₂ (mols)	Outlet Mass of Sulfur from SO ₂ (grams)	Mass of Inlet Sulfur Desulfurized [%]	Mass of Inlet Sulfur Unreacted [%]
Run 1	0,00278	0,08929	0,00088	0,02811	59.22	31.48
Run 2	0,00279	0,08955	0,00089	0,02842	59.01	31.74
Run 3	0,00278	0,08929	0,00089	0,02843	58.83	31.84

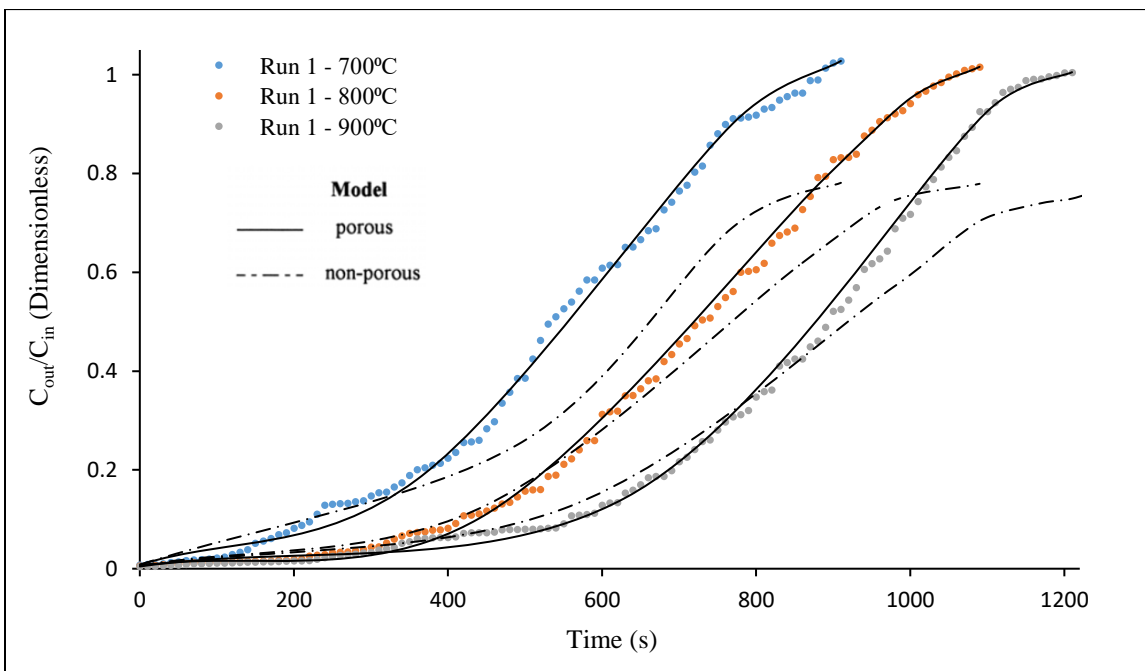


Figure 5. 10: Effect of temperature on Breakthrough - model results vs run 1 experimental data

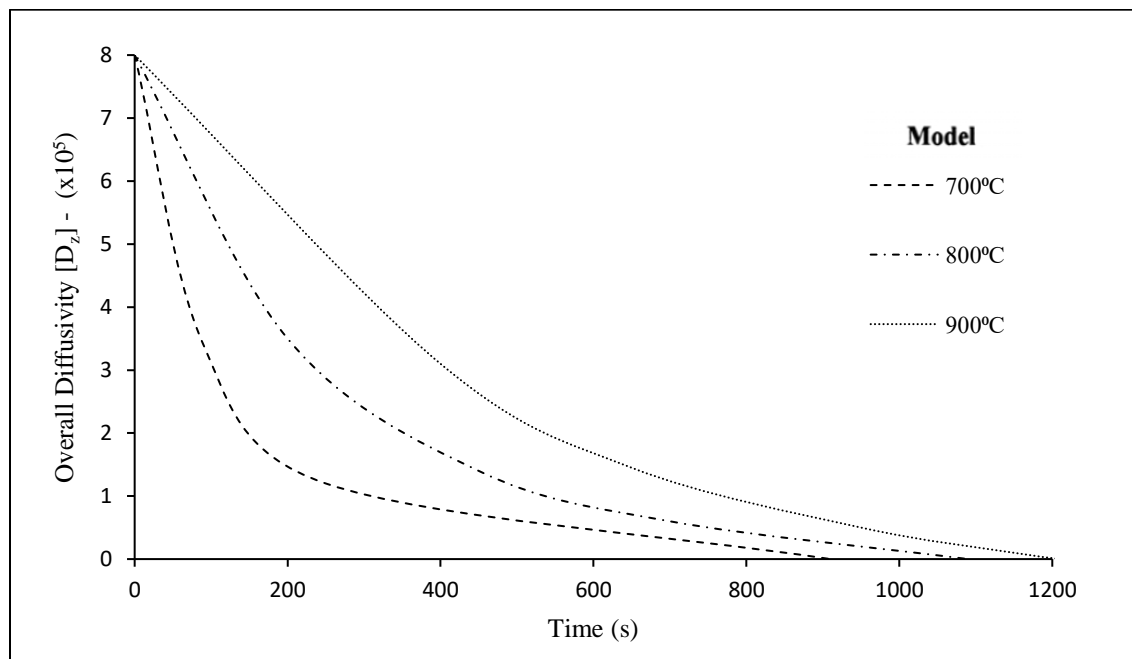


Figure 5. 11: Model prediction - variation in overall diffusivity during SO₂ sorption by porous sorbent

In the current study, limestone sorbent is calcined upon exposure to the elevated experimental operating temperatures, to produce larger surface area CaO. This CaO will subsequently react with SO₂ according to the reaction represented by Equation 3.2 (desulfurization reaction). Model simulations were carried out, assuming a non-porous as well as a porous structure of the CaO particles to explain the breakthrough characteristic of SO₂ in the sorbents bed.

As observed from Figure 5.10, the model based on non-porous structure failed to explain the experimental observations and in each case the data were under-predicted. In the model analysis for non-porous sorbents, the overall diffusivity (D_z) of SO₂ through a fixed bed of non-porous CaO particles was used as an adjustable parameter. This accounts for the net effect of diffusion through CaSO₄ products layers to the active particle surface. The values used in simulations were $8 \times 10^{-5} \frac{m^2}{s}$ at 700°C and $8 \times 10^{-4} \frac{m^2}{s}$ at 900°C. These are the same order of magnitude as values reported elsewhere for overall diffusivity of SO₂ in CaSO₄ product layers (Agnihotri, et al., 1999). Simulations utilizing a broad range of diffusivity values also did not explain the experimental observations.

Model simulations were thereafter carried out assuming a porous structure of the CaO sorbent particles. Overall diffusivity (D_z) of SO₂ through the bed of porous CaO particles was allowed to vary as an adjustable model parameter in the model analysis. This diffusion coefficient accounts for net diffusional effect through product CaSO₄ layers and the pores of porous CaO particles. As observed from Figure 5.10, there is a good agreement between model predictions and the experimental data, within a relatively conservative range of diffusivities: $0.5 \times 10^{-5} \frac{m^2}{s}$ to $8 \times 10^{-5} \frac{m^2}{s}$ - as displayed in Figure 5.11. It can thus be concluded that the particles of CaO utilized in this study are porous in nature.

Experiments were carried out to determine the effect of temperature on flue gas desulfurization (SO₂ removal). The bed height of the limestone was set at 3cm and the inlet flow was adjusted to 6L/min using the rotameter, R-101. This flowrate was chosen based on the findings of Dasgupta, et al., (2003). who state that a residence time of at least 0.3 seconds is sufficient for optimal desulfurization to occur. The residence time, under the aforementioned conditions for flowrate and bed height, was calculated to be 0.3 seconds.

From the results obtained in Figure 5.9, as the operating temperature increased, the time taken to reach breakthrough also increased. This observed trend between the breakthrough time and temperature is in keeping with trends obtained by Dasgupta, et al., (2003).

The reason for such a trend can be explained by considering the steps involved when a heterogeneous solid-gas reaction between porous CaO particles and flue gas occurs. The first step involves the diffusion of gas from the bulk gas phase to the sorbent particle surface through a stagnant boundary layer or gas film. The second step involves diffusion of the gas through the pores of the sorbent particles where a chemical reaction between SO₂ and the active site of the sorbent particle takes place. Therefore it is of vital importance to evaluate which of these steps is rate limiting.

The mass transfer co-efficient controlling gas film diffusion is determined by the particle size and flow rate. In this study the same flow rate and sorbent particles are utilized for all experiments thus the effect of gas film diffusion on the extent of sorption can be considered as identical. Gas film diffusion is therefore not the resistive step that accounted for the observed trend.

According to run 1 data in Tables 5.11, 5.12 & 5.13, only 13.50 $\frac{\text{mg of SO}_2}{\text{gram of Sorbent}}$, 16.20 $\frac{\text{mg of SO}_2}{\text{gram of Sorbent}}$ and 18.73 $\frac{\text{mg of SO}_2}{\text{gram of Sorbent}}$ of sulfur content from the initial/inlet flue gas stream is absorbed by the limestone sorbent, for operating temperatures of 700 °C, 800 °C and 900°C respectively. This implies that a considerable amount of CaO remains unreacted over the experimental temperature range being tested. A mass percent of inlet sulfur unreacted was further defined. This refers to the mass of inlet sulfur that is neither desulfurized nor converted to SO₃. Run 1 data of Tables 5.8, 5.9 & 5.10 indicate that 39.23%, 36.07% and 31.48%, of inlet sulfur content remained unreacted for operating temperatures of 700 °C, 800 °C and 900°C respectively. This information implies that an inhibiting factor exists which prevents necessary utilization of sorbent to remove all of the sulfur content entering the reactor in the form of SO₂. Dasgupta, et al., (2003) state that this inhibiting effect can be attributed to the formation of larger volume product sulfate (CaSO₄) layers, as per Equation 3.2, preventing diffusion of SO₂ through the pores and to the active sorbent particle site. From the XRD test it has been proven that the spent sorbent does in fact contain calcium sulfate (CaSO₄), thus its associated inhibiting effects, as described by Dasgupta, et al., (2003), may be applicable in this instance. Based on the model analysis results this is confirmed by the

relatively steep decline in overall diffusivity, D_z , as reaction proceeds for the various operating temperatures (see Figure 5.11). As previously mentioned, this diffusion coefficient accounts for the net diffusional effect through product CaSO_4 layers and the pores of porous CaO particles. Diffusion of SO_2 gas through product CaSO_4 layers, which ultimately inhibits pore diffusion causing incomplete utilization of the sorbent particles, is thus the rate limiting step and hence is reaction controlling.

According to the model analysis results in Figure 5.11, at lower temperatures (700°C), as the reaction proceeds there is a sharp decline in the overall diffusivity, D_z , while at higher temperatures (800°C and 900°C) larger D_z values prevail with D_z decreasing more gradually as reaction proceeds. Therefore, at higher temperatures a longer time is required for breakthrough to be achieved since the inhibiting effects associated with the decline in the D_z (prevention of the diffusion of SO_2 to the active sorbent particle sites) are not as prominent as they are for lower temperatures. This trend of an increase in breakthrough time with increasing temperature is observed from run 1 experimental results displayed in Tables 5.4, 5.5 & 5.6, with breakthrough times of 100s, 210s and 240s for operating temperatures of 700°C , 800°C and 900°C respectively.

Due to less prominent inhibiting effects associated with enhanced overall diffusivities as temperature increases, it follows that the time taken for the sorbent-gas reaction to reach completion (saturation time) should also increase with increasing temperature. Such a trend is observed with the run 1 experimental results displayed in Tables 5.4, 5.5 & 5.6, where saturation times of 890s, 1060s & 1200s are achieved for operating temperatures of 700°C , 800°C and 900°C respectively.

The variable of interest in an experiment is rarely obtained by measurement of that variable directly. It is often dependent on the measurement of other variables which have associated with them a certain degree of error. This degree of error or uncertainty consequently propagates due to further calculation in an attempt to evaluate the variable of interest.

Data points of the breakthrough curves were calculated by the transient ratio $\frac{C_{\text{out}}}{C_{\text{in}}}$, where C_{in} and C_{out} represent the volume-based concentration of SO_2 at the reactor inlet and outlet respectively.

C_{out} and C_{in} are determined entirely by the calibration curve equation, B-2. Since the calibration curve has an associated absolute uncertainty, this uncertainty will propagate through to calculation of the ratio $\frac{C_{out}}{C_{in}}$, representative of data points on the breakthrough curve. The data points will thus have an associated propagational uncertainty.

According to Harris (2015), the uncertainty which propagates through to the calculation of the quotient $\frac{C_{out}}{C_{in}}$, is a function of the relative uncertainty associated with both C_{out} and C_{in} . As previously mentioned, C_{out} and C_{in} are determined entirely by the calibration curve equation, thus the relative uncertainty in C_{out} and C_{in} is simply the average relative uncertainty associated with the calibration curve. An average relative uncertainty of 3.91% was calculated for the calibration curve. Utilizing this as the relative uncertainty in C_{out} and C_{in} , propagational uncertainties were calculated as per Equation 2.21. The results of these calculations are tabulated in Appendix A, for the respective experimental runs. It is observed that the propagational uncertainty associated with any breakthrough curve data point, irrespective of the operating temperature (700 °C, 800 °C and 900°C) or run number (1, 2 and 3), does not exceed a quantitative value of 0.06. Such insignificant values in propagational uncertainty can be attributed to the negligible absolute uncertainties associated with the calibration curve data and hence relative uncertainty in C_{out} and C_{in} , consequently resulting in such a minimal uncertainty being propagated upon further calculations associated with C_{out} and C_{in} . The propagational uncertainty was incorporated into the response curve plots as error bars however, due to its insignificant order of magnitude ($3 \times 10^{-4} < \delta\left(\frac{C_{out}}{C_{in}}\right) < 6 \times 10^{-2}$), the error bars cannot be viewed.

Based on the experimental design of Chapter 4.2, three runs were to be performed for each operating temperature. The reason for this is to determine if experimental results can in fact be replicated i.e.: are results repeatable? For repeatability to be established, the following conditions must be in place: the same location; the same measurement procedure; the same observer; the same measuring instrument, used under the same conditions; and repetition over a short period of time (Harris, 2015).

In the current study each run was performed in the same location, with the same instrumentation and measurement procedure applied. Each of the three runs were also performed relative to a

constant observer and within a relatively short time frame (48 hours). The requisite conditions to determine repeatability between results was thus satisfied. Having satisfied the necessary conditions, a suitable calculation approach was required to quantify this ‘repeatability’ between breakthrough curve data for the respective runs (i.e.: run 1, 2 & 3). To this end, an average relative uncertainty between breakthrough curve data of run 1 & run 2 and run 1 & run 3, over the operating temperature range (700 °C, 800 °C and 900°C) was calculated. This depicts the average error in breakthrough curve data between run 1 & run 2 and run 1 & run 3 respectively, for a specific operating temperature. From Table 5.7 it is observed that the calculated average relative uncertainties range between 2.5% and 3.9% over the operating temperature range. Harris (2015) states that an average relative uncertainty $\leq 5\%$ may be considered as a negligible error. Thus, the calculated average relative uncertainties of Table 5.7 are indicative of repeatable breakthrough curve data, for a given operating temperature. Consequently, trends observed from run 1 data, over the operating temperature range (700 °C, 800 °C and 900°C), will follow through to run 2 & run 3, thus response curves for run 2 & run 3 are not displayed.

5.3.3) SO₂ SORPTION CAPACITY

Table 5. 11: Limestone sorption capacity - 700°C

	Sorption Capacity $(\frac{\text{mg of SO}_2}{\text{gram of Sorbent}})$
Run 1	13.50
Run 2	13.67
Run 3	13.53

Table 5. 12: Limestone sorption capacity - 800°C

	Sorption Capacity $(\frac{\text{mg of SO}_2}{\text{gram of Sorbent}})$
Run 1	16.20
Run 2	16.37
Run 3	16.59

Table 5. 13: Limestone sorption capacity - 900°C

	Sorption Capacity $(\frac{\text{mg of SO}_2}{\text{gram of Sorbent}})$
Run 1	18.73
Run 2	18.63
Run 3	18.42

Between Tables 5.11, 5.12 & 5.13 the effect of temperature on the sorption capacity of the sorbent is displayed. As explained in Chapter 2.5, the sorption capacity provides an indication of the capability of the sorbent to absorb SO₂.

According to Chapter 2.6.1, the term “saturation time” is defined to be the time taken for the outlet concentration of SO₂ to reach the initial inlet concentration of SO₂ i.e. the time taken for the sorbent-gas reaction, represented by Equation 3.2, to reach completion.

When the sorbent-gas reaction terminates (reaches completion), so too does utilization of the sorbent due to the formation of larger volume product sulfate (CaSO₄) layers preventing diffusion of SO₂ to the active sorbent particle sites.

Since the same amount (mass) of sorbent was utilized in subsequent experiments, it follows that a shorter saturation time will result in premature termination with respect to the utilization of unreacted sorbent and hence reduced amounts of desulfurization.

From the results of Tables 5.4, 5.5 & 5.6, as temperature increases, so too does the saturation time for reaction. It is thus expected that the sorption capacity of the limestone sorbent should also increase with an increase in operating temperature. According to run 1 data in Tables 5.11, 5.12 & 5.13, sorption capacities of 13.50 $\frac{\text{mg of SO}_2}{\text{gram of Sorbent}}$, 16.20 $\frac{\text{mg of SO}_2}{\text{gram of Sorbent}}$ and 18.73 $\frac{\text{mg of SO}_2}{\text{gram of Sorbent}}$ were achieved for operating temperatures of 700 °C, 800 °C and 900°C respectively. It can thus be seen that the sorbent was utilized more effectively at higher temperatures and the expected trend of an increase in limestone sorption capacity with increasing operating temperature is adhered to.

Additionally, run 1 data of Tables 5.8, 5.9 & 5.10 indicate that 57.53%, 58.23% and 59.22% of inlet sulfur mass content was desulfurized at operating temperatures of 700 °C, 800 °C and 900°C respectively. This trend of an increase in desulfurization percent with increasing operating temperature indicates further that a greater sorption capacity is achieved with an increase in operating temperature.

5.4) SULFUR TRIOXIDE (SO_3) FORMATION

Table 5. 14: Desulfurization ratio and molar yield of SO_3 - 700°C

	Desulfurization ratio (dimensionless)	Molar Yield of SO_3 [%]
Run 1	0,947	1.62
Run 2	0,947	1.62
Run 3	0,947	1.63

Table 5. 15: Desulfurization ratio and molar yield of SO_3 - 800°C

	Desulfurization ratio (dimensionless)	Molar Yield of SO_3 [%]
Run 1	0,912	2.80
Run 2	0,913	2.79
Run 3	0,913	2.79

Table 5. 16: Desulfurization ratio and molar yield of SO_3 - 900°C

	Desulfurization ratio (dimensionless)	Molar Yield of SO_3 [%]
Run 1	0,864	4.65
Run 2	0,864	4.64
Run 3	0,863	4.67

Table 5. 17: SO_3 molar yield temperature dependence prior to reactor washing

	Molar Yield of SO_3 [%]
700°C	0.248
800°C	0.245
900°C	0.244

Table 5. 18: SO₃ molar and mass based sulfur analysis - 700°C

	Inlet Moles SO ₃ (mols)	Inlet Mass Sulfur from SO ₃ (grams)	Outlet Moles SO ₃ (mols)	Outlet Mass Sulfur from SO ₃ (grams)	Mass of Inlet Sulfur Converted to SO ₃ [%]
Run 1	0	0	0,000044	0,002808	3.24
Run 2	0	0	0,000044	0,002808	3.22
Run 3	0	0	0,000044	0,002830	3.25

Table 5. 19: SO₃ molar and mass based sulfur analysis - 800°C

	Inlet Moles SO ₃ (mols)	Inlet Mass Sulfur from SO ₃ (grams)	Outlet Moles SO ₃ (mols)	Outlet Mass Sulfur from SO ₃ (grams)	Mass of Inlet Sulfur Converted to SO ₃ [%]
Run 1	0	0	0,000077	0,004936	5.60
Run 2	0	0	0,000077	0,004921	5.57
Run 3	0	0	0,000077	0,004942	5.57

Table 5. 20: SO₃ molar and mass based sulfur analysis - 900°C

	Inlet Moles SO ₃ (mols)	Inlet Mass Sulfur from SO ₃ (grams)	Outlet Moles SO ₃ (mols)	Outlet Mass Sulfur from SO ₃ (grams)	Mass of Inlet Sulfur Converted to SO ₃ [%]
Run 1	0	0	0,000130	0,00830	9.30
Run 2	0	0	0,000130	0,00830	9.27
Run 3	0	0	0,000131	0,00833	9.33

Table 5. 21: Temperature dependence of SO₃ sulfur profile prior to reactor washing

	Inlet Moles SO ₂ (mols)	Inlet Mass of Sulfur from SO ₂ (grams)	Inlet Moles SO ₃ (mols)	Inlet Mass Sulfur from SO ₃ (grams)	Outlet Moles SO ₃ (mols)	Outlet Mass Sulfur from SO ₃ (grams)	Mass of Inlet Sulfur Converted to SO ₃ [%]
700°C	0.00270	0.08654	0	0	0,0000067	0.000217	0.251
800°C	0.00273	0.08725	0	0	0,0000067	0.000217	0.249
900°C	0.00275	0.08801	0	0	0,0000067	0.000217	0.247

The effect of temperature on the amount of SO₃ produced during high temperature flue gas desulfurization is a major objective of this study as it provides insight with respect to the actual degree of desulfurization that can be achieved.

SO₃ analysis was conducted utilizing the Isopropanol Absorption Bottle Method of Chapter 2.2.2. This method was selected over other techniques such as: Salt Method, Controlled Condensation Method or Pentol SO₃ Monitoring Method since it is easily implemented and consists of equipment and chemicals that are relatively inexpensive and readily available. The conventional Isopropanol Absorption Bottle procedure utilizes an isopropanol (IPA) solution for the absorption of SO₃ (in the form of H₂SO₄), a hydrogen peroxide solution for absorption of remaining SO₂ and a silica gel for gas drying. In this study the effluent stream exiting SO₃ analysis is vented due to the insignificant concentration of SO₂ released during the run time of experiments. There is no requirement for gas drying since the moisture content of the effluent stream is not of concern. The current experimental setup thus excludes utilization of hydrogen peroxide solutions and silica gel.

SO₂ is converted to SO₃ through either homogenous gas-phase reactions or heterogeneous catalytic reactions (Belo, et al., 2014). There is very limited data available on high temperature kinetics for the homogenous reaction of SO₂ to SO₃ in the presence of oxygen (in-bed reaction) since the reaction mechanisms and kinetics associated with the conversion are not fully understood (Smith, et al., 1982). Experiments performed by Belo, et al. (2014) however, conclude that the major factors which effect the homogenous conversion of SO₂ to SO₃ at elevated temperatures are: SO₂ partial pressure, O₂ partial pressure, moisture content and temperature.

Hamer (1986) performed experiments investigating the formation of SO₃ in a stainless steel reactor utilized as a bubbling Fluidized Bed Combustor (FBC), at elevated reaction temperatures. For an inlet SO₂ concentration of 2800 ppmv, it was found that 300 ppmv of SO₃ was present at the reactor outlet however, the formation of SO₃ in the bed itself (regardless of the sorbent utilized) was negligible. This indicates that SO₂ was heterogeneously catalysed by the stainless steel walls of the reactor to form SO₃, rather than a homogenous in-bed reaction of SO₂ with O₂ to form SO₃.

Prior to use of the tubular reactor in the current experimental setup, the reactor was utilized in an alternate study involving a thermally intensive biomass-based reaction. These reactions tended to leave behind a carbon-based scale layer on the inner walls of the reactor. This prevents contact between the reacting gas and stainless steel walls of the reactor for the current study.

In the this study the mechanism for SO₃ formation (if SO₃ is in fact produced at all) could not be confirmed prior to experimental runs i.e.: is the production of SO₃ owing to a homogenous reaction of SO₂ with O₂ or heterogeneous catalytic reaction of SO₂ with the stainless steel walls of the reactor. To this end, it was decided to first run a set of experiments over the experimental temperature range of

interest ($700\text{ }^{\circ}\text{C}$ - $900\text{ }^{\circ}\text{C}$), with the carbon-based scale layer of the alternate study present in the reactor tube. As mentioned above, this prevents contact of SO_2 with the stainless steel walls of the reactor. For the initial experiments, preceding washing of the reactor, only SO_3 analysis was performed, as per Chapter 4.6.2. From Table 5.21, the mass of sulfur entering the system which is subsequently converted to SO_3 was calculated to be 0.251%, 0.249% and 0.247% for the operating temperatures of $700\text{ }^{\circ}\text{C}$, $800\text{ }^{\circ}\text{C}$ and $900\text{ }^{\circ}\text{C}$ respectively, and SO_3 molar yields of 0.248%, 0.245% and 0.244% were calculated, as per Table 5.17, at the respective operating temperatures. Based on these minute percentages calculated it can be concluded that SO_3 formation is negligible, thus we may state with certainty that a homogenous reaction of SO_2 to SO_3 in the presence of oxygen (in-bed reaction) does not owe to the production of any appreciable amounts of SO_3 .

Although it has been determined, from experimental results preceding reactor washing, that a homogenous reaction of SO_2 to SO_3 does not owe to the production of any appreciable amounts of SO_3 , it cannot simply be assumed that the driving force for SO_3 formation at elevated temperatures of high temperature flue gas desulfurization is due to heterogeneous catalytic reaction of SO_2 with the stainless steel walls of the reactor. This is required to be proved; to prove that such is true, the stainless steel reactor was washed utilizing a typical ‘pickling’ procedure as explained in Chapter 4.5. A HF-HNO_3 solution was selected since it not only removes scale deposits from the stainless steel surface but also provides corrosion resistance to the underlying exposed surface after the scale deposit is removed. Following reactor washing (scale removal), the stainless steel surfaces of the reactor became exposed to SO_2 component of the reacting flue gas. Experiments were therefore performed, over the experimental temperature range of interest ($700\text{ }^{\circ}\text{C}$ - $900\text{ }^{\circ}\text{C}$), to determine if the presence of stainless steel leads to the formation any significant amount SO_3 via catalytic reaction with SO_2 . Based on run 1 data from Tables 5.18, 5.19 & 5.20, the mass of sulfur entering the system which is subsequently converted to SO_3 was calculated to be 3.24%, 5.60% and 9.30% for operating temperatures of $700\text{ }^{\circ}\text{C}$, $800\text{ }^{\circ}\text{C}$ and $900\text{ }^{\circ}\text{C}$ respectively. It can immediately be seen that the mass of inlet sulfur converted to SO_3 in the presence of stainless steel is orders of magnitude greater, relative to that converted to SO_3 in the absence of stainless steel (carbon-based scale layer present). This result clearly proves that the formation of SO_3 is predominantly due to the heterogeneous catalytic reaction of SO_2 with the stainless steel walls of the reactor at such elevated temperatures utilized during high temperature flue gas desulfurization.

Of significant importance from the above run 1 data is that the mass of sulfur entering the system which is subsequently converted to SO_3 increases by 2.36% for an operating temperature shift from $700\text{ }^{\circ}\text{C}$ to $800\text{ }^{\circ}\text{C}$ and by 6.06% for an operating temperature shift from $700\text{ }^{\circ}\text{C}$ to $900\text{ }^{\circ}\text{C}$. This result indicates that SO_3 formation not only increases with an increase in operating temperature, but also increases more drastically as operating temperature increases and shifts away from $700\text{ }^{\circ}\text{C}$ towards $900\text{ }^{\circ}\text{C}$.

Based on the above observation it is expected that the SO₃ molar yield should also increase in a similar fashion and a greater difference between the actual degree of desulfurization and apparent degree of desulfurization should be realized as operating temperature increases and shifts away from 700 °C towards 900 °C (expressed by a desulfurization ratio straying away from unity). From run 1 data of Tables 5.14, 5.15 & 5.16, SO₃ molar yields of 1.62%, 2.80% and 4.65% were calculated for operating temperatures of 700 °C, 800 °C and 900°C respectively while desulfurization ratios of 0.947, 0.912 and 0.864 % were calculated for operating temperatures of 700 °C, 800 °C and 900°C respectively. The results obtained therefor adhere to the expected trend.

In this discussion only run 1 data was examined and trends established based on this data. The reason for this is simply because data for runs 2 & 3 are nearly identical to that of run 1. This can be viewed from the tabulated data presented above. The trends established between the respective operating temperatures for run 1 will thus follow through to runs 2 & 3.

Considering the experimental results realized, one might be inclined to operate utilizing reactor material other than stainless steel since SO₃ formation may not be an issue. Alternate materials however may be more expensive and not as readily available as stainless steel. Additionally, due to presence of H₂SO₄ which is corrosive in nature, stainless-steel is a requirement. Based on the experimental results it is therefore suggested to operate at a temperature of 700°C since similar performance is achieved in terms of SO₂ removal, relative to 800 °C and 900 °C, while SO₃ production is minimal in the presence of stainless steel.

CHAPTER 6: CONCLUSIONS

- Upon non-linear regression utilizing the Microsoft Excel function, a third-degree polynomial was found to best fit the calibration data relating SO₂ gas volume (ml) to chromatogram area (μV.s). To account for human error implicated with sample extraction and injection, multiple calibration runs were undertaken, and an average of the run areas utilized to generate the calibration plot.
- The third-degree polynomial accurately represents the calibration curve data within the specified data range as expressed by the squared correlation coefficient (R^2) ~ 1 and minute absolute uncertainties calculated (order of 10⁻⁵ ml).
- A dead time of three seconds was experimentally determined for the flue gas to propagate from the flue gas tank exit, V-101, to the sampling point, SP-101.
- The effect of impurities on the desulfurization capacity of the limestone sorbent can be considered negligible due to the minute concentration of impurities present (0.5wt%). From results of the sieve tray analysis a mean particle size of 362.76μm was calculated.
- The XRD test dictates that the ‘white powder assay’ component constituting 99.5wt% of the fresh sorbent makeup, as displayed in Table 5.3, is essentially calcium carbonate (limestone). The test also confirms the presence of larger volume calcium sulfate (CaSO₄) layers on the spent sorbent.
- The results of the model analysis reveal that the morphological structure of the sorbent surface is best described as porous in nature.
- Experimental results for SO₂ removal indicate that breakthrough time, saturation time and SO₂ sorption capacity of sorbent all increase with an increase in operating temperature. This trend is attributed to a more gradual decline in overall diffusivity (D_z) with increasing operating temperature, as expressed by the model analysis results of Figure 5.11. Run 1 experimental data revealed:
 - Breakthrough times of 100s, 210s and 240s for operating temperatures of 700 °C, 800 °C and 900°C respectively.
 - Saturation times of 890s, 1060s & 1200s are achieved for operating temperatures of 700 °C, 800 °C and 900°C respectively.
 - SO₂ sorption capacities of 13.50 $\frac{\text{mg of SO}_2}{\text{gram of Sorbent}}$, 16.20 $\frac{\text{mg of SO}_2}{\text{gram of Sorbent}}$ and 18.73 $\frac{\text{mg of SO}_2}{\text{gram of Sorbent}}$ for operating temperatures of 700 °C, 800 °C and 900°C respectively.

- Relatively low conversions achieved by the limestone particles (low sorption capacities), as per Tables 5.11, 5.12 and 5.13, can be attributed to:
 - High percentage of larger particles present (bigger than 250 μm) - larger particles exhibit a greater diffusion path length leading to incomplete utilization of the particles available internal surface area.
 - Small pore radius - small pore radii attribute to pore blockage due to the formation of larger volume product CaSO_4 layers.
- Error associated with breakthrough curve data was quantified in terms of a propagational uncertainty, $\delta(\frac{C_{\text{out}}}{C_{\text{in}}})$. $3 \times 10^{-4} < \delta(\frac{C_{\text{out}}}{C_{\text{in}}}) < 6 \times 10^{-2}$ for all experimental breakthrough curve data. This error is negligible.
- Run 2 & run 3 were performed to determine repeatability of run 1 breakthrough data. Average relative uncertainties ranging between 2.5% and 3.9% were calculated. According to Harris (2015), an average relative uncertainty $\leq 5\%$ may be considered as a negligible error. Breakthrough curve data for subsequent experimental runs is thus repeatable. Trends observed from run 1 data, over the operating temperature range (700 °C, 800 °C and 900°C), therefore follows through to run 2 & run 3, hence response curves for run 2 & run 3 are not displayed.
- Run 1 experimental data for SO_3 formation reveals:
 - In the absence of stainless steel the mass of sulfur entering the system which is converted to SO_3 was calculated to be 0.251%, 0.249% and 0.247% for the operating temperatures of 700 °C, 800 °C and 900°C respectively. In the presence of stainless steel the mass of sulfur entering the system which is converted to SO_3 was calculated to be 3.24%, 5.60% and 9.30% for operating temperatures of 700 °C, 800 °C and 900°C respectively. The formation of SO_3 is thus predominantly due to the heterogeneous catalytic reaction of SO_2 with the stainless steel walls of the reactor.
 - In the presence of stainless steel SO_3 molar yields of 1.62%, 2.80% and 4.65% were calculated for operating temperatures of 700 °C, 800 °C and 900°C respectively while desulfurization ratios of 0.947, 0.912 and 0.864 % were calculated for the same operating temperatures.
 - Of significant importance is that in the presence of stainless steel the mass of sulfur entering the system which is converted to SO_3 increases by 2.36% for an operating temperature shift from 700 °C to 800 °C and by 6.06% for an operating temperature shift from 700 °C to 900 °C. This result indicates that SO_3 formation not only increases with an increase in operating temperature, but also increases more drastically as operating temperature increases and shifts away from 700 °C towards 900 °C.
 - Due to presence of H_2SO_4 which is corrosive in nature, stainless-steel is a requirement. Based on the experimental results it is therefore suggested to operate at a temperature of

700°C since similar performance is achieved by the sorbent in terms of SO₂ removal, relative to 800 °C and 900 °C, while SO₃ production is minimal in the presence of stainless steel.

- Experimental data for run 2 & run 3 are nearly identical to run 1. This can be viewed in the tabulated data of Chapter 5.4. The trends applicable to run 1 thus follows through to run 2 & run 3.

CHAPTER 7: RECOMMENDATIONS

To further improve on the research undertaken in this dissertation, and its validity, the following recommendations should be considered:

- Utilize an online measurement instrument such as an SO₂ analyzer for transient monitoring of SO₂ concentration. This will significantly minimize the extent of manual labor (sample extraction and injection) and element of human error involved. Additionally, an improved time resolution can be achieved for data analysis purposes. Such an instrument could not be used in the current study due to lack of availability.
- Investigate the effect of varying alternate system parameters on SO₂ removal and SO₃ formation during high temperature desulfurization. Such parameters include:
 - Flow rate
 - Inlet SO₂ concentration
 - Sorbent particle size
 - Amount of sorbent utilized
 - Type of sorbent utilized
- Investigate the effect of intermediate temperatures, other than 800°C, within the temperature range utilized in this study (700°C – 900°C). This will provide greater insight with regards to temperature dependence of SO₃ formation in the presence of stainless steel.
- Investigate the effect of different grades of stainless steel. Different compositions of stainless steel may most significantly attribute to varying amounts of SO₃ formation during high temperature flue gas desulfurization; this could possibly provide insight with regards to the base metal catalyzing the reaction of SO₂ to SO₃ at such elevated temperatures.

REFERENCES

1. Agnihotri, R., Mahuli, S., Chauk, S. & Fan, L., 1999. Combined Calcination, Sintering and Sulfation Model for CaCO₃-SO₂ Reaction. *AIChE Journal*, Volume 45, pp. 366 - 380.
2. Anon., 2002. *Dry Flue Gas Desulfurization Technology Evaluation*, Chicago: Sargent & Lundy.
3. Anon., 2003. *Wet Flue Gas Desulfurization Technology Evaluation*, Chicago: Sargent & Lundy LLC.
4. Arcor Epoxy Technologies, 1990. *Wet Flue Gas Desulfurization (FGD)*, Dennis: Arcor Epoxy Technologies.
5. Arvanitidis, C., Vamvuka, D. & Zachariadis, D., 2009. Flue Gas Desulfurization at High Temperatures: A Review. *Energy Fuels*, pp. 5537-5549.
6. Babcock & Wilcox, 2002. *Dry Flue Gas Desulfurization systems*. s.l. Patent No. E101-3178.
7. Belo, L. P. et al., 2014. *High-Temperature Conversion of SO₂ to SO₃: Homogeneous experiments and Catalytic Effect of Fly Ash from Air and Oxy-fuel Firing*, New South Wales: ACS publications .
8. Candan, N., 1979. *Reaction of Sulfur Dioxide with Calcined Limestone in a Fixed Bed Reactor*, Ankara, Turkey: M.S. thesis: M.E.T.U..
9. Chang, L., Zhu, S., Xie, K. & Bao, W., 1998. *Effect of impurities on desulphurisation properties of limestone during coal gasification*, China: Taiyan University of Technology.
10. Chan, R., Murthi, K. & Harrison, D., 1970. *Thermogravimetric analysis of Ontario limestones and dolomites-Reactivity of sulfur dioxide with calcined samples*, Ontario: Chemical Research Department, Ontario Hydro Research Division.
11. Cooper, C. D. & Alley, F. C., 2002. *Air Pollution Control: A Design Approach*, s.l.: Waveland Press Inc..
12. Dasgupta, K., Rai, K. & Verma, N., 2003. *Breakthrough and Sulfate Conversion Analysis during Removal of Sulfur Dioxide Oxide Sorbents*, Kanpur: Department of Chemical Engineering, Indian Institute of Technology Kanpur.

13. Dogu, T., 1981. Importance of Pore Structure and Diffusion in the Kinetics of Gas-Solid Noncatalytic Reactions: Reaction of Calcined Limestone with SO₂. *Chem. Eng. Journal*, Volume 21, pp. 213 - 222.
14. Ersoy, M. A., 1999. Removal of Sulphur Dioxide from Flue Gases. *Energy Sources*, Volume 21, pp. 611-619.
15. EU Communities, 2001. Emission Limit Values: Combustion Plants in EU and USA. *Journal of European Communities*.
16. Felder, R. M. & Rousseau, R. W., 2005. *Elementary Principles of Chemical Processes*. 3rd ed. s.l.:John Wiley & Sons, Inc..
17. Flieg, D., Vainio, E., Andersson, K. & Brink, A., 2012. Evaluation of SO₃ Measurement Techniques in Air and Oxyfuel Combustion. *Energy Fuels*, Volume 26, pp. 5537-5549.
18. Fuller, E., Schettler, P. & Giddings, J., 1966. Correlations for Prediction of Diffusion Coefficients in Multicomponent Mixtures. *Ind. Eng. Chem.*, 58(5), pp. 18 - 27.
19. Gupta, V. & Verma, N., 2002. Removal of Volatile Organic Compounds by Cryogenic Condensation Followed by Adsorption. *Chem. Eng. Sci.*, Volume 57, pp. 97-114.
20. Hamer, C., 1986. *Evaluation of SO₂ Sorbent Utilization in Fluidized Beds*, s.l.: Energy, Mines and Resources, Canmet Report No 86-9E.
21. Harris, D., 2015. *Quantitative Chemical Analysis*. 9 ed. s.l.:W. H. Freeman.
22. Hartman, M. & Coughlin, R., 1976. Reaction of Sulfur Dioxide with Limestone and the Grain Model. *AIChE Journal*, Volume 22, pp. 490 - 498.
23. Hopkins, J. & Golding, J., 1993. The effect of Heat Transfer Rate on the characteristics and Operation of a Tubular Reactor. *The Chemical Engineering Journal*, Volume 51, pp. 7 - 18.
24. IAPWS , 2012. *Dew Point for Flue Gas of Power-Plant Exhaust*, Yokohama: International Association for the Properties of Water and Steam.
25. Institute, N. D., 1998. *Cleaning and Descaling Stainless Steels*. s.l. Patent No. 9001.
26. Jaworowski, R. J. & Mack, S. S., 1979. Evaluation of Methods for Measurement of SO₃/H₂SO₄ in Flue Gas. *Air Pollution Control Association*, Volume 29, pp. 43-46.
27. Joseph, G. T. & Beachler, D. S., 1998. *Scrubber Systems Operation Review APTI Course*, s.l.: Raleigh N.C..

28. Khinast, D., Krammer, G., Brunner, C. & Staudinger, G., 1996. Decomposition of Limestone: The influence of CO₂ and particle size on reaction rate. *Chem. Eng. Sci.*, 51(4), pp. 623 - 634.
29. Krammer, G. & Staudinger, G., 1991. SO₂ Removal from Flue Gas wih Dry Limestone. *Gas Separation & Purification*, Volume 5, pp. 259-260.
30. Laursen, K. J., 2007. *Advances in Sulfur Recovery by the WSA Process*, s.l.: Hydrocarbon Engineering.
31. Levenspiel, O., 1999. *Chemical Reaction Engineering*. New York: Wiley.
32. Lokhat, D., 2015. *Learn@ukzn*. [Online]
Available at: <http://www.learn@ukzn.ac.za>
[Accessed 20 August 2018].
33. Milne, C., 1998. *High-Temperature, Short Time Sulfation of Calcium Based Sorbents*, Salt Lake City: University of Utah.
34. Montes, D. et al., 2012. *Reactive H₂S chemisorption on mesoporous silica molecular sieve-supported CuO or ZnO*, Venezuela: Elsevier Inc..
35. Munoz, G. M., Linares, S. A. & Salinas, M. d. L., 1995. A New Parameter to Characterize Limestones as SO₂ Sorbents. *App. Surf. Sci.*, Volume 89, pp. 197 - 203.
36. Naidoo, J., Goumri, A. & Marshall, P., 2004. *A kinetic study of the reaction of atomic oxygen with SO₂*, Texas: Elesevier.
37. Nauman, E., 2002. *Chemical Reactor Design, Optimization and Scaleup*. New York: McGraw Hill.
38. Newton, G. et al., 1998. Fundamental Studies of Dry Injection of Calcium Based-Sorbents for SO₂ Control in Utility Boilers. EPA-600/2-88-069(NTIS PB89-134142).
39. Nolan, P. S., 2000. *Flue Gas Desulfurization Technologies for Coal-Fired Power Stations*. Ohio: Babcock & Wilcox.
40. Orbey, N., Dogu, G. & Dogu, T., 1981. *Breakthrough Analysis of Noncatalytic Solid-Gas Reactions-Reaction of SO₂ with Calcined Limestone*, Turkey: Chemical Engineering Department, Middle East Technical University.
41. Perry, R. H., 2008. *Perry's Chemical Engineers Handbook*. s.l.:McGraw Hill Publishers.

42. Satterfield, C., 1991. *Heterogenous Catalysis in Industrial Practice*. 2nd ed. New York: McGraw Hill.
43. Scheisser, W. & Griffiths, G., 2009. *A Copendium of Partial Differential Equation Models, Mehtod of Lines Analysis with MATLAB*. s.l.:Cambridge University Press.
44. Schenelle, K. B. & Brown, C. A., 2002. *Air Pollution Control Technology Handbook*, s.l.: CRC Press LLC.
45. Seader, J., Henley, E. & Roper, D., 2011. *Separation Process Principals*. 3rd ed. New York: Wiley & Sons Inc..
46. Semaru, K. T., 1977. Practical Process Design of Particulate Scrubbers. *Chemical Engineering*, Volume 84, pp. 87 - 91.
47. Smith, J., Van Ness, H. & Abbott, M., 2001. *Introduction to Chemical Engineering Thermodynamics*. 6th ed. New York: McGraw Hill.
48. Smith, O. I., Tseregounis, S. & Wang, S.-n., 1982. *High-Temperature Kinetics of the Reactions of SO₂ and SO₃ with Atomic Oxygen*, Los Angeles : University of California.
49. Srivastava, R. K., 2002. *Controlling SO₂ Emmisions: A Review of Technologies*, Washington D.C.: EPA/600/R-00/93.
50. Srivastava, R. K. & Josewicz, W., 2001. Flue gas Desulfurization: The State of the Art. *Air and Waste Management Association*, Volume 51, pp. 1676 - 1688.
51. Zevenhoven & Kilpinen, 2001. *Suplur*, s.l.: s.n.

APPENDIX A: RAW & CALCULATED DATA

A-1.1) CALIBRATION DATA

Table A- 1: Calibration data

Volume Injected (ml)	0	0,2	0,4	0,6	0,8	1
SO₂ fraction (2000 ppmv)	0,002	0,002	0,002	0,002	0,002	0,002
Volume SO₂ (ml)	0	0,0004	0,0008	0,0012	0,0016	0,002
Run 1 area (µV.s)	0	766453,4	1335023,8	1785929,4	2212041,6	2792863,8
Run 2 area (µV.s)	0	798509,8	1327330,5	1961332,3	2523995	3069082,9
Run 3 area (µV.s)	0	801627,6	1319637,2	1829118,3	2422421,4	2757720,5
Average area (µV.s)	0	788863,6	1327330,5	1858793,3	2386152,7	2873222,4

Table A- 2: Calibration curve relative uncertainty calculation data

Volume Injected (ml)	0	0,2	0,4	0,6	0,8	1
SO₂ fraction (2000 ppmv)	0,002	0,002	0,002	0,002	0,002	0,002
Volume SO₂ (ml) - Y OBSERVED	0	0,0004	0,0008	0,0012	0,0016	0,002
Area (µV.s) - X OBSERVED	0	788863,60	1327330,50	1858793,33	2386152,67	2873222,40
Absolute Uncertainty (ml)	0	2,2E-05	1,0E-05	3,9E-05	8,3 E-05	8,6E-05
Volume SO₂ (ml) - Y PREDICTED	0	0,000422	0,000810	0,001239	0,001683	0,002086
Relative Uncertainty	0	0,0557	0,0127	0,0324	0,0516	0,0429
Relative Uncertainty (%)	0	5,57	1,27	3,24	5,16	4,29

Table A- 3: Average relative uncertainty

Average Relative Uncertainty	0,0391
Average Relative Uncertainty (%)	3.91

A-1.2) DEADTIME RUN DATA

Table A- 4: Deadtime run data

Time (s)	Area (μ V. s)	SO ₂ Volume (ml)	SO ₂ Volume percent	SO ₂ Concentration (ppmv)
0	0	0,000000	0,000000000	0,0
2	0	0,000000	0,000000000	0,0
4	2840334,6	0,002059	0,205920193	2059,2
6	2874256,2	0,002087	0,208661524	2086,6
8	2854693,6	0,002071	0,207082201	2070,8
10	2883659,4	0,002094	0,209419071	2094,2

A-1.3) BARIUM PERCHLORATE STANDARDIZATION DATA

Table A- 5: Volumes obtained from sulfuric acid titration

Sample	Initial Volume (ml)	Final Volume (ml)	Volume Titrated (ml)
1	0,1	26	25,9
2	0,1	25,9	25,8
3	0,1	26	25,9
Average	25,87		

Table A- 6: Volumes obtained from water (blank) titration

Sample	Initial Volume (ml)	Final Volume (ml)	Volume Titrated (ml)
1	0,1	6,1	6
2	0,2	6,3	6,1
3	0	6	6
Average	6,03		

A-1.4) 700°C DATA

A-1.4.1) RUN 1

Green – Breakthrough Time

Red – Saturation Time

Table A- 7: Initial /inlet SO₂ concentration - 700°C run 1

Time (s)	Area ($\mu\text{V.s}$)	SO ₂ Volume (ml)	SO ₂ Volume Percent (%)	SO ₂ Concentration (ppmv)
0	3159201,40	0,002311	0,231087	2311
10	2356158,20	0,001657	0,165735	1657
20	3210309,40	0,002350	0,234977	2350
30	2453942,20	0,001740	0,173963	1740
40	3161036,20	0,002312	0,231228	2312
50	2654647,00	0,001907	0,190706	1907
60	3497063,90	0,002559	0,255870	2559
70	2752561,30	0,001988	0,198769	1988
80	3527904,60	0,002580	0,258012	2580
90	2671142,30	0,001921	0,192070	1921
100	3298515,60	0,002416	0,241579	2416
110	2866365,60	0,002080	0,208025	2080
120	3334383,50	0,002442	0,244221	2442
130	2659319,40	0,001911	0,191092	1911
140	3755945,10	0,002731	0,273124	2731
150	2716297,10	0,001958	0,195793	1958
160	3567153,50	0,002607	0,260706	2607
170	2714174,3	0,001956	0,195618	1956
180	3615489,5	0,002640	0,263972	2640
190	2438419,4	0,001727	0,172659	1727
200	3238347,6	0,002371	0,237091	2371
210	2619914,3	0,001878	0,187827	1878
220	3390934,4	0,002483	0,248335	2483

230	2656712,6	0,001909	0,190877	1909
240	3510646,1	0,002568	0,256816	2568
250	2752828,3	0,001988	0,198791	1988
260	3279041,4	0,002401	0,240134	2401
270	2692154,3	0,001938	0,193804	1938
280	3560778,8	0,002603	0,260271	2603
290	2704270,8	0,001948	0,194803	1948
300	3452064,5	0,002527	0,252705	2527
Average		0,002207	0,220667	2207

Table A- 8: Reactor effluent SO₂ concentration - 700°C run 1

Time (s)	Area (μ V.s)	SO ₂ Volume (ml)	SO ₂ Volume Percent (%)	SO ₂ Concentration (ppmv)	C _{SO₂} (mol/L)	ΔT (s)	C _{SO₂} ΔT (mol.s/L)
0	51168,3	0,000018	0,001799	18	0,00000023	10	0,00000225
10	54829,1	0,000020	0,001953	20	0,00000024	10	0,00000245
20	57156,5	0,000021	0,002051	21	0,00000026	10	0,00000257
30	62833,2	0,000023	0,002292	23	0,00000029	10	0,00000287
40	76221,3	0,000029	0,002864	29	0,00000036	10	0,00000359
50	82104,5	0,000031	0,003117	31	0,00000039	10	0,00000390
60	96189,5	0,000037	0,003730	37	0,00000047	10	0,00000467
70	103380,2	0,000040	0,004046	40	0,00000051	10	0,00000507
80	105384,2	0,000041	0,004134	41	0,00000052	10	0,00000518
90	113547,7	0,000045	0,004495	45	0,00000056	10	0,00000563
100	121573,3	0,000049	0,004853	49	0,00000061	10	0,00000608
110	132182,7	0,000053	0,005330	53	0,00000067	10	0,00000667
120	155708,3	0,000064	0,006402	64	0,00000080	10	0,00000802
130	179252,7	0,000075	0,007495	75	0,00000094	10	0,00000939
140	200915,2	0,000085	0,008520	85	0,00000107	10	0,00001067
150	261195,9	0,000115	0,011459	115	0,00000144	10	0,00001435

160	280271,4	0,000124	0,012416	124	0,00000155	10	0,00001555
170	304060,6	0,000136	0,013627	136	0,00000171	10	0,00001707
180	335173,4	0,000152	0,015241	152	0,00000191	10	0,00001909
190	352326,2	0,000161	0,016145	161	0,00000202	10	0,00002022
200	389145,8	0,000181	0,018118	181	0,00000227	10	0,00002269
210	412330,3	0,000194	0,019383	194	0,00000243	10	0,00002427
220	442796,6	0,000211	0,021073	211	0,00000264	10	0,00002639
230	502908,8	0,000245	0,024493	245	0,00000307	10	0,00003067
240	569887	0,000284	0,028436	284	0,00000356	10	0,00003561
250	577217,8	0,000289	0,028875	289	0,00000362	10	0,00003616
260	581051,2	0,000291	0,029106	291	0,00000365	10	0,00003645
270	584843,7	0,000293	0,029334	293	0,00000367	10	0,00003674
280	597010,3	0,000301	0,030070	301	0,00000377	10	0,00003766
290	604493,7	0,000305	0,030525	305	0,00000382	10	0,00003823
300	638211,1	0,000326	0,032595	326	0,00000408	10	0,00004082
310	661297	0,000340	0,034031	340	0,00000426	10	0,00004262
320	666174,2	0,000343	0,034336	343	0,00000430	10	0,00004300
330	702262,6	0,000366	0,036615	366	0,00000459	10	0,00004585
340	730819,4	0,000384	0,038444	384	0,00000481	10	0,00004815
350	781390,6	0,000417	0,041736	417	0,00000523	10	0,00005227
360	820269,9	0,000443	0,044312	443	0,00000555	10	0,00005549
370	834312	0,000453	0,045252	453	0,00000567	10	0,00005667
380	849918,1	0,000463	0,046302	463	0,00000580	10	0,00005799
390	862820,7	0,000472	0,047175	472	0,00000591	10	0,00005908
400	895951,3	0,000494	0,049435	494	0,00000619	10	0,00006191
410	934089,1	0,000521	0,052069	521	0,00000652	10	0,00006521
420	995918,8	0,000564	0,056410	564	0,00000706	10	0,00007065
430	1000294,1	0,000567	0,056721	567	0,00000710	10	0,00007103
440	1011048,7	0,000575	0,057486	575	0,00000720	10	0,00007199
450	1082415,4	0,000626	0,062625	626	0,00000784	10	0,00007843

460	1125853,6	0,000658	0,065804	658	0,00000824	10	0,00008241
470	1236349,2	0,000741	0,074056	741	0,00000927	10	0,00009274
480	1299894,5	0,000789	0,078901	789	0,00000988	10	0,00009881
490	1379552,3	0,000851	0,085069	851	0,00001065	10	0,00010654
500	1381728,2	0,000852	0,085239	852	0,00001067	10	0,00010675
510	1490403,2	0,000938	0,093810	938	0,00001175	10	0,00011748
520	1593545,6	0,001021	0,102090	1021	0,00001279	10	0,00012785
530	1683545,6	0,001094	0,109413	1094	0,00001370	10	0,00013702
540	1723545,6	0,001127	0,112694	1127	0,00001411	10	0,00014113
550	1766174,2	0,001162	0,116206	1162	0,00001455	10	0,00014553
560	1802262,6	0,001192	0,119191	1192	0,00001493	10	0,00014927
570	1860819,4	0,001241	0,124056	1241	0,00001554	10	0,00015536
580	1920269,9	0,001290	0,129017	1290	0,00001616	10	0,00016157
590	1921390,6	0,001291	0,129111	1291	0,00001617	10	0,00016169
600	1984312	0,001344	0,134383	1344	0,00001683	10	0,00016829
610	1999918,1	0,001357	0,135693	1357	0,00001699	10	0,00016994
620	2002820,7	0,001359	0,135937	1359	0,00001702	10	0,00017024
630	2094089,1	0,001436	0,143619	1436	0,00001799	10	0,00017986
640	2095951,3	0,001438	0,143776	1438	0,00001801	10	0,00018006
650	2135918,8	0,001471	0,147147	1471	0,00001843	10	0,00018428
660	2183545,6	0,001512	0,151167	1512	0,00001893	10	0,00018931
670	2193545,6	0,001520	0,152011	1520	0,00001904	10	0,00019037
680	2293545,6	0,001605	0,160454	1605	0,00002009	10	0,00020095
690	2333545,6	0,001638	0,163829	1638	0,00002052	10	0,00020517
700	2393545,6	0,001689	0,168885	1689	0,00002115	10	0,00021150
710	2423545,6	0,001714	0,171409	1714	0,00002147	10	0,00021466
720	2493545,6	0,001773	0,177284	1773	0,00002220	10	0,00022202
730	2525853,6	0,001800	0,179989	1800	0,00002254	10	0,00022541
740	2636349,2	0,001892	0,189190	1892	0,00002369	10	0,00023693
750	2699894,5	0,001944	0,194442	1944	0,00002435	10	0,00024351

760	2749552,3	0,001985	0,198523	1985	0,00002486	10	0,00024862
770	2781728,2	0,002012	0,201154	2012	0,00002519	10	0,00025192
780	2785556,2	0,002015	0,201467	2015	0,00002523	10	0,00025231
790	2790403,2	0,002019	0,201862	2019	0,00002528	10	0,00025280
800	2800403,2	0,002027	0,202677	2027	0,00002538	10	0,00025382
810	2833545,6	0,002054	0,205370	2054	0,00002572	10	0,00025720
820	2843545,6	0,002062	0,206180	2062	0,00002582	10	0,00025821
830	2883545,6	0,002094	0,209410	2094	0,00002623	10	0,00026226
840	2903545,6	0,002110	0,211018	2110	0,00002643	10	0,00026427
850	2923545,6	0,002126	0,212621	2126	0,00002663	10	0,00026628
860	2923545,6	0,002126	0,212621	2126	0,00002663	10	0,00026628
870	2993545,6	0,002182	0,218190	2182	0,00002733	10	0,00027325
880	2995555,6	0,002183	0,218349	2183	0,00002734	10	0,00027345
890	3063545,6	0,002237	0,223691	2237	0,00002801	10	0,00028014
900	3093545,6	0,002260	0,226026	2260	0,00002831	10	0,00028306
910	3103545,6	0,002268	0,226802	2268	0,00002840	10	0,00028404
Summation						0,01061589	

Table A- 9: Propagational uncertainty data - 700°C run 1

C _{in} (ppmv)	C _{out} (ppmv)	Time (s)	C _{out} /C _{in}	Average relative uncertainty	Propagational uncertainty
2207	18	0	0,0081512	0,039059	0,00045025
2207	20	10	0,0088495	0,039059	0,00048883
2207	21	20	0,0092947	0,039059	0,00051342
2207	23	30	0,0103846	0,039059	0,00057362
2207	29	40	0,0129776	0,039059	0,00071685
2207	31	50	0,0141269	0,039059	0,00078034
2207	37	60	0,0169031	0,039059	0,00093369
2207	40	70	0,0183337	0,039059	0,00101271

2207	41	80	0,018734	0,039059	0,00103483
2207	45	90	0,0203718	0,039059	0,00112529
2207	49	100	0,0219931	0,039059	0,00121485
2207	53	110	0,0241533	0,039059	0,00133417
2207	64	120	0,0290117	0,039059	0,00160254
2207	75	130	0,0339674	0,039059	0,00187628
2207	85	140	0,0386086	0,039059	0,00213265
2207	115	150	0,0519283	0,039059	0,00286841
2207	124	160	0,0562652	0,039059	0,00310797
2207	136	170	0,0617545	0,039059	0,00341118
2207	152	180	0,0690671	0,039059	0,00381511
2207	161	190	0,0731625	0,039059	0,00404133
2207	181	200	0,0821046	0,039059	0,00453527
2207	194	210	0,0878395	0,039059	0,00485206
2207	211	220	0,0954961	0,039059	0,00527499
2207	245	230	0,1109961	0,039059	0,00613118
2207	284	240	0,1288626	0,039059	0,00711808
2207	289	250	0,1308552	0,039059	0,00722815
2207	291	260	0,1319001	0,039059	0,00728587
2207	293	270	0,1329358	0,039059	0,00734307
2207	301	280	0,1362711	0,039059	0,00752731
2207	305	290	0,1383324	0,039059	0,00764117
2207	326	300	0,1477109	0,039059	0,00815922
2207	340	310	0,1542172	0,039059	0,00851861
2207	343	320	0,1556005	0,039059	0,00859502
2207	366	330	0,1659289	0,039059	0,00916554
2207	384	340	0,1742164	0,039059	0,00962333
2207	417	350	0,189135	0,039059	0,01044740
2207	443	360	0,2008094	0,039059	0,01109226
2207	453	370	0,2050686	0,039059	0,01132753

2207	463	380	0,2098284	0,039059	0,01159045
2207	472	390	0,2137842	0,039059	0,01180896
2207	494	400	0,2240259	0,039059	0,01237469
2207	521	410	0,2359623	0,039059	0,01303403
2207	564	420	0,2556365	0,039059	0,01412079
2207	567	430	0,2570435	0,039059	0,01419851
2207	575	440	0,2605098	0,039059	0,01438998
2207	626	450	0,2837972	0,039059	0,01567632
2207	658	460	0,298205	0,039059	0,01647218
2207	741	470	0,3355999	0,039059	0,01853779
2207	789	480	0,3575572	0,039059	0,01975066
2207	851	490	0,3855086	0,039059	0,02129464
2207	852	500	0,3862784	0,039059	0,02133716
2207	938	510	0,4251223	0,039059	0,02348281
2207	1021	520	0,4626424	0,039059	0,02555533
2207	1094	530	0,4958305	0,039059	0,02738857
2207	1127	540	0,5106986	0,039059	0,02820985
2207	1162	550	0,5266152	0,039059	0,02908905
2207	1192	560	0,5401429	0,039059	0,02983629
2207	1241	570	0,5621862	0,039059	0,03105391
2207	1290	580	0,5846692	0,039059	0,03229582
2207	1291	590	0,5850939	0,039059	0,03231928
2207	1344	600	0,6089856	0,039059	0,03363900
2207	1357	610	0,614924	0,039059	0,03396703
2207	1359	620	0,616029	0,039059	0,03402806
2207	1436	630	0,6508405	0,039059	0,03595098
2207	1438	640	0,6515519	0,039059	0,03599027
2207	1471	650	0,666828	0,039059	0,03683409
2207	1512	660	0,6850458	0,039059	0,03784040
2207	1520	670	0,6888721	0,039059	0,03805176

2207	1605	680	0,7271348	0,039059	0,04016530
2207	1638	690	0,7424281	0,039059	0,04101007
2207	1689	700	0,7653392	0,039059	0,04227563
2207	1714	710	0,776777	0,039059	0,04290743
2207	1773	720	0,803404	0,039059	0,04437824
2207	1800	730	0,8156585	0,039059	0,04505516
2207	1892	740	0,8573579	0,039059	0,04735854
2207	1944	750	0,8811592	0,039059	0,04867326
2207	1985	760	0,8996503	0,039059	0,04969468
2207	2012	770	0,9115757	0,039059	0,05035341
2207	2015	780	0,9129914	0,039059	0,05043161
2207	2019	790	0,914783	0,039059	0,05053057
2207	2027	800	0,9184758	0,039059	0,05073455
2207	2054	810	0,9306804	0,039059	0,05140871
2207	2062	820	0,9343523	0,039059	0,05161153
2207	2094	830	0,9489882	0,039059	0,05241999
2207	2110	840	0,9562741	0,039059	0,05282245
2207	2126	850	0,9635379	0,039059	0,05322368
2207	2126	860	0,9635379	0,039059	0,05322368
2207	2182	870	0,9887763	0,039059	0,05461780
2207	2183	880	0,9894966	0,039059	0,05465758
2207	2237	890	1,0137065	0,039059	0,05599488
2207	2260	900	1,0242896	0,039059	0,05657947
2207	2268	910	1,0278031	0,039059	0,05677355

Table A- 10: Volumes obtained from titration for SO₃ analysis - 700°C run 1

Bottle	Initial Volume (ml)	Final Volume (ml)	Volume Titrated (ml)
1	0	2.8	2,8
	2.8	5.7	2,9
	5.7	8.7	3
Average			2,9
2	8.7	11.6	2,9
	11.6	14.4	2,8
	14.4	17.3	2,9
Average			2,866666667
3	17.3	20.4	3,1
	20.4	23.3	2,9
	23.3	26.3	3
Average			3

Table A- 11: Moles of SO₃ produced from titrations - 700°C run 1

Bottle	BaClO ₄ Consumed (moles)	SO ₃ Produced (moles)
1	0,0000145	0,0000145
2	1,43333E-05	1,43333E-05
3	0,000015	0,000015
Total (moles)	4,38333E-05	4,38333E-05

Table A- 12: System sulfur mass balance - 700°C run 1

Into System		
<i>SO₂ Analysis</i>		
Total moles gas	1,22629	moles
Moles SO ₂	0,00271	moles
Moles sulfur from SO ₂	0,00271	moles
Mass sulfur from SO ₂	0,08677	grams
<i>SO₃ Analysis</i>		
Moles SO ₃	0	moles
Mass SO ₃	0	grams
Out of System		
<i>SO₂ Analysis</i>		
Moles SO ₂	0,00106	moles
Moles sulfur from SO ₂	0,00106	moles
Mass sulfur from SO ₂	0,03404	grams
<i>SO₃ Analysis</i>		
Moles SO ₃ formed	0,000044	moles
Moles sulfur from SO ₃	0,000044	moles
Mass sulfur from SO ₃	0,002808	grams

Table A- 13: SO₂ sorption capacity of limestone sorbent - 700°C run 1

Initial/inlet Concentration (C _o)	2207	ppmv
Saturation time (T _{sat})	890	s
Integral	0,01062	mol.s/L
Sorption capacity of limestone	13.498	mg SO₂/g CaCO₃

A-1.4.2) RUN 2

Table A- 14: Initial /inlet SO₂ concentration - 700°C run 2

Time (s)	Area ($\mu\text{V} \cdot \text{s}$)	SO ₂ Volume (ml)	SO ₂ Volume Percent (%)	SO ₂ Concentration (ppmv)
0	3173487,40	0,002322	0,232179	2322
10	2370448,20	0,001669	0,166940	1669
20	3224595,40	0,002361	0,236056	2361
30	2467612,20	0,001751	0,175110	1751
40	3175326,20	0,002323	0,232319	2323
50	2668933,00	0,001919	0,191887	1919
60	3483393,90	0,002549	0,254914	2549
70	2766231,30	0,001999	0,199888	1999
80	3542190,66	0,002590	0,258997	2590
90	2685432,30	0,001932	0,193250	1932
100	3312185,60	0,002426	0,242589	2426
110	2880651,60	0,002092	0,209177	2092
120	3320093,50	0,002432	0,243172	2432
130	2673605,40	0,001923	0,192273	1923
140	3769615,10	0,002740	0,273986	2740
150	2730583,10	0,001970	0,196967	1970
160	3580823,50	0,002616	0,261636	2616
170	2728460,3	0,001968	0,196792	1968
180	3601199,5	0,002630	0,263013	2630
190	2452705,4	0,001739	0,173859	1739
200	3252017,6	0,002381	0,238117	2381
210	2634200,3	0,001890	0,189012	1890
220	3405220,4	0,002494	0,249363	2494

230	2670382,6	0,001920	0,192007	1920
240	3524936,1	0,002578	0,257807	2578
250	2739158,3	0,001977	0,197670	1977
260	3293327,4	0,002412	0,241195	2412
270	2705824,3	0,001949	0,194931	1949
280	3575068,8	0,002612	0,261245	2612
290	2718556,8	0,001960	0,195978	1960
300	3466350,5	0,002537	0,253715	2537
	Average	0,002215	0,221485	2215

Table A- 15: Reactor effluent SO₂ concentration - 700°C run 2

Time (s)	Area (μ V.s)	SO ₂ Volume (ml)	SO ₂ Volume Percent (%)	SO ₂ Concentration (ppmv)	C _{SO₂} (mol/L)	ΔT (s)	C _{SO₂} ΔT (mol.s/L)
0	56362,3	0,000020	0,002017	20	0,00000025	10	0,00000253
10	60067,1	0,000022	0,002174	22	0,00000027	10	0,00000272
20	62593,5	0,000023	0,002281	23	0,00000029	10	0,00000286
30	68027,2	0,000025	0,002513	25	0,00000031	10	0,00000315
40	81658,3	0,000031	0,003098	31	0,00000039	10	0,00000388
50	87342,5	0,000033	0,003344	33	0,00000042	10	0,00000419
60	101626,5	0,000040	0,003968	40	0,00000050	10	0,00000497
70	115561,2	0,000046	0,004585	46	0,00000057	10	0,00000574
80	117069,2	0,000047	0,004652	47	0,00000058	10	0,00000583
90	125327,7	0,000050	0,005021	50	0,00000063	10	0,00000629
100	133754,3	0,000054	0,005401	54	0,00000068	10	0,00000676
110	143867,7	0,000059	0,005860	59	0,00000073	10	0,00000734
120	167889,3	0,000070	0,006965	70	0,00000087	10	0,00000872
130	191032,7	0,000081	0,008050	81	0,00000101	10	0,00001008
140	213096,2	0,000091	0,009103	91	0,00000114	10	0,00001140
150	272880,9	0,000120	0,012044	120	0,00000151	10	0,00001508

160	292051,4	0,000130	0,013013	130	0,00000163	10	0,00001630
170	316241,6	0,000143	0,014255	143	0,00000179	10	0,00001785
180	346858,4	0,000159	0,015855	159	0,00000199	10	0,00001986
190	364507,2	0,000168	0,016792	168	0,00000210	10	0,00002103
200	401326,8	0,000188	0,018780	188	0,00000235	10	0,00002352
210	424110,3	0,000200	0,020033	200	0,00000251	10	0,00002509
220	454481,6	0,000217	0,021729	217	0,00000272	10	0,00002721
230	514688,8	0,000252	0,025177	252	0,00000315	10	0,00003153
240	558202	0,000277	0,027738	277	0,00000347	10	0,00003474
250	588902,8	0,000296	0,029580	296	0,00000370	10	0,00003704
260	593232,2	0,000298	0,029841	298	0,00000374	10	0,00003737
270	596528,7	0,000300	0,030041	300	0,00000376	10	0,00003762
280	608790,3	0,000308	0,030787	308	0,00000386	10	0,00003856
290	616674,7	0,000313	0,031269	313	0,00000392	10	0,00003916
300	649991,1	0,000333	0,033326	333	0,00000417	10	0,00004174
310	673478	0,000348	0,034794	348	0,00000436	10	0,00004357
320	677859,2	0,000351	0,035070	351	0,00000439	10	0,00004392
330	714042,6	0,000374	0,037367	374	0,00000468	10	0,00004680
340	743000,4	0,000392	0,039230	392	0,00000491	10	0,00004913
350	793170,6	0,000425	0,042512	425	0,00000532	10	0,00005324
360	831954,9	0,000451	0,045094	451	0,00000565	10	0,00005647
370	845997	0,000460	0,046038	460	0,00000577	10	0,00005766
380	862099,1	0,000471	0,047126	471	0,00000590	10	0,00005902
390	874600,7	0,000480	0,047976	480	0,00000601	10	0,00006008
400	907731,3	0,000502	0,050245	502	0,00000629	10	0,00006292
410	946270,1	0,000529	0,052917	529	0,00000663	10	0,00006627
420	1007603,8	0,000572	0,057241	572	0,00000717	10	0,00007169
430	1014584,1	0,000577	0,057738	577	0,00000723	10	0,00007231
440	1024718,7	0,000585	0,058462	585	0,00000732	10	0,00007321
450	1096701,4	0,000637	0,063666	637	0,00000797	10	0,00007973

460	1140143,6	0,000669	0,066858	669	0,00000837	10	0,00008373
470	1250635,2	0,000751	0,075139	751	0,00000941	10	0,00009410
480	1314180,5	0,000800	0,080000	800	0,00001002	10	0,00010019
490	1393222,3	0,000861	0,086137	861	0,00001079	10	0,00010787
500	1396014,2	0,000864	0,086356	864	0,00001081	10	0,00010815
510	1504693,2	0,000949	0,094949	949	0,00001189	10	0,00011891
520	1607831,6	0,001032	0,103246	1032	0,00001293	10	0,00012930
530	1697215,6	0,001105	0,110533	1105	0,00001384	10	0,00013843
540	1737835,6	0,001139	0,113870	1139	0,00001426	10	0,00014261
550	1780460,2	0,001174	0,117387	1174	0,00001470	10	0,00014701
560	1815932,6	0,001203	0,120325	1203	0,00001507	10	0,00015069
570	1875105,4	0,001252	0,125246	1252	0,00001569	10	0,00015685
580	1934559,9	0,001302	0,130212	1302	0,00001631	10	0,00016307
590	1935060,6	0,001303	0,130254	1303	0,00001631	10	0,00016312
600	1998598	0,001356	0,135582	1356	0,00001698	10	0,00016980
610	2014208,1	0,001369	0,136894	1369	0,00001714	10	0,00017144
620	2017110,7	0,001371	0,137138	1371	0,00001717	10	0,00017175
630	2080419,1	0,001425	0,142467	1425	0,00001784	10	0,00017842
640	2110237,3	0,001450	0,144980	1450	0,00001816	10	0,00018157
650	2149588,8	0,001483	0,148300	1483	0,00001857	10	0,00018572
660	2169875,6	0,001500	0,150013	1500	0,00001879	10	0,00018787
670	2207835,6	0,001532	0,153218	1532	0,00001919	10	0,00019188
680	2307835,6	0,001617	0,161660	1617	0,00002025	10	0,00020246
690	2347215,6	0,001650	0,164982	1650	0,00002066	10	0,00020662
700	2407831,6	0,001701	0,170087	1701	0,00002130	10	0,00021301
710	2437215,6	0,001726	0,172558	1726	0,00002161	10	0,00021610
720	2479255,6	0,001761	0,176087	1761	0,00002205	10	0,00022052
730	2540139,6	0,001812	0,181182	1812	0,00002269	10	0,00022690
740	2650019,2	0,001903	0,190323	1903	0,00002384	10	0,00023835
750	2714184,5	0,001956	0,195619	1956	0,00002450	10	0,00024498

760	2735882,3	0,001974	0,197402	1974	0,00002472	10	0,00024722
770	2796018,2	0,002023	0,202320	2023	0,00002534	10	0,00025338
780	2799842,2	0,002026	0,202631	2026	0,00002538	10	0,00025377
790	2804073,2	0,002030	0,202976	2030	0,00002542	10	0,00025420
800	2814693,2	0,002038	0,203839	2038	0,00002553	10	0,00025528
810	2847831,6	0,002065	0,206527	2065	0,00002586	10	0,00025864
820	2857835,6	0,002073	0,207336	2073	0,00002597	10	0,00025966
830	2897831,6	0,002106	0,210559	2106	0,00002637	10	0,00026369
840	2917831,6	0,002122	0,212163	2122	0,00002657	10	0,00026570
850	2937215,6	0,002137	0,213713	2137	0,00002676	10	0,00026764
860	2937835,6	0,002138	0,213763	2138	0,00002677	10	0,00026771
870	3007215,6	0,002193	0,219270	2193	0,00002746	10	0,00027460
880	3009841,6	0,002195	0,219477	2195	0,00002749	10	0,00027486
890	3017835,6	0,002201	0,220107	2201	0,00002757	10	0,00027565
900	3089875,6	0,002257	0,225741	2257	0,00002827	10	0,00028271
910	3107835,6	0,002271	0,227134	2271	0,00002845	10	0,00028445
Summation							0,01069676

Table A- 16: Propagational uncertainty data - 700°C run 2

C _{in} (ppmv)	C _{out} (ppmv)	Time (s)	C _{out} /C _{in}	Average relative uncertainty	Propagational uncertainty
2215	20	0	0,0091089	0,039059	0,00050316
2215	22	10	0,0098164	0,039059	0,00054224
2215	23	20	0,0103003	0,039059	0,00056897
2215	25	30	0,0113448	0,039059	0,00062666
2215	31	40	0,0139877	0,039059	0,00077265
2215	33	50	0,0150993	0,039059	0,00083405
2215	40	60	0,0179175	0,039059	0,00098972
2215	46	70	0,0207007	0,039059	0,00114346

2215	47	80	0,0210039	0,039059	0,00116021
2215	50	90	0,0226712	0,039059	0,00125231
2215	54	100	0,0243845	0,039059	0,00134694
2215	59	110	0,0264565	0,039059	0,00146140
2215	70	120	0,0314473	0,039059	0,00173708
2215	81	130	0,0363467	0,039059	0,00200771
2215	91	140	0,0410999	0,039059	0,00227027
2215	120	150	0,0543763	0,039059	0,00300363
2215	130	160	0,0587543	0,039059	0,00324545
2215	143	170	0,0643607	0,039059	0,00355514
2215	159	180	0,0715865	0,039059	0,00395428
2215	168	190	0,0758168	0,039059	0,00418795
2215	188	200	0,0847931	0,039059	0,00468378
2215	200	210	0,0904482	0,039059	0,00499616
2215	217	220	0,0981045	0,039059	0,00541907
2215	252	230	0,1136717	0,039059	0,00627897
2215	277	240	0,1252367	0,039059	0,00691779
2215	296	250	0,1335508	0,039059	0,00737705
2215	298	260	0,1347334	0,039059	0,00744237
2215	300	270	0,1356355	0,039059	0,00749220
2215	308	280	0,1390035	0,039059	0,00767824
2215	313	290	0,1411796	0,039059	0,00779844
2215	333	300	0,150464	0,039059	0,00831130
2215	348	310	0,1570947	0,039059	0,00867756
2215	351	320	0,1583392	0,039059	0,00874631
2215	374	330	0,1687094	0,039059	0,00931913
2215	392	340	0,1771246	0,039059	0,00978397
2215	425	350	0,1919415	0,039059	0,01060242
2215	451	360	0,2035967	0,039059	0,01124622
2215	460	370	0,2078586	0,039059	0,01148165

2215	471	380	0,212773	0,039059	0,01175310
2215	480	390	0,2166082	0,039059	0,01196496
2215	502	400	0,2268545	0,039059	0,01253093
2215	529	410	0,2389206	0,039059	0,01319744
2215	572	420	0,2584393	0,039059	0,01427561
2215	577	430	0,2606846	0,039059	0,01439963
2215	585	440	0,263953	0,039059	0,01458017
2215	637	450	0,28745	0,039059	0,01587810
2215	669	460	0,3018619	0,039059	0,01667418
2215	751	470	0,3392499	0,039059	0,01873941
2215	800	480	0,3611959	0,039059	0,01995165
2215	861	490	0,3889073	0,039059	0,02148237
2215	864	500	0,389894	0,039059	0,02153687
2215	949	510	0,428694	0,039059	0,02368010
2215	1032	520	0,4661546	0,039059	0,02574934
2215	1105	530	0,4990523	0,039059	0,02756653
2215	1139	540	0,5141186	0,039059	0,02839876
2215	1174	550	0,5299981	0,039059	0,02927591
2215	1203	560	0,5432632	0,039059	0,03000865
2215	1252	570	0,5654818	0,039059	0,03123595
2215	1302	580	0,5879056	0,039059	0,03247459
2215	1303	590	0,5880948	0,039059	0,03248504
2215	1356	600	0,61215	0,039059	0,03381380
2215	1369	610	0,6180721	0,039059	0,03414092
2215	1371	620	0,6191737	0,039059	0,03420177
2215	1425	630	0,6432327	0,039059	0,03553074
2215	1450	640	0,6545817	0,039059	0,03615763
2215	1483	650	0,6695712	0,039059	0,03698562
2215	1500	660	0,6773026	0,039059	0,03741268
2215	1532	670	0,6917734	0,039059	0,03821202

2215	1617	680	0,7298913	0,039059	0,04031757
2215	1650	690	0,7448876	0,039059	0,04114593
2215	1701	700	0,7679381	0,039059	0,04241919
2215	1726	710	0,7790932	0,039059	0,04303537
2215	1761	720	0,7950262	0,039059	0,04391547
2215	1812	730	0,8180338	0,039059	0,04518636
2215	1903	740	0,8593018	0,039059	0,04746591
2215	1956	750	0,8832134	0,039059	0,04878674
2215	1974	760	0,8912631	0,039059	0,04923138
2215	2023	770	0,9134676	0,039059	0,05045791
2215	2026	780	0,914874	0,039059	0,05053560
2215	2030	790	0,9164294	0,039059	0,05062151
2215	2038	800	0,9203296	0,039059	0,05083695
2215	2065	810	0,9324645	0,039059	0,05150726
2215	2073	820	0,936117	0,039059	0,05170901
2215	2106	830	0,9506673	0,039059	0,05251274
2215	2122	840	0,9579105	0,039059	0,05291284
2215	2137	850	0,9649091	0,039059	0,05329942
2215	2138	860	0,9651326	0,039059	0,05331177
2215	2193	870	0,9899965	0,039059	0,05468520
2215	2195	880	0,9909317	0,039059	0,05473686
2215	2201	890	0,993776	0,039059	0,05489397
2215	2257	900	1,0192164	0,039059	0,05629924
2215	2271	910	1,0255031	0,039059	0,05664650

Table A- 17: Volumes obtained from titration for SO₃ analysis - 700°C run 2

Bottle	Initial Volume (ml)	Final Volume (ml)	Volume Titrated (ml)
1	0	3.1	3,1
	3.1	6	2,9
	6	9	3
Average			3
2	9	11.9	2,9
	11.9	14.7	2,8
	14.7	17.6	2,9
Average			2,866666667
3	17.6	20.4	2,8
	20.4	23.3	2,9
	23.3	26.3	3
Average			2.9

Table A- 18: Moles of SO₃ produced from titrations - 700°C run 2

Bottle	BaClO ₄ Consumed (moles)	SO ₃ Produced (moles)
1	0,000015	0,000015
2	1,43333E-05	1,43333E-05
3	0,0000145	0,0000145
Total (moles)	4,38333E-05	4,38333E-05

Table A- 19: System sulfur mass balance - 700°C run 2

Into System		
<i>SO₂ Analysis</i>		
Total moles gas	1,22629	moles
Moles SO ₂	0,00272	moles
Moles sulfur from SO ₂	0,00272	moles
Mass sulfur from SO ₂	0,08709	grams
<i>SO₃ Analysis</i>		
Moles SO ₃	0	moles
Mass SO ₃	0	grams
Out of System		
<i>SO₂ Analysis</i>		
Moles SO ₂	0,00107	moles
Moles sulfur from SO ₂	0,00107	moles
Mass sulfur from SO ₂	0,03430	grams
<i>SO₃ Analysis</i>		
Moles SO ₃ formed	0,000044	moles
Moles sulfur from SO ₃	0,000044	moles
Mass sulfur from SO ₃	0,002808	grams

Table A- 20: SO₂ sorption capacity of limestone sorbent - 700°C run 2

Initial/inlet Concentration (C _o)	2215	ppmv
Saturation time (T _{sat})	900	s
Integral	0,01070	mol.s/L
Sorption capacity of limestone	13.670	mg SO₂/g CaCO₃

A-1.4.3) RUN 3

Table A- 21: Initial /inlet SO₂ concentration - 700°C run 3

Time (s)	Area ($\mu\text{V} \cdot \text{s}$)	SO ₂ Volume (ml)	SO ₂ Volume Percent (%)	SO ₂ Concentration (ppmv)
0	3173017,40	0,002321	0,232143	2321
10	2371031,20	0,001670	0,166989	1670
20	3225763,40	0,002361	0,236144	2361
30	2467758,20	0,001751	0,175122	1751
40	3176490,20	0,002324	0,232408	2324
50	2654647,00	0,001907	0,190706	1907
60	3511936,90	0,002569	0,256906	2569
70	2766377,30	0,001999	0,199900	1999
80	3513031,60	0,002570	0,256982	2570
90	2684958,30	0,001932	0,193211	1932
100	3313388,60	0,002427	0,242678	2427
110	2881819,60	0,002093	0,209271	2093
120	3319510,50	0,002431	0,243129	2431
130	2673135,40	0,001922	0,192235	1922
140	3770818,10	0,002741	0,274062	2741
150	2731751,10	0,001971	0,197063	1971
160	3580969,50	0,002616	0,261646	2616
170	2729047,3	0,001968	0,196841	1968
180	3629305,5	0,002649	0,264895	2649
190	2453873,4	0,001740	0,173957	1740
200	3222893,6	0,002359	0,235928	2359
210	2633730,3	0,001890	0,188973	1890
220	3376061,4	0,002473	0,247259	2473
230	2670528,6	0,001920	0,192019	1920

240	3495192,1	0,002557	0,255739	2557
250	2767701,3	0,002000	0,200008	2000
260	3265225,4	0,002391	0,239104	2391
270	2705970,3	0,001949	0,194943	1949
280	3545324,8	0,002592	0,259213	2592
290	2719143,8	0,001960	0,196027	1960
300	3436610,5	0,002516	0,251608	2516
Average		0,002212	0,221197	2212

Table A- 22: Reactor effluent SO₂ concentration - 700°C run 3

Time (s)	Area (μ V.s)	SO ₂ Volume (ml)	SO ₂ Volume Percent (%)	SO ₂ Concentration (ppmv)	C _{SO₂} (mol/L)	ΔT (s)	C _{SO₂} ΔT (mol.s/L)
0	56429,3	0,002020	20	20	0,00000025	10	0,00000253
10	59197,1	0,002137	21	22	0,00000027	10	0,00000268
20	62123,5	0,002261	23	23	0,00000028	10	0,00000283
30	68094,2	0,002516	25	25	0,00000032	10	0,00000315
40	81482,3	0,003090	31	31	0,00000039	10	0,00000387
50	87071,5	0,003333	33	33	0,00000042	10	0,00000417
60	100557,5	0,003921	39	40	0,00000049	10	0,00000491
70	103380,2	0,004046	40	46	0,00000051	10	0,00000507
80	117151,2	0,004656	47	47	0,00000058	10	0,00000583
90	125530,7	0,005030	50	50	0,00000063	10	0,00000630
100	133033,3	0,005368	54	54	0,00000067	10	0,00000672
110	143949,7	0,005863	59	59	0,00000073	10	0,00000734
120	167168,3	0,006932	69	70	0,00000087	10	0,00000868
130	191019,7	0,008050	80	81	0,00000101	10	0,00001008
140	212375,2	0,009068	91	91	0,00000114	10	0,00001136
150	272655,9	0,012032	120	120	0,00000151	10	0,00001507
160	292254,4	0,013024	130	130	0,00000163	10	0,00001631

170	315827,6	0,014234	142	143	0,00000178	10	0,00001783
180	346633,4	0,015843	158	159	0,00000198	10	0,00001984
190	364093,2	0,016770	168	168	0,00000210	10	0,00002100
200	400912,8	0,018758	188	188	0,00000235	10	0,00002349
210	423790,3	0,020015	200	200	0,00000251	10	0,00002507
220	454779,6	0,021745	217	217	0,00000272	10	0,00002723
230	514368,8	0,025158	252	252	0,00000315	10	0,00003151
240	581654	0,029142	291	277	0,00000365	10	0,00003650
250	589200,8	0,029598	296	296	0,00000371	10	0,00003707
260	592511,2	0,029798	298	298	0,00000373	10	0,00003732
270	596303,7	0,030028	300	300	0,00000376	10	0,00003761
280	608777,3	0,030786	308	308	0,00000386	10	0,00003856
290	616260,7	0,031244	312	313	0,00000391	10	0,00003913
300	650194,1	0,033338	333	333	0,00000418	10	0,00004175
310	672757	0,034749	347	348	0,00000435	10	0,00004352
320	677634,2	0,035056	351	351	0,00000439	10	0,00004390
330	713722,6	0,037346	373	374	0,00000468	10	0,00004677
340	742586,4	0,039204	392	392	0,00000491	10	0,00004910
350	792850,6	0,042491	425	425	0,00000532	10	0,00005321
360	832036,9	0,045099	451	451	0,00000565	10	0,00005648
370	846295	0,046058	461	460	0,00000577	10	0,00005768
380	861901,1	0,047113	471	471	0,00000590	10	0,00005900
390	874587,7	0,047975	480	480	0,00000601	10	0,00006008
400	907411,3	0,050223	502	502	0,00000629	10	0,00006290
410	945549,1	0,052867	529	529	0,00000662	10	0,00006621
420	1011372,8	0,057509	575	572	0,00000720	10	0,00007202
430	1015167,1	0,057779	578	577	0,00000724	10	0,00007236
440	1024864,7	0,058472	585	585	0,00000732	10	0,00007323
450	1097869,4	0,063751	638	637	0,00000798	10	0,00007984
460	1141307,6	0,066944	669	669	0,00000838	10	0,00008384

470	1251222,2	0,075183	752	751	0,00000942	10	0,00009416
480	1314767,5	0,080045	800	800	0,00001002	10	0,00010024
490	1395006,3	0,086277	863	861	0,00001080	10	0,00010805
500	1395544,2	0,086319	863	864	0,00001081	10	0,00010810
510	1504219,2	0,094912	949	949	0,00001189	10	0,00011886
520	1608418,6	0,103294	1033	1032	0,00001294	10	0,00012936
530	1698999,6	0,110679	1107	1105	0,00001386	10	0,00013861
540	1737361,6	0,113831	1138	1139	0,00001426	10	0,00014256
550	1781047,2	0,117435	1174	1174	0,00001471	10	0,00014707
560	1816078,6	0,120337	1203	1203	0,00001507	10	0,00015070
570	1875692,4	0,125295	1253	1252	0,00001569	10	0,00015691
580	1935723,9	0,130310	1303	1302	0,00001632	10	0,00016319
590	1944823,6	0,131072	1311	1303	0,00001641	10	0,00016415
600	1998128	0,135543	1355	1356	0,00001697	10	0,00016975
610	2013734,1	0,136854	1369	1369	0,00001714	10	0,00017139
620	2017693,7	0,137187	1372	1371	0,00001718	10	0,00017181
630	2107905,1	0,144784	1448	1425	0,00001813	10	0,00018132
640	2110824,3	0,145030	1450	1450	0,00001816	10	0,00018163
650	2151372,8	0,148451	1485	1483	0,00001859	10	0,00018591
660	2197361,6	0,152333	1523	1500	0,00001908	10	0,00019077
670	2208418,6	0,153267	1533	1532	0,00001919	10	0,00019194
680	2307361,6	0,161620	1616	1617	0,00002024	10	0,00020241
690	2347361,6	0,164994	1650	1650	0,00002066	10	0,00020663
700	2408418,6	0,170136	1701	1701	0,00002131	10	0,00021307
710	2438418,6	0,172659	1727	1726	0,00002162	10	0,00021623
720	2508999,6	0,178579	1786	1761	0,00002236	10	0,00022364
730	2541307,6	0,181280	1813	1812	0,00002270	10	0,00022703
740	2651222,2	0,190422	1904	1903	0,00002385	10	0,00023848
750	2714767,5	0,195667	1957	1956	0,00002450	10	0,00024504
760	2763368,3	0,199654	1997	1974	0,00002500	10	0,00025004

770	2795544,2	0,202281	2023	2023	0,00002533	10	0,00025333
780	2799372,2	0,202593	2026	2026	0,00002537	10	0,00025372
790	2804219,2	0,202988	2030	2030	0,00002542	10	0,00025421
800	2815276,2	0,203887	2039	2038	0,00002553	10	0,00025534
810	2847361,6	0,206489	2065	2065	0,00002586	10	0,00025860
820	2829729,6	0,205061	2051	2073	0,00002568	10	0,00025681
830	2898418,6	0,210606	2106	2106	0,00002638	10	0,00026375
840	2918418,6	0,212210	2122	2122	0,00002658	10	0,00026576
850	2937361,6	0,213725	2137	2137	0,00002677	10	0,00026766
860	2938418,6	0,213809	2138	2138	0,00002678	10	0,00026776
870	3007361,6	0,219281	2193	2193	0,00002746	10	0,00027462
880	3009371,6	0,219440	2194	2195	0,00002748	10	0,00027482
890	3018418,6	0,220153	2202	2201	0,00002757	10	0,00027571
900	3107361,6	0,227097	2271	2257	0,00002844	10	0,00028441
910	3110418,6	0,227334	2273	2271	0,00002847	10	0,00028470
Summation							0,01071118

Table A- 23: Propagational uncertainty data - 700°C run 3

C _{in} (ppmv)	C _{out} (ppmv)	Time (s)	C _{out} /C _{in}	Average relative uncertainty	Propagational uncertainty
2212	20	0	0,0091336	0,039059	0,00050452
2212	21	10	0,0096626	0,039059	0,00053374
2212	23	20	0,0102235	0,039059	0,00056472
2212	25	30	0,0113725	0,039059	0,00062819
2212	31	40	0,0139715	0,039059	0,00077176
2212	33	50	0,0150658	0,039059	0,00083220
2212	39	60	0,0177285	0,039059	0,00097928
2212	40	70	0,0182898	0,039059	0,00101029
2212	47	80	0,0210478	0,039059	0,00116263

2212	50	90	0,022742	0,039059	0,00125621
2212	54	100	0,024269	0,039059	0,00134056
2212	59	110	0,0265079	0,039059	0,00146424
2212	69	120	0,0313369	0,039059	0,00173098
2212	80	130	0,0363913	0,039059	0,00201017
2212	91	140	0,0409967	0,039059	0,00226456
2212	120	150	0,0543961	0,039059	0,00300472
2212	130	160	0,0588776	0,039059	0,00325227
2212	142	170	0,0643478	0,039059	0,00355443
2212	158	180	0,0716261	0,039059	0,00395647
2212	168	190	0,0758157	0,039059	0,00418789
2212	188	200	0,0848014	0,039059	0,00468424
2212	200	210	0,090486	0,039059	0,00499825
2212	217	220	0,0983083	0,039059	0,00543033
2212	252	230	0,1137357	0,039059	0,00628250
2212	291	240	0,1317479	0,039059	0,00727746
2212	296	250	0,1338063	0,039059	0,00739116
2212	298	260	0,1347116	0,039059	0,00744117
2212	300	270	0,1357505	0,039059	0,00749856
2212	308	280	0,1391811	0,039059	0,00768805
2212	312	290	0,141249	0,039059	0,00780228
2212	333	300	0,1507172	0,039059	0,00832528
2212	347	310	0,1570946	0,039059	0,00867755
2212	351	320	0,1584816	0,039059	0,00875417
2212	373	330	0,1688368	0,039059	0,00932617
2212	392	340	0,1772343	0,039059	0,00979002
2212	425	350	0,1920961	0,039059	0,01061096
2212	451	360	0,2038869	0,039059	0,01126226
2212	461	370	0,2082204	0,039059	0,01150163
2212	471	380	0,2129896	0,039059	0,01176507

2212	480	390	0,2168866	0,039059	0,01198033
2212	502	400	0,2270505	0,039059	0,01254176
2212	529	410	0,2390045	0,039059	0,01320208
2212	575	420	0,2599895	0,039059	0,01436124
2212	578	430	0,2612123	0,039059	0,01442879
2212	585	440	0,2643442	0,039059	0,01460178
2212	638	450	0,2882104	0,039059	0,01592010
2212	669	460	0,3026443	0,039059	0,01671740
2212	752	470	0,3398936	0,039059	0,01877497
2212	800	480	0,3618711	0,039059	0,01998895
2212	863	490	0,3900454	0,039059	0,02154524
2212	863	500	0,3902358	0,039059	0,02155576
2212	949	510	0,4290818	0,039059	0,02370152
2212	1033	520	0,4669772	0,039059	0,02579478
2212	1107	530	0,5003639	0,039059	0,02763898
2212	1138	540	0,5146122	0,039059	0,02842603
2212	1174	550	0,5309084	0,039059	0,02932619
2212	1203	560	0,544026	0,039059	0,03005078
2212	1253	570	0,56644	0,039059	0,03128888
2212	1303	580	0,5891123	0,039059	0,03254125
2212	1311	590	0,5925568	0,039059	0,03273151
2212	1355	600	0,6127694	0,039059	0,03384802
2212	1369	610	0,6186975	0,039059	0,03417547
2212	1372	620	0,6202023	0,039059	0,03425859
2212	1448	630	0,6545457	0,039059	0,03615564
2212	1450	640	0,6556586	0,039059	0,03621712
2212	1485	650	0,6711246	0,039059	0,03707142
2212	1523	660	0,6886767	0,039059	0,03804096
2212	1533	670	0,6928976	0,039059	0,03827412
2212	1616	680	0,7306618	0,039059	0,04036013

2212	1650	690	0,7459141	0,039059	0,04120263
2212	1701	700	0,7691623	0,039059	0,04248681
2212	1727	710	0,7805657	0,039059	0,04311670
2212	1786	720	0,8073279	0,039059	0,04459499
2212	1813	730	0,8195411	0,039059	0,04526962
2212	1904	740	0,8608721	0,039059	0,04755265
2212	1957	750	0,8845814	0,039059	0,04886230
2212	1997	760	0,9026067	0,039059	0,04985798
2212	2023	770	0,9144836	0,039059	0,05051403
2212	2026	780	0,9158934	0,039059	0,05059191
2212	2030	790	0,9176776	0,039059	0,05069046
2212	2039	800	0,9217434	0,039059	0,05091505
2212	2065	810	0,9335079	0,039059	0,05156489
2212	2051	820	0,9270492	0,039059	0,05120813
2212	2106	830	0,9521195	0,039059	0,05259296
2212	2122	840	0,9593716	0,039059	0,05299354
2212	2137	850	0,9662194	0,039059	0,05337180
2212	2138	860	0,9666009	0,039059	0,05339288
2212	2193	870	0,9913389	0,039059	0,05475935
2212	2194	880	0,9920557	0,039059	0,05479894
2212	2202	890	0,9952788	0,039059	0,05497698
2212	2271	900	1,0266738	0,039059	0,05671117
2212	2273	910	1,0277431	0,039059	0,05677023

Table A- 24: Volumes obtained from titration for SO₃ analysis - 700°C run 3

Bottle	Initial Volume (ml)	Final Volume (ml)	Volume Titrated (ml)
1	0	2.9	2,9
	2.9	5.9	3
	5.9	8.8	2,9
Average			2,933333333
2	8.8	11.6	2,8
	11.6	14.5	2,9
	14.5	17.5	3
Average			2,9
3	17.5	20.6	3,1
	20.6	23.5	2,9
	23.5	26.5	3
Average			3

Table A- 25: Moles of SO₃ produced from titrations - 700°C run 3

Bottle	BaClO ₄ Consumed (moles)	SO ₃ Produced (moles)
1	1,46667E-05	1,46667E-05
2	0,0000145	0,0000145
3	0,000015	0,000015
Total (moles)	4,41667E-05	4,41667E-05

Table A- 26: System sulfur mass balance - 700°C run 3

Into System		
<i>SO₂ Analysis</i>		
Total moles gas	1,22629	moles
Moles SO ₂	0,00271	moles
Moles sulfur from SO ₂	0,00271	moles
Mass sulfur from SO ₂	0,08698	grams
<i>SO₃ Analysis</i>		
Moles SO ₃	0	moles
Mass SO ₃	0	grams
Out of System		
<i>SO₂ Analysis</i>		
Moles SO ₂	0,00107	0,00107
Moles sulfur from SO ₂	0,00107	0,00107
Mass sulfur from SO ₂	0,03435	0,03435
<i>SO₃ Analysis</i>		
Moles SO ₃ formed	0,000044	moles
Moles sulfur from SO ₃	0,000044	moles
Mass sulfur from SO ₃	0,002830	grams

Table A- 27: SO₂ sorption capacity of limestone sorbent – 700°C run 3

Initial/inlet Concentration (C _o)	2212	ppmv
Saturation time (T _{sat})	890	s
Integral	0,01071	mol.s/L
Sorption capacity of limestone	13.530	mg SO₂/g CaCO₃

A-1.5) 800°C DATA

A-1.5.1) RUN 1

Table A- 28: Initial /inlet SO₂ concentration - 800°C run 1

Time (s)	Area ($\mu\text{V} \cdot \text{s}$)	SO ₂ Volume (ml)	SO ₂ Volume Percent (%)	SO ₂ Concentration (ppmv)
0	3159201,40	0,002311	0,231087	2311
10	2356158,20	0,001657	0,165735	1657
20	3210309,40	0,002350	0,234977	2350
30	2453942,20	0,001740	0,173963	1740
40	3161036,20	0,002312	0,231228	2312
50	2654647,00	0,001907	0,190706	1907
60	3497063,90	0,002559	0,255870	2559
70	2752561,30	0,001988	0,198769	1988
80	3527904,60	0,002580	0,258012	2580
90	2692154,30	0,001938	0,193804	1938
100	3560778,80	0,002603	0,260271	2603
110	2704270,80	0,001948	0,194803	1948
120	3452064,50	0,002527	0,252705	2527
130	3527904,60	0,002580	0,258012	2580
140	3452064,50	0,002527	0,252705	2527
150	3298515,60	0,002416	0,241579	2416
160	2866365,60	0,002080	0,208025	2080
170	3334383,5	0,002442	0,244221	2442
180	3615489,5	0,002640	0,263972	2640
190	2438419,4	0,001727	0,172659	1727
200	3238347,6	0,002371	0,237091	2371

210	2619914,3	0,001878	0,187827	1878
220	3390934,4	0,002483	0,248335	2483
230	2656712,6	0,001909	0,190877	1909
240	3510646,1	0,002568	0,256816	2568
250	2752828,3	0,001988	0,198791	1988
260	3279041,4	0,002401	0,240134	2401
270	2692154,3	0,001938	0,193804	1938
280	3560778,8	0,002603	0,260271	2603
290	2704270,8	0,001948	0,194803	1948
300	3452064,5	0,002527	0,252705	2527
Average		0,002240	0,224018	2240

Table A- 29: Reactor effluent SO₂ concentration - 800°C run 1

Time (s)	Area (μ V. s)	SO ₂ Volume (ml)	SO ₂ Volume Percent (%)	SO ₂ Concentration (ppmv)	C _{SO₂} (mol/L)	ΔT (s)	C _{SO₂} ΔT (mols/L)
0	41168,3	0,000014	0,001380	14	0,00000016	10	0,00000157
10	44830,1	0,000015	0,001533	15	0,00000017	10	0,00000174
20	47156,5	0,000016	0,001630	16	0,00000019	10	0,00000185
30	52833,2	0,000019	0,001869	19	0,00000021	10	0,00000212
40	56221,3	0,000020	0,002012	20	0,00000023	10	0,00000228
50	62104,5	0,000023	0,002261	23	0,00000026	10	0,00000257
60	66189,5	0,000024	0,002434	24	0,00000028	10	0,00000276
70	73380,2	0,000027	0,002742	27	0,00000031	10	0,00000311
80	75384,2	0,000028	0,002828	28	0,00000032	10	0,00000321
90	78547,7	0,000030	0,002964	30	0,00000034	10	0,00000337
100	81573,3	0,000031	0,003094	31	0,00000035	10	0,00000351
110	82182,7	0,000031	0,003121	31	0,00000035	10	0,00000354
120	85708,3	0,000033	0,003273	33	0,00000037	10	0,00000372
130	89252,7	0,000034	0,003427	34	0,00000039	10	0,00000389

140	90915,2	0,000035	0,003500	35	0,00000040	10	0,00000397
150	91195,9	0,000035	0,003512	35	0,00000040	10	0,00000399
160	95271,4	0,000037	0,003690	37	0,00000042	10	0,00000419
170	94060,6	0,000036	0,003637	36	0,00000041	10	0,00000413
180	99173,4	0,000039	0,003861	39	0,00000044	10	0,00000438
190	102326,2	0,000040	0,003999	40	0,00000045	10	0,00000454
200	109145,8	0,000043	0,004300	43	0,00000049	10	0,00000488
210	112330,3	0,000044	0,004441	44	0,00000050	10	0,00000504
220	142796,6	0,000058	0,005811	58	0,00000066	10	0,00000660
230	152908,8	0,000063	0,006273	63	0,00000071	10	0,00000712
240	159887	0,000066	0,006594	66	0,00000075	10	0,00000749
250	177217,8	0,000074	0,007400	74	0,00000084	10	0,00000840
260	181051,2	0,000076	0,007580	76	0,00000086	10	0,00000861
270	184843,7	0,000078	0,007758	78	0,00000088	10	0,00000881
280	197010,3	0,000083	0,008334	83	0,00000095	10	0,00000946
290	204493,7	0,000087	0,008690	87	0,00000099	10	0,00000987
300	228211,1	0,000098	0,009834	98	0,00000112	10	0,00001117
310	231297	0,000100	0,009985	100	0,00000113	10	0,00001134
320	266174,2	0,000117	0,011707	117	0,00000133	10	0,00001330
330	302262,6	0,000135	0,013535	135	0,00000154	10	0,00001537
340	330819,4	0,000150	0,015013	150	0,00000170	10	0,00001705
350	351390,6	0,000161	0,016095	161	0,00000183	10	0,00001828
360	360269,9	0,000166	0,016566	166	0,00000188	10	0,00001881
370	364312	0,000168	0,016782	168	0,00000191	10	0,00001906
380	379918,1	0,000176	0,017619	176	0,00000200	10	0,00002001
390	382820,7	0,000178	0,017776	178	0,00000202	10	0,00002019
400	395951,3	0,000185	0,018487	185	0,00000210	10	0,00002100
410	434089,1	0,000206	0,020587	206	0,00000234	10	0,00002338
420	495918,8	0,000241	0,024090	241	0,00000274	10	0,00002736
430	500294,1	0,000243	0,024342	243	0,00000276	10	0,00002764

440	511048,7	0,000250	0,024965	250	0,00000284	10	0,00002835
450	532415,4	0,000262	0,026213	262	0,00000298	10	0,00002977
460	555853,6	0,000276	0,027598	276	0,00000313	10	0,00003134
470	586349,2	0,000294	0,029425	294	0,00000334	10	0,00003342
480	599894,5	0,000302	0,030246	302	0,00000343	10	0,00003435
490	639552,3	0,000327	0,032678	327	0,00000371	10	0,00003711
500	681728,2	0,000353	0,035314	353	0,00000401	10	0,00004010
510	690403,2	0,000359	0,035862	359	0,00000407	10	0,00004073
520	693545,6	0,000361	0,036061	361	0,00000410	10	0,00004095
530	783545,6	0,000419	0,041878	419	0,00000476	10	0,00004756
540	793545,6	0,000425	0,042537	425	0,00000483	10	0,00004831
550	866174,2	0,000474	0,047403	474	0,00000538	10	0,00005383
560	902262,6	0,000499	0,049869	499	0,00000566	10	0,00005663
570	960819,4	0,000539	0,053935	539	0,00000613	10	0,00006125
580	1020269,9	0,000581	0,058144	581	0,00000660	10	0,00006603
590	1021390,6	0,000582	0,058224	582	0,00000661	10	0,00006612
600	1184312	0,000701	0,070141	701	0,00000797	10	0,00007966
610	1199918,1	0,000713	0,071310	713	0,00000810	10	0,00008098
620	1202820,7	0,000715	0,071528	715	0,00000812	10	0,00008123
630	1294089,1	0,000785	0,078455	785	0,00000891	10	0,00008910
640	1295951,3	0,000786	0,078598	786	0,00000893	10	0,00008926
650	1335918,8	0,000817	0,081678	817	0,00000928	10	0,00009276
660	1383545,6	0,000854	0,085381	854	0,00000970	10	0,00009696
670	1393545,6	0,000862	0,086163	862	0,00000979	10	0,00009785
680	1493545,6	0,000941	0,094061	941	0,00001068	10	0,00010682
690	1533545,6	0,000973	0,097257	973	0,00001105	10	0,00011045
700	1593545,6	0,001021	0,102090	1021	0,00001159	10	0,00011594
710	1623545,6	0,001045	0,104521	1045	0,00001187	10	0,00011870
720	1693545,6	0,001102	0,110232	1102	0,00001252	10	0,00012519
730	1725853,6	0,001129	0,112884	1129	0,00001282	10	0,00012820

740	1736349,2	0,001137	0,113747	1137	0,00001292	10	0,00012918
750	1799894,5	0,001190	0,118995	1190	0,00001351	10	0,00013514
760	1849552,3	0,001231	0,123118	1231	0,00001398	10	0,00013982
770	1881728,2	0,001258	0,125798	1258	0,00001429	10	0,00014286
780	1985556,2	0,001345	0,134487	1345	0,00001527	10	0,00015273
790	1990403,2	0,001349	0,134894	1349	0,00001532	10	0,00015319
800	2000403,2	0,001357	0,135734	1357	0,00001541	10	0,00015415
810	2033545,6	0,001385	0,138520	1385	0,00001573	10	0,00015731
820	2143545,6	0,001478	0,147790	1478	0,00001678	10	0,00016784
830	2183545,6	0,001512	0,151167	1512	0,00001717	10	0,00017167
840	2203545,6	0,001529	0,152855	1529	0,00001736	10	0,00017359
850	2223545,6	0,001545	0,154544	1545	0,00001755	10	0,00017551
860	2323545,6	0,001630	0,162986	1630	0,00001851	10	0,00018510
870	2393545,6	0,001689	0,168885	1689	0,00001918	10	0,00019179
880	2495555,6	0,001775	0,177453	1775	0,00002015	10	0,00020152
890	2503545,6	0,001781	0,178122	1781	0,00002023	10	0,00020228
900	2593545,6	0,001856	0,185635	1856	0,00002108	10	0,00021082
910	2603545,6	0,001865	0,186467	1865	0,00002118	10	0,00021176
920	2604645,6	0,001866	0,186558	1866	0,00002119	10	0,00021187
930	2623545,6	0,001881	0,188128	1881	0,00002136	10	0,00021365
940	2723545,6	0,001964	0,196388	1964	0,00002230	10	0,00022303
950	2754545,6	0,001989	0,198932	1989	0,00002259	10	0,00022592
960	2803545,6	0,002029	0,202933	2029	0,00002305	10	0,00023046
970	2823545,6	0,002046	0,204559	2046	0,00002323	10	0,00023231
980	2845545,6	0,002063	0,206342	2063	0,00002343	10	0,00023433
990	2863545,6	0,002078	0,207797	2078	0,00002360	10	0,00023599
1000	2903545,6	0,002110	0,211018	2110	0,00002396	10	0,00023964
1010	2953545,6	0,002150	0,215015	2150	0,00002442	10	0,00024418
1020	2973545,6	0,002166	0,216605	2166	0,00002460	10	0,00024599
1030	3003545,6	0,002190	0,218980	2190	0,00002487	10	0,00024869

1040	3023545,6	0,002206	0,220556	2206	0,00002505	10	0,00025048
1050	3055945,6	0,002231	0,223097	2231	0,00002534	10	0,00025336
1060	3073545,6	0,002245	0,224471	2245	0,00002549	10	0,00025492
1070	3093545,6	0,002260	0,226026	2260	0,00002567	10	0,00025669
1080	3103545,6	0,002268	0,226802	2268	0,00002576	10	0,00025757
1090	3113545,6	0,002276	0,227575	2276	0,00002584	10	0,00025845
Summation							0,00990744

Table A- 30: Propagational uncertainty data - 800°C run 1

C _{in} (ppmv)	C _{out} (ppmv)	Time (s)	C _{out} /C _{in}	Average relative uncertainty	Propagational uncertainty
2240	14	0	0,0061621	0,039059	0,00034038
2240	15	10	0,0068438	0,039059	0,00037803
2240	16	20	0,0072781	0,039059	0,00040202
2240	19	30	0,0083418	0,039059	0,00046078
2240	20	40	0,0089793	0,039059	0,00049600
2240	23	50	0,0100912	0,039059	0,00055741
2240	24	60	0,0108667	0,039059	0,00060025
2240	27	70	0,0122388	0,039059	0,00067604
2240	28	80	0,0126228	0,039059	0,00069726
2240	30	90	0,0132304	0,039059	0,00073082
2240	31	100	0,0138131	0,039059	0,00076301
2240	31	110	0,0139307	0,039059	0,00076950
2240	33	120	0,014612	0,039059	0,00080714
2240	34	130	0,0152992	0,039059	0,00084509
2240	35	140	0,0156222	0,039059	0,00086294
2240	35	150	0,0156768	0,039059	0,00086595
2240	37	160	0,016471	0,039059	0,00090982
2240	36	170	0,0162347	0,039059	0,00089677

2240	39	180	0,017234	0,039059	0,00095197
2240	40	190	0,0178523	0,039059	0,00098612
2240	43	200	0,0191957	0,039059	0,00106033
2240	44	210	0,0198257	0,039059	0,00109513
2240	58	220	0,0259396	0,039059	0,00143285
2240	63	230	0,0280033	0,039059	0,00154684
2240	66	240	0,0294373	0,039059	0,00162605
2240	74	250	0,0330337	0,039059	0,00182471
2240	76	260	0,0338358	0,039059	0,00186901
2240	78	270	0,0346318	0,039059	0,00191298
2240	83	280	0,0372012	0,039059	0,00205491
2240	87	290	0,0387935	0,039059	0,00214287
2240	98	300	0,0439	0,039059	0,00242494
2240	100	310	0,0445711	0,039059	0,00246201
2240	117	320	0,0522608	0,039059	0,00288677
2240	135	330	0,0604188	0,039059	0,00333740
2240	150	340	0,0670169	0,039059	0,00370186
2240	161	350	0,0718467	0,039059	0,00396865
2240	166	360	0,0739512	0,039059	0,00408490
2240	168	370	0,0749131	0,039059	0,00413803
2240	176	380	0,0786498	0,039059	0,00434444
2240	178	390	0,0793487	0,039059	0,00438305
2240	185	400	0,0825263	0,039059	0,00455857
2240	206	410	0,0918981	0,039059	0,00507625
2240	241	420	0,107534	0,039059	0,00593994
2240	243	430	0,1086608	0,039059	0,00600218
2240	250	440	0,1114417	0,039059	0,00615579
2240	262	450	0,1170137	0,039059	0,00646357
2240	276	460	0,1231971	0,039059	0,00680513
2240	294	470	0,1313524	0,039059	0,00725561

2240	302	480	0,1350141	0,039059	0,00745788
2240	327	490	0,1458715	0,039059	0,00805762
2240	353	500	0,1576377	0,039059	0,00870755
2240	359	510	0,1600853	0,039059	0,00884276
2240	361	520	0,1609742	0,039059	0,00889186
2240	419	530	0,1869382	0,039059	0,01032605
2240	425	540	0,189882	0,039059	0,01048866
2240	474	550	0,2116015	0,039059	0,01168839
2240	499	560	0,2226094	0,039059	0,01229644
2240	539	570	0,2407629	0,039059	0,01329921
2240	581	580	0,259549	0,039059	0,01433690
2240	582	590	0,2599064	0,039059	0,01435665
2240	701	600	0,3131044	0,039059	0,01729519
2240	713	610	0,3183219	0,039059	0,01758339
2240	715	620	0,3192945	0,039059	0,01763711
2240	785	630	0,350219	0,039059	0,01934532
2240	786	640	0,3508567	0,039059	0,01938054
2240	817	650	0,3646035	0,039059	0,02013988
2240	854	660	0,3811329	0,039059	0,02105293
2240	862	670	0,3846232	0,039059	0,02124573
2240	941	680	0,4198792	0,039059	0,02319319
2240	973	690	0,4341501	0,039059	0,02398148
2240	1021	700	0,4557207	0,039059	0,02517300
2240	1045	710	0,4665754	0,039059	0,02577258
2240	1102	720	0,4920674	0,039059	0,02718071
2240	1129	730	0,503905	0,039059	0,02783459
2240	1137	740	0,5077596	0,039059	0,02804751
2240	1190	750	0,531186	0,039059	0,02934153
2240	1231	760	0,549589	0,039059	0,03035807
2240	1258	770	0,5615534	0,039059	0,03101896

2240	1345	780	0,6003406	0,039059	0,03316147
2240	1349	790	0,602157	0,039059	0,03326181
2240	1357	800	0,6059059	0,039059	0,03346889
2240	1385	810	0,6183428	0,039059	0,03415588
2240	1478	820	0,6597243	0,039059	0,03644170
2240	1512	830	0,6747967	0,039059	0,03727426
2240	1529	840	0,6823351	0,039059	0,03769067
2240	1545	850	0,6898741	0,039059	0,03810710
2240	1630	860	0,7275555	0,039059	0,04018854
2240	1689	870	0,7538889	0,039059	0,04164314
2240	1775	880	0,7921358	0,039059	0,04375581
2240	1781	890	0,7951229	0,039059	0,04392082
2240	1856	900	0,8286613	0,039059	0,04577340
2240	1865	910	0,8323739	0,039059	0,04597848
2240	1866	920	0,8327821	0,039059	0,04600103
2240	1881	930	0,8397899	0,039059	0,04638812
2240	1964	940	0,8766636	0,039059	0,04842494
2240	1989	950	0,8880164	0,039059	0,04905204
2240	2029	960	0,9058764	0,039059	0,05003859
2240	2046	970	0,9131345	0,039059	0,05043951
2240	2063	980	0,921096	0,039059	0,05087929
2240	2078	990	0,927592	0,039059	0,05123811
2240	2110	1000	0,9419672	0,039059	0,05203216
2240	2150	1010	0,9598123	0,039059	0,05301789
2240	2166	1020	0,9669097	0,039059	0,05340993
2240	2190	1030	0,9775105	0,039059	0,05399550
2240	2206	1040	0,9845464	0,039059	0,05438414
2240	2231	1050	0,9958896	0,039059	0,05501072
2240	2245	1060	1,002022	0,039059	0,05534946
2240	2260	1070	1,008965	0,039059	0,05573297

2240	2268	1080	1,012426	0,039059	0,05592415
2240	2276	1090	1,0158799	0,039059	0,05611494

Table A- 31: Volumes obtained from titration for SO₃ analysis - 800°C run 1

Bottle	Initial Volume (ml)	Final Volume (ml)	Volume Titrated (ml)
1	0	5.2	5.2
	5.2	10.3	5.1
	10.3	15.5	5.2
Average			5.1666
2	15.5	20.6	5.1
	20.6	25.7	5.1
	25.7	30.9	5.2
Average			5.1333
3	0	5.1	5.1
	5.1	10.2	5.1
	10.2	15.3	5.1
Average			5.1

Table A- 32: Moles of SO₃ produced from titrations - 800°C run 1

Bottle	BaClO ₄ Consumed (moles)	SO ₃ Produced (moles)
1	0,0000258	0,0000258
2	0,0000257	0,0000257
3	0,0000255	0,0000255
Total (moles)	0,000077	0,000077

Table A- 33: System sulfur mass balance - 800°C run 1

Into System		
<i>SO₂ Analysis</i>		
Total moles gas	1,22629	moles
Moles SO ₂	0,00275	moles
Moles sulfur from SO ₂	0,00275	moles
Mass sulfur from SO ₂	0,08809	grams
<i>SO₃ Analysis</i>		
Moles SO ₃	0	moles
Mass SO ₃	0	grams
Out of System		
<i>SO₂ Analysis</i>		
Moles SO ₂	0,00099	moles
Moles sulfur from SO ₂	0,00099	moles
Mass sulfur from SO ₂	0,03177	grams
<i>SO₃ Analysis</i>		
Moles SO ₃ formed	0,000077	moles
Moles sulfur from SO ₃	0,000077	moles
Mass sulfur from SO ₃	0,004936	grams

Table A- 34: SO₂ sorption capacity of limestone sorbent - 800°C run 1

Initial/inlet Concentration (C _o)	2240	ppmv
Saturation time (T _{sat})	1060	s
Integral	0,00991	mol.s/L
Sorption capacity of limestone	16.320	mg SO₂/g CaCO₃

A-1.5.2) RUN 2

Table A- 35: Initial /inlet SO₂ concentration - 800°C run 2

Time (s)	Area ($\mu\text{V} \cdot \text{s}$)	SO ₂ Volume (ml)	SO ₂ Volume Percent (%)	SO ₂ Concentration (ppmv)
0	3172871,40	0,002321	0,232132	2321
10	2369828,20	0,001669	0,166887	1669
20	3224595,40	0,002361	0,236056	2361
30	2467612,20	0,001751	0,175110	1751
40	3146746,20	0,002301	0,230133	2301
50	2668933,00	0,001919	0,191887	1919
60	3511353,90	0,002569	0,256865	2569
70	2738891,30	0,001976	0,197649	1976
80	3542190,60	0,002590	0,258997	2590
90	2705824,30	0,001949	0,194931	1949
100	3546488,80	0,002593	0,259292	2593
110	2718556,80	0,001960	0,195978	1960
120	3466354,50	0,002537	0,253715	2537
130	3542190,60	0,002590	0,258997	2590
140	3465734,50	0,002537	0,253672	2537
150	3312801,60	0,002426	0,242635	2426
160	2880655,60	0,002092	0,209177	2092
170	3348673,5	0,002453	0,245267	2453
180	3601203,5	0,002630	0,263013	2630
190	2452089,4	0,001738	0,173807	1738
200	3252633,6	0,002382	0,238163	2382
210	2634204,3	0,001890	0,189012	1890
220	3376644,4	0,002473	0,247302	2473

230	2670998,6	0,001921	0,192058	1921
240	3524936,1	0,002578	0,257807	2578
250	2738542,3	0,001976	0,197620	1976
260	3293331,4	0,002412	0,241195	2412
270	2705824,3	0,001949	0,194931	1949
280	3575068,8	0,002612	0,261245	2612
290	2718556,8	0,001960	0,195978	1960
300	3465734,5	0,002537	0,253672	2537
Average		0,002247	0,224683	2247

Table A- 36: Reactor effluent SO₂ concentration - 800°C run 2

Time (s)	Area (μ V.s)	SO ₂ Volume (ml)	SO ₂ Volume Percent (%)	SO ₂ Concentration (ppmv)	C _{SO₂} (mol/L)	ΔT (s)	C _{SO₂} ΔT (mol.s/L)
0	48345,3	0,000017	0,001680	17	0,00000019	10	0,00000191
10	50220,1	0,000018	0,001759	18	0,00000020	10	0,00000200
20	52702,5	0,000019	0,001863	19	0,00000021	10	0,00000212
30	58010,2	0,000021	0,002087	21	0,00000024	10	0,00000237
40	61611,3	0,000022	0,002240	22	0,00000025	10	0,00000254
50	67650,5	0,000025	0,002497	25	0,00000028	10	0,00000284
60	71579,5	0,000027	0,002665	27	0,00000030	10	0,00000303
70	78770,2	0,000030	0,002973	30	0,00000034	10	0,00000338
80	80561,2	0,000031	0,003051	31	0,00000035	10	0,00000346
90	84093,7	0,000032	0,003203	32	0,00000036	10	0,00000364
100	86963,3	0,000033	0,003328	33	0,00000038	10	0,00000378
110	87728,7	0,000034	0,003361	34	0,00000038	10	0,00000382
120	91254,3	0,000035	0,003514	35	0,00000040	10	0,00000399
130	94642,7	0,000037	0,003662	37	0,00000042	10	0,00000416
140	96092,2	0,000037	0,003726	37	0,00000042	10	0,00000423
150	96741,9	0,000038	0,003754	38	0,00000043	10	0,00000426

160	99448,4	0,000039	0,003873	39	0,00000044	10	0,00000440
170	99606,6	0,000039	0,003880	39	0,00000044	10	0,00000441
180	104719,4	0,000041	0,004105	41	0,00000047	10	0,00000466
190	114106,2	0,000045	0,004520	45	0,00000051	10	0,00000513
200	120830,8	0,000048	0,004820	48	0,00000055	10	0,00000547
210	124511,3	0,000050	0,004985	50	0,00000057	10	0,00000566
220	154481,6	0,000063	0,006345	63	0,00000072	10	0,00000721
230	164593,8	0,000068	0,006812	68	0,00000077	10	0,00000774
240	171667	0,000071	0,007141	71	0,00000081	10	0,00000811
250	188997,8	0,000080	0,007954	80	0,00000090	10	0,00000903
260	192736,2	0,000081	0,008131	81	0,00000092	10	0,00000923
270	196528,7	0,000083	0,008311	83	0,00000094	10	0,00000944
280	209191,3	0,000089	0,008915	89	0,00000101	10	0,00001012
290	216178,7	0,000093	0,009252	93	0,00000105	10	0,00001051
300	239896,1	0,000104	0,010405	104	0,00000118	10	0,00001182
310	243478	0,000106	0,010581	106	0,00000120	10	0,00001202
320	277859,2	0,000123	0,012294	123	0,00000140	10	0,00001396
330	314443,6	0,000142	0,014162	142	0,00000161	10	0,00001608
340	342599,4	0,000156	0,015631	156	0,00000178	10	0,00001775
350	363571,6	0,000167	0,016742	167	0,00000190	10	0,00001901
360	371954,9	0,000172	0,017191	172	0,00000195	10	0,00001952
370	376092	0,000174	0,017413	174	0,00000198	10	0,00001978
380	391603,1	0,000183	0,018251	183	0,00000207	10	0,00002073
390	395001,7	0,000184	0,018436	184	0,00000209	10	0,00002094
400	407636,3	0,000191	0,019126	191	0,00000217	10	0,00002172
410	445869,1	0,000212	0,021245	212	0,00000241	10	0,00002413
420	508099,8	0,000248	0,024794	248	0,00000282	10	0,00002816
430	511979,1	0,000250	0,025019	250	0,00000284	10	0,00002841
440	522828,7	0,000257	0,025651	257	0,00000291	10	0,00002913
450	544195,4	0,000269	0,026907	269	0,00000306	10	0,00003056

460	567538,6	0,000283	0,028295	283	0,00000321	10	0,00003213
470	598530,2	0,000302	0,030163	302	0,00000343	10	0,00003425
480	611674,5	0,000310	0,030963	310	0,00000352	10	0,00003516
490	651237,3	0,000334	0,033403	334	0,00000379	10	0,00003793
500	693508,2	0,000361	0,036059	361	0,00000410	10	0,00004095
510	702584,2	0,000366	0,036635	366	0,00000416	10	0,00004161
520	705230,6	0,000368	0,036804	368	0,00000418	10	0,00004180
530	795230,6	0,000426	0,042648	426	0,00000484	10	0,00004843
540	805325,6	0,000433	0,043317	433	0,00000492	10	0,00004919
550	878355,2	0,000482	0,048231	482	0,00000548	10	0,00005477
560	913947,6	0,000507	0,050674	507	0,00000575	10	0,00005755
570	973000,4	0,000548	0,054791	548	0,00000622	10	0,00006222
580	1034559,9	0,000592	0,059167	592	0,00000672	10	0,00006719
590	1035676,6	0,000592	0,059247	592	0,00000673	10	0,00006728
600	1197982	0,000712	0,071165	712	0,00000808	10	0,00008082
610	1213588,1	0,000723	0,072337	723	0,00000822	10	0,00008215
620	1216490,7	0,000726	0,072556	726	0,00000824	10	0,00008240
630	1308375,1	0,000796	0,079553	796	0,00000903	10	0,00009034
640	1310241,3	0,000797	0,079696	797	0,00000905	10	0,00009051
650	1349588,8	0,000827	0,082737	827	0,00000940	10	0,00009396
660	1397835,6	0,000865	0,086498	865	0,00000982	10	0,00009823
670	1407215,6	0,000872	0,087234	872	0,00000991	10	0,00009907
680	1507215,6	0,000952	0,095151	952	0,00001081	10	0,00010806
690	1547215,6	0,000984	0,098355	984	0,00001117	10	0,00011170
700	1607831,6	0,001032	0,103246	1032	0,00001173	10	0,00011725
710	1637215,6	0,001056	0,105633	1056	0,00001200	10	0,00011996
720	1707831,6	0,001114	0,111403	1114	0,00001265	10	0,00012652
730	1740143,6	0,001141	0,114060	1141	0,00001295	10	0,00012953
740	1750639,2	0,001149	0,114925	1149	0,00001305	10	0,00013051
750	1814180,5	0,001202	0,120179	1202	0,00001365	10	0,00013648

760	1863838,3	0,001243	0,124307	1243	0,00001412	10	0,00014117
770	1895398,2	0,001269	0,126939	1269	0,00001442	10	0,00014416
780	1999842,2	0,001357	0,135687	1357	0,00001541	10	0,00015409
790	2004693,2	0,001361	0,136094	1361	0,00001546	10	0,00015456
800	2014073,2	0,001369	0,136883	1369	0,00001555	10	0,00015545
810	2047835,6	0,001397	0,139722	1397	0,00001587	10	0,00015868
820	2157831,6	0,001490	0,148996	1490	0,00001692	10	0,00016921
830	2197215,6	0,001523	0,152321	1523	0,00001730	10	0,00017298
840	2217835,6	0,001541	0,154062	1541	0,00001750	10	0,00017496
850	2237215,6	0,001557	0,155699	1557	0,00001768	10	0,00017682
860	2337831,6	0,001642	0,164190	1642	0,00001865	10	0,00018646
870	2407215,6	0,001700	0,170035	1700	0,00001931	10	0,00019310
880	2509845,6	0,001786	0,178649	1786	0,00002029	10	0,00020288
890	2517831,6	0,001793	0,179318	1793	0,00002036	10	0,00020364
900	2607835,6	0,001868	0,186823	1868	0,00002122	10	0,00021217
910	2617215,6	0,001876	0,187603	1876	0,00002131	10	0,00021305
920	2618935,6	0,001877	0,187745	1877	0,00002132	10	0,00021321
930	2637831,6	0,001893	0,189313	1893	0,00002150	10	0,00021499
940	2737215,6	0,001975	0,197511	1975	0,00002243	10	0,00022430
950	2768835,6	0,002001	0,200101	2001	0,00002272	10	0,00022725
960	2817215,6	0,002040	0,204044	2040	0,00002317	10	0,00023172
970	2837831,6	0,002057	0,205717	2057	0,00002336	10	0,00023362
980	2859215,6	0,002074	0,207448	2074	0,00002356	10	0,00023559
990	2877835,6	0,002090	0,208950	2090	0,00002373	10	0,00023729
1000	2917835,6	0,002122	0,212163	2122	0,00002409	10	0,00024094
1010	2967831,6	0,002162	0,216152	2162	0,00002455	10	0,00024547
1020	2987835,6	0,002177	0,217738	2177	0,00002473	10	0,00024728
1030	3017215,6	0,002201	0,220058	2201	0,00002499	10	0,00024991
1040	3037831,6	0,002217	0,221679	2217	0,00002518	10	0,00025175
1050	3070235,6	0,002242	0,224213	2242	0,00002546	10	0,00025463

1060	3087215,6	0,002255	0,225535	2255	0,00002561	10	0,00025613
1070	3107215,6	0,002271	0,227086	2271	0,00002579	10	0,00025789
1080	3117215,6	0,002279	0,227859	2279	0,00002588	10	0,00025877
1090	3121835,6	0,002282	0,228216	2282	0,00002592	10	0,00025917
Summation							0,01000765

Table A- 37: Propagational uncertainty data - 800°C run 2

C _{in} (ppmv)	C _{out} (ppmv)	Time (s)	C _{out} /C _{in}	Average relative uncertainty	Propagational uncertainty
2247	17	0	0,0074782	0,039059	0,00041308
2247	18	10	0,0078282	0,039059	0,00043241
2247	19	20	0,0082926	0,039059	0,00045807
2247	21	30	0,0092892	0,039059	0,00051311
2247	22	40	0,0099681	0,039059	0,00055062
2247	25	50	0,0111117	0,039059	0,00061379
2247	27	60	0,0118591	0,039059	0,00065507
2247	30	70	0,0132339	0,039059	0,00073101
2247	31	80	0,0135777	0,039059	0,00075000
2247	32	90	0,0142574	0,039059	0,00078755
2247	33	100	0,0148111	0,039059	0,00081813
2247	34	110	0,014959	0,039059	0,00082630
2247	35	120	0,0156417	0,039059	0,00086401
2247	37	130	0,0162999	0,039059	0,00090037
2247	37	140	0,016582	0,039059	0,00091595
2247	38	150	0,0167086	0,039059	0,00092294
2247	39	160	0,0172366	0,039059	0,00095211
2247	39	170	0,0172675	0,039059	0,00095382
2247	41	180	0,0182686	0,039059	0,00100912
2247	45	190	0,0201181	0,039059	0,00111128

2247	48	200	0,0214522	0,039059	0,00118497
2247	50	210	0,0221855	0,039059	0,00122548
2247	63	220	0,0282419	0,039059	0,00156002
2247	68	230	0,0303191	0,039059	0,00167476
2247	71	240	0,031782	0,039059	0,00175557
2247	80	250	0,0354012	0,039059	0,00195548
2247	81	260	0,0361883	0,039059	0,00199896
2247	83	270	0,0369892	0,039059	0,00204320
2247	89	280	0,0396799	0,039059	0,00219183
2247	93	290	0,0411757	0,039059	0,00227446
2247	104	300	0,0463115	0,039059	0,00255815
2247	106	310	0,0470949	0,039059	0,00260142
2247	123	320	0,0547176	0,039059	0,00302248
2247	142	330	0,0630308	0,039059	0,00348168
2247	156	340	0,0695682	0,039059	0,00384279
2247	167	350	0,0745154	0,039059	0,00411607
2247	172	360	0,0765113	0,039059	0,00422632
2247	174	370	0,0775002	0,039059	0,00428094
2247	183	380	0,08123	0,039059	0,00448696
2247	184	390	0,0820519	0,039059	0,00453237
2247	191	400	0,0851224	0,039059	0,00470197
2247	212	410	0,0945546	0,039059	0,00522298
2247	248	420	0,1103499	0,039059	0,00609548
2247	250	430	0,1113523	0,039059	0,00615085
2247	257	440	0,1141669	0,039059	0,00630632
2247	269	450	0,1197565	0,039059	0,00661508
2247	283	460	0,1259334	0,039059	0,00695628
2247	302	470	0,1342455	0,039059	0,00741542
2247	310	480	0,1378087	0,039059	0,00761225
2247	334	490	0,1486675	0,039059	0,00821206

2247	361	500	0,160487	0,039059	0,00886495
2247	366	510	0,1630536	0,039059	0,00900671
2247	368	520	0,1638038	0,039059	0,00904816
2247	426	530	0,1898154	0,039059	0,01048498
2247	433	540	0,1927919	0,039059	0,01064939
2247	482	550	0,2146638	0,039059	0,01185755
2247	507	560	0,2255336	0,039059	0,01245797
2247	548	570	0,2438592	0,039059	0,01347024
2247	592	580	0,263334	0,039059	0,01454598
2247	592	590	0,2636907	0,039059	0,01456568
2247	712	600	0,3167329	0,039059	0,01749562
2247	723	610	0,3219524	0,039059	0,01778393
2247	726	620	0,3229254	0,039059	0,01783768
2247	796	630	0,3540659	0,039059	0,01955781
2247	797	640	0,3547049	0,039059	0,01959311
2247	827	650	0,3682381	0,039059	0,02034065
2247	865	660	0,3849793	0,039059	0,02126540
2247	872	670	0,3882522	0,039059	0,02144618
2247	952	680	0,4234883	0,039059	0,02339255
2247	984	690	0,4377477	0,039059	0,02418021
2247	1032	700	0,4595195	0,039059	0,02538283
2247	1056	710	0,4701398	0,039059	0,02596947
2247	1114	720	0,495824	0,039059	0,02738821
2247	1141	730	0,5076467	0,039059	0,02804127
2247	1149	740	0,5114957	0,039059	0,02825388
2247	1202	750	0,5348837	0,039059	0,02954578
2247	1243	760	0,5532545	0,039059	0,03056054
2247	1269	770	0,5649674	0,039059	0,03120754
2247	1357	780	0,6039021	0,039059	0,03335820
2247	1361	790	0,6057159	0,039059	0,03345839

2247	1369	800	0,6092242	0,039059	0,03365219
2247	1397	810	0,6218638	0,039059	0,03435037
2247	1490	820	0,6631372	0,039059	0,03663022
2247	1523	830	0,6779358	0,039059	0,03744766
2247	1541	840	0,6856854	0,039059	0,03787573
2247	1557	850	0,692969	0,039059	0,03827806
2247	1642	860	0,7307637	0,039059	0,04036576
2247	1700	870	0,7567769	0,039059	0,04180267
2247	1786	880	0,795116	0,039059	0,04392043
2247	1793	890	0,7980902	0,039059	0,04408472
2247	1868	900	0,8314964	0,039059	0,04593000
2247	1876	910	0,8349645	0,039059	0,04612158
2247	1877	920	0,8356002	0,039059	0,04615669
2247	1893	930	0,8425771	0,039059	0,04654208
2247	1975	940	0,8790642	0,039059	0,04855754
2247	2001	950	0,8905912	0,039059	0,04919427
2247	2040	960	0,9081424	0,039059	0,05016376
2247	2057	970	0,9155881	0,039059	0,05057504
2247	2074	980	0,923289	0,039059	0,05100042
2247	2090	990	0,9299755	0,039059	0,05136977
2247	2122	1000	0,9442774	0,039059	0,05215978
2247	2162	1010	0,9620275	0,039059	0,05314025
2247	2177	1020	0,9690882	0,039059	0,05353027
2247	2201	1030	0,9794137	0,039059	0,05410062
2247	2217	1040	0,9866264	0,039059	0,05449904
2247	2242	1050	0,9979068	0,039059	0,05512214
2247	2255	1060	1,0037895	0,039059	0,05544709
2247	2271	1070	1,0106929	0,039059	0,05582842
2247	2279	1080	1,014134	0,039059	0,05601850
2247	2282	1090	1,0157214	0,039059	0,05610618

Table A- 38: Volumes obtained from titration for SO₃ analysis - 800°C run 2

Bottle	Initial Volume (ml)	Final Volume (ml)	Volume Titrated (ml)
1	0	5.1	5.1
	5.1	10.2	5.1
	10.2	15.4	5.2
Average			5.1333
2	15.4	20.5	5.1
	20.5	25.6	5.1
	25.6	30.8	5.2
Average			5.1333
3	0	5.1	5.1
	5.1	10.2	5.1
	10.2	15.3	5.1
Average			5.1

Table A- 39: Moles of SO₃ produced from titrations - 800°C run 2

Bottle	BaClO ₄ Consumed (moles)	SO ₃ Produced (moles)
1	0,0000256	0,0000256
2	0,0000256	0,0000256
3	0,0000255	0,0000255
Total (moles)	0,000077	0,000077

Table A- 40: System sulfur mass balance - 800°C run 2

Into System		
<i>SO₂ Analysis</i>		
Total moles gas	1,22629	moles
Moles SO ₂	0,00276	moles
Moles sulfur from SO ₂	0,00276	moles
Mass sulfur from SO ₂	0,08835	grams
<i>SO₃ Analysis</i>		
Moles SO ₃	0	moles
Mass SO ₃	0	grams
Out of System		
<i>SO₂ Analysis</i>		
Moles SO ₂	0,00100	moles
Moles sulfur from SO ₂	0,00100	moles
Mass sulfur from SO ₂	0,03209	grams
<i>SO₃ Analysis</i>		
Moles SO ₃ formed	0,000077	moles
Moles sulfur from SO ₃	0,000077	moles
Mass sulfur from SO ₃	0,004921	grams

Table A- 41: SO₂ sorption capacity of limestone sorbent - 800°C run 2

Initial/inlet Concentration (C _o)	2247	ppmv
Saturation time (T _{sat})	1060	s
Integral	0,01001	mol.s/L
Sorption capacity of limestone	16.368	mg SO₂/g CaCO₃

A-1.5.3) RUN 3

Table A- 42: Initial /inlet SO₂ concentration - 800°C run 3

Time (s)	Area ($\mu\text{V} \cdot \text{s}$)	SO ₂ Volume (ml)	SO ₂ Volume Percent (%)	SO ₂ Concentration (ppmv)
0	3174074,40	0,002322	0,232224	2322
10	2869974,20	0,002083	0,208316	2083
20	3196493,40	0,002339	0,233930	2339
30	2467758,20	0,001751	0,175122	1751
40	3174852,20	0,002323	0,232283	2323
50	2669520,00	0,001919	0,191936	1919
60	3510879,90	0,002568	0,256833	2568
70	2766377,30	0,001999	0,199900	1999
80	3514088,60	0,002571	0,257055	2571
90	2707608,30	0,001951	0,195078	1951
100	3546962,80	0,002593	0,259325	2593
110	2718086,80	0,001959	0,195940	1959
120	3437191,50	0,002516	0,251649	2516
130	3512450,60	0,002569	0,256942	2569
140	3438248,50	0,002517	0,251725	2517
150	3283642,60	0,002405	0,240476	2405
160	2881238,60	0,002092	0,209224	2092
170	3348199,5	0,002452	0,245232	2452
180	3600035,5	0,002629	0,262934	2629
190	2453873,4	0,001740	0,173957	1740
200	3224531,6	0,002361	0,236051	2361
210	2633730,3	0,001890	0,188973	1890
220	3377118,4	0,002473	0,247336	2473
230	2670528,6	0,001920	0,192019	1920

240	3496830,1	0,002559	0,255854	2559
250	2767701,3	0,002000	0,200008	2000
260	3292857,4	0,002412	0,241160	2412
270	2705970,3	0,001949	0,194943	1949
280	3545324,8	0,002592	0,259213	2592
290	2718086,8	0,001959	0,195940	1959
300	3437191,5	0,002516	0,251649	2516
Average		0,002256	0,225588	2256

Table A- 43: Reactor effluent SO₂ concentration - 800°C run 3

Time (s)	Area (μ V.s)	SO ₂ Volume (ml)	SO ₂ Volume Percent (%)	SO ₂ Concentration (ppmv)	C _{SO₂} (mol/L)	ΔT (s)	C _{SO₂} ΔT (mol.s/L)
0	45536,3	0,000016	0,001563	16	0,00000018	10	0,00000177
10	49797,1	0,000017	0,001741	17	0,00000020	10	0,00000198
20	52417,5	0,000019	0,001851	19	0,00000021	10	0,00000210
30	57201,2	0,000021	0,002053	21	0,00000023	10	0,00000233
40	61482,3	0,000022	0,002234	22	0,00000025	10	0,00000254
50	67071,5	0,000025	0,002472	25	0,00000028	10	0,00000281
60	70557,5	0,000026	0,002621	26	0,00000030	10	0,00000298
70	78347,2	0,000030	0,002955	30	0,00000034	10	0,00000336
80	80645,2	0,000031	0,003054	31	0,00000035	10	0,00000347
90	83808,7	0,000032	0,003191	32	0,00000036	10	0,00000362
100	86834,3	0,000033	0,003322	33	0,00000038	10	0,00000377
110	87443,7	0,000033	0,003349	33	0,00000038	10	0,00000380
120	90969,3	0,000035	0,003502	35	0,00000040	10	0,00000398
130	94513,7	0,000037	0,003657	37	0,00000042	10	0,00000415
140	96176,2	0,000037	0,003729	37	0,00000042	10	0,00000424
150	96456,9	0,000037	0,003742	37	0,00000042	10	0,00000425
160	100532,4	0,000039	0,003920	39	0,00000045	10	0,00000445

170	101321,6	0,000040	0,003955	40	0,00000045	10	0,00000449
180	104434,4	0,000041	0,004092	41	0,00000046	10	0,00000465
190	114093,2	0,000045	0,004520	45	0,00000051	10	0,00000513
200	121128,8	0,000048	0,004833	48	0,00000055	10	0,00000549
210	123790,3	0,000050	0,004952	50	0,00000056	10	0,00000562
220	154256,6	0,000063	0,006335	63	0,00000072	10	0,00000719
230	164675,8	0,000068	0,006816	68	0,00000077	10	0,00000774
240	171870	0,000072	0,007150	72	0,00000081	10	0,00000812
250	188677,8	0,000079	0,007939	79	0,00000090	10	0,00000902
260	193034,2	0,000081	0,008145	81	0,00000092	10	0,00000925
270	196610,7	0,000083	0,008315	83	0,00000094	10	0,00000944
280	208470,3	0,000089	0,008881	89	0,00000101	10	0,00001009
290	216476,7	0,000093	0,009266	93	0,00000105	10	0,00001052
300	239671,1	0,000104	0,010394	104	0,00000118	10	0,00001180
310	243280	0,000106	0,010572	106	0,00000120	10	0,00001201
320	277941,2	0,000123	0,012298	123	0,00000140	10	0,00001397
330	314029,6	0,000141	0,014141	141	0,00000161	10	0,00001606
340	342279,4	0,000156	0,015614	156	0,00000177	10	0,00001773
350	362850,6	0,000167	0,016704	167	0,00000190	10	0,00001897
360	372036,9	0,000172	0,017195	172	0,00000195	10	0,00001953
370	376295	0,000174	0,017424	174	0,00000198	10	0,00001979
380	391378,1	0,000182	0,018239	182	0,00000207	10	0,00002071
390	394280,7	0,000184	0,018396	184	0,00000209	10	0,00002089
400	407411,3	0,000191	0,019113	191	0,00000217	10	0,00002171
410	445856,1	0,000212	0,021244	212	0,00000241	10	0,00002413
420	507901,8	0,000248	0,024782	248	0,00000281	10	0,00002814
430	512061,1	0,000250	0,025024	250	0,00000284	10	0,00002842
440	522508,7	0,000256	0,025633	256	0,00000291	10	0,00002911
450	544398,4	0,000269	0,026919	269	0,00000306	10	0,00003057
460	567313,6	0,000283	0,028282	283	0,00000321	10	0,00003212

470	598116,2	0,000301	0,030138	301	0,00000342	10	0,00003423
480	611877,5	0,000310	0,030976	310	0,00000352	10	0,00003518
490	651012,3	0,000334	0,033389	334	0,00000379	10	0,00003792
500	693495,2	0,000361	0,036058	361	0,00000409	10	0,00004095
510	701863,2	0,000366	0,036590	366	0,00000416	10	0,00004155
520	705312,6	0,000368	0,036809	368	0,00000418	10	0,00004180
530	795528,6	0,000427	0,042668	427	0,00000485	10	0,00004846
540	805005,6	0,000433	0,043296	433	0,00000492	10	0,00004917
550	877941,2	0,000482	0,048203	482	0,00000547	10	0,00005474
560	913722,6	0,000507	0,050658	507	0,00000575	10	0,00005753
570	972802,4	0,000548	0,054777	548	0,00000622	10	0,00006221
580	1035142,9	0,000592	0,059209	592	0,00000672	10	0,00006724
590	1036263,6	0,000593	0,059289	593	0,00000673	10	0,00006733
600	1198128	0,000712	0,071176	712	0,00000808	10	0,00008083
610	1214791,1	0,000724	0,072428	724	0,00000823	10	0,00008225
620	1218274,7	0,000727	0,072690	727	0,00000826	10	0,00008255
630	1307905,1	0,000795	0,079517	795	0,00000903	10	0,00009030
640	1310824,3	0,000797	0,079741	797	0,00000906	10	0,00009056
650	1349734,8	0,000827	0,082748	827	0,00000940	10	0,00009397
660	1398418,6	0,000865	0,086544	865	0,00000983	10	0,00009828
670	1408999,6	0,000874	0,087374	874	0,00000992	10	0,00009923
680	1507361,6	0,000952	0,095162	952	0,00001081	10	0,00010807
690	1548999,6	0,000985	0,098498	985	0,00001119	10	0,00011186
700	1608418,6	0,001033	0,103294	1033	0,00001173	10	0,00011731
710	1637361,6	0,001056	0,105644	1056	0,00001200	10	0,00011998
720	1708418,6	0,001115	0,111452	1115	0,00001266	10	0,00012657
730	1741307,6	0,001142	0,114156	1142	0,00001296	10	0,00012964
740	1750165,2	0,001149	0,114885	1149	0,00001305	10	0,00013047
750	1815348,5	0,001203	0,120276	1203	0,00001366	10	0,00013659
760	1864425,3	0,001244	0,124356	1244	0,00001412	10	0,00014123

770	1896601,2	0,001270	0,127039	1270	0,00001443	10	0,00014427
780	1999372,2	0,001356	0,135647	1356	0,00001540	10	0,00015405
790	2005276,2	0,001361	0,136143	1361	0,00001546	10	0,00015461
800	2015857,2	0,001370	0,137032	1370	0,00001556	10	0,00015562
810	2048418,6	0,001398	0,139772	1398	0,00001587	10	0,00015873
820	2157361,6	0,001490	0,148956	1490	0,00001692	10	0,00016916
830	2197361,6	0,001523	0,152333	1523	0,00001730	10	0,00017300
840	2218418,6	0,001541	0,154111	1541	0,00001750	10	0,00017502
850	2237361,6	0,001557	0,155711	1557	0,00001768	10	0,00017683
860	2338418,6	0,001642	0,164240	1642	0,00001865	10	0,00018652
870	2408418,6	0,001701	0,170136	1701	0,00001932	10	0,00019322
880	2511009,6	0,001787	0,178747	1787	0,00002030	10	0,00020299
890	2517361,6	0,001793	0,179278	1793	0,00002036	10	0,00020360
900	2608418,6	0,001869	0,186872	1869	0,00002122	10	0,00021222
910	2617361,6	0,001876	0,187615	1876	0,00002131	10	0,00021307
920	2619518,6	0,001878	0,187794	1878	0,00002133	10	0,00021327
930	2638418,6	0,001894	0,189362	1894	0,00002150	10	0,00021505
940	2737361,6	0,001975	0,197523	1975	0,00002243	10	0,00022432
950	2769999,6	0,002002	0,200196	2002	0,00002274	10	0,00022735
960	2818418,6	0,002041	0,204142	2041	0,00002318	10	0,00023184
970	2838418,6	0,002058	0,205765	2058	0,00002337	10	0,00023368
980	2860999,6	0,002076	0,207592	2076	0,00002358	10	0,00023575
990	2878418,6	0,002090	0,208997	2090	0,00002373	10	0,00023735
1000	2917361,6	0,002121	0,212125	2121	0,00002409	10	0,00024090
1010	2968418,6	0,002162	0,216198	2162	0,00002455	10	0,00024553
1020	2988999,6	0,002178	0,217830	2178	0,00002474	10	0,00024738
1030	3018418,6	0,002202	0,220153	2202	0,00002500	10	0,00025002
1040	3038999,6	0,002218	0,221770	2218	0,00002519	10	0,00025185
1050	3069761,6	0,002242	0,224176	2242	0,00002546	10	0,00025459
1060	3087361,6	0,002255	0,225546	2255	0,00002561	10	0,00025614

1070	3107361,6	0,002271	0,227097	2271	0,00002579	10	0,00025790
1080	3117361,6	0,002279	0,227870	2279	0,00002588	10	0,00025878
1090	3120061,6	0,002281	0,228079	2281	0,00002590	10	0,00025902
Summation						0,01000963	

Table A- 44: Propagational uncertainty data - 800°C run 3

C _{in} (ppmv)	C _{out} (ppmv)	Time (s)	C _{out} /C _{in}	Average relative uncertainty	Propagational uncertainty
2256	16	0	0,006927	0,039059	0,00038263
2256	17	10	0,0077181	0,039059	0,00042633
2256	19	20	0,0082062	0,039059	0,00045329
2256	21	30	0,0091003	0,039059	0,00050268
2256	22	40	0,0099039	0,039059	0,00054707
2256	25	50	0,0109577	0,039059	0,00060528
2256	26	60	0,0116177	0,039059	0,00064174
2256	30	70	0,0131	0,039059	0,00072362
2256	31	80	0,0135393	0,039059	0,00074788
2256	32	90	0,0141455	0,039059	0,00078137
2256	33	100	0,0147269	0,039059	0,00081348
2256	33	110	0,0148442	0,039059	0,00081996
2256	35	120	0,015524	0,039059	0,00085751
2256	37	130	0,0162095	0,039059	0,00089538
2256	37	140	0,0165318	0,039059	0,00091318
2256	37	150	0,0165863	0,039059	0,00091619
2256	39	160	0,0173785	0,039059	0,00095995
2256	40	170	0,0175322	0,039059	0,00096844
2256	41	180	0,0181397	0,039059	0,00100199
2256	45	190	0,0200348	0,039059	0,00110668
2256	48	200	0,0214252	0,039059	0,00118348
2256	50	210	0,0219533	0,039059	0,00121265

2256	63	220	0,0280829	0,039059	0,00155123
2256	68	230	0,0302144	0,039059	0,00166897
2256	72	240	0,0316965	0,039059	0,00175085
2256	79	250	0,0351922	0,039059	0,00194394
2256	81	260	0,0361058	0,039059	0,00199440
2256	83	270	0,0368581	0,039059	0,00203596
2256	89	280	0,0393675	0,039059	0,00217457
2256	93	290	0,0410743	0,039059	0,00226885
2256	104	300	0,0460769	0,039059	0,00254518
2256	106	310	0,0468629	0,039059	0,00258860
2256	123	320	0,0545165	0,039059	0,00301137
2256	141	330	0,0626832	0,039059	0,00346248
2256	156	340	0,0692146	0,039059	0,00382326
2256	167	350	0,0740461	0,039059	0,00409014
2256	172	360	0,076224	0,039059	0,00421044
2256	174	370	0,0772378	0,039059	0,00426644
2256	182	380	0,0808501	0,039059	0,00446598
2256	184	390	0,0815491	0,039059	0,00450459
2256	191	400	0,0847264	0,039059	0,00468010
2256	212	410	0,0941722	0,039059	0,00520186
2256	248	420	0,1098565	0,039059	0,00606823
2256	250	430	0,1109269	0,039059	0,00612736
2256	256	440	0,1136262	0,039059	0,00627646
2256	269	450	0,1193295	0,039059	0,00659149
2256	283	460	0,1253687	0,039059	0,00692509
2256	301	470	0,1335957	0,039059	0,00737953
2256	310	480	0,1373111	0,039059	0,00758476
2256	334	490	0,1480092	0,039059	0,00817570
2256	361	500	0,1598398	0,039059	0,00882919
2256	366	510	0,1621963	0,039059	0,00895936

2256	368	520	0,1631701	0,039059	0,00901315
2256	427	530	0,1891416	0,039059	0,01044776
2256	433	540	0,1919246	0,039059	0,01060149
2256	482	550	0,2136779	0,039059	0,01180309
2256	507	560	0,2245603	0,039059	0,01240421
2256	548	570	0,2428195	0,039059	0,01341281
2256	592	580	0,2624635	0,039059	0,01449790
2256	593	590	0,26282	0,039059	0,01451759
2256	712	600	0,3155113	0,039059	0,01742814
2256	724	610	0,3210629	0,039059	0,01773480
2256	727	620	0,3222263	0,039059	0,01779906
2256	795	630	0,3524858	0,039059	0,01947053
2256	797	640	0,3534815	0,039059	0,01952553
2256	827	650	0,3668116	0,039059	0,02026186
2256	865	660	0,3836379	0,039059	0,02119130
2256	874	670	0,3873159	0,039059	0,02139446
2256	952	680	0,4218418	0,039059	0,02330160
2256	985	690	0,4366278	0,039059	0,02411834
2256	1033	700	0,4578877	0,039059	0,02529270
2256	1056	710	0,4683071	0,039059	0,02586824
2256	1115	720	0,4940493	0,039059	0,02729018
2256	1142	730	0,5060359	0,039059	0,02795229
2256	1149	740	0,5092714	0,039059	0,02813101
2256	1203	750	0,5331683	0,039059	0,02945103
2256	1244	760	0,5512526	0,039059	0,03044996
2256	1270	770	0,563147	0,039059	0,03110698
2256	1356	780	0,6013054	0,039059	0,03321477
2256	1361	790	0,603504	0,039059	0,03333622
2256	1370	800	0,6074459	0,039059	0,03355396
2256	1398	810	0,6195876	0,039059	0,03422464

2256	1490	820	0,6603021	0,039059	0,03647361
2256	1523	830	0,6752719	0,039059	0,03730051
2256	1541	840	0,6831539	0,039059	0,03773590
2256	1557	850	0,6902448	0,039059	0,03812758
2256	1642	860	0,7280527	0,039059	0,04021601
2256	1701	870	0,7541909	0,039059	0,04165982
2256	1787	880	0,7923594	0,039059	0,04376816
2256	1793	890	0,7947155	0,039059	0,04389831
2256	1869	900	0,8283768	0,039059	0,04575769
2256	1876	910	0,83167	0,039059	0,04593959
2256	1878	920	0,8324639	0,039059	0,04598345
2256	1894	930	0,839414	0,039059	0,04636735
2256	1975	940	0,8755922	0,039059	0,04836576
2256	2002	950	0,8874417	0,039059	0,04902030
2256	2041	960	0,904934	0,039059	0,04998653
2256	2058	970	0,9121274	0,039059	0,05038388
2256	2076	980	0,9202254	0,039059	0,05083119
2256	2090	990	0,9264545	0,039059	0,05117528
2256	2121	1000	0,9403225	0,039059	0,05194132
2256	2162	1010	0,9583764	0,039059	0,05293857
2256	2178	1020	0,9656105	0,039059	0,05333817
2256	2202	1030	0,9759061	0,039059	0,05390687
2256	2218	1040	0,9830761	0,039059	0,05430293
2256	2242	1050	0,9937413	0,039059	0,05489205
2256	2255	1060	0,9998145	0,039059	0,05522752
2256	2271	1070	1,00669	0,039059	0,05560731
2256	2279	1080	1,0101172	0,039059	0,05579662
2256	2281	1090	1,0110413	0,039059	0,05584767

Table A- 45: Volumes obtained from titration for SO₃ analysis - 800°C run 3

Bottle	Initial Volume (ml)	Final Volume (ml)	Volume Titrated (ml)
1	0	5.1	5,1
	5.1	10.3	5,2
	10.3	15.4	5,1
Average			5.1333
<hr/>			
2	15.4	20.5	5,1
	20.5	25.7	5,2
	25.7	30.9	5,2
Average			5.1666
<hr/>			
3	0	5.1	5,1
	5.1	10.2	5,1
	10.2	15.4	5,2
Average			5.1333

Table A- 46: Moles of SO₃ produced from titrations - 800°C run 3

Bottle	BaClO₄ Consumed (moles)	SO₃ Produced (moles)
1	0,0000257	0,0000257
2	0,0000258	0,0000258
3	0,0000257	0,0000257
Total (moles)	0,000077	0,000077

Table A- 47: System sulfur mass balance - 800°C run 3

Into System		
<i>SO₂ Analysis</i>		
Total moles gas	1,22629	moles
Moles SO ₂	0,00277	moles
Moles sulfur from SO ₂	0,00277	moles
Mass sulfur from SO ₂	0,08870	grams
<i>SO₃ Analysis</i>		
Moles SO ₃	0	moles
Mass SO ₃	0	grams
Out of System		
<i>SO₂ Analysis</i>		
Moles SO ₂	0,00100	moles
Moles sulfur from SO ₂	0,00100	moles
Mass sulfur from SO ₂	0,03210	grams
<i>SO₃ Analysis</i>		
Moles SO ₃ formed	0,000077	moles
Moles sulfur from SO ₃	0,000077	moles
Mass sulfur from SO ₃	0,004942	grams

Table A- 48: SO₂ sorption capacity of limestone sorbent - 800°C run 3

Initial/inlet Concentration (C _o)	2256	ppmv
Saturation time (T _{sat})	1070	s
Integral	0,01001	mol.s/L
Sorption capacity of limestone	16.589	mg SO₂/g CaCO₃

A-1.6) 900°C DATA

A-1.6.1) RUN 1

Table A- 49: Initial /inlet SO₂ concentration - 900°C run 1

Time (s)	Area ($\mu\text{V.s}$)	SO ₂ Volume (ml)	SO ₂ Volume Percent (%)	SO ₂ Concentration (ppmv)
0	3159201,40	0,002311	0,231087	2311
10	2971125,10	0,002164	0,216413	2164
20	3051277,80	0,002227	0,222732	2227
30	2973000,50	0,002166	0,216562	2166
40	3005203,40	0,002191	0,219111	2191
50	2962860,60	0,002158	0,215756	2158
60	2928464,30	0,002130	0,213014	2130
70	3112856,10	0,002275	0,227522	2275
80	3000060,40	0,002187	0,218705	2187
90	3682358,00	0,002684	0,268394	2684
100	3050660,90	0,002227	0,222684	2227
110	2931594,80	0,002133	0,213264	2133
120	3101544,10	0,002266	0,226647	2266
130	3152213,70	0,002306	0,230552	2306
140	3159201,40	0,002311	0,231087	2311
150	3298515,60	0,002416	0,241579	2416
160	2866365,60	0,002080	0,208025	2080
170	3134383,5	0,002292	0,229183	2292
180	3615489,5	0,002640	0,263972	2640
190	3159201,4	0,002311	0,231087	2311
200	3238347,6	0,002371	0,237091	2371
210	2931594,8	0,002133	0,213264	2133
220	3390934,4	0,002483	0,248335	2483

230	3390934,4	0,002483	0,248335	2483
240	3510646,1	0,002568	0,256816	2568
250	2752828,3	0,001988	0,198791	1988
260	3079041,4	0,002249	0,224899	2249
270	2692154,3	0,001938	0,193804	1938
280	3060778,8	0,002235	0,223475	2235
290	2704270,8	0,001948	0,194803	1948
300	3452064,5	0,002527	0,252705	2527
Average		0,002271	0,227087	2271

Table A- 50: Reactor effluent SO₂ concentration - 900°C run 1

Time (s)	Area (μ V.s)	SO ₂ Volume (ml)	SO ₂ Volume Percent (%)	SO ₂ Concentration (ppmv)	C _{SO₂} (mol/L)	ΔT (s)	C _{SO₂} ΔT (mol.s/L)
0	32424,3	0,000010	0,001018	10	0,00000011	10	0,00000106
10	34830,1	0,000011	0,001117	11	0,00000012	10	0,00000116
20	37156,5	0,000012	0,001214	12	0,00000013	10	0,00000126
30	42833,2	0,000014	0,001450	14	0,00000015	10	0,00000151
40	46221,3	0,000016	0,001591	16	0,00000017	10	0,00000165
50	52104,5	0,000018	0,001838	18	0,00000019	10	0,00000191
60	56189,5	0,000020	0,002010	20	0,00000021	10	0,00000209
70	63380,2	0,000023	0,002315	23	0,00000024	10	0,00000240
80	65384,2	0,000024	0,002400	24	0,00000025	10	0,00000249
90	68547,7	0,000025	0,002535	25	0,00000026	10	0,00000263
100	71573,3	0,000027	0,002664	27	0,00000028	10	0,00000277
110	72182,7	0,000027	0,002690	27	0,00000028	10	0,00000279
120	75708,3	0,000028	0,002842	28	0,00000030	10	0,00000295
130	79252,7	0,000030	0,002994	30	0,00000031	10	0,00000311
140	80915,2	0,000031	0,003066	31	0,00000032	10	0,00000319
150	81195,9	0,000031	0,003078	31	0,00000032	10	0,00000320

160	84060,6	0,000032	0,003202	32	0,00000033	10	0,00000333
170	85271,4	0,000033	0,003254	33	0,00000034	10	0,00000338
180	89173,4	0,000034	0,003424	34	0,00000036	10	0,00000356
190	92326,2	0,000036	0,003561	36	0,00000037	10	0,00000370
200	94145,8	0,000036	0,003641	36	0,00000038	10	0,00000378
210	96330,3	0,000037	0,003736	37	0,00000039	10	0,00000388
220	98796,6	0,000038	0,003844	38	0,00000040	10	0,00000399
230	112908,8	0,000045	0,004467	45	0,00000046	10	0,00000464
240	129887	0,000052	0,005226	52	0,00000054	10	0,00000543
250	142217,8	0,000058	0,005785	58	0,00000060	10	0,00000601
260	152051,2	0,000062	0,006234	62	0,00000065	10	0,00000648
270	156843,7	0,000065	0,006454	65	0,00000067	10	0,00000670
280	165010,3	0,000068	0,006832	68	0,00000071	10	0,00000710
290	175297	0,000073	0,007310	73	0,00000076	10	0,00000759
300	180262,6	0,000075	0,007543	75	0,00000078	10	0,00000784
310	204493,7	0,000087	0,008690	87	0,00000090	10	0,00000903
320	215819,4	0,000092	0,009234	92	0,00000096	10	0,00000959
330	230174,2	0,000099	0,009930	99	0,00000103	10	0,00001032
340	268390,6	0,000118	0,011818	118	0,00000123	10	0,00001228
350	283211,1	0,000126	0,012564	126	0,00000131	10	0,00001305
360	309269,9	0,000139	0,013895	139	0,00000144	10	0,00001443
370	312312	0,000141	0,014052	141	0,00000146	10	0,00001460
380	315918,1	0,000142	0,014238	142	0,00000148	10	0,00001479
390	318820,7	0,000144	0,014389	144	0,00000149	10	0,00001495
400	320951,3	0,000145	0,014499	145	0,00000151	10	0,00001506
410	325089,1	0,000147	0,014714	147	0,00000153	10	0,00001529
420	355918,8	0,000163	0,016335	163	0,00000170	10	0,00001697
430	360294,1	0,000166	0,016568	166	0,00000172	10	0,00001721
440	361048,7	0,000166	0,016608	166	0,00000173	10	0,00001725
450	362415,4	0,000167	0,016681	167	0,00000173	10	0,00001733

460	365853,6	0,000169	0,016864	169	0,00000175	10	0,00001752
470	386349,2	0,000180	0,017966	180	0,00000187	10	0,00001866
480	389552,3	0,000181	0,018140	181	0,00000188	10	0,00001884
490	389894,5	0,000182	0,018158	182	0,00000189	10	0,00001886
500	391728,2	0,000183	0,018258	183	0,00000190	10	0,00001897
510	392403,2	0,000183	0,018294	183	0,00000190	10	0,00001901
520	393545,6	0,000184	0,018357	184	0,00000191	10	0,00001907
530	398545,6	0,000186	0,018629	186	0,00000194	10	0,00001935
540	403545,6	0,000189	0,018902	189	0,00000196	10	0,00001964
550	436174,2	0,000207	0,020703	207	0,00000215	10	0,00002151
560	502262,6	0,000245	0,024456	245	0,00000254	10	0,00002541
570	506819,4	0,000247	0,024720	247	0,00000257	10	0,00002568
580	512269,9	0,000250	0,025036	250	0,00000260	10	0,00002601
590	522390,6	0,000256	0,025626	256	0,00000266	10	0,00002662
600	584312	0,000293	0,029302	293	0,00000304	10	0,00003044
610	599918,1	0,000302	0,030247	302	0,00000314	10	0,00003142
620	602820,7	0,000304	0,030424	304	0,00000316	10	0,00003161
630	674089,1	0,000348	0,034833	348	0,00000362	10	0,00003619
640	695951,3	0,000362	0,036214	362	0,00000376	10	0,00003762
650	735918,8	0,000388	0,038773	388	0,00000403	10	0,00004028
660	783545,6	0,000419	0,041878	419	0,00000435	10	0,00004350
670	793545,6	0,000425	0,042537	425	0,00000442	10	0,00004419
680	793545,6	0,000425	0,042537	425	0,00000442	10	0,00004419
690	833545,6	0,000452	0,045200	452	0,00000470	10	0,00004696
700	893545,6	0,000493	0,049270	493	0,00000512	10	0,00005118
710	923545,6	0,000513	0,051337	513	0,00000533	10	0,00005333
720	973545,6	0,000548	0,054829	548	0,00000570	10	0,00005696
730	1025853,6	0,000585	0,058543	585	0,00000608	10	0,00006082
740	1036349,2	0,000593	0,059295	593	0,00000616	10	0,00006160
750	1099894,5	0,000639	0,063899	639	0,00000664	10	0,00006638

760	1149552,3	0,000676	0,067554	676	0,00000702	10	0,00007018
770	1181728,2	0,000699	0,069948	699	0,00000727	10	0,00007267
780	1195556,2	0,000710	0,070983	710	0,00000737	10	0,00007374
790	1220403,2	0,000729	0,072851	729	0,00000757	10	0,00007568
800	1300403,2	0,000789	0,078940	789	0,00000820	10	0,00008201
810	1333545,6	0,000815	0,081494	815	0,00000847	10	0,00008466
820	1343545,6	0,000823	0,082268	823	0,00000855	10	0,00008546
830	1483545,6	0,000933	0,093265	933	0,00000969	10	0,00009689
840	1503545,6	0,000949	0,094858	949	0,00000985	10	0,00009854
850	1523545,6	0,000965	0,096456	965	0,00001002	10	0,00010020
860	1523545,6	0,000965	0,096456	965	0,00001002	10	0,00010020
870	1593545,6	0,001021	0,102090	1021	0,00001061	10	0,00010606
880	1625555,6	0,001047	0,104685	1047	0,00001088	10	0,00010875
890	1703545,6	0,001111	0,111052	1111	0,00001154	10	0,00011537
900	1793545,6	0,001185	0,118469	1185	0,00001231	10	0,00012307
910	1803545,6	0,001193	0,119298	1193	0,00001239	10	0,00012393
920	1854645,6	0,001235	0,123542	1235	0,00001283	10	0,00012834
930	1923545,6	0,001293	0,129291	1293	0,00001343	10	0,00013431
940	2023545,6	0,001377	0,137679	1377	0,00001430	10	0,00014303
950	2054545,6	0,001403	0,140287	1403	0,00001457	10	0,00014574
960	2080545,6	0,001425	0,142477	1425	0,00001480	10	0,00014801
970	2123545,6	0,001461	0,146103	1461	0,00001518	10	0,00015178
980	2245545,6	0,001564	0,156402	1564	0,00001625	10	0,00016248
990	2303545,6	0,001613	0,161298	1613	0,00001676	10	0,00016756
1000	2323545,6	0,001630	0,162986	1630	0,00001693	10	0,00016932
1010	2393545,6	0,001689	0,168885	1689	0,00001754	10	0,00017545
1020	2473545,6	0,001756	0,175608	1756	0,00001824	10	0,00018243
1030	2513545,6	0,001790	0,178959	1790	0,00001859	10	0,00018591
1040	2583545,6	0,001848	0,184803	1848	0,00001920	10	0,00019198
1050	2635945,6	0,001892	0,189157	1892	0,00001965	10	0,00019651

1060	2673545,6	0,001923	0,192268	1923	0,00001997	10	0,00019974
1070	2753545,6	0,001988	0,198850	1988	0,00002066	10	0,00020658
1080	2803545,6	0,002029	0,202933	2029	0,00002108	10	0,00021082
1090	2893545,6	0,002102	0,210214	2102	0,00002184	10	0,00021838
1100	2893545,6	0,002102	0,210214	2102	0,00002184	10	0,00021838
1110	2945545,6	0,002144	0,214378	2144	0,00002227	10	0,00022271
1120	3003545,6	0,002190	0,218980	2190	0,00002275	10	0,00022749
1130	3023545,6	0,002206	0,220556	2206	0,00002291	10	0,00022912
1140	3033545,6	0,002213	0,221342	2213	0,00002299	10	0,00022994
1150	3073545,6	0,002245	0,224471	2245	0,00002332	10	0,00023319
1160	3081545,6	0,002251	0,225094	2251	0,00002338	10	0,00023384
1170	3083545,6	0,002252	0,225249	2252	0,00002340	10	0,00023400
1180	3095945,6	0,002262	0,226213	2262	0,00002350	10	0,00023500
1190	3103545,6	0,002268	0,226802	2268	0,00002356	10	0,00023561
1200	3118545,6	0,002280	0,227962	2280	0,00002368	10	0,00023682
1210	3121965,6	0,002282	0,228226	2282	0,00002371	10	0,00023709
Summation							0,00876652

Table A- 51: Propagational uncertainty data - 900°C run 1

C _{in} (ppmv)	C _{out} (ppmv)	Time (s)	C _{out} /C _{in}	Average relative uncertainty	Propagational uncertainty
2271	10	0	0,0044824	0,039059	0,00024760
2271	11	10	0,0049203	0,039059	0,00027179
2271	12	20	0,0053447	0,039059	0,00029523
2271	14	30	0,0063843	0,039059	0,00035265
2271	16	40	0,0070074	0,039059	0,00038707
2271	18	50	0,008094	0,039059	0,00044710
2271	20	60	0,0088521	0,039059	0,00048897
2271	23	70	0,0101934	0,039059	0,00056306
2271	24	80	0,0105688	0,039059	0,00058380

2271	25	90	0,0111628	0,039059	0,00061661
2271	27	100	0,0117325	0,039059	0,00064807
2271	27	110	0,0118474	0,039059	0,00065442
2271	28	120	0,0125136	0,039059	0,00069122
2271	30	130	0,0131854	0,039059	0,00072833
2271	31	140	0,0135013	0,039059	0,00074578
2271	31	150	0,0135547	0,039059	0,00074873
2271	32	160	0,0141002	0,039059	0,00077886
2271	33	170	0,0143312	0,039059	0,00079162
2271	34	180	0,0150772	0,039059	0,00083283
2271	36	190	0,015682	0,039059	0,00086624
2271	36	200	0,0160317	0,039059	0,00088556
2271	37	210	0,0164524	0,039059	0,00090879
2271	38	220	0,0169283	0,039059	0,00093508
2271	45	230	0,0196709	0,039059	0,00108658
2271	52	240	0,0230146	0,039059	0,00127128
2271	58	250	0,0254731	0,039059	0,00140708
2271	62	260	0,0274516	0,039059	0,00151636
2271	65	270	0,0284216	0,039059	0,00156994
2271	68	280	0,0300832	0,039059	0,00166173
2271	73	290	0,0321916	0,039059	0,00177819
2271	75	300	0,0332156	0,039059	0,00183475
2271	87	310	0,0382692	0,039059	0,00211391
2271	92	320	0,0406636	0,039059	0,00224617
2271	99	330	0,0437277	0,039059	0,00241542
2271	118	340	0,052043	0,039059	0,00287474
2271	126	350	0,0553289	0,039059	0,00305624
2271	139	360	0,0611881	0,039059	0,00337989
2271	141	370	0,0618788	0,039059	0,00341805
2271	142	380	0,0626994	0,039059	0,00346338

2271	144	390	0,0633614	0,039059	0,00349994
2271	145	400	0,0638481	0,039059	0,00352682
2271	147	410	0,0647952	0,039059	0,00357914
2271	163	420	0,071933	0,039059	0,00397342
2271	166	430	0,0729575	0,039059	0,00403001
2271	166	440	0,0731344	0,039059	0,00403978
2271	167	450	0,0734552	0,039059	0,00405750
2271	169	460	0,0742632	0,039059	0,00410214
2271	180	470	0,0791163	0,039059	0,00437021
2271	181	480	0,0798803	0,039059	0,00441241
2271	182	490	0,079962	0,039059	0,00441692
2271	183	500	0,0804001	0,039059	0,00444112
2271	183	510	0,0805615	0,039059	0,00445004
2271	184	520	0,0808348	0,039059	0,00446513
2271	186	530	0,0820332	0,039059	0,00453133
2271	189	540	0,0832353	0,039059	0,00459773
2271	207	550	0,0911676	0,039059	0,00503590
2271	245	560	0,1076933	0,039059	0,00594874
2271	247	570	0,1088549	0,039059	0,00601290
2271	250	580	0,1102481	0,039059	0,00608986
2271	256	590	0,1128457	0,039059	0,00623335
2271	293	600	0,129036	0,039059	0,00712766
2271	302	610	0,1331958	0,039059	0,00735744
2271	304	620	0,1339729	0,039059	0,00740036
2271	348	630	0,1533887	0,039059	0,00847285
2271	362	640	0,1594709	0,039059	0,00880882
2271	388	650	0,170739	0,039059	0,00943124
2271	419	660	0,1844119	0,039059	0,01018650
2271	425	670	0,1873159	0,039059	0,01034691
2271	425	680	0,1873159	0,039059	0,01034691

2271	452	690	0,1990442	0,039059	0,01099476
2271	493	700	0,2169654	0,039059	0,01198468
2271	513	710	0,2260692	0,039059	0,01248756
2271	548	720	0,2414471	0,039059	0,01333700
2271	585	730	0,2577995	0,039059	0,01424027
2271	593	740	0,2611122	0,039059	0,01442326
2271	639	750	0,2813868	0,039059	0,01554318
2271	676	760	0,2974816	0,039059	0,01643222
2271	699	770	0,3080228	0,039059	0,01701449
2271	710	780	0,3125794	0,039059	0,01726619
2271	729	790	0,320806	0,039059	0,01772061
2271	789	800	0,3476199	0,039059	0,01920175
2271	815	810	0,3588678	0,039059	0,01982305
2271	823	820	0,3622769	0,039059	0,02001136
2271	933	830	0,4106996	0,039059	0,02268613
2271	949	840	0,4177159	0,039059	0,02307369
2271	965	850	0,424755	0,039059	0,02346252
2271	965	860	0,424755	0,039059	0,02346252
2271	1021	870	0,449562	0,039059	0,02483280
2271	1047	880	0,460989	0,039059	0,02546400
2271	1111	890	0,4890274	0,039059	0,02701278
2271	1185	900	0,5216921	0,039059	0,02881711
2271	1193	910	0,5253395	0,039059	0,02901858
2271	1235	920	0,5440281	0,039059	0,03005090
2271	1293	930	0,5693451	0,039059	0,03144935
2271	1377	940	0,6062827	0,039059	0,03348970
2271	1403	950	0,617769	0,039059	0,03412418
2271	1425	960	0,6274126	0,039059	0,03465687
2271	1461	970	0,6433777	0,039059	0,03553875
2271	1564	980	0,6887317	0,039059	0,03804400

2271	1613	990	0,7102926	0,039059	0,03923498
2271	1630	1000	0,7177232	0,039059	0,03964543
2271	1689	1010	0,7437006	0,039059	0,04108036
2271	1756	1020	0,7733061	0,039059	0,04271570
2271	1790	1030	0,7880636	0,039059	0,04353087
2271	1848	1040	0,8137972	0,039059	0,04495234
2271	1892	1050	0,8329703	0,039059	0,04601142
2271	1923	1060	0,8466732	0,039059	0,04676834
2271	1988	1070	0,8756549	0,039059	0,04836922
2271	2029	1080	0,8936342	0,039059	0,04936236
2271	2102	1090	0,9256999	0,039059	0,05113360
2271	2102	1100	0,9256999	0,039059	0,05113360
2271	2144	1110	0,944034	0,039059	0,05214633
2271	2190	1120	0,9643002	0,039059	0,05326579
2271	2206	1130	0,971241	0,039059	0,05364918
2271	2213	1140	0,9747019	0,039059	0,05384036
2271	2245	1150	0,9884805	0,039059	0,05460145
2271	2251	1160	0,9912234	0,039059	0,05475297
2271	2252	1170	0,9919085	0,039059	0,05479081
2271	2262	1180	0,9961496	0,039059	0,05502508
2271	2268	1190	0,9987438	0,039059	0,05516838
2271	2280	1200	1,0038521	0,039059	0,05545055
2271	2282	1210	1,0050145	0,039059	0,05551476

Table A- 52: Volumes obtained from titration for SO₃ analysis - 900°C run 1

Bottle	Initial Volume (ml)	Final Volume (ml)	Volume Titrated (ml)
1	0	8.7	8,7
	8.7	17.3	8,6
	17.3	25.9	8.6
Average			8.6333
2	25.9	34.5	8.6
	0	8.6	8.6
	8.6	17.2	8.6
Average			8.6
3	17.2	25.9	8.7
	25.9	34.6	8.7
	0	8.6	8.6
Average			8.6666

Table A- 53: Moles of SO₃ produced from titrations - 900°C run 1

Bottle	BaClO ₄ Consumed (moles)	SO ₃ Produced (moles)
1	0,0000432	0,0000432
2	0,0000430	0,0000430
3	0,0000433	0,0000433
Total (moles)	0,000130	0,000130

Table A- 54: System sulfur mass balance - 900°C run 1

Into System		
<i>SO₂ Analysis</i>		
Total moles gas	1,22629	moles
Moles SO ₂	0,00278	moles
Moles sulfur from SO ₂	0,00278	moles
Mass sulfur from SO ₂	0,08929	grams
<i>SO₃ Analysis</i>		
Moles SO ₃	0	moles
Mass SO ₃	0	grams
Out of System		
<i>SO₂ Analysis</i>		
Moles SO ₂	0,00088	moles
Moles sulfur from SO ₂	0,00088	moles
Mass sulfur from SO ₂	0,02811	grams
<i>SO₃ Analysis</i>		
Moles SO ₃ formed	0,000130	moles
Moles sulfur from SO ₃	0,000130	moles
Mass sulfur from SO ₃	0,00830	grams

Table A- 55: SO₂ sorption capacity of limestone sorbent - 900°C run 1

Initial/inlet Concentration (C _o)	2271	ppmv
Saturation time (T _{sat})	1200	s
Integral	0,00877	mol.s/L
Sorption capacity of limestone	18.728	mg SO₂/g CaCO₃

A-1.6.2) RUN 2

Table A- 56: Initial /inlet SO₂ concentration - 900°C run 2

Time (s)	Area ($\mu\text{V} \cdot \text{s}$)	SO ₂ Volume (ml)	SO ₂ Volume Percent (%)	SO ₂ Concentration (ppmv)
0	2973487,40	0,002166	0,216601	2166
10	2985411,10	0,002175	0,217546	2175
20	3064947,80	0,002238	0,223801	2238
30	2987290,50	0,002177	0,217695	2177
40	3019489,40	0,002202	0,220237	2202
50	2976530,60	0,002168	0,216842	2168
60	2942754,30	0,002142	0,214155	2142
70	3127142,10	0,002286	0,228625	2286
80	3013730,40	0,002198	0,219783	2198
90	3096644,00	0,002263	0,226267	2263
100	3164330,90	0,002315	0,231480	2315
110	2945880,80	0,002144	0,214405	2144
120	3115834,10	0,002278	0,227752	2278
130	3766499,70	0,002738	0,273790	2738
140	3187157,40	0,002332	0,233221	2332
150	3012185,60	0,002197	0,219662	2197
160	2880655,60	0,002092	0,209177	2092
170	3348669,5	0,002453	0,245267	2453
180	3129159,5	0,002288	0,228780	2288
190	3187773,4	0,002333	0,233267	2333
200	3252017,6	0,002381	0,238117	2381
210	2960170,8	0,002155	0,215543	2155
220	3405220,4	0,002494	0,249363	2494
230	3404604,4	0,002493	0,249319	2493

240	3524932,1	0,002578	0,257807	2578
250	2767118,3	0,002000	0,199961	2000
260	3093327,4	0,002260	0,226009	2260
270	2705824,3	0,001949	0,194931	1949
280	3575068,8	0,002612	0,261245	2612
290	2718560,8	0,001960	0,195979	1960
300	3466350,5	0,002537	0,253715	2537
Average		0,002278	0,227753	2278

Table A- 57: Reactor effluent SO₂ concentration - 900°C run 2

Time (s)	Area (μ V.s)	SO ₂ Volume (ml)	SO ₂ Volume Percent (%)	SO ₂ Concentration (ppmv)	C _{SO₂} (mol/L)	ΔT (s)	C _{SO₂} ΔT (mol.s/L)
0	36345,3	0,000012	0,001180	12	0,00000012	10	0,00000123
10	40220,1	0,000013	0,001341	13	0,00000014	10	0,00000139
20	42702,5	0,000014	0,001444	14	0,00000015	10	0,00000150
30	48379,2	0,000017	0,001682	17	0,00000017	10	0,00000175
40	51767,3	0,000018	0,001824	18	0,00000019	10	0,00000189
50	57281,5	0,000021	0,002056	21	0,00000021	10	0,00000214
60	61735,5	0,000022	0,002245	22	0,00000023	10	0,00000233
70	68770,2	0,000025	0,002544	25	0,00000026	10	0,00000264
80	70561,2	0,000026	0,002621	26	0,00000027	10	0,00000272
90	73937,7	0,000028	0,002766	28	0,00000029	10	0,00000287
100	77119,3	0,000029	0,002902	29	0,00000030	10	0,00000302
110	77359,7	0,000029	0,002913	29	0,00000030	10	0,00000303
120	81098,3	0,000031	0,003074	31	0,00000032	10	0,00000319
130	84429,7	0,000032	0,003218	32	0,00000033	10	0,00000334
140	86092,2	0,000033	0,003290	33	0,00000034	10	0,00000342
150	86585,9	0,000033	0,003311	33	0,00000034	10	0,00000344
160	89606,6	0,000034	0,003443	34	0,00000036	10	0,00000358

170	90661,4	0,000035	0,003489	35	0,00000036	10	0,00000362
180	94719,4	0,000037	0,003666	37	0,00000038	10	0,00000381
190	97716,2	0,000038	0,003797	38	0,00000039	10	0,00000394
200	99691,8	0,000039	0,003883	39	0,00000040	10	0,00000403
210	101507,3	0,000040	0,003963	40	0,00000041	10	0,00000412
220	104186,6	0,000041	0,004081	41	0,00000042	10	0,00000424
230	124688,8	0,000050	0,004993	50	0,00000052	10	0,00000519
240	141572	0,000058	0,005755	58	0,00000060	10	0,00000598
250	154398,8	0,000063	0,006342	63	0,00000066	10	0,00000659
260	163736,2	0,000068	0,006772	68	0,00000070	10	0,00000704
270	168623,7	0,000070	0,006999	70	0,00000073	10	0,00000727
280	176790,3	0,000074	0,007380	74	0,00000077	10	0,00000767
290	187478	0,000079	0,007882	79	0,00000082	10	0,00000819
300	192443,6	0,000081	0,008117	81	0,00000084	10	0,00000843
310	216178,7	0,000093	0,009252	93	0,00000096	10	0,00000961
320	228000,4	0,000098	0,009824	98	0,00000102	10	0,00001021
330	241859,2	0,000105	0,010502	105	0,00000109	10	0,00001091
340	280170,6	0,000124	0,012411	124	0,00000129	10	0,00001289
350	295392,1	0,000132	0,013183	132	0,00000137	10	0,00001370
360	321049,9	0,000145	0,014504	145	0,00000151	10	0,00001507
370	323997	0,000147	0,014657	147	0,00000152	10	0,00001523
380	328099,1	0,000149	0,014871	149	0,00000154	10	0,00001545
390	330505,7	0,000150	0,014997	150	0,00000156	10	0,00001558
400	332731,3	0,000151	0,015113	151	0,00000157	10	0,00001570
410	336774,1	0,000153	0,015325	153	0,00000159	10	0,00001592
420	368099,8	0,000170	0,016984	170	0,00000176	10	0,00001764
430	372074,1	0,000172	0,017197	172	0,00000179	10	0,00001787
440	372733,7	0,000172	0,017233	172	0,00000179	10	0,00001790
450	374195,4	0,000173	0,017311	173	0,00000180	10	0,00001798
460	377538,6	0,000175	0,017491	175	0,00000182	10	0,00001817

470	398530,2	0,000186	0,018628	186	0,00000194	10	0,00001935
480	401332,3	0,000188	0,018781	188	0,00000195	10	0,00001951
490	401579,5	0,000188	0,018794	188	0,00000195	10	0,00001952
500	403909,2	0,000189	0,018922	189	0,00000197	10	0,00001966
510	404088,2	0,000189	0,018931	189	0,00000197	10	0,00001967
520	405325,6	0,000190	0,018999	190	0,00000197	10	0,00001974
530	410726,6	0,000193	0,019295	193	0,00000200	10	0,00002004
540	415325,6	0,000195	0,019548	195	0,00000203	10	0,00002031
550	447954,2	0,000214	0,021362	214	0,00000222	10	0,00002219
560	514443,6	0,000252	0,025162	252	0,00000261	10	0,00002614
570	518504,4	0,000254	0,025399	254	0,00000264	10	0,00002639
580	523954,9	0,000257	0,025717	257	0,00000267	10	0,00002672
590	534170,6	0,000263	0,026316	263	0,00000273	10	0,00002734
600	595997	0,000300	0,030009	300	0,00000312	10	0,00003117
610	612099,1	0,000310	0,030989	310	0,00000322	10	0,00003219
620	614505,7	0,000311	0,031136	311	0,00000323	10	0,00003235
630	686270,1	0,000356	0,035601	356	0,00000370	10	0,00003698
640	708132,3	0,000370	0,036989	370	0,00000384	10	0,00003843
650	747698,8	0,000395	0,039535	395	0,00000411	10	0,00004107
660	795325,6	0,000427	0,042655	427	0,00000443	10	0,00004431
670	805230,6	0,000433	0,043311	433	0,00000450	10	0,00004499
680	805230,6	0,000433	0,043311	433	0,00000450	10	0,00004499
690	845726,6	0,000460	0,046019	460	0,00000478	10	0,00004781
700	905230,6	0,000501	0,050073	501	0,00000520	10	0,00005202
710	935325,6	0,000522	0,052155	522	0,00000542	10	0,00005418
720	985726,6	0,000557	0,055689	557	0,00000579	10	0,00005785
730	1040143,6	0,000596	0,059568	596	0,00000619	10	0,00006188
740	1050019,2	0,000603	0,060279	603	0,00000626	10	0,00006262
750	1114184,5	0,000649	0,064946	649	0,00000675	10	0,00006747
760	1163838,3	0,000686	0,068615	686	0,00000713	10	0,00007128

770	1195398,2	0,000710	0,070971	710	0,00000737	10	0,00007373
780	1209846,2	0,000721	0,072056	721	0,00000749	10	0,00007486
790	1234689,2	0,000739	0,073930	739	0,00000768	10	0,00007680
800	1314689,2	0,000800	0,080039	800	0,00000831	10	0,00008315
810	1347215,6	0,000826	0,082553	826	0,00000858	10	0,00008576
820	1357835,6	0,000834	0,083377	834	0,00000866	10	0,00008662
830	1497831,6	0,000944	0,094402	944	0,00000981	10	0,00009807
840	1517835,6	0,000960	0,095999	960	0,00000997	10	0,00009973
850	1537831,6	0,000976	0,097601	976	0,00001014	10	0,00010139
860	1537835,6	0,000976	0,097602	976	0,00001014	10	0,00010139
870	1607831,6	0,001032	0,103246	1032	0,00001073	10	0,00010726
880	1639225,6	0,001058	0,105796	1058	0,00001099	10	0,00010991
890	1717835,6	0,001122	0,112225	1122	0,00001166	10	0,00011658
900	1807831,6	0,001197	0,119653	1197	0,00001243	10	0,00012430
910	1817215,6	0,001204	0,120431	1204	0,00001251	10	0,00012511
920	1868931,6	0,001247	0,124731	1247	0,00001296	10	0,00012958
930	1937835,6	0,001305	0,130487	1305	0,00001356	10	0,00013556
940	2037835,6	0,001389	0,138881	1389	0,00001443	10	0,00014428
950	2068831,6	0,001415	0,141490	1415	0,00001470	10	0,00014699
960	2094215,6	0,001436	0,143629	1436	0,00001492	10	0,00014921
970	2137831,6	0,001473	0,147308	1473	0,00001530	10	0,00015303
980	2259215,6	0,001576	0,157556	1576	0,00001637	10	0,00016368
990	2317835,6	0,001625	0,162504	1625	0,00001688	10	0,00016882
1000	2337215,6	0,001641	0,164139	1641	0,00001705	10	0,00017052
1010	2407831,6	0,001701	0,170087	1701	0,00001767	10	0,00017669
1020	2487215,6	0,001768	0,176754	1768	0,00001836	10	0,00018362
1030	2527831,6	0,001802	0,180154	1802	0,00001872	10	0,00018715
1040	2597215,6	0,001859	0,185940	1859	0,00001932	10	0,00019316
1050	2650235,6	0,001903	0,190341	1903	0,00001977	10	0,00019774
1060	2687215,6	0,001934	0,193397	1934	0,00002009	10	0,00020091

1070	2767215,6	0,002000	0,199969	2000	0,00002077	10	0,00020774
1080	2817831,6	0,002041	0,204095	2041	0,00002120	10	0,00021202
1090	2907831,6	0,002114	0,211362	2114	0,00002196	10	0,00021957
1100	2907835,6	0,002114	0,211362	2114	0,00002196	10	0,00021957
1110	2959831,6	0,002155	0,215516	2155	0,00002239	10	0,00022389
1120	3017215,6	0,002201	0,220058	2201	0,00002286	10	0,00022861
1130	3037831,6	0,002217	0,221679	2217	0,00002303	10	0,00023029
1140	3047835,6	0,002225	0,222463	2225	0,00002311	10	0,00023111
1150	3087835,6	0,002256	0,225583	2256	0,00002343	10	0,00023435
1160	3095215,6	0,002262	0,226156	2262	0,00002349	10	0,00023494
1170	3097831,6	0,002264	0,226359	2264	0,00002352	10	0,00023515
1180	3110235,6	0,002273	0,227320	2273	0,00002362	10	0,00023615
1190	3117835,6	0,002279	0,227907	2279	0,00002368	10	0,00023676
1200	3127831,6	0,002287	0,228678	2287	0,00002376	10	0,00023756
1210	3134635,6	0,002292	0,229202	2292	0,00002381	10	0,00023811
Summation							0,00886300

Table A- 58: Propagational uncertainty data - 900°C run 2

C _{in} (ppmv)	C _{out} (ppmv)	Time (s)	C _{out} /C _{in}	Average relative uncertainty	Propagational uncertainty
2278	12	0	0,0051814	0,039059	0,00028621
2278	13	10	0,0058878	0,039059	0,00032523
2278	14	20	0,0063417	0,039059	0,00035030
2278	17	30	0,0073836	0,039059	0,00040785
2278	18	40	0,0080081	0,039059	0,00044235
2278	21	50	0,0090287	0,039059	0,00049873
2278	22	60	0,0098569	0,039059	0,00054447
2278	25	70	0,0111718	0,039059	0,00061711
2278	26	80	0,011508	0,039059	0,00063567
2278	28	90	0,0121431	0,039059	0,00067076

2278	29	100	0,0127434	0,039059	0,00070392
2278	29	110	0,0127888	0,039059	0,00070643
2278	31	120	0,0134965	0,039059	0,00074552
2278	32	130	0,0141291	0,039059	0,00078046
2278	33	140	0,0144455	0,039059	0,00079794
2278	33	150	0,0145396	0,039059	0,00080313
2278	34	160	0,0151159	0,039059	0,00083497
2278	35	170	0,0153175	0,039059	0,00084611
2278	37	180	0,0160949	0,039059	0,00088905
2278	38	190	0,0166708	0,039059	0,00092086
2278	39	200	0,0170512	0,039059	0,00094187
2278	40	210	0,0174014	0,039059	0,00096122
2278	41	220	0,0179193	0,039059	0,00098982
2278	50	230	0,0219215	0,039059	0,00121089
2278	58	240	0,0252696	0,039059	0,00139584
2278	63	250	0,0278446	0,039059	0,00153807
2278	68	260	0,029736	0,039059	0,00164255
2278	70	270	0,0307317	0,039059	0,00169755
2278	74	280	0,0324041	0,039059	0,00178993
2278	79	290	0,0346091	0,039059	0,00191173
2278	81	300	0,0356397	0,039059	0,00196866
2278	93	310	0,0406208	0,039059	0,00224380
2278	98	320	0,0431351	0,039059	0,00238269
2278	105	330	0,0461107	0,039059	0,00254705
2278	124	340	0,0544922	0,039059	0,00301003
2278	132	350	0,0578851	0,039059	0,00319744
2278	145	360	0,0636839	0,039059	0,00351775
2278	147	370	0,0643563	0,039059	0,00355490
2278	149	380	0,0652944	0,039059	0,00360672
2278	150	390	0,0658459	0,039059	0,00363718

2278	151	400	0,0663568	0,039059	0,00366540
2278	153	410	0,0672866	0,039059	0,00371676
2278	170	420	0,0745734	0,039059	0,00411927
2278	172	430	0,0755082	0,039059	0,00417091
2278	172	440	0,0756636	0,039059	0,00417949
2278	173	450	0,0760081	0,039059	0,00419852
2278	175	460	0,0767973	0,039059	0,00424211
2278	186	470	0,0817897	0,039059	0,00451788
2278	188	480	0,0824609	0,039059	0,00455496
2278	188	490	0,0825202	0,039059	0,00455823
2278	189	500	0,0830792	0,039059	0,00458911
2278	189	510	0,0831222	0,039059	0,00459149
2278	190	520	0,0834195	0,039059	0,00460791
2278	193	530	0,0847196	0,039059	0,00467972
2278	195	540	0,0858299	0,039059	0,00474105
2278	214	550	0,0937936	0,039059	0,00518095
2278	252	560	0,1104809	0,039059	0,00610272
2278	254	570	0,1115196	0,039059	0,00616010
2278	257	580	0,1129173	0,039059	0,00623730
2278	263	590	0,1155477	0,039059	0,00638260
2278	300	600	0,1317613	0,039059	0,00727820
2278	310	610	0,1360653	0,039059	0,00751595
2278	311	620	0,1367115	0,039059	0,00755164
2278	356	630	0,156312	0,039059	0,00863432
2278	370	640	0,1624086	0,039059	0,00897109
2278	395	650	0,1735873	0,039059	0,00958857
2278	427	660	0,1872848	0,039059	0,01034519
2278	433	670	0,1901659	0,039059	0,01050434
2278	433	680	0,1901659	0,039059	0,01050434
2278	460	690	0,2020585	0,039059	0,01116126

2278	501	700	0,2198555	0,039059	0,01214433
2278	522	710	0,2289979	0,039059	0,01264933
2278	557	720	0,2445143	0,039059	0,01350642
2278	596	730	0,2615454	0,039059	0,01444719
2278	603	740	0,2646663	0,039059	0,01461957
2278	649	750	0,2851602	0,039059	0,01575161
2278	686	760	0,3012677	0,039059	0,01664136
2278	710	770	0,3116135	0,039059	0,01721283
2278	721	780	0,3163769	0,039059	0,01747595
2278	739	790	0,3246063	0,039059	0,01793053
2278	800	800	0,3514281	0,039059	0,01941210
2278	826	810	0,3624668	0,039059	0,02002186
2278	834	820	0,366087	0,039059	0,02022183
2278	944	830	0,4144935	0,039059	0,02289570
2278	960	840	0,421507	0,039059	0,02328311
2278	976	850	0,4285399	0,039059	0,02367159
2278	976	860	0,4285413	0,039059	0,02367167
2278	1032	870	0,4533263	0,039059	0,02504073
2278	1058	880	0,4645216	0,039059	0,02565914
2278	1122	890	0,4927481	0,039059	0,02721831
2278	1197	900	0,5253632	0,039059	0,02901989
2278	1204	910	0,5287803	0,039059	0,02920864
2278	1247	920	0,5476609	0,039059	0,03025157
2278	1305	930	0,5729308	0,039059	0,03164742
2278	1389	940	0,6097876	0,039059	0,03368330
2278	1415	950	0,621245	0,039059	0,03431619
2278	1436	960	0,6306368	0,039059	0,03483497
2278	1473	970	0,6467887	0,039059	0,03572716
2278	1576	980	0,6917859	0,039059	0,03821271
2278	1625	990	0,7135097	0,039059	0,03941268

2278	1641	1000	0,7206868	0,039059	0,03980913
2278	1701	1010	0,746805	0,039059	0,04125184
2278	1768	1020	0,7760775	0,039059	0,04286879
2278	1802	1030	0,7910059	0,039059	0,04369340
2278	1859	1040	0,816413	0,039059	0,04509683
2278	1903	1050	0,8357331	0,039059	0,04616403
2278	1934	1060	0,8491527	0,039059	0,04690530
2278	2000	1070	0,8780066	0,039059	0,04849913
2278	2041	1080	0,8961227	0,039059	0,04949982
2278	2114	1090	0,9280302	0,039059	0,05126232
2278	2114	1100	0,9280317	0,039059	0,05126240
2278	2155	1110	0,9462694	0,039059	0,05226981
2278	2201	1120	0,9662136	0,039059	0,05337148
2278	2217	1130	0,9733291	0,039059	0,05376452
2278	2225	1140	0,976772	0,039059	0,05395471
2278	2256	1150	0,9904725	0,039059	0,05471149
2278	2262	1160	0,9929884	0,039059	0,05485046
2278	2264	1170	0,9938793	0,039059	0,05489967
2278	2273	1180	0,9980972	0,039059	0,05513266
2278	2279	1190	1,0006762	0,039059	0,05527512
2278	2287	1200	1,004062	0,039059	0,05546215
2278	2292	1210	1,0063626	0,039059	0,05558922

Table A- 59: Volumes obtained from titration for SO₃ analysis - 900°C run 2

Bottle	Initial Volume (ml)	Final Volume (ml)	Volume Titrated (ml)
1	0	8.6	8.6
	8.6	17.2	8.6
	17.2	25.8	8.6
Average			8.6
<hr/>			
2	25.8	34.5	8.7
	0	8.6	8.6
	8.6	17.2	8.6
Average			8.6333
<hr/>			
3	17.2	25.9	8.7
	25.9	34.6	8.7
	0	8.6	8.6
Average			8.6666

Table A- 60: Moles of SO₃ produced from titrations - 900°C run 2

Bottle	BaClO₄ Consumed (moles)	SO₃ Produced (moles)
1	0.0000430	0.0000430
2	0.0000432	0.0000432
3	0.0000433	0.0000433
Total (moles)	0.000130	0.000130

Table A- 61: System sulfur mass balance - 900°C run 2

Into System		
<i>SO₂ Analysis</i>		
Total moles gas	1,22629	moles
Moles SO ₂	0,00279	moles
Moles sulfur from SO ₂	0,00279	moles
Mass sulfur from SO ₂	0,08955	grams
<i>SO₃ Analysis</i>		
Moles SO ₃	0	moles
Mass SO ₃	0	grams
Out of System		
<i>SO₂ Analysis</i>		
Moles SO ₂	0,00089	moles
Moles sulfur from SO ₂	0,00089	moles
Mass sulfur from SO ₂	0,02842	grams
<i>SO₃ Analysis</i>		
Moles SO ₃ formed	0,000130	moles
Moles sulfur from SO ₃	0,000130	moles
Mass sulfur from SO ₃	0,00830	grams

Table A- 62: SO₂ sorption capacity of limestone sorbent - 900° run 2

Initial/inlet Concentration (C _o)	2278	ppmv
Saturation time (T _{sat})	1190	s
Integral	0,00886	mol.s/L
Sorption capacity of limestone	18.627	mg SO₂/g CaCO₃

A-1.6.3) RUN 3

Table A- 63: Initial /inlet SO₂ concentration - 900°C run 3

Time (s)	Area ($\mu\text{V} \cdot \text{s}$)	SO ₂ Volume (ml)	SO ₂ Volume Percent (%)	SO ₂ Concentration (ppmv)
0	3173017,40	0,002321	0,232143	2321
10	2985998,10	0,002176	0,217592	2176
20	3065093,80	0,002238	0,223812	2238
30	2986816,50	0,002177	0,217657	2177
40	3019019,40	0,002202	0,220200	2202
50	2977733,60	0,002169	0,216938	2169
60	2943337,30	0,002142	0,214202	2142
70	3126672,10	0,002286	0,228589	2286
80	3013876,40	0,002198	0,219795	2198
90	3668542,00	0,002675	0,267490	2675
100	3165533,90	0,002316	0,231572	2316
110	2947048,80	0,002145	0,214498	2145
120	3115360,10	0,002277	0,227716	2277
130	2786759,70	0,002016	0,201565	2016
140	3187890,40	0,002333	0,233276	2333
150	3012331,60	0,002197	0,219673	2197
160	2881238,60	0,002092	0,209224	2092
170	3320567,5	0,002432	0,243207	2432
180	3301673,5	0,002418	0,241813	2418
190	3186833,4	0,002332	0,233196	2332
200	3252163,6	0,002381	0,238128	2381
210	2960864,8	0,002156	0,215598	2156
220	3376061,4	0,002473	0,247259	2473
230	3375480,4	0,002472	0,247217	2472

240	3195192,1	0,002338	0,233831	2338
250	2766644,3	0,001999	0,199922	1999
260	3292857,4	0,002412	0,241160	2412
270	2707608,3	0,001951	0,195078	1951
280	3545324,8	0,002592	0,259213	2592
290	2718086,8	0,001959	0,195940	1959
300	3436610,5	0,002516	0,251608	2516
Average		0,002271	0,227068	2271

Table A- 64: Reactor effluent SO₂ concentration - 900°C run 3

Time (s)	Area (μ V.s)	SO ₂ Volume (ml)	SO ₂ Volume Percent (%)	SO ₂ Concentration (ppmv)	C _{SO₂} (mol/L)	ΔT (s)	C _{SO₂} ΔT (mol.s/L)
0	33792,3	0,000011	0,001074	11	0,00000011	10	0,00000112
10	39198,1	0,000013	0,001298	13	0,00000013	10	0,00000135
20	41524,5	0,000014	0,001395	14	0,00000014	10	0,00000145
30	47800,2	0,000017	0,001657	17	0,00000017	10	0,00000172
40	51188,3	0,000018	0,001800	18	0,00000019	10	0,00000187
50	57071,5	0,000020	0,002047	20	0,00000021	10	0,00000213
60	60557,5	0,000022	0,002195	22	0,00000023	10	0,00000228
70	67748,2	0,000025	0,002501	25	0,00000026	10	0,00000260
80	70351,2	0,000026	0,002612	26	0,00000027	10	0,00000271
90	72915,7	0,000027	0,002722	27	0,00000028	10	0,00000283
100	76540,3	0,000029	0,002877	29	0,00000030	10	0,00000299
110	77149,7	0,000029	0,002904	29	0,00000030	10	0,00000302
120	80675,3	0,000031	0,003056	31	0,00000032	10	0,00000317
130	84219,7	0,000032	0,003209	32	0,00000033	10	0,00000333
140	85283,2	0,000033	0,003255	33	0,00000034	10	0,00000338
150	86162,9	0,000033	0,003293	33	0,00000034	10	0,00000342
160	88428,6	0,000034	0,003391	34	0,00000035	10	0,00000352

170	90238,4	0,000035	0,003470	35	0,00000036	10	0,00000361
180	93541,4	0,000036	0,003614	36	0,00000038	10	0,00000375
190	96694,2	0,000038	0,003752	38	0,00000039	10	0,00000390
200	98513,8	0,000038	0,003832	38	0,00000040	10	0,00000398
210	100698,3	0,000039	0,003928	39	0,00000041	10	0,00000408
220	103763,6	0,000041	0,004063	41	0,00000042	10	0,00000422
230	124368,8	0,000050	0,004978	50	0,00000052	10	0,00000517
240	141347	0,000057	0,005745	57	0,00000060	10	0,00000597
250	153984,8	0,000063	0,006323	63	0,00000066	10	0,00000657
260	165867,2	0,000069	0,006871	69	0,00000071	10	0,00000714
270	171716,7	0,000071	0,007143	71	0,00000074	10	0,00000742
280	178826,3	0,000075	0,007475	75	0,00000078	10	0,00000777
290	189113	0,000080	0,007960	80	0,00000083	10	0,00000827
300	195135,6	0,000082	0,008245	82	0,00000086	10	0,00000857
310	219366,7	0,000094	0,009405	94	0,00000098	10	0,00000977
320	229635,4	0,000099	0,009904	99	0,00000103	10	0,00001029
330	243990,2	0,000106	0,010607	106	0,00000110	10	0,00001102
340	283263,6	0,000126	0,012567	126	0,00000131	10	0,00001306
350	297027,1	0,000133	0,013267	133	0,00000138	10	0,00001378
360	324142,9	0,000147	0,014665	147	0,00000152	10	0,00001523
370	326128	0,000148	0,014768	148	0,00000153	10	0,00001534
380	330791,1	0,000150	0,015012	150	0,00000156	10	0,00001559
390	333693,7	0,000152	0,015163	152	0,00000158	10	0,00001575
400	336405,3	0,000153	0,015305	153	0,00000159	10	0,00001590
410	340543,1	0,000155	0,015523	155	0,00000161	10	0,00001613
420	370791,8	0,000171	0,017128	171	0,00000178	10	0,00001779
430	375167,1	0,000174	0,017363	174	0,00000180	10	0,00001804
440	376502,7	0,000174	0,017435	174	0,00000181	10	0,00001811
450	377869,4	0,000175	0,017509	175	0,00000182	10	0,00001819
460	380726,6	0,000177	0,017663	177	0,00000183	10	0,00001835

470	401222,2	0,000188	0,018775	188	0,00000195	10	0,00001950
480	404425,3	0,000189	0,018950	189	0,00000197	10	0,00001969
490	405348,5	0,000190	0,019000	190	0,00000197	10	0,00001974
500	407182,2	0,000191	0,019101	191	0,00000198	10	0,00001984
510	404170,2	0,000189	0,018936	189	0,00000197	10	0,00001967
520	405005,6	0,000190	0,018982	190	0,00000197	10	0,00001972
530	410528,6	0,000193	0,019284	193	0,00000200	10	0,00002003
540	415005,6	0,000195	0,019530	195	0,00000203	10	0,00002029
550	447634,2	0,000213	0,021344	213	0,00000222	10	0,00002217
560	514245,6	0,000252	0,025151	252	0,00000261	10	0,00002613
570	518802,4	0,000254	0,025416	254	0,00000264	10	0,00002640
580	523729,9	0,000257	0,025704	257	0,00000267	10	0,00002670
590	534157,6	0,000263	0,026316	263	0,00000273	10	0,00002734
600	596295	0,000300	0,030027	300	0,00000312	10	0,00003119
610	611378,1	0,000309	0,030945	309	0,00000321	10	0,00003215
620	614803,7	0,000312	0,031155	312	0,00000324	10	0,00003237
630	686072,1	0,000356	0,035588	356	0,00000370	10	0,00003697
640	707718,3	0,000370	0,036963	370	0,00000384	10	0,00003840
650	747685,8	0,000395	0,039534	395	0,00000411	10	0,00004107
660	795005,6	0,000426	0,042633	426	0,00000443	10	0,00004429
670	805528,6	0,000433	0,043331	433	0,00000450	10	0,00004501
680	805312,6	0,000433	0,043316	433	0,00000450	10	0,00004500
690	845312,6	0,000460	0,045992	460	0,00000478	10	0,00004778
700	905312,6	0,000501	0,050078	501	0,00000520	10	0,00005202
710	935005,6	0,000521	0,052133	521	0,00000542	10	0,00005416
720	985005,6	0,000556	0,055638	556	0,00000578	10	0,00005780
730	1039669,6	0,000595	0,059534	595	0,00000618	10	0,00006185
740	1051222,2	0,000604	0,060365	604	0,00000627	10	0,00006271
750	1114767,5	0,000650	0,064989	650	0,00000675	10	0,00006751
760	1163368,3	0,000686	0,068580	686	0,00000712	10	0,00007124

770	1196601,2	0,000711	0,071061	711	0,00000738	10	0,00007382
780	1209372,2	0,000720	0,072020	720	0,00000748	10	0,00007482
790	1235276,2	0,000740	0,073974	740	0,00000768	10	0,00007685
800	1314219,2	0,000800	0,080003	800	0,00000831	10	0,00008311
810	1348418,6	0,000826	0,082646	826	0,00000859	10	0,00008586
820	1358418,6	0,000834	0,083423	834	0,00000867	10	0,00008666
830	1497361,6	0,000944	0,094365	944	0,00000980	10	0,00009803
840	1517361,6	0,000960	0,095962	960	0,00000997	10	0,00009969
850	1537361,6	0,000976	0,097564	976	0,00001014	10	0,00010135
860	1538418,6	0,000976	0,097648	976	0,00001014	10	0,00010144
870	1608418,6	0,001033	0,103294	1033	0,00001073	10	0,00010731
880	1640428,6	0,001059	0,105894	1059	0,00001100	10	0,00011001
890	1717361,6	0,001122	0,112186	1122	0,00001165	10	0,00011654
900	1808418,6	0,001197	0,119702	1197	0,00001244	10	0,00012435
910	1817361,6	0,001204	0,120443	1204	0,00001251	10	0,00012512
920	1869518,6	0,001248	0,124780	1248	0,00001296	10	0,00012963
930	1937361,6	0,001304	0,130447	1304	0,00001355	10	0,00013551
940	2037361,6	0,001388	0,138841	1388	0,00001442	10	0,00014424
950	2068361,6	0,001415	0,141451	1415	0,00001469	10	0,00014695
960	2095418,6	0,001437	0,143731	1437	0,00001493	10	0,00014931
970	2138418,6	0,001474	0,147358	1474	0,00001531	10	0,00015308
980	2260418,6	0,001577	0,157658	1577	0,00001638	10	0,00016378
990	2317361,6	0,001625	0,162464	1625	0,00001688	10	0,00016878
1000	2338418,6	0,001642	0,164240	1642	0,00001706	10	0,00017062
1010	2408418,6	0,001701	0,170136	1701	0,00001767	10	0,00017675
1020	2488418,6	0,001769	0,176855	1769	0,00001837	10	0,00018373
1030	2527361,6	0,001801	0,180115	1801	0,00001871	10	0,00018711
1040	2597361,6	0,001860	0,185953	1860	0,00001932	10	0,00019318
1050	2649761,6	0,001903	0,190301	1903	0,00001977	10	0,00019769
1060	2687361,6	0,001934	0,193409	1934	0,00002009	10	0,00020092

1070	2768418,6	0,002001	0,200067	2001	0,00002078	10	0,00020784
1080	2818418,6	0,002041	0,204142	2041	0,00002121	10	0,00021207
1090	2908418,6	0,002114	0,211409	2114	0,00002196	10	0,00021962
1100	2908999,6	0,002115	0,211455	2115	0,00002197	10	0,00021967
1110	2959361,6	0,002155	0,215478	2155	0,00002238	10	0,00022385
1120	3018418,6	0,002202	0,220153	2202	0,00002287	10	0,00022871
1130	3038418,6	0,002217	0,221725	2217	0,00002303	10	0,00023034
1140	3048418,6	0,002225	0,222508	2225	0,00002312	10	0,00023115
1150	3087361,6	0,002255	0,225546	2255	0,00002343	10	0,00023431
1160	3095361,6	0,002262	0,226167	2262	0,00002350	10	0,00023495
1170	3097361,6	0,002263	0,226322	2263	0,00002351	10	0,00023512
1180	3109761,6	0,002273	0,227283	2273	0,00002361	10	0,00023611
1190	3117361,6	0,002279	0,227870	2279	0,00002367	10	0,00023672
1200	3127361,6	0,002286	0,228642	2286	0,00002375	10	0,00023752
1210	3135838,6	0,002293	0,229295	2293	0,00002382	10	0,00023820
Summation							0,00886684

Table A- 65: Propagational uncertainty data - 900°C run 3

C _{in} (ppmv)	C _{out} (ppmv)	Time (s)	C _{out} /C _{in}	Average relative uncertainty	Propagational uncertainty
2271	11	0	0,0047317	0,039059	0,00026137
2271	13	10	0,0057184	0,039059	0,00031587
2271	14	20	0,0061446	0,039059	0,00033942
2271	17	30	0,007299	0,039059	0,00040318
2271	18	40	0,0079251	0,039059	0,00043776
2271	20	50	0,0090169	0,039059	0,00049807
2271	22	60	0,0096666	0,039059	0,00053396
2271	25	70	0,0110134	0,039059	0,00060836
2271	26	80	0,0115031	0,039059	0,00063541
2271	27	90	0,0119867	0,039059	0,00066212

2271	29	100	0,0126721	0,039059	0,00069998
2271	29	110	0,0127876	0,039059	0,00070636
2271	31	120	0,0134568	0,039059	0,00074332
2271	32	130	0,0141317	0,039059	0,00078060
2271	33	140	0,0143346	0,039059	0,00079181
2271	33	150	0,0145026	0,039059	0,00080109
2271	34	160	0,0149359	0,039059	0,00082502
2271	35	170	0,0152826	0,039059	0,00084418
2271	36	180	0,0159168	0,039059	0,00087921
2271	38	190	0,0165239	0,039059	0,00091274
2271	38	200	0,016875	0,039059	0,00093214
2271	39	210	0,0172973	0,039059	0,00095547
2271	41	220	0,0178912	0,039059	0,00098827
2271	50	230	0,0219244	0,039059	0,00121106
2271	57	240	0,0253007	0,039059	0,00139756
2271	63	250	0,0278448	0,039059	0,00153808
2271	69	260	0,0302607	0,039059	0,00167153
2271	71	270	0,0314585	0,039059	0,00173769
2271	75	280	0,0329217	0,039059	0,00181852
2271	80	290	0,0350534	0,039059	0,00193627
2271	82	300	0,0363093	0,039059	0,00200565
2271	94	310	0,0414212	0,039059	0,00228802
2271	99	320	0,0436157	0,039059	0,00240924
2271	106	330	0,0467114	0,039059	0,00258023
2271	126	340	0,0553452	0,039059	0,00305714
2271	133	350	0,0584273	0,039059	0,00322739
2271	147	360	0,0645838	0,039059	0,00356746
2271	148	370	0,0650389	0,039059	0,00359260
2271	150	380	0,0661102	0,039059	0,00365178
2271	152	390	0,0667787	0,039059	0,00368871

2271	153	400	0,0674043	0,039059	0,00372327
2271	155	410	0,0683612	0,039059	0,00377612
2271	171	420	0,0754332	0,039059	0,00416676
2271	174	430	0,0764673	0,039059	0,00422388
2271	174	440	0,0767835	0,039059	0,00424135
2271	175	450	0,0771074	0,039059	0,00425924
2271	177	460	0,0777853	0,039059	0,00429669
2271	188	470	0,0826832	0,039059	0,00456723
2271	189	480	0,0834541	0,039059	0,00460982
2271	190	490	0,0836766	0,039059	0,00462211
2271	191	500	0,0841189	0,039059	0,00464654
2271	189	510	0,0833927	0,039059	0,00460642
2271	190	520	0,083594	0,039059	0,00461754
2271	193	530	0,0849272	0,039059	0,00469119
2271	195	540	0,0860112	0,039059	0,00475106
2271	213	550	0,0939974	0,039059	0,00519221
2271	252	560	0,1107634	0,039059	0,00611832
2271	254	570	0,1119325	0,039059	0,00618290
2271	257	580	0,1131999	0,039059	0,00625291
2271	263	590	0,1158929	0,039059	0,00640166
2271	300	600	0,1322383	0,039059	0,00730455
2271	309	610	0,1362817	0,039059	0,00752790
2271	312	620	0,1372041	0,039059	0,00757885
2271	356	630	0,1567283	0,039059	0,00865732
2271	370	640	0,1627821	0,039059	0,00899172
2271	395	650	0,1741071	0,039059	0,00961729
2271	426	660	0,1877564	0,039059	0,01037125
2271	433	670	0,1908265	0,039059	0,01054083
2271	433	680	0,1907634	0,039059	0,01053734
2271	460	690	0,202545	0,039059	0,01118814

2271	501	700	0,2205434	0,039059	0,01218233
2271	521	710	0,2295906	0,039059	0,01268207
2271	556	720	0,2450273	0,039059	0,01353476
2271	595	730	0,2621842	0,039059	0,01448247
2271	604	740	0,2658464	0,039059	0,01468476
2271	650	750	0,2862087	0,039059	0,01580953
2271	686	760	0,3020225	0,039059	0,01668305
2271	711	770	0,3129505	0,039059	0,01728669
2271	720	780	0,3171741	0,039059	0,01751999
2271	740	790	0,3257809	0,039059	0,01799541
2271	800	800	0,3523286	0,039059	0,01946184
2271	826	810	0,363971	0,039059	0,02010494
2271	834	820	0,3673907	0,039059	0,02029384
2271	944	830	0,4155786	0,039059	0,02295564
2271	960	840	0,4226113	0,039059	0,02334411
2271	976	850	0,4296664	0,039059	0,02373381
2271	976	860	0,4300398	0,039059	0,02375444
2271	1033	870	0,4549031	0,039059	0,02512783
2271	1059	880	0,4663538	0,039059	0,02576034
2271	1122	890	0,4940628	0,039059	0,02729093
2271	1197	900	0,5271621	0,039059	0,02911926
2271	1204	910	0,5304285	0,039059	0,02929969
2271	1248	920	0,5495281	0,039059	0,03035471
2271	1304	930	0,574484	0,039059	0,03173321
2271	1388	940	0,6114511	0,039059	0,03377519
2271	1415	950	0,6229444	0,039059	0,03441006
2271	1437	960	0,6329854	0,039059	0,03496470
2271	1474	970	0,6489576	0,039059	0,03584697
2271	1577	980	0,6943197	0,039059	0,03835267
2271	1625	990	0,7154856	0,039059	0,03952183

2271	1642	1000	0,7233071	0,039059	0,03995387
2271	1701	1010	0,7492749	0,039059	0,04138827
2271	1769	1020	0,7788622	0,039059	0,04302261
2271	1801	1030	0,7932186	0,039059	0,04381562
2271	1860	1040	0,8189288	0,039059	0,04523580
2271	1903	1050	0,8380809	0,039059	0,04629372
2271	1934	1060	0,8517669	0,039059	0,04704970
2271	2001	1070	0,8810879	0,039059	0,04866933
2271	2041	1080	0,8990355	0,039059	0,04966071
2271	2114	1090	0,9310366	0,039059	0,05142838
2271	2115	1100	0,9312418	0,039059	0,05143972
2271	2155	1110	0,9489587	0,039059	0,05241836
2271	2202	1120	0,9695449	0,039059	0,05355550
2271	2217	1130	0,9764675	0,039059	0,05393788
2271	2225	1140	0,9799191	0,039059	0,05412854
2271	2255	1150	0,9932976	0,039059	0,05486754
2271	2262	1160	0,9960332	0,039059	0,05501865
2271	2263	1170	0,9967164	0,039059	0,05505639
2271	2273	1180	1,000946	0,039059	0,05529003
2271	2279	1190	1,0035331	0,039059	0,05543293
2271	2286	1200	1,0069308	0,039059	0,05562061
2271	2293	1210	1,0098055	0,039059	0,05577940

Table A- 66: Volumes obtained from titration for SO₃ analysis - 900°C run 3

Bottle	Initial Volume (ml)	Final Volume (ml)	Volume Titrated (ml)
1	0	8.6	8.6
	8.6	17.3	8.7
	17.3	25.9	8.6
Average			8.6333
2	25.9	34.6	8.7
	0	8.7	8.7
	8.7	17.4	8.7
Average			8.7
3	17.4	26.1	8.7
	26.1	34.7	8.6
	0	8.7	8.7
Average			8,6666

Table A- 67: Moles of SO₃ produced from titrations - 900°C run3

Bottle	BaClO ₄ Consumed (moles)	SO ₃ Produced (moles)
1	0,0000432	0,0000432
2	0,0000435	0,0000435
3	0,0000433	0,0000433
Total (moles)	0,000130	0,000130

Table A- 68: System sulfur mass balance – 900°C run 3

Into System		
<i>SO₂ Analysis</i>		
Total moles gas	1,22629	moles
Moles SO ₂	0,00278	moles
Moles sulfur from SO ₂	0,00278	moles
Mass sulfur from SO ₂	0,08929	grams
<i>SO₃ Analysis</i>		
Moles SO ₃	0	moles
Mass SO ₃	0	grams
Out of System		
<i>SO₂ Analysis</i>		
Moles SO ₂	0,00089	moles
Moles sulfur from SO ₂	0,00089	moles
Mass sulfur from SO ₂	0,02843	grams
<i>SO₃ Analysis</i>		
Moles SO ₃ formed	0,000131	moles
Moles sulfur from SO ₃	0,000131	moles
Mass sulfur from SO ₃	0,00833	grams

Table A- 69: SO₂ sorption capacity of limestone sorbent – 900°C run 3

Initial/inlet Concentration (C _o)	2271	ppmv
Saturation time (T _{sat})	1180	s
Integral	0,00887	mol.s/L
Sorption capacity of limestone	18.415	mg SO₂/g CaCO₃

A-1.7) RESPONSE CURVE DATA AVERAGE RELATIVE UNCERTAINTY CALCULATIONS

A-1.7.1) 700°C

Table A- 70: Calculation for average relative uncertainty between response curve data - 700°C

Time (s)	$(\frac{C_{out}}{C_{in}}) - \text{Run 1}$	$(\frac{C_{out}}{C_{in}}) - \text{Run 2}$	$(\frac{C_{out}}{C_{in}}) - \text{Run 3}$	$\left \frac{(y_{1,k} - y_{2,k})}{y_{1,k}} \right \ell$	$\left \frac{(y_{1,k} - y_{3,k})}{y_{1,k}} \right \ell$
0	0,008151187	0,009108907	0,00913357	0,117494522	0,120520194
10	0,008849527	0,00981643	0,009662643	0,10926045	0,091882443
20	0,009294737	0,010300292	0,010223499	0,10818537	0,099923425
30	0,010384648	0,01134476	0,011372474	0,092454904	0,095123684
40	0,01297758	0,013987655	0,013971511	0,077832306	0,076588301
50	0,014126941	0,015099311	0,015065795	0,068830899	0,066458419
60	0,016903148	0,017917533	0,017728477	0,060011621	0,048826936
70	0,018333742	0,020700724	0,018289772	0,129105238	0,002398295
80	0,018734033	0,021003916	0,021047811	0,121163614	0,123506685
90	0,020371817	0,022671225	0,022741958	0,112871997	0,116344093
100	0,021993111	0,024384452	0,024268982	0,108731374	0,103481113
110	0,024153302	0,026456533	0,026507909	0,095358809	0,097485888
120	0,02901169	0,031447286	0,031336873	0,083952247	0,080146426
130	0,033967365	0,036346717	0,03639131	0,070048175	0,071360986
140	0,038608558	0,041099873	0,040996651	0,064527545	0,061853987
150	0,051928331	0,054376324	0,054396092	0,047141764	0,047522437
160	0,056265221	0,058754264	0,058877572	0,044237679	0,046429225
170	0,06175449	0,064360742	0,064347785	0,042203449	0,041993635
180	0,069067116	0,071586506	0,071626114	0,036477414	0,037050894
190	0,073162516	0,0758168	0,075815715	0,0362793	0,03626446
200	0,082104582	0,084793073	0,084801405	0,032744711	0,03284619
210	0,087839472	0,090448212	0,090486041	0,029698953	0,030129605

220	0,095496075	0,098104526	0,098308274	0,02731474	0,029448323
230	0,11099607	0,113671712	0,113735674	0,024105736	0,024681995
240	0,128862583	0,125236664	0,131747854	0,028137874	0,022390295
250	0,130855235	0,133550788	0,133806279	0,020599505	0,022551977
260	0,1319001	0,134733358	0,134711597	0,021480334	0,021315348
270	0,132935753	0,135635458	0,135750543	0,020308341	0,021174064
280	0,136271144	0,139003468	0,139181056	0,020050649	0,021353841
290	0,138332423	0,141179575	0,141248969	0,020581956	0,021083601
300	0,14771094	0,150464034	0,150717228	0,018638385	0,020352502
310	0,154217208	0,157094665	0,157094566	0,018658468	0,018657827
320	0,155600459	0,158339245	0,158481562	0,017601402	0,018516031
330	0,165928896	0,168709447	0,168836796	0,016757484	0,017524979
340	0,174216433	0,177124572	0,17723425	0,01669268	0,017322233
350	0,189135031	0,191941491	0,192096094	0,014838395	0,015655817
360	0,200809421	0,203596651	0,203886869	0,013879973	0,015325217
370	0,205068622	0,207858629	0,208220352	0,013605236	0,015369146
380	0,209828392	0,212772978	0,212989617	0,014033306	0,015065766
390	0,213784211	0,216608238	0,216886557	0,013209705	0,014511574
400	0,224025889	0,226854459	0,227050474	0,012626083	0,013501049
410	0,235962285	0,238920591	0,239004531	0,012537196	0,012892931
420	0,255636529	0,258439295	0,259989458	0,010963874	0,017027806
430	0,257043465	0,260684577	0,261212336	0,014165355	0,016218542
440	0,260509847	0,263952975	0,264344224	0,013216881	0,014718739
450	0,283797174	0,287450001	0,288210413	0,01287126	0,01555068
460	0,298205009	0,301861935	0,302644349	0,012263127	0,014886874
470	0,3355999	0,339249894	0,339893625	0,010876029	0,012794179
480	0,357557212	0,361195897	0,361871083	0,010176511	0,012064843
490	0,385508619	0,388907259	0,390045435	0,00881599	0,011768391
500	0,386278435	0,389894006	0,390235817	0,009360013	0,010244896
510	0,425122328	0,428694031	0,429081761	0,00840159	0,009313632

520	0,462642429	0,466154589	0,466977249	0,007591522	0,0093697
530	0,495830537	0,499052281	0,500363855	0,006497672	0,009142878
540	0,510698587	0,514118577	0,51461224	0,006696689	0,007663332
550	0,526615206	0,52999814	0,530908364	0,006423919	0,008152363
560	0,540142943	0,543263186	0,544026018	0,005776699	0,007188976
570	0,562186195	0,565481756	0,56644001	0,005862045	0,00756656
580	0,584669197	0,587905554	0,589112281	0,005535363	0,007599312
590	0,585093914	0,588094772	0,592556759	0,005128849	0,012754952
600	0,608985557	0,612150047	0,612769437	0,005196331	0,006213416
610	0,614923969	0,618072063	0,618697524	0,005119486	0,00613662
620	0,616028958	0,619173689	0,620202275	0,005104841	0,006774546
630	0,650840479	0,643232664	0,654545715	0,011689217	0,005693002
640	0,651551875	0,65458168	0,65565864	0,004650136	0,006303051
650	0,666827967	0,669571171	0,671124561	0,004113811	0,006443332
660	0,685045793	0,677302557	0,688676688	0,011303238	0,005300223
670	0,688872117	0,691773449	0,69289765	0,004211713	0,005843657
680	0,727134768	0,729891342	0,730661849	0,003791009	0,004850656
690	0,742428106	0,74488758	0,745914091	0,003312744	0,004695384
700	0,765339239	0,767938138	0,769162317	0,003395748	0,004995272
710	0,776777041	0,779093219	0,780565652	0,00298178	0,004877347
720	0,80340396	0,795026164	0,807327924	0,010427875	0,004884172
730	0,815658541	0,818033841	0,81954112	0,002912125	0,004760055
740	0,857357879	0,859301795	0,860872062	0,002267333	0,004098852
750	0,881159157	0,883213416	0,884581392	0,002331315	0,003883787
760	0,899650332	0,891263072	0,902606669	0,0093228	0,003286096
770	0,911575731	0,913467581	0,91448356	0,002075362	0,003189892
780	0,912991417	0,914874034	0,915893404	0,002062032	0,003178548
790	0,914782985	0,91642938	0,917677555	0,001799765	0,003164215
800	0,918475777	0,920329626	0,921743391	0,002018397	0,003557649
810	0,930680407	0,932464509	0,93350791	0,001916987	0,003038103

820	0,934352269	0,936117017	0,927049224	0,00188874	0,007816158
830	0,948988216	0,950667283	0,95211954	0,001769323	0,003299645
840	0,956274149	0,957910527	0,95937157	0,001711202	0,003239051
850	0,963537852	0,964909107	0,966219443	0,001423146	0,002783068
860	0,963537852	0,9651326	0,966600938	0,001655097	0,003178999
870	0,988776325	0,989996484	0,991338894	0,001234009	0,002591658
880	0,98949661	0,990931709	0,992055691	0,001450333	0,002586246
890	1,013706501	0,993775975	0,995278777	0,019661041	0,01817856
900	1,024289552	1,019216411	1,026673834	0,004952839	0,002327742
910	1,027803129	1,025503057	1,027743091	0,002237853	5,84142E-05
Summation				2,354880802	2,262085902
Average Relative Deviation				0,02559653	0,02458789
% Average Relative Deviation				2,559653045	2,458789024

A-1.7.2) 800°C

Table A- 71: Calculation for average relative uncertainty between response curve data - 800°C

Time (s)	$(\frac{C_{out}}{C_{in}}) - \text{Run 1}$	$(\frac{C_{out}}{C_{in}}) - \text{Run 2}$	$(\frac{C_{out}}{C_{in}}) - \text{Run 3}$	$\left \frac{y_{1,k} - y_{2,k}}{y_{1,k}} \right \ell$	$\left \frac{y_{1,k} - y_{3,k}}{y_{1,k}} \right \ell$
0	0,006162089	0,007478161	0,006926964	0,213575755	0,124126005
10	0,006843771	0,007828195	0,007718091	0,143842369	0,127754117
20	0,007278074	0,008292612	0,008206199	0,139396549	0,127523446
30	0,008341793	0,009289189	0,009100335	0,113572125	0,090932626
40	0,008979345	0,009968115	0,00990388	0,110116035	0,10296242
50	0,010091153	0,01111174	0,010957705	0,101136765	0,085872425
60	0,010866672	0,011859144	0,0116177	0,091331708	0,069112929
70	0,012238814	0,013233898	0,013100037	0,081305577	0,070368158
80	0,012622813	0,013577693	0,013539319	0,07564714	0,072607054
90	0,013230401	0,014257393	0,014145523	0,077623691	0,069168151
100	0,013813116	0,014811117	0,0147269	0,072250223	0,0661534
110	0,013930674	0,014959047	0,014844187	0,073820824	0,065575675
120	0,014612041	0,015641743	0,015523974	0,070469377	0,062409645
130	0,015299194	0,016299871	0,016209516	0,065407192	0,059501349
140	0,015622244	0,016582005	0,016531805	0,061435508	0,058222152
150	0,015676835	0,01670858	0,016586267	0,065813309	0,058011171
160	0,016470968	0,017236636	0,017378511	0,046485896	0,055099549
170	0,016234741	0,01726754	0,01753225	0,063616631	0,079921788
180	0,017233953	0,018268616	0,018139663	0,060036325	0,052553793
190	0,017852339	0,02011807	0,020034834	0,126915059	0,122252568
200	0,019195716	0,021452151	0,021425185	0,117548888	0,116144064
210	0,019825729	0,022185544	0,021953306	0,119027887	0,107313917
220	0,02593963	0,028241947	0,028082854	0,088756735	0,082623536

230	0,028003314	0,030319101	0,030214364	0,082696912	0,078956744
240	0,029437334	0,031782036	0,031696526	0,079650599	0,076745791
250	0,033033663	0,035401209	0,035192247	0,071670688	0,065344967
260	0,033835816	0,036188324	0,036105796	0,069527168	0,067088077
270	0,034631781	0,036989152	0,036858094	0,06806958	0,064285254
280	0,037201165	0,039679881	0,039367475	0,066630075	0,058232317
290	0,038793508	0,041175745	0,041074341	0,061408134	0,058794193
300	0,043900003	0,046311525	0,046076866	0,054932162	0,049586859
310	0,044571064	0,047094942	0,046862903	0,056625939	0,051419885
320	0,052260817	0,054717564	0,05451647	0,047009349	0,043161457
330	0,060418834	0,063030785	0,062683181	0,043230735	0,03747751
340	0,067016866	0,069568242	0,069214594	0,038070663	0,032793665
350	0,071846732	0,074515422	0,074046126	0,037144205	0,030612302
360	0,073951179	0,076511341	0,07622402	0,034619624	0,030734349
370	0,074913091	0,077500155	0,077237763	0,034534205	0,031031586
380	0,078649767	0,081229976	0,080850099	0,032806309	0,027976322
390	0,079348742	0,082051931	0,08154908	0,034067188	0,027729963
400	0,08252625	0,085122424	0,084726413	0,031458761	0,026660154
410	0,091898121	0,094554552	0,094172152	0,028906267	0,024745127
420	0,107534041	0,11034987	0,109856454	0,026185473	0,021597006
430	0,108660809	0,111352318	0,110926914	0,024769822	0,020854844
440	0,111441678	0,11416689	0,113626163	0,024454154	0,01960204
450	0,117013655	0,119756539	0,119329493	0,023440719	0,019791181
460	0,123197097	0,125933374	0,125368728	0,022210564	0,017627289
470	0,131352371	0,134245489	0,133595737	0,022025626	0,017078993
480	0,135014059	0,137808732	0,137311092	0,020699122	0,017013288
490	0,145871496	0,148667462	0,148009227	0,01916732	0,014654887
500	0,157637673	0,160487034	0,159839814	0,01807538	0,013969637
510	0,160085312	0,163053562	0,16219627	0,018541671	0,013186454
520	0,160974224	0,163803806	0,163170107	0,017577858	0,013641209

530	0,186938215	0,189815427	0,189141599	0,015391249	0,011786696
540	0,189881973	0,1927919	0,19192464	0,015324925	0,01075756
550	0,2116015	0,214663841	0,213677888	0,01447221	0,009812728
560	0,222609375	0,225533606	0,224560341	0,013136154	0,008764078
570	0,24076291	0,243859217	0,242819534	0,0128604	0,008542115
580	0,259548953	0,263334007	0,26246346	0,014583199	0,011229121
590	0,259906419	0,263690669	0,262820026	0,014560048	0,011210215
600	0,313104412	0,316732888	0,315511306	0,011588709	0,007687196
610	0,318321874	0,32195239	0,321062887	0,011405173	0,008610821
620	0,319294493	0,322925353	0,322226337	0,011371507	0,009182258
630	0,350219025	0,354065861	0,352485761	0,010984087	0,006472339
640	0,35085667	0,354704949	0,353481456	0,010968237	0,007481079
650	0,364603495	0,36823809	0,366811644	0,009968623	0,006056302
660	0,381132858	0,384979268	0,38363791	0,010092046	0,006572647
670	0,384623166	0,388252169	0,38731588	0,009435215	0,007000913
680	0,419879209	0,423488348	0,421841801	0,008595659	0,004674183
690	0,434150065	0,437747693	0,436627752	0,008286601	0,005706984
700	0,455720748	0,459519531	0,457887722	0,008335768	0,004755047
710	0,466575369	0,470139757	0,468307119	0,007639468	0,003711618
720	0,492067433	0,495824007	0,494049256	0,007634266	0,004027544
730	0,503904987	0,507646663	0,506035915	0,007425361	0,004228829
740	0,507759633	0,511495711	0,50927135	0,007357967	0,002977231
750	0,531185973	0,534883725	0,533168281	0,006961314	0,003731854
760	0,549589031	0,553254478	0,551252613	0,006669433	0,003026957
770	0,56155338	0,564967384	0,563147032	0,006079572	0,002837936
780	0,6003406	0,603902086	0,601305386	0,005932442	0,001607063
790	0,60215701	0,605715873	0,603504042	0,005910192	0,002237012
800	0,605905875	0,609224206	0,607445917	0,005476645	0,00254172
810	0,618342811	0,621863781	0,619587588	0,005694203	0,002013085
820	0,659724293	0,663137165	0,660302076	0,00517318	0,000875795

830	0,674796694	0,677935796	0,675271869	0,004651923	0,000704175
840	0,68233508	0,685685359	0,683153941	0,00491002	0,001200086
850	0,689874067	0,692969045	0,690244836	0,004486294	0,000537444
860	0,727555507	0,730763731	0,728052729	0,004409594	0,000683414
870	0,753888855	0,756776945	0,754190876	0,003830923	0,000400618
880	0,79213577	0,795115982	0,792359368	0,003762248	0,000282271
890	0,79512294	0,798090216	0,794715512	0,003731844	0,00051241
900	0,8286613	0,831496401	0,828376806	0,003421303	0,000343317
910	0,832373938	0,834964517	0,831669987	0,003112279	0,000845714
920	0,832782142	0,835600162	0,832463908	0,003383862	0,000382133
930	0,839789941	0,842577102	0,839413982	0,003318879	0,000447681
940	0,876663621	0,879064166	0,875592157	0,002738274	0,001222207
950	0,888016422	0,890591182	0,887441657	0,00289945	0,000647246
960	0,905876394	0,908142417	0,904933989	0,00250147	0,001040324
970	0,913134484	0,915588089	0,912127358	0,002687014	0,001102934
980	0,921096037	0,923288976	0,92022536	0,002380794	0,000945262
990	0,927592043	0,929975503	0,926454457	0,002569514	0,001226386
1000	0,941967152	0,944277437	0,940322522	0,002452618	0,001745952
1010	0,959812259	0,962027453	0,95837635	0,002307945	0,001496031
1020	0,966909731	0,969088187	0,965610526	0,002253008	0,001343668
1030	0,977510461	0,979413654	0,975906069	0,001946979	0,001641305
1040	0,984546359	0,986626351	0,983076077	0,00211264	0,001493359
1050	0,995889574	0,997906788	0,993741262	0,002025539	0,002157179
1060	1,002022019	1,003789531	0,99981455	0,001763945	0,002203015
1070	1,008964963	1,010692902	1,006690033	0,001712586	0,002254716
1080	1,012425973	1,014133992	1,010117221	0,001687056	0,002280415
1090	1,015879902	1,01572136	1,011041341	0,000156064	0,004762926
Summation				3,755865757	3,212624401
Average Relative Deviation				0,034144234	0,032126244
% Average Relative Deviation				3,414423416	3,212624401

A-1.7.3) 900°C

Table A- 72: Calculation for average relative uncertainty between response curve data - 900°C

Time (s)	$(\frac{C_{out}}{C_{in}}) - \text{Run 1}$	$(\frac{C_{out}}{C_{in}}) - \text{Run 2}$	$(\frac{C_{out}}{C_{in}}) - \text{Run 3}$	$\left \frac{y_{1,k} - y_{2,k}}{y_{1,k}} \right _\ell$	$\left \frac{y_{1,k} - y_{3,k}}{y_{1,k}} \right _\ell$
0	0,004482408	0,005181438	0,004731686	0,155949773	0,055612494
10	0,004920317	0,005887793	0,005718432	0,196628772	0,162207958
20	0,005344728	0,006341682	0,006144638	0,186530277	0,149663228
30	0,006384276	0,007383613	0,007299035	0,156530998	0,143283087
40	0,007007376	0,008008121	0,007925089	0,142813093	0,13096378
50	0,008094049	0,009028731	0,00901688	0,115477577	0,11401353
60	0,008852084	0,009856909	0,009666609	0,113512816	0,092015042
70	0,010193386	0,011171841	0,011013401	0,095989186	0,080445827
80	0,010568775	0,011507962	0,011503112	0,088864267	0,088405395
90	0,01116276	0,012143121	0,011986711	0,087824256	0,073812428
100	0,011732451	0,012743389	0,012672127	0,086165978	0,080092064
110	0,011847384	0,012788814	0,012787585	0,079463188	0,079359391
120	0,012513554	0,013496516	0,013456789	0,078551773	0,075377102
130	0,013185408	0,014129128	0,014131689	0,071573091	0,071767299
140	0,013501276	0,014445529	0,014334609	0,069937996	0,061722484
150	0,013554655	0,014539577	0,014502603	0,072663074	0,069935303
160	0,014100173	0,01511591	0,014935883	0,072037213	0,059269505
170	0,014331161	0,015317523	0,015282603	0,068826335	0,066389737
180	0,015077248	0,016094908	0,015916816	0,067496409	0,055684476
190	0,015681963	0,016670778	0,016523906	0,063054297	0,053688659
200	0,016031731	0,017051237	0,016875043	0,063593059	0,052602724
210	0,016452378	0,017401442	0,017297333	0,057685531	0,051357619
220	0,016928255	0,017919281	0,017891245	0,058542681	0,056886517

230	0,019670884	0,021921487	0,02192441	0,114412878	0,114561455
240	0,023014612	0,02526958	0,025300731	0,097979831	0,099333339
250	0,025473062	0,027844606	0,027844802	0,093100076	0,093107781
260	0,027451566	0,029736042	0,030260693	0,083218408	0,102330296
270	0,028421585	0,030731741	0,031458457	0,081281744	0,106850902
280	0,030083191	0,032404117	0,03292173	0,077150235	0,094356285
290	0,032191633	0,03460905	0,035053388	0,075094595	0,08889748
300	0,03321557	0,035639738	0,03630934	0,072982878	0,093142166
310	0,038269244	0,040620797	0,041421213	0,061447596	0,082362971
320	0,040663621	0,043135093	0,043615721	0,060778431	0,072598046
330	0,043727682	0,046110685	0,046711359	0,05449643	0,068233145
340	0,052043032	0,05449221	0,055345187	0,047060633	0,063450469
350	0,055328873	0,057885055	0,058427288	0,046199785	0,055999954
360	0,061188054	0,063683852	0,064583796	0,040788974	0,055496816
370	0,061878793	0,064356271	0,065038869	0,040037596	0,051068806
380	0,062699407	0,065294386	0,066110185	0,041387611	0,054398888
390	0,063361359	0,065845928	0,066778685	0,039212679	0,05393392
400	0,063848061	0,066356759	0,067404336	0,039291673	0,055699018
410	0,064795231	0,067286574	0,068361173	0,038449477	0,055034008
420	0,07193303	0,074573415	0,075433187	0,036706161	0,048658551
430	0,072957461	0,075508228	0,076467281	0,034962385	0,04810776
440	0,073134429	0,075663599	0,076783507	0,034582485	0,049895486
450	0,073455159	0,076008134	0,077107366	0,034755559	0,04972022
460	0,074263236	0,076797328	0,077785302	0,0341231	0,047426782
470	0,079116276	0,081789708	0,082683177	0,03379118	0,045084295
480	0,07988026	0,082460945	0,083454125	0,032306915	0,044740267
490	0,079961968	0,082520216	0,083676602	0,031993304	0,046455012
500	0,080400094	0,083079234	0,084118861	0,033322598	0,046253272
510	0,080561494	0,083122218	0,083392671	0,031785946	0,035143051
520	0,080834806	0,083419484	0,083593954	0,031974815	0,034133167

530	0,082033249	0,084719565	0,084927206	0,032746677	0,035277853
540	0,083235305	0,085829888	0,086011168	0,031171665	0,033349589
550	0,091167635	0,093793598	0,093997415	0,028803667	0,031039297
560	0,107693292	0,110480887	0,110763361	0,025884572	0,028507517
570	0,108854943	0,111519623	0,111932517	0,02447918	0,028272251
580	0,11024813	0,112917327	0,113199941	0,02421082	0,026774256
590	0,112845722	0,115547731	0,115892863	0,023944268	0,027002713
600	0,129036029	0,131761272	0,132238265	0,021120022	0,024816604
610	0,133195765	0,136065329	0,136281697	0,021543962	0,023168396
620	0,133972903	0,13671145	0,137204079	0,020441054	0,024118135
630	0,153388697	0,156311977	0,156728305	0,019057987	0,021772193
640	0,159470913	0,162408634	0,162782133	0,018421673	0,020763788
650	0,170739039	0,1735873	0,174107136	0,016681956	0,019726575
660	0,184411892	0,187284762	0,187756449	0,015578554	0,018136342
670	0,187315868	0,190165854	0,190826518	0,015214869	0,018741873
680	0,187315868	0,190165854	0,190763375	0,015214869	0,01840478
690	0,199044222	0,20205849	0,202545048	0,015143706	0,017588178
700	0,216965389	0,219855465	0,22054342	0,013320448	0,016491254
710	0,22606922	0,228997917	0,229590594	0,012954869	0,015576529
720	0,241447094	0,244514289	0,245027343	0,012703381	0,014828296
730	0,257799485	0,261545421	0,262184244	0,014530427	0,017008409
740	0,26111221	0,264666263	0,265846446	0,01361121	0,01813104
750	0,281386838	0,285160156	0,286208672	0,013409717	0,017135963
760	0,297481624	0,301267727	0,302022456	0,012727181	0,015264244
770	0,30802283	0,31161349	0,312950504	0,011657125	0,015997757
780	0,312579433	0,316376863	0,317174062	0,012148688	0,014699077
790	0,320805978	0,324606287	0,325780942	0,011846127	0,015507702
800	0,347619944	0,351428083	0,352328574	0,010954893	0,013545337
810	0,35886775	0,362466838	0,363970987	0,010029008	0,014220382
820	0,362276859	0,366087012	0,36739071	0,010517241	0,014115866

830	0,410699614	0,414493518	0,415578648	0,009237661	0,011879811
840	0,417715905	0,421506992	0,422611334	0,009075754	0,011719516
850	0,424754983	0,428539925	0,42966637	0,008910884	0,011562871
860	0,424754983	0,428541334	0,430039838	0,008914201	0,012442127
870	0,449562041	0,453326339	0,454903124	0,008373257	0,011880636
880	0,460988952	0,464521593	0,466353829	0,00766318	0,011637757
890	0,489027434	0,492748145	0,494062811	0,00760839	0,010296717
900	0,521692071	0,52536324	0,527162077	0,007037041	0,010485122
910	0,525339522	0,52878032	0,5304285	0,006549665	0,009687026
920	0,544028106	0,54766094	0,549528118	0,006677657	0,010109793
930	0,569345112	0,572930751	0,57448399	0,006297831	0,009025945
940	0,60628267	0,609787586	0,611451106	0,005780994	0,008524796
950	0,617768991	0,621245006	0,622944369	0,005626724	0,00837753
960	0,627412626	0,630636777	0,632985425	0,005138805	0,008882191
970	0,643377708	0,646788665	0,648957553	0,005301641	0,008672737
980	0,688731703	0,691785895	0,694319679	0,004434517	0,00811343
990	0,710292615	0,713509715	0,715485597	0,00452926	0,007311047
1000	0,717723167	0,720686764	0,723307145	0,004129165	0,007780128
1010	0,74370064	0,746805016	0,749274919	0,004174227	0,007495326
1020	0,773306116	0,776077513	0,77886223	0,00358383	0,007184883
1030	0,78806358	0,791005934	0,793218604	0,003733651	0,006541381
1040	0,813797187	0,816412977	0,818928809	0,003214303	0,006305775
1050	0,832970275	0,835733078	0,83808086	0,003316808	0,006135374
1060	0,846673239	0,849152731	0,85176687	0,002928511	0,006016053
1070	0,875654929	0,878006626	0,881087936	0,002685643	0,006204507
1080	0,893634187	0,896122663	0,89903546	0,002784669	0,006044165
1090	0,925699899	0,928030249	0,931036596	0,002517392	0,00576504
1100	0,925699899	0,928031657	0,931241812	0,002518914	0,005986728
1110	0,944034002	0,946269385	0,948958729	0,002367905	0,005216684
1120	0,964300177	0,96621357	0,96954493	0,00198423	0,005438922

1130	0,971240989	0,973329058	0,976467487	0,002149897	0,005381257
1140	0,974701908	0,976772048	0,9799191	0,00212387	0,005352602
1150	0,98848048	0,990472455	0,993297571	0,002015189	0,004873229
1160	0,991223401	0,99298837	0,996033166	0,001780597	0,004852353
1170	0,991908451	0,993879289	0,996716374	0,001986915	0,004847144
1180	0,996149645	0,998097195	1,000946046	0,001955078	0,00481494
1190	0,998743832	1,000676204	1,003533088	0,001934802	0,004795279
1200	1,003852065	1,004062049	1,006930841	0,000209178	0,003066962
1210	1,005014514	1,006362614	1,0098055	0,001341374	0,004767081
Summation				4,527051044	4,796486311
Average Relative Deviation				0,037106976	0,039315462
% Average Relative Deviation				3,710697577	3,931546156

APPENDIX B: SAMPLE CALCULATIONS

Table B- 1: System operating conditions

Flue gas flow rate (Q)	6	$\frac{\text{L}}{\text{min}}$
	0,1	$\frac{\text{L}}{\text{s}}$
Flue gas composition (vol %)		
<i>Sulfur Dioxide</i>	2073	ppm
<i>Oxygen</i>	20	%
<i>Nitrogen</i>	Balance	%
Operating pressure	101,325	KPa
Operating temperature prior to Reaction	25	°C
	700	°C
Operating temperatures during Reaction	800	°C
	900	°C

Table B- 2: Calibration curve equation coefficients

Calibration Curve Equation $y = -3E-23x^3 + 2E-16x^2 + 4E-10x - 3E-06$	
x³ co-efficient	-3,00E-23
x² co-efficient	2,00E-16
x co-efficient	4,00E-10
constant	-3,00E-06

Table B- 3: Auxiliary data for subsequent calculations

Sulfur Dioxide Molar Mass	64,066	$\frac{\text{g}}{\text{mol}}$
Sulfur Trioxide Molar Mass	80,066	$\frac{\text{g}}{\text{mol}}$
Sulfur Molar Mass	32,065	$\frac{\text{g}}{\text{mol}}$
R Value	8,314	$\frac{\text{L. KPa}}{\text{mol. K}}$
Molar gas volume (V_m)	22,4	$\frac{\text{cm}^3}{\text{mmol}}$
Reactor Diameter (D_t)	3,5	cm
Limestone bed length (L_{bed})	3	cm
Limestone Bulk Density (ρ_B)	1441660	$\frac{\text{g}}{\text{m}^3}$

B-1.1) CALIBRATION CURVE (REFER TO TABLE A-1)

Given that 1ml syringe samples were utilized for all experimental runs, a calibration curve was generated with the range:

[0.0; 0.2; 0.4; 0.6; 0.8; 1.0] ml flue gas

A 2073 ppmv SO₂ flue gas concentration yields the following SO₂ gas volumes with respect to the above samples:

$$\begin{aligned} & [0.0; 0.2; 0.4; 0.6; 0.8; 1.0] \times (2073 \times 10^{-6}) \text{ ml SO}_2 \\ & = [0.000; 0.0004; 0.0008; 0.0012; 0.0016; 0.002] \text{ ml SO}_2 \end{aligned}$$

A Gas Chromatograph (GC) was utilized to determine the SO₂ concentration at the reactor inlet and outlet for all experimental runs. The GC outputs a chromatogram for each sample injected and an area is assigned to each such chromatogram. Three calibration samples were injected for each respective SO₂ gas volume above, and the areas were recorded for each sample. An average area was then calculated for the appropriate SO₂ gas volume. For a 0.002 ml SO₂ gas volume, the average area was calculated as follows (the tabulated range of SO₂ gas volume average areas, as per Table A-1, were similarly calculated):

$$\begin{aligned} \text{Average Area} &= \frac{\text{Run 1 Area} + \text{Run 2 Area} + \text{Run 3 Area}}{3} & (B-1) \\ &= \frac{2792863,8 + 3069082,9 + 2757720,5}{3} \\ &= 2873222,4 \mu\text{V.s} \end{aligned}$$

The area is related to the SO₂ gas volume via a calibration curve. This curve consists of a plot of chromatogram area (μm) vs SO₂ gas volume (ppmv) - Figure 5.1. Upon non-linear regression using the Microsoft Excel function a third-degree polynomial was found to best fit the data of this plot. The calibration curve equation coefficients are tabulated in Table B-2 and the equation takes the following form:

$$y = (-3 \times 10^{-23})x^3 + (2 \times 10^{-16})x^2 + (4 \times 10^{-10})x + (-3 \times 10^{-6}) \quad (B-2)$$

Where: y – SO₂ volume (ml) of injected sample

x – Chromatogram area (μm)

B-1.2) BARIUM PERCHLORATE STANDARDIZATION

Average Volume from Sulfuric Acid (H_2SO_4) Titration (Table A-5): 25.87 ml

Average Volume from water (blank) Titration (Table A-6): 6.03 ml

$$\text{H}_2\text{SO}_4 \text{ Nomality} = 0.02 \frac{\text{mol}}{\text{L}}$$

$$\text{H}_2\text{SO}_4 \text{ Molarity} = \frac{\text{H}_2\text{SO}_4 \text{ Nomality}}{2} \quad (\text{B-3})$$

$$= \frac{0.02}{2}$$

$$= 0.01 \frac{\text{mol}}{\text{L}}$$

Volume H_2SO_4 used = 10 ml

BaClO_4 Molarity (as per Equation 4.1):

$$\text{BaClO}_4 \text{ Molarity} = \frac{\text{Vol. H}_2\text{SO}_4 \times \text{Molarity H}_2\text{SO}_4}{[\text{Avg. Vol. from H}_2\text{SO}_4 \text{ Titration} - \text{Avg. Vol. from H}_2\text{O Titration}]}$$

$$= \frac{(10 \times 10^{-3} \text{ L}) \times (0.01 \frac{\text{mol}}{\text{L}})}{[25.87 - 6.03] \times 10^{-3} \text{ L}}$$

$$= 0.005 \frac{\text{mol}}{\text{L}}$$

BaClO_4 Nomality:

$$\text{BaClO}_4 \text{ Nomality} = \text{BaClO}_4 \text{ Molarity} \times 2 \quad (\text{B-4})$$

$$= 0.005 \times 2$$

$$= 0.01 \frac{\text{mol}}{\text{L}}$$

B-1.3) 700°C - RUN 1 SAMPLE CALCULATIONS

Note: The calculation approach for the remaining experiments are identical to the **700°C - Run 1** sample calculation approach that follows below.

B-1.3.1) INLET SULFUR MASS FROM SO₂

B-1.3.1.1) INITIAL/INLET SO₂ VOLUME CONCENTRATION (**REFER TO TABLE A-7**)

As the run proceeds, 1ml sample volumes of flue gas were injected into the GC. The GC outputted chromatograms with an associated area. Calibration curve Equation B-2 was utilized to determine the corresponding SO₂ volume from this area.

Note: The calculation below is based on the initial value obtained (t = 0 s) for 700°C - Run 1 inlet/initial data (An identical approach was adopted to determine the inlet SO₂ volume concentration at future time steps for the run).

$$y = (-3 \times 10^{-23})x^3 + (2 \times 10^{-16})x^2 + (4 \times 10^{-10})x + (-3 \times 10^{-6})$$

$$x = 3159201,40 \mu\text{V.s}$$

Thus,

$$y = (-3 \times 10^{-23})(3159201,40)^3 + (2 \times 10^{-16})(3159201,40)^2 + (4 \times 10^{-10})(3159201,40) + (-3 \times 10^{-6})$$

$$y = 0,002311 \text{ ml SO}_2$$

Since 1ml flue gas samples were injected, the SO₂ volume fraction and volume percent could be determined:

$$\begin{aligned} \text{SO}_2 \text{ volume fraction} &= \frac{\text{SO}_2 \text{ volume}}{\text{Sample Volume}} \\ &= \frac{0,002311 \text{ ml}}{1\text{ml}} \\ &= 0,002311 \end{aligned} \tag{B-5}$$

$$\begin{aligned}
 \text{SO}_2 \text{ volume \%} &= \text{SO}_2 \text{ volume fraction} \times 100 & (\text{B-6}) \\
 &= 0,002311 \times 100 \\
 &= 0.2311 \%
 \end{aligned}$$

The volume fraction is finally converted to a part per million based concentration due to the minute volumes of SO₂ dealt with in this study:

$$\begin{aligned}
 \text{SO}_2 \text{ Concentration} &= \text{SO}_2 \text{ volume fraction} \times 10^6 & (\text{B-7}) \\
 &= 0,002311 \times 10^6 \\
 &= 2311 \text{ ppmv}
 \end{aligned}$$

An average inlet concentration was determined by summation of the SO₂ concentration across all time steps:

$$\begin{aligned}
 \text{Average SO}_2 \text{ Concentration} &= \frac{\sum_{t=0}^{300 \text{ sec}} (\text{SO}_2 \text{ Concentration})}{n} & (\text{B-8}) \\
 &= \frac{68407}{31} \\
 &= 2207 \text{ ppmv}
 \end{aligned}$$

B-1.3.1.2) INLET MASS FROM SO₂ (REFER TO TABLE A-12)

Flue Gas Flowrate = 6L/min

Initial/Inlet Concentration Sampling Time = 5 min

$$\begin{aligned}
 \therefore \text{Volume of Gas} &= \text{Flowrate} \times \text{Time} & (\text{B-9}) \\
 &= 6 \times 5 \\
 &= 30 \text{ L}
 \end{aligned}$$

Due to small volumes and the ideal operating pressure utilized, an ideal gas approximation was assumed to calculate the total number of moles entering the system:

$$PV = nRT$$

$$n_{\text{total}} = \frac{PV}{RT} \quad (\text{B-10})$$

$$= \frac{101.325 \times 30}{8.314 \times (25 + 273.15)}$$

$$= 1.23 \text{ moles}$$

The number of moles of SO_2 entering the system is then calculated by multiplying by the average inlet mole/volume fraction of SO_2 :

$$n_{\text{SO}_2} = n_{\text{total}} \times \text{Average } \text{SO}_2 \text{ volume fraction} \quad (\text{B-11})$$

Where,

$$\text{Average } \text{SO}_2 \text{ Volume Fraction} = \text{Average } \text{SO}_2 \text{ Concentration (ppmv)} \times 10^{-6} \quad (\text{B-12})$$

$$= 2207 \text{ ppmv} \times 10^{-6}$$

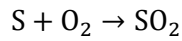
$$= 0.002207$$

Thus,

$$n_{\text{SO}_2} = 1.23 \times 0.002207$$

$$= 0.00271 \text{ moles}$$

From an elemental balance, 1 of mole of Sulfur is equivalent to the 1 of mole of SO_2 :



Thus,

$$n_{\text{sulfur}} = n_{\text{SO}_2} = 0.00271 \text{ moles}$$

Therefore, the mass of sulfur entering the system is calculated as:

$$n_{\text{sulphur}} = \frac{m_{\text{sulphur}}}{MW_{\text{sulphur}}} \quad (\text{B-13})$$

$$m_{\text{sulphur}} = n_{\text{sulphur}} \times MW_{\text{sulphur}} \quad (\text{B-14})$$

$$= 0.00271 \times 32$$

$$= 0.08677 \text{ grams.}$$

B-1.3.2) OUTLET SULFUR MASS FROM SO₂

B-1.3.2.1) REACTOR EFFLUENT SO₂ VOLUME CONCENTRATION (REFER TO TABLE A-8)

Refer to the calculation approach in **Appendix B-1.3.1.1**. The approach is identical in this instance, however now applies to the **reactor effluent data** as opposed to the Initial/inlet data used in **Appendix B-1.3.1.1**.

B-1.3.2.2) OUTLET MASS FROM SO₂ (REFER TO TABLE A-8 & TABLE A-12)

To calculate the mass of sulfur from the reactor effluent, the molar concentration of SO₂ is to first be determined. From the ideal gas Equation:

$$PV = nRT$$

Concentration of component i within a gas mixture under, under ideal conditions, is typically defined as:

$$C_i = \frac{n_i}{V} \quad (B-16)$$

From re-arrangement of the ideal gas equation, the molar concentration of SO₂ at the reactor outlet, for each respective time step, is calculated as:

$$C_i = \frac{n_i}{V} = \frac{P_i}{RT} \quad (B-17)$$

Thus,

$$C_{SO_2} = \frac{n_{SO_2}}{V} = \frac{P_{SO_2}}{RT} \quad (B-18)$$

$$P_{SO_2} = P_{\text{system}} \times \text{Volume fraction of SO}_2 \text{ at each time step } (x_{SO_2}) \quad (B-19)$$

Note: The calculation below is based on the initial value obtained ($t = 0$ s) for the 700°C - Run 1 reactor effluent data (An identical approach was adopted to determine the outlet molar SO₂ concentration at future time steps for the run).

$$C_{SO_2} = \frac{P_{SO_2}}{RT}$$

$$\begin{aligned}
 C_{SO_2} &= \frac{P_{system} \times x_{SO_2}}{RT} && \text{(B-20)} \\
 &= \frac{101.325 \times 0.000018}{8.314 \times (700 + 273.15)} \\
 &= 0.00000023 \frac{\text{mol}}{\text{L}}
 \end{aligned}$$

Samples were analyzed every 10 seconds at the reactor outlet thus: Δt (time step) = 10 s. At each time step the product ($C_{SO_2} \Delta t$) was also evaluated.

At the initial time step ($t = 0$ s) for the 700°C - Run 1 reactor effluent data (An identical approach was adopted to determine the product, $C_{SO_2} \Delta t$, at future time steps):

$$C_{SO_2} \Delta t = 0.00000023 \times 10$$

$$= 0.0000023 \frac{\text{mol.s}}{\text{L}}$$

The summation of ($C_{SO_2} \Delta t$) across all time steps for the entire run time at the reactor outlet was lastly determined:

$$\sum_{t=0}^{910 \text{ sec}} (C_{SO_2} \Delta t) = 0.01062 \frac{\text{mol.s}}{\text{L}} \quad \text{(B-21)}$$

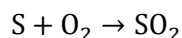
The total number of moles of SO₂ at the reactor outlet was then calculated as:

$$\text{Flue Gas Flowrate} = 6\text{L/min} = 0.1\text{L/s}$$

Thus,

$$\begin{aligned}
 n_{SO_2} &= \text{Flue Gas Flowrate} \times \sum C_{SO_2} \Delta t && \text{(B-22)} \\
 &= 0.1 \times 0.01062 \\
 &= 0.00106 \text{ moles}
 \end{aligned}$$

From an elemental balance, 1 of mole of Sulfur is equivalent to the 1 of mole of SO₂:



Thus,

$$n_{\text{sulfur}} = n_{SO_2} = 0.00106 \text{ moles}$$

Therefore, the mass of sulfur exiting the system is calculated as:

$$n_{\text{sulphur}} = \frac{m_{\text{sulphur}}}{MW_{\text{sulphur}}}$$

$$m_{\text{sulphur}} = n_{\text{sulphur}} \times MW_{\text{sulphur}}$$

$$= 0.00106 \times 32$$

$$= 0.03404 \text{ grams}$$

B-1.3.3) OUTLET SULFUR MASS FROM SO₃ (REFER TO TABLE A-12)

Three dreschel bottles, containing an 80% by volume aqueous isopropanol (IPA) solution, were utilized for the SO₃ analysis. Three samples from each dreschel bottle were collected and titrated against a standardized barium perchlorate [Ba(ClO₄)₂] solution. The volume of Ba(ClO₄)₂ used to titrate the three samples was recorded, for each respective dreschel bottle, and an average volume titrated for each bottle was determined (Table A-10). From the titration procedure the concentration of Ba(ClO₄)₂ was also known as a result of the standardization test ([C_{Ba(ClO₄)₂}] = 0.005 mol/L).

With this information at hand, the number of moles of Ba(ClO₄)₂ titrated could be determined for each dreschel bottle. The sample calculation below is applicable to the first dreschel bottle (bottle 1) for 700°C - Run 1, with an identical calculation approach for dreschel bottles 2 & 3:

$$C_{[Ba(ClO_4)_2],(Bottle\ 1)} = \frac{n_{[Ba(ClO_4)_2],(Bottle\ 1)}}{(Bottle\ 1\ Volume\ Titrated)_{Average}} \quad (B-23)$$

Thus,

$$n_{[Ba(ClO_4)_2],(Bottle\ 1)} = C_{[Ba(ClO_4)_2],(Bottle\ 1)} \times (Bottle\ 1\ Volume\ Titrated)_{Average} \quad (B-24)$$

$$\begin{aligned} &= 0.005 \times \left(\frac{2.9\text{ml}}{1000\text{L}}\right) \\ &= 1.45 \times 10^{-5} \text{ moles} \end{aligned}$$

Similarly, for bottles 2 & 3:

$$n_{[Ba(ClO_4)_2],(Bottle\ 2)} = 1.43 \times 10^{-5} \text{ moles}$$

$$n_{[Ba(ClO_4)_2],(Bottle\ 3)} = 1.5 \times 10^{-5} \text{ moles}$$

The total number of moles of BaClO₄ titrated is then calculated as a summation of the number of moles titrated from each dreschel bottle (Table A-11):

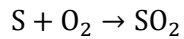
$$\begin{aligned} n_{[Ba(ClO_4)_2],((Total))} &= n_{[Ba(ClO_4)_2],((Bottle\ 1))} + n_{[Ba(ClO_4)_2],((Bottle\ 2))} + n_{[Ba(ClO_4)_2],((Bottle\ 3))} \\ &= 1.45 \times 10^{-5} + 1.43 \times 10^{-5} + 1.55 \times 10^{-5} \end{aligned} \quad (B-25)$$

$$= 4.38 \times 10^{-5} \text{ moles}$$

Literature states that for every 1 mole of $\text{Ba}(\text{ClO}_4)_2$ titrated, 1 mole of SO_2 is consumed (Frieg, et al., 2012):

$$n_{[\text{Ba}(\text{ClO}_4)_2],(\text{Total})} = n_{\text{SO}_2} = 4.38 \times 10^{-5} \text{ moles}$$

From an elemental balance, 1 of mole of Sulfur is equivalent to the 1 of mole of SO_2 :



Thus,

$$n_{\text{sulfur}} = n_{\text{SO}_2} = 4.38 \times 10^{-5} \text{ moles}$$

Therefore, the mass of sulfur exiting the system is calculated as:

$$n_{\text{sulphur}} = \frac{m_{\text{sulphur}}}{MW_{\text{sulphur}}}$$

$$m_{\text{sulphur}} = n_{\text{sulphur}} \times MW_{\text{sulphur}}$$

$$= 4.38 \times 10^{-5} \text{ moles} \times 32$$

$$= 0.00281 \text{ grams}$$

B-1.3.4) DESULFURIZATION RATIO

The desulfurization ratio is defined as the ratio between the actual desulfurization that occurs to the apparent desulfurization based on the mass of sulfur in the inlet and outlet streams (see Equation 2.14).

$$\text{Desulfurization Ratio} = \frac{S_{\text{in}} - S_{2\text{out}}}{S_{\text{in}} - S_{1\text{out}}}$$

Where:

$$S_{\text{in}} = 0.008677 \text{ grams}$$

$$S_{1\text{out}} = 0.03404 \text{ grams}$$

$$S_{2\text{out}} = 0.03404 + 0.00281$$

$$= 0.03685 \text{ grams}$$

Therefore,

$$\begin{aligned}\text{Desulphurisation Ratio} &= \frac{0.008677 - 0.03685}{0.008677 - 0.03404} \\ &= 0.9467\end{aligned}$$

B-1.3.5) SO₃ MOLAR YIELD

The molar yield of SO₃ is defined as the ratio between the moles of SO₃ produced to the moles of SO₂ introduced to the system for the total runtime (see Equation 2.13).

$$\text{Molar Yield of SO}_3(\%) = \frac{\text{Moles of SO}_3 \text{ produced}}{\text{Total moles of SO}_2 \text{ introduced}} \times 100$$

Literature states that for every 1 mole of Ba(ClO₄)₂ titrated, 1 mole of SO₃ is produced (Frieg, et al., 2012):

$$n_{[\text{Ba}(\text{ClO}_4)_2],(\text{Total})} = n_{\text{SO}_3} = 4.38 \times 10^{-5} \text{ moles}$$

Given that the total number of moles of SO₂ entering the system was calculated previously as 0.00271 moles, the molar yield of SO₃ is calculated as:

$$\begin{aligned}\text{Molar Yield of SO}_3(\%) &= \frac{0.00271}{4.38 \times 10^{-5}} \times 100 \\ &= 1.62\%\end{aligned}$$

B-1.3.6) SO₂ SORPTION CAPACITY OF LIMESTONE

Montes, et al. (2012) defines the sorption capacity of limestone sorbent as the mass of SO₂ removed in milligrams per gram of sorbent (X/M) and is calculated by integration of the area above the breakthrough curve, from the SO₂ concentration in the inlet gas, the flue gas flow rate and the saturation time (see Equation 2.10).

$$\frac{X}{M} = \frac{Q \times MW_{SO_2}}{W \times V_m} (C_0 t_{sat} - \int_0^{t_{sat}} (C(t) dt))$$

Flue Gas Flowrate = 6 L/min

$$= 0.0001 \text{ m}^3/\text{s}$$

SO₂ Molar Mass = 64.06 g/mol

Reactor Diameter (D_t) = 3.5cm

Limestone Bed Length (L_{bed}) = 3cm

Volume of limestone used:

$$\text{Volume of Limestone} = \frac{\pi(D_t)^2}{4} \times L_{bed} \quad (\text{B-26})$$

$$= \frac{\pi(3.5)^2}{4} \times 3$$

$$= 28.86 \text{ cm}^3$$

$$= 2.886 \times 10^{-5} \text{ m}^3$$

Limestone Bulk Density = 1441660 g/m³

Mass of limestone used:

Mass of Limestone = Limestone Density × Volume of Limestone

$$= 1441660 \times 2.886 \times 10^{-5}$$

$$= 41.61 \text{ grams}$$

$$\text{Molar Gas Volume} = 22.4 \frac{\text{cm}^3}{\text{mmol}}$$

From Table A-7, the average inlet/initial SO₂ gas concentration (C_o) is: 2207 ppmv

From Table A-9, saturation time (t_{sat}) is: 890 s

The definite integral is calculated as the summation of the SO₂ concentration at each time step, and the time difference between each time step (refer to table A-8):

$$\sum_{t=0}^{910 \text{ sec}} (C_{SO_2} \Delta t) = 0.01062 \frac{\text{mol.s}}{\text{L}}$$

Finally, the limestone sorption capacity is calculated as:

$$\begin{aligned} \frac{x}{m} &= \frac{Q \times MW_{SO_2}}{W \times V_m} (C_0 t_{sat} - \int_0^{t_{sat}} (C(t) dt)) \\ &= \frac{0.0001 \times 64.06}{41.61 \times 22.4} ((2207 \times 890) - 0.01062) \\ &= 13.498 \frac{\text{mg SO}_2}{\text{g CaCO}_3} \end{aligned}$$

B-1.4) STATISTICAL ANALYSIS

B-1.4.1) ABSOLUTE UNCERTAINTY (REFER TO TABLE A-2)

Direct measurements specified x_{observed} and y_{observed} values. Using the cubic calibration curve equation, B-2, together with the respective x_{observed} values in Table A-2, $y_{\text{predicted}}$ values were calculated. The sample calculation below is for an SO_2 gas volume (y_{observed}) of 0.002 ml (similar calculations apply to the range of tabulated y_{observed} data):

$$\begin{aligned}y_{\text{predicted}} &= (-3 \times 10^{-23})x_{\text{observed}}^3 + (2 \times 10^{-16})x_{\text{observed}}^2 + (4 \times 10^{-10})x_{\text{observed}} + (-3 \times 10^{-6}) \\&= (-3 \times 10^{-23})(2873222,40)^3 + (2 \times 10^{-16})(2873222,40)^2 + (4 \times 10^{-10})(2873222,40) \\&\quad + (-3 \times 10^{-6}) \\&= 0.002086 \text{ ml}\end{aligned}$$

For the SO_2 gas volume (y_{observed}) of 0.002 ml, the absolute uncertainty was calculated from Equation 2.15 as follows (similar calculations apply to the range of tabulated y_{observed} data):

$$\begin{aligned}\text{Absolute Uncertainty} &= |y_{\text{observed}} - y_{\text{predicted}}| \\&= 0.002 - 0.002086 \\&= 8.6 \times 10^{-5} \text{ ml}\end{aligned}$$

B-1.4.2) RELATIVE UNCERTAINTY (REFER TO TABLE A-2)

Direct measurements specified x_{observed} and y_{observed} values as per Table A-2. $y_{\text{predicted}}$ values are calculated as per section B-1.4.1 above.

For the SO_2 gas volume (y_{observed}) of 0.002 ml, the relative uncertainty was calculated as Equation 2.16 (similar calculations apply to the range of tabulated y_{observed} data):

$$\begin{aligned}\text{Relative uncertainty} &= \left| \frac{\text{Absolute Uncertainty}}{\text{Observed Value}} \right| \\ &= \left| \frac{y_{\text{observed}} - y_{\text{predicted}}}{y_{\text{observed}}} \right| \\ &= \left| \frac{0.002 - 0.002086}{0.002} \right| \\ &= 0.0429\end{aligned}$$

$$\% \text{ Relative uncertainty} = 0.0429 \times 100$$

$$= 4.29 \%$$

The average relative uncertainty is then calculated as the average of the relative uncertainties, across the tabulated range of y_{observed} data, as per Equation 2.19 (Table A-3).

$$\begin{aligned}\text{Average relative uncertainty} &= \frac{\sum(\text{relative uncertainty})}{n} \\ &= \frac{(0.0557 + 0.0127 + 0.0324 + 0.0516 + 0.0429)}{5} \\ &= 0.0391\end{aligned}$$

$$\% \text{ Average relative uncertainty} = 0.0391 \times 100$$

$$= 3.91 \%$$

B-1.4.3) PROPAGATIONAL UNCERTAINTY (REFER TO TABLE A-9)

Note: The calculation procedure below is with respect to section **A-1.4.1: 700°C - Run 1**, of Appendix A. The calculation approach of ‘Propagational Uncertainty’ for data points of the remaining experimental runs of Appendix A are identical to the **700°C - Run 1** Sample Calculation below.

According to Harris (2015), Equation 2.21 is utilized to calculate the propagational uncertainty:

$$\frac{\delta F}{|F|} = \sqrt{\left(\frac{\delta a}{a}\right)^2 + \left(\frac{\delta b}{b}\right)^2 + \dots + \left(\frac{\delta c}{c}\right)^2 + \left(\frac{\delta x}{x}\right)^2 + \left(\frac{\delta y}{y}\right)^2 + \dots + \left(\frac{\delta z}{z}\right)^2}$$

The breakthrough curve was generated by calculating ratios of $\frac{C_{out}}{C_{in}}$ at each respective time step for the entire run time of the experiment. Based on calculations in section B-1.3.1.1 & B1.3.2.1 of Appendix B, C_{out} and C_{in} are determined by the calibration curve equation, B-2. Since the calibration curve has an associated absolute uncertainty, this uncertainty will propagate through to the calculation of the ratio $\frac{C_{out}}{C_{in}}$, representative of data points on the response curve. The response curve data points will thus have an associated propagational uncertainty. It should be noted that since C_{out} and C_{in} are determined by the calibration curve equation, the relative uncertainty in C_{out} and C_{in} is thus the average relative uncertainty calculated for the calibration curve. Equation 2.21 can thus be adapted to our current study in the following manner:

$$\delta \left(\frac{C_{out}}{C_{in}} \right) = \left| \frac{C_{out}}{C_{in}} \right| \times \sqrt{\left(\frac{\delta C_{in}}{C_{in}} \right)^2 + \left(\frac{\delta C_{out}}{C_{out}} \right)^2}$$

Where: $\left(\frac{\delta C_{in}}{C_{in}} \right)^2 = \left(\frac{\delta C_{out}}{C_{out}} \right)^2$ = the average relative uncertainty calculated for the calibration curve

The sample calculation below is applicable to the initial time step ($t = 0$ s) (An identical approach was adopted to determine the propagational uncertainty at all future time steps for this run):

$$\begin{aligned} \delta \left(\frac{C_{out}}{C_{in}} \right) &= \left| \frac{C_{out}}{C_{in}} \right| \times \sqrt{\left(\frac{\delta C_{in}}{C_{in}} \right)^2 + \left(\frac{\delta C_{out}}{C_{out}} \right)^2} \\ &= \left| \frac{18}{2207} \right| \times \sqrt{(0.0391)^2 + (0.0391)^2} \\ &= 0.00045 \end{aligned}$$

B-1.4.4) BREAKTHROUGH CURVE DATA AVERAGE RELATIVE UNCERTAINTY

Note: The calculation approach for the average relative uncertainty between breakthrough curve data for **800°C,900°C Run1 & Run 2** and **800°C,900°C Run1 & Run 3** is identical to the calculations performed below. All calculated data is tabulated in Chapter A1.7 of Appendix A.

The average relative uncertainty is calculated as per Equation 2.19:

$$\begin{aligned}\text{Average relative uncertainty} &= \frac{\sum(\text{relative uncertainty})}{n} \\ &= \frac{\sum \left| \frac{\text{Absolute Uncertainty}}{\text{Observed Value}} \right|}{n} \\ &= \frac{\sum \left| \frac{y_{\text{observed}} - y_{\text{predicted}}}{y_{\text{observed}}} \right|}{n}\end{aligned}$$

The above equation was modified by the author to calculate an average relative uncertainty between breakthrough curve data obtained from separate experimental runs (i.e.: run 1, run 2 & run 3), for a particular operating temperature. This is done to test for repeatability between breakthrough curve data, generated under identical experimental operating conditions. The modified equation is represented as:

$$\text{Average Relative Uncertainty} = \frac{\sum_{k=1}^{k=n} \left| \left(\frac{y_{i,k} - y_{j,k}}{y_{i,k}} \right)_{\ell} \right|}{n} \quad (\text{B-27})$$

Where: i, j = Run number

$k = \left(\frac{C_{\text{out}}}{C_{\text{in}}} \right)$ Breakthrough curve data point for run i, j at time step ℓ

n = Total number of data points obtained for run i, j through entire run time of experiment

The average relative uncertainty calculations performed below are applicable to the 700°C breakthrough curve data of runs 1, 2 & 3 whereby an average relative uncertainty calculation between 700°C Run 1 & Run 2 and 700°C Run 1 & Run 3 is performed. The calculated data is tabulated in section A1.7 of Appendix A.

Average relative uncertainty calculation between 700°C Run 1 & Run 2:

$$\begin{aligned}
 \text{Average Relative Uncertainty} &= \frac{\sum_{k=1}^n \left| \left(\frac{y_{1,k} - y_{2,k}}{y_{1,k}} \right) \right|}{n} \\
 &= \frac{\left(\left| \left(\frac{y_{1,1} - y_{2,1}}{y_{1,1}} \right) \right| + \left| \left(\frac{y_{1,2} - y_{2,2}}{y_{1,2}} \right) \right| + \dots + \left| \left(\frac{y_{1,92} - y_{2,92}}{y_{1,92}} \right) \right| \right)}{92} \\
 &= \frac{\left(\left| \frac{0.0081 - 0.0091}{0.0081} \right| + \left| \frac{0.0089 - 0.0098}{0.0089} \right| + \dots + \left| \frac{0.0093 - 0.001}{0.0093} \right| \right)}{92} \\
 &= 0.0256
 \end{aligned}$$

% Average Relative Uncertainty = Average Relative Uncertainty × 100

$$\begin{aligned}
 &= 0.0256 \times 100 \\
 &= 2.56 \%
 \end{aligned}$$

Average relative uncertainty calculation between 700°C Run 1 & Run 3:

$$\begin{aligned}
 \text{Average Relative Uncertainty} &= \frac{\sum_{k=1}^n \left| \left(\frac{y_{1,k} - y_{3,k}}{y_{3,k}} \right) \right|}{n} \\
 &= \frac{\left(\left| \left(\frac{y_{1,1} - y_{3,1}}{y_{1,1}} \right) \right| + \left| \left(\frac{y_{1,2} - y_{3,2}}{y_{1,2}} \right) \right| + \dots + \left| \left(\frac{y_{1,92} - y_{3,92}}{y_{1,92}} \right) \right| \right)}{92} \\
 &= \frac{\left(\left| \frac{0.0081 - 0.0091}{0.0081} \right| + \left| \frac{0.0089 - 0.0097}{0.0089} \right| + \dots + \left| \frac{0.0093 - 0.001}{0.0093} \right| \right)}{92}
 \end{aligned}$$

$$= 0.0246$$

% Average Relative Uncertainty = Average Relative Uncertainty $\times 100$

$$= 0.0246 \times 100$$

$$= 2.46 \%$$

APPENDIX C: MATLAB CODE – MODEL SOLUTION FOR REACTION OF SO₂ WITH LIMESTONE

C-1.1) NON-POROUS MODEL

C-1.1.1) MATLAB SCRIPT: ODE45 SOLVER

```
%%
clear all
close all
clc

%% Initial & Boundary Conditions: SO2 Concentrations and Particle Radius for ODE solver

time = linspace(0,1210,10);

Rp = 8.45e-4; % Particle Radius [m]
Cb_z0 = 0.027; % Initial Conc at z=0 [mol/m^3]
Cb_t0 = 0; % Initial Conc at t = 0 along bed length [mol/m^3]
Rc_t0 = Rp; % Initial Radius at t=0 [s]

%% Prompt User to input reactor temperature

Temp=input('Input reactor temperature\n') % Prompting the user to input the reactor temperature

if Temp==700;

    %Initial Concentrations of SO2 in bulk gas phase
```

```

C1_Initial = Cb_z0; % [mol/m^3]
C2_Initial = 0; % [mol/m^3]
C3_Initial = 0; % [mol/m^3]
C4_Initial = 0; % [mol/m^3]
C5_Initial = 0; % [mol/m^3]
C6_Initial = 0; % [mol/m^3]

% Initial Particle Radius

C7_Initial = Rp;
C8_Initial = Rp;
C9_Initial = Rp;
C10_Initial = Rp;
C11_Initial = Rp;
C12_Initial = Rp;

% Initial guess for Dz

Dz1_Initial = 8.5e-4; % [m^2/s]
Dz2_Initial = 8.5e-4; % [m^2/s]
Dz3_Initial = 8.5e-4; % [m^2/s]
Dz4_Initial = 8.5e-4; % [m^2/s]
Dz5_Initial = 8.5e-4; % [m^2/s]

IC= [C1_Initial C2_Initial C3_Initial C4_Initial C5_Initial C6_Initial C7_Initial C8_Initial C9_Initial
C10_Initial C11_Initial C12_Initial ]

% Solver for the set of the ODEs using ode45 as the base solver method
% using Runge-Kutta 4th order

[t,C] = ode45(@NONPORUS700, time,[C1_Initial C2_Initial C3_Initial C4_Initial C5_Initial C6_Initial
C7_Initial C8_Initial C9_Initial C10_Initial C11_Initial C12_Initial Dz1_Initial Dz2_Initial Dz3_Initial
Dz4_Initial Dz5_Initial ])

DimC=C(:,6)/C1_Initial

% Experimental Transient SO2 Concentrations at Z=L

```

```

C_out_exp_700 = [0.00022526 0.000244559 0.000256862 0.000286982 0.000358639 0.000390401 0.000467123
0.000506657 0.000517719 0.00056298 0.000607785 0.000667482 0.000801745 0.000938696 0.001066957 0.001435052
0.001554903 0.0017066 0.001908686 0.002021864 0.00226898 0.002427465 0.002639057 0.003067403 0.003561148
0.003616216 0.003645091 0.003673711 0.003765886 0.003822849 0.004082027 0.004261829 0.004300056 0.004585485
0.004814513 0.005226792 0.005549416 0.00566712 0.005798658 0.005907978 0.006191009 0.006520874 0.007064576
0.007103457 0.007199252 0.007842803 0.008240966 0.009274383 0.009881179 0.010653623 0.010674897 0.011748357
0.012785234 0.013702395 0.014113277 0.014553137 0.014926979 0.015536149 0.016157473 0.01616921 0.016829461
0.01699357 0.017024107 0.017986132 0.018005791 0.01842795 0.018931404 0.019037145 0.020094543 0.020517178
0.021150332 0.021466419 0.02220226 0.022540918 0.023693289 0.024351043 0.024862051 0.025191613 0.025230735
0.025280246 0.025382297 0.025719575 0.025821048 0.026225515 0.026426864 0.026627598 0.026627598 0.027325069
0.027344975 0.028014021 0.028306486 0.028403584]

% Squared Error Between Experimental and Model Results

Delta_C_700 = ((C_out_exp_700 - C(:,6))/(C_out_exp_700))^2

end

%%
if Temp==800;

%Initial Concentrations of SO2 in bulk gas phase

C1_Initial = Cb_z0; % [mol/m^3]
C2_Initial = 0; % [mol/m^3]
C3_Initial = 0; % [mol/m^3]
C4_Initial = 0; % [mol/m^3]
C5_Initial = 0; % [mol/m^3]
C6_Initial = 0; % [mol/m^3]

% Initial Particle Radius

C7_Initial = Rp;
C8_Initial = Rp;
C9_Initial = Rp;
C10_Initial = Rp;
C11_Initial = Rp;
C12_Initial = Rp;

```

```

% Initial guess for Dz

Dz1_Initial = 0; % [m^2/s]
Dz2_Initial = 0; % [m^2/s]
Dz3_Initial = 0; % [m^2/s]
Dz4_Initial = 0; % [m^2/s]
Dz5_Initial = 0; % [m^2/s]

IC= [C1_Initial C2_Initial C3_Initial C4_Initial C5_Initial C6_Initial C7_Initial C8_Initial C9_Initial
C10_Initial C11_Initial C12_Initial ]

% Solver for the set of the ODEs using ode45 as the base solver method
% using Runge-Kutta 4th order

[t,C] = ode45(@NONPORUS800, time,[C1_Initial C2_Initial C3_Initial C4_Initial C5_Initial C6_Initial
C7_Initial C8_Initial C9_Initial C10_Initial C11_Initial C12_Initial Dz1_Initial Dz2_Initial Dz3_Initial
Dz4_Initial Dz5_Initial ])

DimC=C(:,6)/C1_Initial

% Experimental Transient SO2 Concentrations at Z=L

C_out_exp_800 = [0.000156768 0.00017411 0.000185159 0.000212221 0.000228441 0.000256726 0.000276456
0.000311364 0.000321133 0.000336591 0.000351415 0.000354406 0.000371741 0.000389222 0.000397441 0.00039883
0.000419033 0.000413023 0.000438444 0.000454176 0.000488353 0.000504381 0.000659923 0.000712424 0.000748907
0.0008404 0.000860807 0.000881057 0.000946424 0.000986934 0.001116847 0.00113392 0.001329552 0.001537098
0.001704957 0.001827832 0.001881371 0.001905842 0.002000906 0.002018688 0.002099526 0.002337953 0.002735742
0.002764408 0.002835155 0.00297691 0.003134222 0.003341698 0.003434854 0.003711074 0.004010414 0.004072684
0.004095299 0.004755841 0.004830732 0.005383292 0.005663341 0.006125179 0.00660311 0.006612204 0.007965599
0.008098335 0.008123079 0.008909821 0.008926043 0.009275772 0.009696291 0.009785086 0.010682025 0.011045086
0.011593859 0.011870009 0.012518545 0.012819701 0.012917766 0.013513748 0.013981935 0.014286317 0.015273091
0.015319302 0.015414676 0.01573108 0.016783854 0.017167307 0.017359089 0.017550886 0.018509529 0.019179468
0.020152496 0.020228492 0.021081732 0.021176184 0.021186569 0.021364852 0.022302945 0.022591768 0.023046139
0.02323079 0.023433337 0.0235986 0.023964313 0.024418305 0.02459887 0.02486856 0.025047558 0.025336138
0.025492152 0.025668785 0.025756836 0.025844706]

% Squared Error Between Experimental and Model Results

```

```

Delta_C_700 = ((C_out_exp_800 - C(:,6))/(C_out_exp_800))^2
end

%%
if Temp==900;

    %Initial Concentrations of SO2 in bulk gas phase

    C1_Initial = Cb_z0;    % [mol/m^3]
    C2_Initial = 0;        % [mol/m^3]
    C3_Initial = 0;        % [mol/m^3]
    C4_Initial = 0;        % [mol/m^3]
    C5_Initial = 0;        % [mol/m^3]
    C6_Initial = 0;        % [mol/m^3]

    % Initial Particle Radius

    C7_Initial = Rp;
    C8_Initial = Rp;
    C9_Initial = Rp;
    C10_Initial = Rp;
    C11_Initial = Rp;
    C12_Initial = Rp;

    % Initial guess for Dz

    Dz1_Initial = 0;    % [m^2/s]
    Dz2_Initial = 0;    % [m^2/s]
    Dz3_Initial = 0;    % [m^2/s]
    Dz4_Initial = 0;    % [m^2/s]
    Dz5_Initial = 0;    % [m^2/s]

    IC= [C1_Initial C2_Initial C3_Initial C4_Initial C5_Initial C6_Initial C7_Initial C8_Initial C9_Initial
          C10_Initial C11_Initial C12_Initial ]

    % Solver for the set of the ODEs using ode45 as the base solver method

```

```

% using Runge-Kutta 4th order

[t,C] = ode45(@NONPORUS900, time,[C1_Initial C2_Initial C3_Initial C4_Initial C5_Initial C6_Initial
C7_Initial C8_Initial C9_Initial C10_Initial C11_Initial C12_Initial Dz1_Initial Dz2_Initial Dz3_Initial
Dz4_Initial Dz5_Initial ])

DimC=C(:,6)/C1_Initial

Dz = C(:,6);

% Experimental Transient SO2 Concentrations at Z=L

C_out_exp_900 = [0.000105744    0.000116075  0.000126087  0.000150611  0.000165311  0.000190946  0.000208829
0.000240472  0.000249327  0.00026334   0.00027678  0.000279491  0.000295207  0.000311056  0.000318508  0.000319767
0.000332636  0.000338086  0.000355686  0.000369952  0.000378204  0.000388127  0.000399353  0.000464055  0.000542936
0.000600934  0.000647608  0.000670492  0.000709691  0.000759431  0.000783587  0.000902808  0.000959293  0.001031577
0.001227744  0.00130526   0.001443484  0.001459779  0.001479138  0.001494754  0.001506236  0.001528581  0.001696968
0.001721135  0.00172531   0.001732876  0.00175194   0.001866427  0.001884451  0.001886378  0.001896714  0.001900522
0.001906969  0.001935242  0.001963599  0.00215073   0.002540586  0.002567991  0.002600857  0.002662137  0.003044081
0.003142214  0.003160547  0.003618584  0.003762069  0.004027895  0.00435045   0.004418958  0.004418958  0.004695641
0.005118418  0.005333186  0.005695964  0.006081733  0.006159883  0.006638181  0.007017872  0.007266549  0.007374043
0.007568115  0.008200682  0.008466028  0.008546452  0.009688791  0.009854312  0.01002037  0.01002037  0.010605592
0.010875164  0.011536618  0.012307207  0.012393254  0.012834135  0.013431387  0.014302779  0.014573752  0.014801255
0.015177886  0.01624783   0.016756472  0.016931766  0.017544599  0.01824302   0.018591162  0.019198242  0.019650553
0.019973819  0.020657525  0.021081672  0.021838133  0.021838133  0.022270651  0.022748749  0.02291249   0.022994136
0.023319186  0.023383894  0.023400055  0.023500108  0.023561308  0.023681816  0.023709239]

% Squared Error Between Experimental and Model Results

Delta_C_900 = ((C_out_exp_900 - C(:,6))/(C_out_exp_900))^2

end

```

C-1.1.2) 700°C FUNCTION [DC_B/D_T]: TEMPORAL ODE'S TO BE SOLVED

```
%%
% Creating a function that contains ODE's to be solved

%%
function dCb_dt=NONPORUS700(t,C)

dCb_dt      = zeros(17,1);

%Constants

Vz          = 0.104;           % Superficial Velocity [m/s]
Eb          = 0.28;            % Bed Porosity [Dimensionless]
Dz          = 0.17e-4;          % Diffusion Coefficient [m^2/s]
Rp          = 181.38e-6;        % Particle/Grain Radius [m]
Ds          = 1.163e-6;          % Diffusion Coefficient [m^2/s]
Km          = 0.313;            % Average Mass Tranfer Coefficeint [m/s]
De          = 3.708e-7;          % Effective Diffusivity [m^2/s]
deltaZ     = 0.006;            % Distance Between Nodes [m]
rhoB        = 2711;             % Solid Sorbent Density [kg/m^3]
Rc0         = C(7);
Rc1         = C(8);
Rc2         = C(9);
Rc3         = C(10);
Rc4         = C(11);
Rc5         = C(12);

%% Initial & Boundary Conditions: SO2 Concentrations and Particle Radius for ODE solver

Rp = 8.45e-4;    % Particle Radius [m]
Cb_z0 = 0.027;   % Initial Conc at z=0 [mol/m^3]
Cb_t0 = 0;        % Initial Conc at t = 0 along bed length [mol/m^3]
Rc_t0 = Rp;       % Initial Radius at t=0 [m]
```

```

%% Calculations of Reaction Rate Constant (Kr)

T = linspace(973.15,973.15,1000);
t = linspace(0,1210,10);
Beta_0 = 2.76e-1; %[s^-1]
alpha_b = -6938.82; %[K^-1]
Beta = Beta_0*exp(alpha_b/T); %[s^-1]
Ko = 7.08e4; %[s^-1]
alpha_K = -2889.27; %[K^-1]
K = Ko*exp(alpha_K/T); %[s^-1]

Kr= Ko*exp(-Beta*t');

%% Calculation of Constants

A_700_0 = Ds/(Rp^2*Km) + Ds/((Rc0).^2*Kr)-1/Rp +1/Rc0;
A_700_1 = Ds/(Rp^2*Km) + Ds/((Rc1).^2*Kr)-1/Rp +1/Rc1;
A_700_2 = Ds/(Rp^2*Km) + Ds/((Rc2).^2*Kr)-1/Rp +1/Rc2;
A_700_3 = Ds/(Rp^2*Km) + Ds/((Rc3).^2*Kr)-1/Rp +1/Rc3;
A_700_4 = Ds/(Rp^2*Km) + Ds/((Rc4).^2*Kr)-1/Rp +1/Rc4;
A_700_5 = Ds/(Rp^2*Km) + Ds/((Rc5).^2*Kr)-1/Rp +1/Rc5;

B_700_0 = 1/Rc0 + Ds/((Rc0).^2*Kr);
B_700_1 = 1/Rc1 + Ds/((Rc1).^2*Kr);
B_700_2 = 1/Rc2 + Ds/((Rc2).^2*Kr);
B_700_3 = 1/Rc3 + Ds/((Rc3).^2*Kr);
B_700_4 = 1/Rc4 + Ds/((Rc4).^2*Kr);
B_700_5 = 1/Rc5 + Ds/((Rc5).^2*Kr);

%% Temporal ODE's across reactor length for governing equation 3.13: Solves SO2 concentration in bulk phase

dCb_dt(1) = 0

dCb_dt(2) = 5*(-Vz/Eb)*((C(2)-C(1))/deltaZ)+ dCb_dt(13)*((C(3)-2*C(2)+C(1))/((deltaZ)^2))-(3*(1-Eb)*(Km*C(2))/(Rp*Eb))*(1+(1/(A_700_1*Rp)))-(B_700_1)/(A_700_1))

dCb_dt(3) = 5*(-Vz/Eb)*((C(3)-C(2))/deltaZ)+ dCb_dt(14)*((C(4)-2*C(3)+C(2))/((deltaZ)^2))-(3*(1-Eb)*(Km*C(3))/(Rp*Eb))*(1+(1/(A_700_2*Rp)))-(B_700_2)/(A_700_2))

```

```

dCb_dt(4) = 5*(-Vz/Eb)*((C(4)-C(3))/deltaZ)+ dCb_dt(15)*((C(5)-2*C(4)+C(3))/((deltaZ)^2))-(3*(1-
Eb)*(Km*C(4))/(Rp*Eb))*(1+(1/(A_700_3*Rp)))-(B_700_3)/(A_700_3))

dCb_dt(5) = 5*(-Vz/Eb)*((C(5)-C(4))/deltaZ)+ dCb_dt(16)*((C(6)-2*C(5)+C(4))/((deltaZ)^2))-(3*(1-
Eb)*(Km*C(5))/(Rp*Eb))*(1+(1/(A_700_4*Rp)))-(B_700_4)/(A_700_4))

dCb_dt(6) = 5*(-Vz/Eb)*((C(6)-C(5))/deltaZ)+ dCb_dt(17)*((2*C(5)-2*C(6))/((deltaZ)^2))-(3*(1-
Eb)*(Km*C(6))/(Rp*Eb))*(1+(1/(A_700_5*Rp)))-(B_700_5)/(A_700_5))

%% Temporal ODE's across reactor length for governing equation 3.15: Solves particle radius changing with
time 't'

dCb_dt(7) = ((-Kr*C(1))/rhoB)*((B_700_0/A_700_0)- 1/(A_700_0*C(7)))

dCb_dt(8) = ((-Kr*C(2))/rhoB)*((B_700_1/A_700_1)- 1/(A_700_1*C(8)))

dCb_dt(9) = ((-Kr*C(3))/rhoB)*((B_700_2/A_700_2)- 1/(A_700_2*C(9)))

dCb_dt(10) = ((-Kr*C(4))/rhoB)*((B_700_3/A_700_3)- 1/(A_700_3*C(10)))

dCb_dt(11)= ((-Kr*C(5))/rhoB)*((B_700_4/A_700_4)- 1/(A_700_4*C(11)))

dCb_dt(12) = ((-Kr*C(6))/rhoB)*((B_700_5/A_700_5)- 1/(A_700_5*C(12)))

%% Evalution of Dz at time 't' along reactor length 'z'

dCb_dt(13)= (dCb_dt(2) + ((-Vz/Eb)*((C(2)-C(1))/deltaZ))+ (3*(1-Eb)*(Km*C(2))/(Rp*Eb))*(1+(1/(A_700_1*Rp))-
(B_700_1)/(A_700_1)))/((C(3)-2*C(2)+C(1))/((deltaZ)^2))

dCb_dt(14)= (dCb_dt(3) + ((-Vz/Eb)*((C(3)-C(2))/deltaZ))+ (3*(1-Eb)*(Km*C(3))/(Rp*Eb))*(1+(1/(A_700_1*Rp))-
(B_700_1)/(A_700_1)))/((C(4)-2*C(3)+C(2))/((deltaZ)^2))

dCb_dt(15)= (dCb_dt(4) + ((-Vz/Eb)*((C(4)-C(3))/deltaZ))+ (3*(1-Eb)*(Km*C(2))/(Rp*Eb))*(1+(1/(A_700_1*Rp))-
(B_700_1)/(A_700_1)))/((C(5)-2*C(4)+C(3))/((deltaZ)^2))

dCb_dt(16)= (dCb_dt(5) + ((-Vz/Eb)*((C(5)-C(4))/deltaZ))+ (3*(1-Eb)*(Km*C(2))/(Rp*Eb))*(1+(1/(A_700_1*Rp))-
(B_700_1)/(A_700_1)))/((C(6)-2*C(5)+C(4))/((deltaZ)^2))

```

```
dCb_dt(17)= (dCb_dt(6) + ((-Vz/Eb)*(C(6)-C(5))/deltaZ)) + (3*(1-Eb)*(Km*C(2))/(Rp*Eb))*(1+(1/(A_700_1*Rp))-  
(B_700_1)/(A_700_1)))/((2*C(5)-2*C(6))/((deltaZ)^2))
```

```
end
```

C-1.1.3) 800°C FUNCTION [DC_B/D_T]: TEMPORAL ODE'S TO BE SOLVED

```
%%
% Creating a function that contains ODE's to be solved

%%
function dCb_dt=NONPORUS800(t,C)

dCb_dt      = zeros(17,1);

%Constants

Vz          = 0.104;           % Superficial Velocity [m/s]
Eb          = 0.28;            % Bed Porosity [Dimensionless]
Dz          = 0.17e-4;          % Diffusion Coefficient [m^2/s]
Rp          = 181.38e-6;        % Particle/Grain Radius [m]
Ds          = 4.875e-6;         % Diffusion Coefficient [m^2/s]
Km          = 0.336;            % Average Mass Tranfer Coefficeint [m/s]
De          = 3.935e-7;          % Effective Diffusivity [m^2/s]
deltaZ     = 0.006;            % Distance Between Nodes [m]
rhoB        = 2711;             % Solid Sorbent Density [kg/m^3]
Rc0         = C(7);            %
Rc1         = C(8);            %
Rc2         = C(9);            %
Rc3         = C(10);           %
Rc4         = C(11);           %
Rc5         = C(12);           %

%% Initial & Boundary Conditions: SO2 Concentrations and Particle Radius for ODE solver

Rp = 8.45e-4;    % Particle Radius [m]
Cb_z0 = 0.027;   % Initial Conc at z=0 [mol/m^3]
Cb_t0 = 0;        % Initial Conc at t = 0 along bed length [mol/m^3]
Rc_t0 = Rp;       % Initial Radius at t=0 [s]
```

```

%% Calculations of Reaction Rate Constant (Kr)

T = linspace(1073.15,1073.15,1000);
t = linspace(0,1210,10);
Beta_0 = 2.76e-1; % [s^-1]
alpha_b = -6938.82; % [K^-1]
Beta = Beta_0*exp(alpha_b/T); % [s^-1]
Ko = 7.08e4; % [s^-1]
alpha_K = -2889.27; % [K^-1]
K = Ko*exp(alpha_K/T); % [s^-1]

Kr= Ko*exp(-Beta*t');

%% Calculation of Constants

A_800_0 = Ds/(Rp^2*Km) + Ds/((Rc0).^2*Kr)-1/Rp +1/Rc0;
A_800_1 = Ds/(Rp^2*Km) + Ds/((Rc1).^2*Kr)-1/Rp +1/Rc1;
A_800_2 = Ds/(Rp^2*Km) + Ds/((Rc2).^2*Kr)-1/Rp +1/Rc2;
A_800_3 = Ds/(Rp^2*Km) + Ds/((Rc3).^2*Kr)-1/Rp +1/Rc3;
A_800_4 = Ds/(Rp^2*Km) + Ds/((Rc4).^2*Kr)-1/Rp +1/Rc4;
A_800_5 = Ds/(Rp^2*Km) + Ds/((Rc5).^2*Kr)-1/Rp +1/Rc5;

B_800_0 = 1/Rc0 + Ds/((Rc0).^2*Kr);
B_800_1 = 1/Rc1 + Ds/((Rc1).^2*Kr);
B_800_2 = 1/Rc2 + Ds/((Rc2).^2*Kr);
B_800_3 = 1/Rc3 + Ds/((Rc3).^2*Kr);
B_800_4 = 1/Rc4 + Ds/((Rc4).^2*Kr);
B_800_5 = 1/Rc5 + Ds/((Rc5).^2*Kr);

%% Temporal ODE's across reactor length for governing equation 3.13: Solves SO2 concentration in bulk phase

dCb_dt(1) = 0

dCb_dt(2) = (-Vz/Eb)*((C(2)-C(1))/deltaZ)+ dCb_dt(13)*((C(3)-2*C(2)+C(1))/((deltaZ)^2))-(3*(1-Eb)*(Km*C(2))/(Rp*Eb))*(1+(1/(A_800_1*Rp)))-(B_800_1)/(A_800_1))

dCb_dt(3) = (-Vz/Eb)*((C(3)-C(2))/deltaZ)+ dCb_dt(14)*((C(4)-2*C(3)+C(2))/((deltaZ)^2))-(3*(1-Eb)*(Km*C(3))/(Rp*Eb))*(1+(1/(A_800_2*Rp)))-(B_800_2)/(A_800_2))

```

```

dCb_dt(4) = (-Vz/Eb) * ((C(4)-C(3))/deltaZ) + dCb_dt(15) * ((C(5)-2*C(4)+C(3)) / ((deltaZ)^2)) - (3*(1-Eb) * (Km*C(4)) / (Rp*Eb)) * (1+(1/(A_800_3*Rp)) - (B_800_3)/(A_800_3))

dCb_dt(5) = (-Vz/Eb) * ((C(5)-C(4))/deltaZ) + dCb_dt(16) * ((C(6)-2*C(5)+C(4)) / ((deltaZ)^2)) - (3*(1-Eb) * (Km*C(5)) / (Rp*Eb)) * (1+(1/(A_800_4*Rp)) - (B_800_4)/(A_800_4))

dCb_dt(6) = (-Vz/Eb) * ((C(6)-C(5))/deltaZ) + dCb_dt(17) * ((2*C(5)-2*C(6)) / ((deltaZ)^2)) - (3*(1-Eb) * (Km*C(6)) / (Rp*Eb)) * (1+(1/(A_800_5*Rp)) - (B_800_5)/(A_800_5))

%% Temporal ODE's across reactor length for governing equation 3.15 : Solves particle radius changing with time 't'

dCb_dt(7) = ((-Kr*C(1))/rhoB) * ((B_800_0/A_800_0) - 1/(A_800_0*C(7)))

dCb_dt(8) = ((-Kr*C(2))/rhoB) * ((B_800_1/A_800_1) - 1/(A_800_1*C(8)))

dCb_dt(9) = ((-Kr*C(3))/rhoB) * ((B_800_2/A_800_2) - 1/(A_800_2*C(9)))

dCb_dt(10) = ((-Kr*C(4))/rhoB) * ((B_800_3/A_800_3) - 1/(A_800_3*C(10)))

dCb_dt(11)= ((-Kr*C(5))/rhoB) * ((B_800_4/A_800_4) - 1/(A_800_4*C(11)))

dCb_dt(12) = ((-Kr*C(6))/rhoB) * ((B_800_5/A_800_5) - 1/(A_800_5*C(12)))

%% Evalution of Dz at time 't' along reactor length 'z'

dCb_dt(13)= (dCb_dt(2) + ((-Vz/Eb) * ((C(2)-C(1))/deltaZ)) + (3*(1-Eb) * (Km*C(2)) / (Rp*Eb)) * (1+(1/(A_800_1*Rp)) - (B_800_1)/(A_800_1))) / ((C(3)-2*C(2)+C(1)) / ((deltaZ)^2))

dCb_dt(14)= (dCb_dt(3) + ((-Vz/Eb) * ((C(3)-C(2))/deltaZ)) + (3*(1-Eb) * (Km*C(3)) / (Rp*Eb)) * (1+(1/(A_800_1*Rp)) - (B_800_1)/(A_800_1))) / ((C(4)-2*C(3)+C(2)) / ((deltaZ)^2))

dCb_dt(15)= (dCb_dt(4) + ((-Vz/Eb) * ((C(4)-C(3))/deltaZ)) + (3*(1-Eb) * (Km*C(2)) / (Rp*Eb)) * (1+(1/(A_800_1*Rp)) - (B_800_1)/(A_800_1))) / ((C(5)-2*C(4)+C(3)) / ((deltaZ)^2))

dCb_dt(16)= (dCb_dt(5) + ((-Vz/Eb) * ((C(5)-C(4))/deltaZ)) + (3*(1-Eb) * (Km*C(2)) / (Rp*Eb)) * (1+(1/(A_800_1*Rp)) - (B_800_1)/(A_800_1))) / ((C(6)-2*C(5)+C(4)) / ((deltaZ)^2))

```

```
dCb_dt(17)= (dCb_dt(6) + ((-Vz/Eb)*(C(6)-C(5))/deltaZ)) + (3*(1-Eb)*(Km*C(2))/(Rp*Eb))*(1+(1/(A_800_1*Rp))-  
(B_800_1)/(A_800_1)))/((2*C(5)-2*C(6))/((deltaZ)^2))
```

```
end
```

C-1.1.4) 900°C FUNCTION [DC_B/D_T]: TEMPORAL ODE'S TO BE SOLVED

```
%%
% Creating a function that contains ODE's to be solved

%%
function dCb_dt=NONPORUS900(t,C)

dCb_dt = zeros(17,1);

%Constants

Vz = 0.104; % Superficial Velocity [m/s]
Eb = 0.28; % Bed Porosity [Dimensionless]
Dz = 0.17e-4; % Diffusion Coefficient [m^2/s]
Rp = 181.38e-6; % Particle/Grain Radius [m]
Ds = 1.5e-7; % Diffusion Coefficient [m^2/s]
Km = 0.367; % Average Mass Tranfer Coefficeint [m/s]
De = 4.151e-7; % Effective Diffusivity [m^2/s]
deltaZ = 0.006; % Distance Between Nodes [m]
rhoB = 2711; % Solid Sorbent Density [kg/m^3]
Rc0 = C(7);
Rc1 = C(8);
Rc2 = C(9);
Rc3 = C(10);
Rc4 = C(11);
Rc5 = C(12);

%% Initial & Boundary Conditions: SO2 Concentrations and Particle Radius for ODE solver

Rp = 8.45e-4; % Particle Radius [m]
Cb_z0 = 0.027; % Initial Conc at z=0 [mol/m^3]
Cb_t0 = 0; % Initial Conc at t = 0 along bed length [mol/m^3]
Rc_t0 = Rp; % Initial Radius at t=0 [s]
```

```

%% Calculations of Reaction Rate Constant (Kr)
T = linspace(1173.15,1173.15,1000);
t = linspace(0,1210,10);
Beta_0 = 2.76e-1; % [s^-1]
alpha_b = -6938.82; % [K^-1]
Beta = Beta_0*exp(alpha_b/T); % [s^-1]
Ko = 7.08e4; % [s^-1]
alpha_K = -2889.27; % [K^-1]
K = Ko*exp(alpha_K/T); % [s^-1]

Kr= Ko*exp(-Beta*t');

%% Calculation of Constants

A_900_0 = Ds/(Rp^2*Km) + Ds/((Rc0).^2*Kr)-1/Rp +1/Rc0;
A_900_1 = Ds/(Rp^2*Km) + Ds/((Rc1).^2*Kr)-1/Rp +1/Rc1;
A_900_2 = Ds/(Rp^2*Km) + Ds/((Rc2).^2*Kr)-1/Rp +1/Rc2;
A_900_3 = Ds/(Rp^2*Km) + Ds/((Rc3).^2*Kr)-1/Rp +1/Rc3;
A_900_4 = Ds/(Rp^2*Km) + Ds/((Rc4).^2*Kr)-1/Rp +1/Rc4;
A_900_5 = Ds/(Rp^2*Km) + Ds/((Rc5).^2*Kr)-1/Rp +1/Rc5;

B_900_0 = 1/Rc0 + Ds/((Rc0).^2*Kr);
B_900_1 = 1/Rc1 + Ds/((Rc1).^2*Kr);
B_900_2 = 1/Rc2 + Ds/((Rc2).^2*Kr);
B_900_3 = 1/Rc3 + Ds/((Rc3).^2*Kr);
B_900_4 = 1/Rc4 + Ds/((Rc4).^2*Kr);
B_900_5 = 1/Rc5 + Ds/((Rc5).^2*Kr);

%% Temporal ODE's across reactor length for governing equation 3.13: Solves SO2 concentration in bulk phase

dCb_dt(1) = 0

dCb_dt(2) = (-Vz/Eb)*((C(2)-C(1))/deltaZ)+ dCb_dt(13)*((C(3)-2*C(2)+C(1))/((deltaZ)^2))-(3*(1-Eb)*(Km*C(2))/(Rp*Eb))*(1+(1/(A_900_1*Rp)))-(B_900_1)/(A_900_1))

dCb_dt(3) = (-Vz/Eb)*((C(3)-C(2))/deltaZ)+ dCb_dt(14)*((C(4)-2*C(3)+C(2))/((deltaZ)^2))-(3*(1-Eb)*(Km*C(3))/(Rp*Eb))*(1+(1/(A_900_2*Rp)))-(B_900_2)/(A_900_2))

```

```

dCb_dt(4) = (-Vz/Eb) * ((C(4)-C(3))/deltaZ) + dCb_dt(15) * ((C(5)-2*C(4)+C(3)) / ((deltaZ)^2)) - (3*(1-
Eb)*(Km*C(4)) / (Rp*Eb)) * (1+(1/(A_900_3*Rp))-(B_900_3)/(A_900_3))

dCb_dt(5) = (-Vz/Eb) * ((C(5)-C(4))/deltaZ) + dCb_dt(16) * ((C(6)-2*C(5)+C(4)) / ((deltaZ)^2)) - (3*(1-
Eb)*(Km*C(5)) / (Rp*Eb)) * (1+(1/(A_900_4*Rp))-(B_900_4)/(A_900_4))

dCb_dt(6) = (-Vz/Eb) * ((C(6)-C(5))/deltaZ) + dCb_dt(17) * ((2*C(5)-2*C(6)) / ((deltaZ)^2)) - (3*(1-
Eb)*(Km*C(6)) / (Rp*Eb)) * (1+(1/(A_900_5*Rp))-(B_900_5)/(A_900_5))

%% Temporal ODE's across reactor length for governing equation 3.15: Solves particle radius changing with
time 't'

dCb_dt(7) = ((-Kr*C(1))/rhoB) * ((B_900_0/A_900_0)- 1/(A_900_0*C(7)))

dCb_dt(8) = ((-Kr*C(2))/rhoB) * ((B_900_1/A_900_1)- 1/(A_900_1*C(8)))

dCb_dt(9) = ((-Kr*C(3))/rhoB) * ((B_900_2/A_900_2)- 1/(A_900_2*C(9)))

dCb_dt(10) = ((-Kr*C(4))/rhoB) * ((B_900_3/A_900_3)- 1/(A_900_3*C(10)))

dCb_dt(11)= ((-Kr*C(5))/rhoB) * ((B_900_4/A_900_4)- 1/(A_900_4*C(11)))

dCb_dt(12) = ((-Kr*C(6))/rhoB) * ((B_900_5/A_900_5)- 1/(A_900_5*C(12)))

%% Evalution of Dz at time 't' along reactor length 'z'

dCb_dt(13)= (dCb_dt(2) + ((-Vz/Eb)*((C(2)-C(1))/deltaZ)) + (3*(1-Eb)*(Km*C(2)) / (Rp*Eb)) * (1+(1/(A_900_1*Rp))-
(B_900_1)/(A_900_1))) / ((C(3)-2*C(2)+C(1)) / ((deltaZ)^2))

dCb_dt(14)= (dCb_dt(3) + ((-Vz/Eb)*((C(3)-C(2))/deltaZ)) + (3*(1-Eb)*(Km*C(3)) / (Rp*Eb)) * (1+(1/(A_900_1*Rp))-
(B_900_1)/(A_900_1))) / ((C(4)-2*C(3)+C(2)) / ((deltaZ)^2))

dCb_dt(15)= (dCb_dt(4) + ((-Vz/Eb)*((C(4)-C(3))/deltaZ)) + (3*(1-Eb)*(Km*C(2)) / (Rp*Eb)) * (1+(1/(A_900_1*Rp))-
(B_900_1)/(A_900_1))) / ((C(5)-2*C(4)+C(3)) / ((deltaZ)^2))

dCb_dt(16)= (dCb_dt(5) + ((-Vz/Eb)*((C(5)-C(4))/deltaZ)) + (3*(1-Eb)*(Km*C(2)) / (Rp*Eb)) * (1+(1/(A_900_1*Rp))-
(B_900_1)/(A_900_1))) / ((C(6)-2*C(5)+C(4)) / ((deltaZ)^2))

```

$$dCb_dt(17) = (dCb_dt(6) + ((-Vz/Eb) * ((C(6) - C(5)) / deltaZ)) + (3 * (1 - Eb) * (Km * C(2)) / (Rp * Eb)) * (1 + (1 / (A_900_1 * Rp)) - (B_900_1) / (A_900_1))) / ((2 * C(5) - 2 * C(6)) / ((deltaZ)^2))$$

end

C-1.2) POROUS MODEL

C-1.2.1) MATLAB SCRIPT: ODE45 SOLVER

```
%%
clear all
close all
clc

%% Initial & Boundary Conditions: SO2 Concentrations and Particle Radius for ODE solver
time = linspace(0,1210,10);

Cb_z0 = 0.027; % Initial Conc at z=0 [mol/m^3]
Cb_t0 = 0;      % Initial Conc at t = 0 along bed length [mol/m^3]
Cp_t0 = 0;      % Initial Average Particle SO2 Concentration t=0 [mol/m^3]

%% Prompt User to select reactor operation temperature
Temp=input('Input reactor temperature\n') % Prompting the user to input the reactor temperature

if Temp==700;

    %Initial Concentrations of SO2 in bulk gas phase

    C1_Initial = Cb_z0; % [mol/m^3]
    C2_Initial = 0;      % [mol/m^3]
    C3_Initial = 0;      % [mol/m^3]
    C4_Initial = 0;      % [mol/m^3]
    C5_Initial = 0;      % [mol/m^3]
    C6_Initial = 0;      % [mol/m^3]

    % Initial Average Particle SO2 Concentration
```

```

C7_Initial = Cp_t0;
C8_Initial = Cp_t0;
C9_Initial = Cp_t0;
C10_Initial = Cp_t0;
C11_Initial = Cp_t0;
C12_Initial = Cp_t0;

% Initial guess for Dz

Dz1_Initial = 8.5e-4; % [m^2/s]
Dz2_Initial = 8.5e-4; % [m^2/s]
Dz3_Initial = 8.5e-4; % [m^2/s]
Dz4_Initial = 8.5e-4; % [m^2/s]
Dz5_Initial = 8.5e-4; % [m^2/s]

IC= [C1_Initial C2_Initial C3_Initial C4_Initial C5_Initial C6_Initial C7_Initial C8_Initial C9_Initial
C10_Initial C11_Initial C12_Initial ]

% Solver for the set of the ODEs using ode45 as the base solver method
% using Runge-Kutta 4th order

[t,C] = ode45(@PORUS700, time,[C1_Initial C2_Initial C3_Initial C4_Initial C5_Initial C6_Initial
C7_Initial C8_Initial C9_Initial C10_Initial C11_Initial C12_Initial Dz1_Initial Dz2_Initial Dz3_Initial
Dz4_Initial Dz5_Initial ])
DimC=C(:,6)/C1_Initial;

% Experimental Transient SO2 Concentrations at Z=L

C_out_exp_700 = [0.00022526 0.000244559 0.000256862 0.000286982 0.000358639 0.000390401 0.000467123
0.000506657 0.000517719 0.00056298 0.000607785 0.000667482 0.000801745 0.000938696 0.001066957 0.001435052
0.001554903 0.0017066 0.001908686 0.002021864 0.00226898 0.002427465 0.002639057 0.003067403 0.003561148
0.003616216 0.003645091 0.003673711 0.003765886 0.003822849 0.004082027 0.004261829 0.004300056 0.004585485
0.004814513 0.005226792 0.005549416 0.00566712 0.005798658 0.005907978 0.006191009 0.006520874 0.007064576
0.007103457 0.007199252 0.007842803 0.008240966 0.009274383 0.009881179 0.010653623 0.010674897 0.011748357
0.012785234 0.013702395 0.014113277 0.014553137 0.014926979 0.015536149 0.016157473 0.01616921 0.016829461
0.01699357 0.017024107 0.017986132 0.018005791 0.01842795 0.018931404 0.019037145 0.020094543 0.020517178
0.021150332 0.021466419 0.02220226 0.022540918 0.023693289 0.024351043 0.024862051 0.025191613 0.025230735

```

```

0.025280246 0.025382297 0.025719575 0.025821048 0.026225515 0.026426864 0.026627598 0.026627598 0.027325069
0.027344975 0.028014021 0.028306486 0.028403584]

% Squared Error Between Experimental and Model Results

Delta_C_700 = ((C_out_exp_700 - C(:,6)) / (C_out_exp_700))^2

end
%%
if Temp==800;

%Initial Concentrations of SO2 in bulk gas phase

C1_Initial = Cb_z0; % [mol/m^3]
C2_Initial = 0; % [mol/m^3]
C3_Initial = 0; % [mol/m^3]
C4_Initial = 0; % [mol/m^3]
C5_Initial = 0; % [mol/m^3]
C6_Initial = 0; % [mol/m^3]

% Initial Average Particle SO2 Concentration

C7_Initial = Cp_t0;
C8_Initial = Cp_t0;
C9_Initial = Cp_t0;
C10_Initial = Cp_t0;
C11_Initial = Cp_t0;
C12_Initial = Cp_t0;

% Initial guess for Dz

Dz1_Initial = 8.5e-4; % [m^2/s]
Dz2_Initial = 8.5e-4; % [m^2/s]
Dz3_Initial = 8.5e-4; % [m^2/s]
Dz4_Initial = 8.5e-4; % [m^2/s]
Dz5_Initial = 8.5e-4; % [m^2/s]

```

```

IC= [C1_Initial C2_Initial C3_Initial C4_Initial C5_Initial C6_Initial C7_Initial C8_Initial C9_Initial
C10_Initial C11_Initial C12_Initial ]

% Solver for the set of the ODEs using ode45 as the base solver method
% using Runge-Kutta 4th order

[t,C] = ode45(@PORUS800, time,[C1_Initial C2_Initial C3_Initial C4_Initial C5_Initial C6_Initial
C7_Initial C8_Initial C9_Initial C10_Initial C11_Initial C12_Initial Dz1_Initial Dz2_Initial Dz3_Initial
Dz4_Initial Dz5_Initial ])
DimC=C(:,6)/C1_Initial

% Experimental Transient SO2 Concentrations at Z=L

C_out_exp_800 = [0.000156768 0.00017411 0.000185159 0.000212221 0.000228441 0.000256726 0.000276456
0.000311364 0.000321133 0.000336591 0.000351415 0.000354406 0.000371741 0.000389222 0.000397441 0.00039883
0.000419033 0.000413023 0.000438444 0.000454176 0.000488353 0.000504381 0.000659923 0.000712424 0.000748907
0.0008404 0.000860807 0.000881057 0.000946424 0.000986934 0.001116847 0.00113392 0.001329552 0.001537098
0.001704957 0.001827832 0.001881371 0.001905842 0.002000906 0.002018688 0.002099526 0.002337953 0.002735742
0.002764408 0.002835155 0.00297691 0.003134222 0.003341698 0.003434854 0.003711074 0.004010414 0.004072684
0.004095299 0.004755841 0.004830732 0.005383292 0.005663341 0.006125179 0.00660311 0.006612204 0.007965599
0.008098335 0.008123079 0.008909821 0.008926043 0.009275772 0.009696291 0.009785086 0.010682025 0.011045086
0.011593859 0.011870009 0.012518545 0.012819701 0.012917766 0.013513748 0.013981935 0.014286317 0.015273091
0.015319302 0.015414676 0.01573108 0.016783854 0.017167307 0.017359089 0.017550886 0.018509529 0.019179468
0.020152496 0.020228492 0.021081732 0.021176184 0.021186569 0.021364852 0.022302945 0.022591768 0.023046139
0.02323079 0.023433337 0.0235986 0.023964313 0.024418305 0.02459887 0.02486856 0.025047558 0.025336138
0.025492152 0.025668785 0.025756836 0.025844706]

% Squared Error Between Experimental and Model Results

Delta_C_700 = ((C_out_exp_800 - C(:,6))/(C_out_exp_800))^2

end

%%
if Temp==900;

%Initial Concentrations of SO2 in bulk gas phase
C1_Initial = Cb_z0; % [mol/m^3]
C2_Initial = 0; % [mol/m^3]

```

```

C3_Initial = 0;          % [mol/m^3]
C4_Initial = 0;          % [mol/m^3]
C5_Initial = 0;          % [mol/m^3]
C6_Initial = 0;          % [mol/m^3]

% Initial Average Particle SO2 Concentration

C7_Initial = Cp_t0;
C8_Initial = Cp_t0;
C9_Initial = Cp_t0;
C10_Initial = Cp_t0;
C11_Initial = Cp_t0;
C12_Initial = Cp_t0;

% Initial guess for Dz

Dz1_Initial = 8.5e-4;   % [m^2/s]
Dz2_Initial = 8.5e-4;   % [m^2/s]
Dz3_Initial = 8.5e-4;   % [m^2/s]
Dz4_Initial = 8.5e-4;   % [m^2/s]
Dz5_Initial = 8.5e-4;   % [m^2/s]

IC= [C1_Initial C2_Initial C3_Initial C4_Initial C5_Initial C6_Initial C7_Initial C8_Initial C9_Initial
      C10_Initial C11_Initial C12_Initial ]

% Solver for the set of the ODEs using ode45 as the base solver method
% using Runge-Kutta 4th order

[t,C] = ode45(@PORUS900, time,[C1_Initial C2_Initial C3_Initial C4_Initial C5_Initial C6_Initial
      C7_Initial C8_Initial C9_Initial C10_Initial C11_Initial C12_Initial Dz1_Initial Dz2_Initial Dz3_Initial
      Dz4_Initial Dz5_Initial ])
DimC=C(:,6)/C1_Initial

% Experimental Transient SO2 Concentrations at Z=L

C_out_exp_900 = [0.000105744    0.000116075  0.000126087  0.000150611  0.000165311  0.000190946  0.000208829
0.000240472 0.000249327 0.00026334 0.00027678 0.000279491 0.000295207 0.000311056 0.000318508 0.000319767
0.000332636 0.000338086 0.000355686 0.000369952 0.000378204 0.000388127 0.000399353 0.000464055 0.000542936

```

```

0.000600934 0.000647608 0.000670492 0.000709691 0.000759431 0.000783587 0.000902808 0.000959293 0.001031577
0.001227744 0.00130526 0.001443484 0.001459779 0.001479138 0.001494754 0.001506236 0.001528581 0.001696968
0.001721135 0.00172531 0.001732876 0.00175194 0.001866427 0.001884451 0.001886378 0.001896714 0.001900522
0.001906969 0.001935242 0.001963599 0.00215073 0.002540586 0.002567991 0.002600857 0.002662137 0.003044081
0.003142214 0.003160547 0.003618584 0.003762069 0.004027895 0.00435045 0.004418958 0.004418958 0.004695641
0.005118418 0.005333186 0.005695964 0.006081733 0.006159883 0.006638181 0.007017872 0.007266549 0.007374043
0.007568115 0.008200682 0.008466028 0.008546452 0.009688791 0.009854312 0.01002037 0.01002037 0.010605592
0.010875164 0.011536618 0.012307207 0.012393254 0.012834135 0.013431387 0.014302779 0.014573752 0.014801255
0.015177886 0.01624783 0.016756472 0.016931766 0.017544599 0.01824302 0.018591162 0.019198242 0.019650553
0.019973819 0.020657525 0.021081672 0.021838133 0.021838133 0.022270651 0.022748749 0.02291249 0.022994136
0.023319186 0.023383894 0.023400055 0.023500108 0.023561308 0.023681816 0.023709239]

```

% Squared Error Between Experimental and Model Results

```
Delta_C_900 = ((C_out_exp_900 - C(:,6))/(C_out_exp_900))^2
```

```
end
```

C-1.2.2) 700°C FUNCTION [DC_B/D_T]: TEMPORAL ODE'S TO BE SOLVED

```
%%
% Creating a function that contains ODE's to be solved

%%
function dCb_dt=PORUS700(t,C)

dCb_dt      = zeros(17,1);

%Constants

Vz          = 0.104 ;           % Superficial Velocity           [m/s]
Eb          = 0.28;            % Bed Porosity                  [Dimensionless]
Dz          = 0.17e-4;          % Diffusion Coefficient         [m^2/s]
Rp          = 181.38e-6;        % Particle/Grain Radius        [m]
Km          = 0.313;            % Average Mass Tranfer Coefficeint [m/s]
a           = 5.76e7;           % External Surface Area per unit volume of particle [m^2/m^3]
alpha        = 0.2;              % Intraparticle Porosity        [Dimensionless]
deltaZ      = 0.006;            % Distance Between Nodes        [m]
Cp0         = C(7);
Cp1         = C(8);
Cp2         = C(9);
Cp3         = C(10);
Cp4         = C(11);
Cp5         = C(12);

%% Initial & Boundary Conditions: SO2 Concentrations and Particle Radius for ODE solver

Cb_z0 = 0.027; % Initial Conc at z=0 [mol/m^3]
Cb_t0 = 0;       % Initial Conc at t = 0 along bed length [mol/m^3]
Cp_t0 = 0;       % Initial Average Particle SO2 Concentration t=0 [mol/m^3]

%% Calculations of Reaction Rate Constant (Kr)

T           = linspace(973.15,973.15,1000);
t           =linspace(0,1210,1000);
```

```

Beta_0      = 2.76e-1;          %[s^-1]
alpha_b     = -6938.82;         %[K^-1]
Beta        = Beta_0*exp(alpha_b/T);    %[s^-1]
Ko          = 7.08e4;           %[s^-1]
alpha_K     = -2889.27;          %[K^-1]
K           = Ko*exp(alpha_K/T);    %[s^-1]

Kr= Ko*exp(-Beta*t');

%% Temporal ODE's across reactor length for governing equation 3.3: Solves SO2 concentration in bulk phase

dCb_dt(1) = 0;

dCb_dt(2) = (Vz/Eb)*((C(2)-C(1))/deltaZ)+ Dz*((C(3)-2*C(2)+C(1))/((deltaZ)^2))-(((1-Eb)/(Eb))*Km*a)*(C(2)-(Km*C(2)+((5*De*C(8))/Rp))/(Km+(5*De)/Rp));

dCb_dt(3) = (Vz/Eb)*((C(3)-C(2))/deltaZ)+ Dz*((C(4)-2*C(3)+C(2))/((deltaZ)^2))-(((1-Eb)/(Eb))*Km*a)*(C(3)-(Km*C(3)+((5*De*C(9))/Rp))/(Km+(5*De)/Rp));

dCb_dt(4) = (Vz/Eb)*((C(4)-C(3))/deltaZ)+ Dz*((C(5)-2*C(4)+C(3))/((deltaZ)^2))-(((1-Eb)/(Eb))*Km*a)*(C(4)-(Km*C(4)+((5*De*C(10))/Rp))/(Km+(5*De)/Rp));

dCb_dt(5) = (Vz/Eb)*((C(5)-C(4))/deltaZ)+ Dz*((C(6)-2*C(5)+C(4))/((deltaZ)^2))-(((1-Eb)/(Eb))*Km*a)*(C(5)-(Km*C(5)+((5*De*C(11))/Rp))/(Km+(5*De)/Rp));

dCb_dt(6) = (Vz/Eb)*((C(6)-C(5))/deltaZ)+ Dz*((2*C(5)-2*C(6))/((deltaZ)^2))-(((1-Eb)/(Eb))*Km*a)*(C(6)-(Km*C(6)+((5*De*C(12))/Rp))/(Km+(5*De)/Rp));

%% Temporal ODE's across reactor length for governing equation 3.18: Solves average particle SO2 concentration at position 'z'

dCb_dt(7) = (3/Rp)*Km*(C(1)-(Km*C(1)+((5*De*C(7))/Rp))/(Km+(5*De)/Rp))-((3*(1-alpha)*Kr*C(7))/(Rp*alpha));

dCb_dt(8) = (3/Rp)*Km*(C(2)-(Km*C(2)+((5*De*C(8))/Rp))/(Km+(5*De)/Rp))-((3*(1-alpha)*Kr*C(8))/(Rp*alpha));

dCb_dt(9) = (3/Rp)*Km*(C(3)-(Km*C(3)+((5*De*C(9))/Rp))/(Km+(5*De)/Rp))-((3*(1-alpha)*Kr*C(9))/(Rp*alpha));

```

```
dCb_dt(10) = (3/Rp)*Km*(C(4)-(Km*C(4)+((5*De*C(10))/Rp))/(Km+(5*De)/Rp))-((3*(1-alpha)*Kr*C(10))/(Rp*alpha));
```

```
dCb_dt(11)= (3/Rp)*Km*(C(5)-(Km*C(5)+((5*De*C(11))/Rp))/(Km+(5*De)/Rp))-((3*(1-alpha)*Kr*C(11))/(Rp*alpha));
```

```
dCb_dt(12) = (3/Rp)*Km*(C(6)-(Km*C(6)+((5*De*C(12))/Rp))/(Km+(5*De)/Rp))-((3*(1-alpha)*Kr*C(12))/(Rp*alpha));
```

```
%% Evalution of Dz at time 't' along reactor length 'z':
```

```
dCb_dt(13)= (Vz/Eb)*((C(2)-C(1))/deltaZ)+(((1-Eb)/(Eb))*Km*a)*(C(2)-(Km*C(2)+((5*De*C(8))/Rp))/(Km+(5*De)/Rp))/((C(3)-2*C(2)+C(1))/((deltaZ)^2));
```

```
dCb_dt(14)= (Vz/Eb)*((C(3)-C(2))/deltaZ)+(((1-Eb)/(Eb))*Km*a)*(C(3)-(Km*C(3)+((5*De*C(9))/Rp))/(Km+(5*De)/Rp))/((C(4)-2*C(3)+C(2))/((deltaZ)^2));
```

```
dCb_dt(15)= (Vz/Eb)*((C(4)-C(3))/deltaZ)+(((1-Eb)/(Eb))*Km*a)*(C(4)-(Km*C(4)+((5*De*C(10))/Rp))/(Km+(5*De)/Rp))/((C(5)-2*C(4)+C(3))/((deltaZ)^2));
```

```
dCb_dt(16)= (Vz/Eb)*((C(5)-C(4))/deltaZ)+(((1-Eb)/(Eb))*Km*a)*(C(5)-(Km*C(5)+((5*De*C(11))/Rp))/(Km+(5*De)/Rp))/((C(6)-2*C(5)+C(4))/((deltaZ)^2));
```

```
dCb_dt(17)= (Vz/Eb)*((C(6)-C(5))/deltaZ)+(((1-Eb)/(Eb))*Km*a)*(C(6)-(Km*C(6)+((5*De*C(12))/Rp))/(Km+(5*De)/Rp))/((2*C(5)-2*C(6))/((deltaZ)^2));
```

```
end
```

C-1.2.3) 800°C FUNCTION [DC_B/D_T]: TEMPORAL ODE'S TO BE SOLVED

```
%%
% Creating a function that contains ODE's to be solved

%%
function dCb_dt=PORUS800(t,C)

dCb_dt      = zeros(17,1);

%Constants

Vz          = 0.104 ;           % Superficial Velocity          [m/s]
Eb          = 0.28;            % Bed Porosity                  [Dimensionless]
Dz          = 0.17e-4;          % Diffusion Coefficient         [m^2/s]
Rp          = 181.38e-6;        % Particle/Grain Radius        [m]
Km          = 0.336;            % Average Mass Tranfer Coefficeint [m/s]
a           = 5.76e7;           % External Surface Area per unit volume of particle [m^2/m^3]
alpha        = 0.2;              % Intraparticle Porosity        [Dimensionless]
deltaZ      = 0.006;            % Distance Between Nodes        [m]
Cp0         = C(7);
Cp1         = C(8);
Cp2         = C(9);
Cp3         = C(10);
Cp4         = C(11);
Cp5         = C(12);

%% Initial & Boundary Conditions: SO2 Concentrations and Particle Radius for ODE solver

Cb_z0 = 0.027; % Initial Conc at z=0 [mol/m^3]
Cb_t0 = 0;       % Initial Conc at t = 0 along bed length [mol/m^3]
Cp_t0 = 0;       % Initial Average Particle SO2 Concentration t=0 [mol/m^3]

%% Calculations of Reaction Rate Constant (Kr)

T           = linspace(1073.15,1073.15,1000);
t           =linspace(0,1210,10);
```

```

Beta_0      = 2.76e-1;          %[s^-1]
alpha_b     = -6938.82;         %[K^-1]
Beta        = Beta_0*exp(alpha_b/T); %[s^-1]
Ko          = 7.08e4;           %[s^-1]
alpha_K     = -2889.27;          %[K^-1]
K           = Ko*exp(alpha_K/T); %[s^-1]

Kr= Ko*exp(-Beta*t');

%% Temporal ODE's across reactor length for governing equation 3.3 : Solves SO2 concentration in bulk phase

dCb_dt(1) = 0;

dCb_dt(2) = (Vz/Eb)*((C(2)-C(1))/deltaZ)+ Dz*((C(3)-2*C(2)+C(1))/((deltaZ)^2))-(((1-Eb)/(Eb))*Km*a)*(C(2)-(Km*C(2)+((5*De*C(8))/Rp))/(Km+(5*De)/Rp));

dCb_dt(3) = (Vz/Eb)*((C(3)-C(2))/deltaZ)+ Dz*((C(4)-2*C(3)+C(2))/((deltaZ)^2))-(((1-Eb)/(Eb))*Km*a)*(C(3)-(Km*C(3)+((5*De*C(9))/Rp))/(Km+(5*De)/Rp));

dCb_dt(4) = (Vz/Eb)*((C(4)-C(3))/deltaZ)+ Dz*((C(5)-2*C(4)+C(3))/((deltaZ)^2))-(((1-Eb)/(Eb))*Km*a)*(C(4)-(Km*C(4)+((5*De*C(10))/Rp))/(Km+(5*De)/Rp));

dCb_dt(5) = (Vz/Eb)*((C(5)-C(4))/deltaZ)+ Dz*((C(6)-2*C(5)+C(4))/((deltaZ)^2))-(((1-Eb)/(Eb))*Km*a)*(C(5)-(Km*C(5)+((5*De*C(11))/Rp))/(Km+(5*De)/Rp));

dCb_dt(6) = (Vz/Eb)*((C(6)-C(5))/deltaZ)+ Dz*((2*C(5)-2*C(6))/((deltaZ)^2))-(((1-Eb)/(Eb))*Km*a)*(C(6)-(Km*C(6)+((5*De*C(12))/Rp))/(Km+(5*De)/Rp));

%% Temporal ODE's across reactor length for governing equation 3.18: Solves average particle SO2 concentration at position 'z'

dCb_dt(7) = (3/Rp)*Km*(C(1)-(Km*C(1)+((5*De*C(7))/Rp))/(Km+(5*De)/Rp))-((3*(1-alpha)*Kr*C(7))/(Rp*alpha));

dCb_dt(8) = (3/Rp)*Km*(C(2)-(Km*C(2)+((5*De*C(8))/Rp))/(Km+(5*De)/Rp))-((3*(1-alpha)*Kr*C(8))/(Rp*alpha));

dCb_dt(9) = (3/Rp)*Km*(C(3)-(Km*C(3)+((5*De*C(9))/Rp))/(Km+(5*De)/Rp))-((3*(1-alpha)*Kr*C(9))/(Rp*alpha));

```

```

dCb_dt(10) = (3/Rp)*Km*(C(4)-(Km*C(4)+((5*De*C(10))/Rp))/(Km+(5*De)/Rp))-((3*(1-alpha)*Kr*C(10))/(Rp*alpha));

dCb_dt(11)= (3/Rp)*Km*(C(5)-(Km*C(5)+((5*De*C(11))/Rp))/(Km+(5*De)/Rp))-((3*(1-alpha)*Kr*C(11))/(Rp*alpha));

dCb_dt(12) = (3/Rp)*Km*(C(6)-(Km*C(6)+((5*De*C(12))/Rp))/(Km+(5*De)/Rp))-((3*(1-alpha)*Kr*C(12))/(Rp*alpha));

%% Evalution of Dz at time 't' along reactor length 'z':

dCb_dt(13)= (Vz/Eb)*((C(2)-C(1))/deltaZ)+(((1-Eb)/(Eb))*Km*a)*(C(2)-(Km*C(2)+((5*De*C(8))/Rp))/(Km+(5*De)/Rp))/((C(3)-2*C(2)+C(1))/((deltaZ)^2));

dCb_dt(14)= (Vz/Eb)*((C(3)-C(2))/deltaZ)+(((1-Eb)/(Eb))*Km*a)*(C(3)-(Km*C(3)+((5*De*C(9))/Rp))/(Km+(5*De)/Rp))/((C(4)-2*C(3)+C(2))/((deltaZ)^2));

dCb_dt(15)= (Vz/Eb)*((C(4)-C(3))/deltaZ)+(((1-Eb)/(Eb))*Km*a)*(C(4)-(Km*C(4)+((5*De*C(10))/Rp))/(Km+(5*De)/Rp))/((C(5)-2*C(4)+C(3))/((deltaZ)^2));

dCb_dt(16)= (Vz/Eb)*((C(5)-C(4))/deltaZ)+(((1-Eb)/(Eb))*Km*a)*(C(5)-(Km*C(5)+((5*De*C(11))/Rp))/(Km+(5*De)/Rp))/((C(6)-2*C(5)+C(4))/((deltaZ)^2));

dCb_dt(17)= (Vz/Eb)*((C(6)-C(5))/deltaZ)+(((1-Eb)/(Eb))*Km*a)*(C(6)-(Km*C(6)+((5*De*C(12))/Rp))/(Km+(5*De)/Rp))/((2*C(5)-2*C(6))/((deltaZ)^2));

```

end

C-1.2.4) 900°C FUNCTION [DC_B/D_T]: TEMPORAL ODE'S TO BE SOLVED

```
%%
% Creating a function that contains ODE's to be solved

%%
function dCb_dt=PORUS900(t,C)

dCb_dt      = zeros(17,1);

%Constants

Vz          = 0.104 ;           % Superficial Velocity           [m/s]
Eb          = 0.28;            % Bed Porosity                  [Dimensionless]
Dz          = 0.17e-4;          % Diffusion Coefficient         [m^2/s]
Rp          = 181.38e-6;        % Particle/Grain Radius        [m]
Km          = 0.367;            % Average Mass Tranfer Coefficeint [m/s]
a           = 5.76e7;           % External Surface Area per unit volume of particle [m^2/m^3]
alpha        = 0.2;              % Intraparticle Porosity        [Dimensionless]
deltaZ      = 0.006;            % Distance Between Nodes        [m]
Cp0         = C(7);
Cp1         = C(8);
Cp2         = C(9);
Cp3         = C(10);
Cp4         = C(11);
Cp5         = C(12);

%% Initial & Boundary Conditions: SO2 Concentrations and Particle Radius for ODE solver

Cb_z0 = 0.027; % Initial Conc at z=0 [mol/m^3]
Cb_t0 = 0;       % Initial Conc at t = 0 along bed length [mol/m^3]
Cp_t0 = 0;       % Initial Average Particle SO2 Concentration t=0 [mol/m^3]

%% Calculations of Reaction Rate Constant (Kr)

T           = linspace(1173.15,1173.15,1000);
t           = linspace(0,1210,10);
```

```

Beta_0      = 2.76e-1;          %[s^-1]
alpha_b     = -6938.82;         %[K^-1]
Beta        = Beta_0*exp(alpha_b/T);    %[s^-1]
Ko          = 7.08e4;           %[s^-1]
alpha_K     = -2889.27;          %[K^-1]
K           = Ko*exp(alpha_K/T);    %[s^-1]

Kr= Ko*exp(-Beta*t');

%% Temporal ODE's across reactor length for governing equation 3.3: Solves SO2 concentration in bulk phase

dCb_dt(1) = 0;

dCb_dt(2) = (Vz/Eb)*((C(2)-C(1))/deltaZ)+ Dz*((C(3)-2*C(2)+C(1)) / ((deltaZ)^2))-(((1-Eb)/(Eb))*Km*a)*(C(2)-(Km*C(2)+((5*De*C(8))/Rp))/(Km+(5*De)/Rp));

dCb_dt(3) = (Vz/Eb)*((C(3)-C(2))/deltaZ)+ Dz*((C(4)-2*C(3)+C(2)) / ((deltaZ)^2))-(((1-Eb)/(Eb))*Km*a)*(C(3)-(Km*C(3)+((5*De*C(9))/Rp))/(Km+(5*De)/Rp));

dCb_dt(4) = (Vz/Eb)*((C(4)-C(3))/deltaZ)+ Dz*((C(5)-2*C(4)+C(3)) / ((deltaZ)^2))-(((1-Eb)/(Eb))*Km*a)*(C(4)-(Km*C(4)+((5*De*C(10))/Rp))/(Km+(5*De)/Rp));

dCb_dt(5) = (Vz/Eb)*((C(5)-C(4))/deltaZ)+ Dz*((C(6)-2*C(5)+C(4)) / ((deltaZ)^2))-(((1-Eb)/(Eb))*Km*a)*(C(5)-(Km*C(5)+((5*De*C(11))/Rp))/(Km+(5*De)/Rp));

dCb_dt(6) = (Vz/Eb)*((C(6)-C(5))/deltaZ)+ Dz*((2*C(5)-2*C(6)) / ((deltaZ)^2))-(((1-Eb)/(Eb))*Km*a)*(C(6)-(Km*C(6)+((5*De*C(12))/Rp))/(Km+(5*De)/Rp));

%% Temporal ODE's across reactor length for governing equation 3.18: Solves average particle SO2 concentration at position 'z'

dCb_dt(7) = (3/Rp)*Km*(C(1)-(Km*C(1)+((5*De*C(7))/Rp))/(Km+(5*De)/Rp))-((3*(1-alpha)*Kr*C(7))/(Rp*alpha));

dCb_dt(8) = (3/Rp)*Km*(C(2)-(Km*C(2)+((5*De*C(8))/Rp))/(Km+(5*De)/Rp))-((3*(1-alpha)*Kr*C(8))/(Rp*alpha));

dCb_dt(9) = (3/Rp)*Km*(C(3)-(Km*C(3)+((5*De*C(9))/Rp))/(Km+(5*De)/Rp))-((3*(1-alpha)*Kr*C(9))/(Rp*alpha));

```

```

dCb_dt(10) = (3/Rp)*Km*(C(4)-(Km*C(4)+((5*De*C(10))/Rp))/(Km+(5*De)/Rp))-(3*(1-alpha)*Kr*C(10))/(Rp*alpha));

dCb_dt(11)= (3/Rp)*Km*(C(5)-(Km*C(5)+((5*De*C(11))/Rp))/(Km+(5*De)/Rp))-(3*(1-alpha)*Kr*C(11))/(Rp*alpha));

dCb_dt(12) = (3/Rp)*Km*(C(6)-(Km*C(6)+((5*De*C(12))/Rp))/(Km+(5*De)/Rp))-(3*(1-alpha)*Kr*C(12))/(Rp*alpha));

%% Evalution of Dz at time 't' along reactor length 'z':

dCb_dt(13)= (Vz/Eb)*((C(2)-C(1))/deltaZ)+(((1-Eb)/(Eb))*Km*a)*(C(2)-(Km*C(2)+((5*De*C(8))/Rp))/(Km+(5*De)/Rp))/((C(3)-2*C(2)+C(1))/((deltaZ)^2));

dCb_dt(14)= (Vz/Eb)*((C(3)-C(2))/deltaZ)+(((1-Eb)/(Eb))*Km*a)*(C(3)-(Km*C(3)+((5*De*C(9))/Rp))/(Km+(5*De)/Rp))/((C(4)-2*C(3)+C(2))/((deltaZ)^2));

dCb_dt(15)= (Vz/Eb)*((C(4)-C(3))/deltaZ)+(((1-Eb)/(Eb))*Km*a)*(C(4)-(Km*C(4)+((5*De*C(10))/Rp))/(Km+(5*De)/Rp))/((C(5)-2*C(4)+C(3))/((deltaZ)^2));

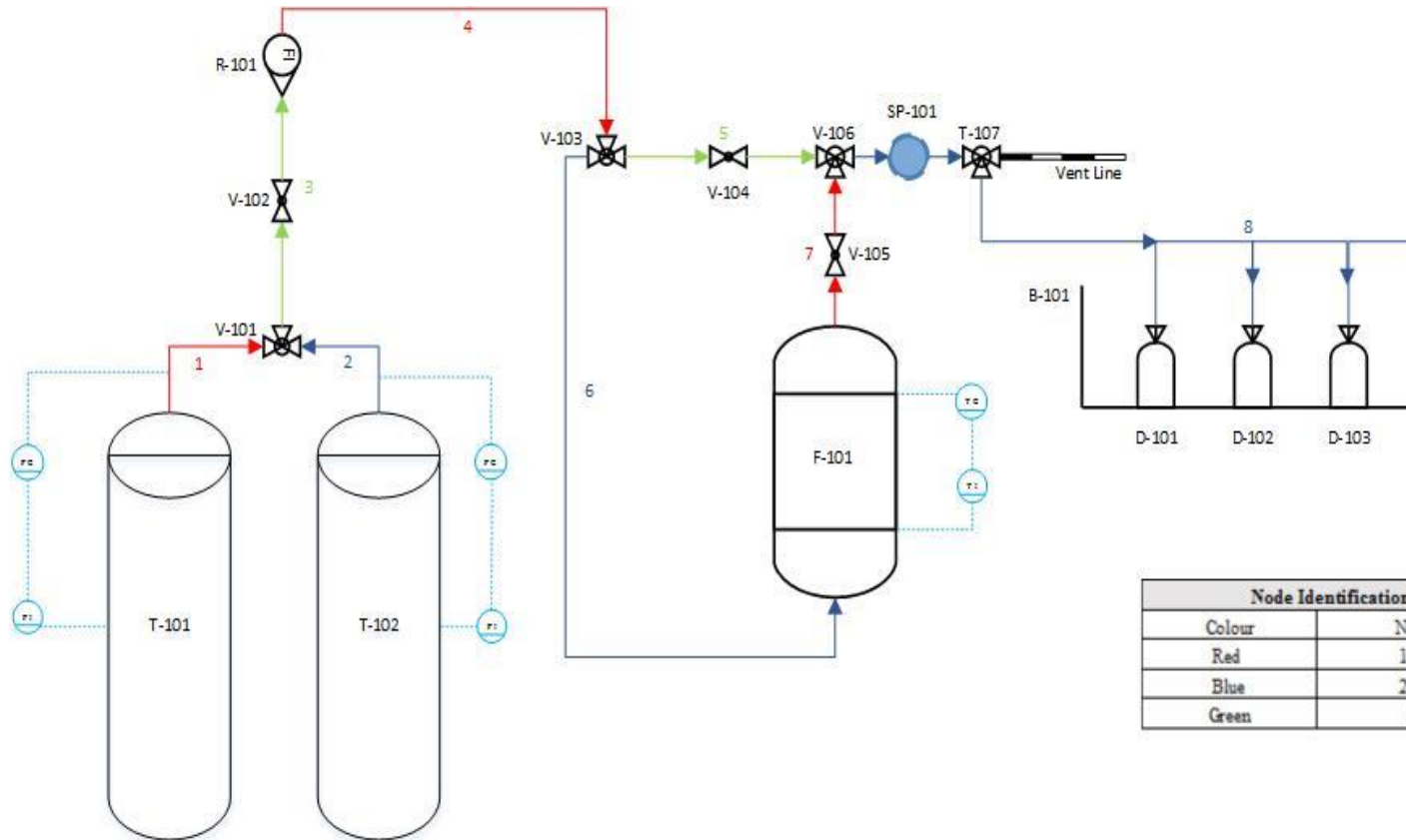
dCb_dt(16)= (Vz/Eb)*((C(5)-C(4))/deltaZ)+(((1-Eb)/(Eb))*Km*a)*(C(5)-(Km*C(5)+((5*De*C(11))/Rp))/(Km+(5*De)/Rp))/((C(6)-2*C(5)+C(4))/((deltaZ)^2));

dCb_dt(17)= (Vz/Eb)*((C(6)-C(5))/deltaZ)+(((1-Eb)/(Eb))*Km*a)*(C(6)-(Km*C(6)+((5*De*C(12))/Rp))/(Km+(5*De)/Rp))/((2*C(5)-2*C(6))/((deltaZ)^2));

```

end

APPENDIX D: HAZOP STUDY



Process Flow Diagram-HAZOP NODAL ANALYSIS					
Dry Sorbent Desulphurisation of Flue Gas					
Sheet		1	Drawn by	C. Moodley	
Revision		2	Checked by	Dr. D Lokhat	
DH001/0001-01			Supervisor	Dr. D Lokhat	
Drawing No. 16104-215-A1-0001			Project	Drv Sorbent Desulphurisation of Flue Gas	

Figure D- 1: HAZOP nodal scheme

Table D- 1: Hazard-And-Operability-Study-Record-Node 1

HAZARD-AND-OPERABILITY-STUDY-RECORD-NODE: 1 (INERT GAS FEED)						
Unit: Inert Gas Tank T-101						
Key Words	Deviation	Causes	Consequences or Hazards	Safeguards Provided	Recommendations and/or Actions	By
Flow	No/Low	<ul style="list-style-type: none"> • Pipe Rupture • Blockage at tank outlet • Semi closed valves 	<ul style="list-style-type: none"> • No inert to remove any SO₂ absorbed into isopropanol solution • Trace amounts of SO₃ still within the system 	<ul style="list-style-type: none"> • None 	<ol style="list-style-type: none"> 1. Routine inspection to be done 2. Install a flow indicator and automate flow control 	Calvin Moodley
	High	<ul style="list-style-type: none"> • Valve saturates • Flow control valve failure 	<ul style="list-style-type: none"> • Excess amounts of inert gas purged (hazardous) • Furnace temperature decreases • Effects rate of desulfurization 	<ul style="list-style-type: none"> • None 	<ol style="list-style-type: none"> 1. Routine inspection to be done 2. Install a flow indicator and automate flow control 	Calvin Moodley
	Reverse	<ul style="list-style-type: none"> • Pressure at suction greater than discharge (vacuum) 	<ul style="list-style-type: none"> • Pressure build up in inert tank (explosive hazard) 	<ul style="list-style-type: none"> • None 	<ol style="list-style-type: none"> 1. Routine inspection to be done 2. Install a flow indicator and automate flow control 	Calvin Moodley
Temperature	High	<ul style="list-style-type: none"> • Tank heated externally 	<ul style="list-style-type: none"> • Effect amount of desulfurization during reaction due to SO₂ converted to alternate SO₃ form prior to reaction 	<ul style="list-style-type: none"> • None 	<ol style="list-style-type: none"> 1. Install a temperature alarm 2. Maintain an isothermal temperature through automated thermal control 	Calvin Moodley
	Low	<ul style="list-style-type: none"> • Tank cooled externally 	<ul style="list-style-type: none"> • None 	<ul style="list-style-type: none"> • None 	<ol style="list-style-type: none"> 1. Install a temperature alarm 2. Maintain an isothermal temperature through automated thermal control 	Calvin Moodley
Pressure	High	<ul style="list-style-type: none"> • Blocked streams and screens downstream • Valves downstream partially closed 	<ul style="list-style-type: none"> • Rupture of tank (explosive hazard) 	<ul style="list-style-type: none"> • Pressure indicator and pressure controller 	<ol style="list-style-type: none"> 1. Install a vent line 2. Install a pressure alarm 	Calvin Moodley
	Less	<ul style="list-style-type: none"> • Downstream valve saturates • Leakages in pipeline 	<ul style="list-style-type: none"> • Decreased flow downstream • No inert to remove any SO₂ absorbed into isopropanol solution • Trace amounts of SO₃ still within the system 	<ul style="list-style-type: none"> • Pressure indicator and pressure controller 	<ol style="list-style-type: none"> 1. Install a pressure alarm 	Calvin Moodley

Table D- 2: Hazard-And-Operability-Study-Record-Node 2

Unit: Flue Gas Tank T-102						
HAZARD-AND-OPERABILITY-STUDY-RECORD-NODE: 2 (FLUE GAS FEED)						
Key Words	Deviation	Causes	Consequences or Hazards	Safeguards Provided	Recommendations and/or Actions	By
Flow	No/Low	<ul style="list-style-type: none"> • Pipe Rupture • Blockage at tank outlet • Semi closed valves 	<ul style="list-style-type: none"> • No flow through the furnace therefore no results can be recorded 	<ul style="list-style-type: none"> • None 	<ol style="list-style-type: none"> 1. Routine inspection to be done 2. Install a flow indicator and automate flow control 	Calvin Moodley
	High	<ul style="list-style-type: none"> • Valve saturates • Flow control valve failure 	<ul style="list-style-type: none"> • Excess amounts of flue gas purged (hazardous) • Inefficient contact time of flue gas and sorbent therefore desulfurization will not be optimal 	<ul style="list-style-type: none"> • None 	<ol style="list-style-type: none"> 1. Routine inspection to be done 2. Install a flow indicator and automate flow control 	Calvin Moodley
	Reverse	<ul style="list-style-type: none"> • Pressure at suction greater than discharge (vacuum) 	<ul style="list-style-type: none"> • Pressure build up in flue gas tank (explosive hazard) • No flow through the furnace therefore no results can be recorded 	<ul style="list-style-type: none"> • None 	<ol style="list-style-type: none"> 1. Routine inspection to be done 2. Install a flow indicator and automate flow control 	Calvin Moodley
Temperature	High	<ul style="list-style-type: none"> • Tank heated externally 	<ul style="list-style-type: none"> • Effect amount of desulfurization during reaction due to SO₂ converted to alternate SO₃ form prior to reaction 	<ul style="list-style-type: none"> • None 	<ol style="list-style-type: none"> 1. Install a temperature alarm 2. Maintain an isothermal temperature through automated thermal control 	Calvin Moodley
	Low	<ul style="list-style-type: none"> • Tank cooled externally 	<ul style="list-style-type: none"> • None 	<ul style="list-style-type: none"> • None 	<ol style="list-style-type: none"> 1. Install a temperature alarm 2. Maintain an isothermal temperature through automated thermal control 	Calvin Moodley
Pressure	High	<ul style="list-style-type: none"> • Blocked streams and screens downstream • Valves downstream partially closed 	<ul style="list-style-type: none"> • Rupture of flue gas tank (explosive hazard) 	<ul style="list-style-type: none"> • Pressure indicator and pressure controller 	<ol style="list-style-type: none"> 1. Install a vent line 2. Install a pressure alarm 	Calvin Moodley
	Less	<ul style="list-style-type: none"> • Downstream valve saturates • Leakages in pipeline 	<ul style="list-style-type: none"> • Decreased flow downstream • No inert to remove any SO₂ absorbed into isopropanol solution • Trace amounts of SO₃ still within the system 	<ul style="list-style-type: none"> • Pressure indicator and pressure controller 	<ol style="list-style-type: none"> 1. Install a pressure alarm 	Calvin Moodley

Table D- 3: Hazard-And-Operability-Study-Record-Node 3

Unit: Turn Down Valve (TV-101)						
HAZARD-AND-OPERABILITY-STUDY-RECORD-NODE: 3 (TURN DOWN VALVE)						
Key Words	Deviation	Causes	Consequences or Hazards	Safeguards Provided	Recommendations and/or Actions	By
Flow	No/Low	<ul style="list-style-type: none"> • Pipe Rupture • Blockage at tank outlet • Semi closed valves 	<ul style="list-style-type: none"> • No flow through the furnace therefore no results can be recorded 	<ul style="list-style-type: none"> • None 	<ol style="list-style-type: none"> 1. Routine inspection to be done 2. Install a flow indicator and automate flow control 	Calvin Moodley
	High	<ul style="list-style-type: none"> • Valve saturates • Flow control valve failure 	<ul style="list-style-type: none"> • Excess amounts of flue gas purged (hazardous) • Inefficient contact time of flue gas and sorbent therefore desulfurization will not be optimal 	<ul style="list-style-type: none"> • None 	<ol style="list-style-type: none"> 1. Routine inspection to be done 2. Install a flow indicator and automate flow control 	Calvin Moodley
	Reverse	<ul style="list-style-type: none"> • Pressure at suction greater than discharge (vacuum) 	<ul style="list-style-type: none"> • Pressure build up in flue gas tank (explosive hazard) • No flow through the furnace therefore no results can be recorded 	<ul style="list-style-type: none"> • None 	<ol style="list-style-type: none"> 1. Routine inspection to be done 2. Install a flow indicator and automate flow control 	Calvin Moodley
Temperature	High	<ul style="list-style-type: none"> • External heat source introduced 	<ul style="list-style-type: none"> • Effect amount of desulfurization during reaction due to SO₂ converted to alternate SO₃ form prior to reaction 	<ul style="list-style-type: none"> • None 	<ol style="list-style-type: none"> 1. Install a temperature alarm 2. Maintain an isothermal temperature through automated thermal control 	Calvin Moodley
	Low	<ul style="list-style-type: none"> • External cooling introduced 	<ul style="list-style-type: none"> • None 	<ul style="list-style-type: none"> • None 	<ol style="list-style-type: none"> 1. Install a temperature alarm 2. Maintain an isothermal temperature through automated thermal control 	Calvin Moodley
Pressure	High	<ul style="list-style-type: none"> • Blocked streams and screens downstream • Valves downstream partially closed 	<ul style="list-style-type: none"> • Rupture of flue gas tank (explosive hazard) 	<ul style="list-style-type: none"> • None 	<ol style="list-style-type: none"> 1. Install a vent line 2. Install a pressure alarm 	Calvin Moodley
	Less	<ul style="list-style-type: none"> • Downstream valve saturates • Leakages in pipeline 	<ul style="list-style-type: none"> • Decreased flow downstream • No inert to remove any SO₂ absorbed into isopropanol solution • Trace amounts of SO₃ still within the system 	<ul style="list-style-type: none"> • None 	<ol style="list-style-type: none"> 1. Install a pressure alarm 	Calvin Moodley

Table D- 4: Hazard-And-Operability-Study-Record-Node 4

Unit: Rotameter (R-101)						
HAZARD-AND-OPERABILITY-STUDY-RECORD-NODE: 4 (ROTAMETER)						
Key Words	Deviation	Causes	Consequences or Hazards	Safeguards Provided	Recommendations and/or Actions	By
Flow	No/Low	<ul style="list-style-type: none"> • Pipe Rupture • Blockage at tank outlet • Semi closed valves 	<ul style="list-style-type: none"> • No flow through the furnace therefore no results can be recorded 	<ul style="list-style-type: none"> • None 	<ul style="list-style-type: none"> 3. Routine inspection to be done 4. Install a flow indicator and automate flow control 	Calvin Moodley
	High	<ul style="list-style-type: none"> • Valve saturates • Flow control valve failure 	<ul style="list-style-type: none"> • Excess amounts of flue gas purged (hazardous) • Inefficient contact time of flue gas and sorbent therefore desulfurization will not be optimal 	<ul style="list-style-type: none"> • None 	<ul style="list-style-type: none"> 3. Routine inspection to be done 4. Install a flow indicator and automate flow control 	Calvin Moodley
	Reverse	<ul style="list-style-type: none"> • Pressure at suction greater than discharge (vacuum) 	<ul style="list-style-type: none"> • Pressure build up in flue gas tank (explosive hazard) • No flow through the furnace therefore no results can be recorded 	<ul style="list-style-type: none"> • None 	<ul style="list-style-type: none"> 3. Routine inspection to be done 4. Install a flow indicator and automate flow control 	Calvin Moodley
Temperature	High	<ul style="list-style-type: none"> • External heat source introduced 	<ul style="list-style-type: none"> • Effect amount of desulfurization during reaction due to SO₂ converted to alternate SO₃ form prior to reaction 	<ul style="list-style-type: none"> • None 	<ul style="list-style-type: none"> 3. Install a temperature alarm 4. Maintain an isothermal temperature through automated thermal control 	Calvin Moodley
	Low	<ul style="list-style-type: none"> • External cooling introduced 	<ul style="list-style-type: none"> • None 	<ul style="list-style-type: none"> • None 	<ul style="list-style-type: none"> 3. Install a temperature alarm 4. Maintain an isothermal temperature through automated thermal control 	Calvin Moodley
Pressure	High	<ul style="list-style-type: none"> • Blocked streams and screens downstream • Valves downstream partially closed 	<ul style="list-style-type: none"> • Rupture of flue gas tank (explosive hazard) 	<ul style="list-style-type: none"> • None 	<ul style="list-style-type: none"> 3. Install a vent line 4. Install a pressure alarm 	Calvin Moodley
	Less	<ul style="list-style-type: none"> • Downstream valve saturates • Leakages in pipeline 	<ul style="list-style-type: none"> • Decreased flow downstream • No inert to remove any SO₂ absorbed into isopropanol solution • Trace amounts of SO₃ still within the system 	<ul style="list-style-type: none"> • None 	<ul style="list-style-type: none"> 2. Install a pressure alarm 	Calvin Moodley

Table D- 5: Hazard-And-Operability-Study-Record-Node 6

Unit: Reactor (F-101)						
HAZARD-AND-OPERABILITY-STUDY-RECORD-NODE: 6 (REACTOR FEED)						
Key Words	Deviation	Causes	Consequences or Hazards	Safeguards Provided	Recommendations and/or Actions	By
Flow	No/Low	<ul style="list-style-type: none"> • Pipe Rupture • Blockage upstream • Semi closed valves 	<ul style="list-style-type: none"> • No flow through the furnace therefore effluent results cannot be recorded 	<ul style="list-style-type: none"> • None 	<ul style="list-style-type: none"> 5. Routine inspection to be done 6. Install a flow indicator and automate flow control 	Calvin Moodley
	High	<ul style="list-style-type: none"> • Valve saturates • Flow control valve failure 	<ul style="list-style-type: none"> • Excess amounts of flue gas purged (hazardous)/ Wastage of flue gas 	<ul style="list-style-type: none"> • None 	<ul style="list-style-type: none"> 5. Routine inspection to be done 6. Install a flow indicator and automate flow control 	Calvin Moodley
	Reverse	<ul style="list-style-type: none"> • Pressure at suction greater than discharge (vacuum) 	<ul style="list-style-type: none"> • Pressure build up in flue gas tank (explosive hazard) • No results can be recorded 	<ul style="list-style-type: none"> • None 	<ul style="list-style-type: none"> 5. Routine inspection to be done 6. Install a flow indicator and automate flow control 	Calvin Moodley
Temperature	High	<ul style="list-style-type: none"> • External heat source introduced 	<ul style="list-style-type: none"> • Effect amount of desulfurization during reaction due to SO₂ converted to alternate SO₃ form prior to reaction 	<ul style="list-style-type: none"> • None 	<ul style="list-style-type: none"> 5. Install a temperature alarm 6. Maintain an isothermal temperature through automated thermal control 	Calvin Moodley
	Low	<ul style="list-style-type: none"> • External cooling introduced 	<ul style="list-style-type: none"> • None 	<ul style="list-style-type: none"> • None 	<ul style="list-style-type: none"> 5. None 	Calvin Moodley
Pressure	High	<ul style="list-style-type: none"> • Blocked streams and screens downstream • Valves downstream partially closed 	<ul style="list-style-type: none"> • Rupture of flue gas tank (explosive hazard) 	<ul style="list-style-type: none"> • None 	<ul style="list-style-type: none"> 5. Install a vent line 6. Install a pressure alarm 	Calvin Moodley
	Less	<ul style="list-style-type: none"> • Downstream valve saturates • Leakages in pipeline 	<ul style="list-style-type: none"> • Decreased flow downstream 	<ul style="list-style-type: none"> • None 	<ul style="list-style-type: none"> 3. Install a pressure alarm 	Calvin Moodley

Table D- 6: Hazard-And-Operability-Study-Record-Nodes - 5, 7 & 8

Unit: Non-Return Valve (V-104)						
HAZARD-AND-OPERABILITY-STUDY-RECORD-NODES: 5,7 and 8 (BYPASS, REACTOR EFFLUENT & PURGE)						
Key Words	Deviation	Causes	Consequences or Hazards	Safeguards Provided	Recommendations and/or Actions	By
Flow	No/Low	<ul style="list-style-type: none"> • Pipe Rupture • Blockage upstream • Semi closed valves 	<ul style="list-style-type: none"> • Initial concentration of SO₂ cannot be determined 	<ul style="list-style-type: none"> • None 	<ul style="list-style-type: none"> 7. Routine inspection to be done 8. Install a flow indicator and automate flow control 	Calvin Moodley
	High	<ul style="list-style-type: none"> • Valve saturates • Flow control valve failure 	<ul style="list-style-type: none"> • Excess amounts of flue gas purged (hazardous) • Wastage of flue gas 	<ul style="list-style-type: none"> • None 	<ul style="list-style-type: none"> 7. Routine inspection to be done 8. Install a flow indicator and automate flow control 	Calvin Moodley
	Reverse	<ul style="list-style-type: none"> • Pressure at suction greater than discharge (vacuum) 	<ul style="list-style-type: none"> • Pressure build up in flue gas tank (explosive hazard) • No results can be recorded 	<ul style="list-style-type: none"> • None 	<ul style="list-style-type: none"> 7. Routine inspection to be done 8. Install a flow indicator and automate flow control 	Calvin Moodley
Temperature	High	<ul style="list-style-type: none"> • External heat source introduced 	<ul style="list-style-type: none"> • Higher temperatures can cause downstream vent piping to melt • Prevent condensation required for SO₃ analysis 	<ul style="list-style-type: none"> • None 	<ul style="list-style-type: none"> 7. Install a temperature alarm 8. Maintain an isothermal temperature through automated thermal control 	Calvin Moodley
	Low	<ul style="list-style-type: none"> • External cooling introduced 	<ul style="list-style-type: none"> • None 	<ul style="list-style-type: none"> • None 	<ul style="list-style-type: none"> 6. None 	Calvin Moodley
Pressure	High	<ul style="list-style-type: none"> • Blocked streams and screens downstream • Valves downstream partially closed 	<ul style="list-style-type: none"> • Rupture of flue gas tank (explosive hazard) 	<ul style="list-style-type: none"> • None 	<ul style="list-style-type: none"> 7. Install a vent line 8. Install a pressure alarm 	Calvin Moodley
	Less	<ul style="list-style-type: none"> • Downstream valve saturates • Leakages in pipeline 	<ul style="list-style-type: none"> • Decreased flow downstream 	<ul style="list-style-type: none"> • None 	<ul style="list-style-type: none"> 4. Install a pressure alarm 	Calvin Moodley

APPENDIX E: MATERIAL AND SAFETY DATA SHEETS

Table E- 1: Material Safety Data Sheet - Barium Perchlorate, Anhydrous

Section 1: Chemical Product	
Product Name: Barium Perchlorate, anhydrous	
Synonym: Barium diperchlorate	
Chemical Name: Perchloric Acid, barium salt	
Chemical Formula: Ba(ClO ₄) ₂	
Section 2: Hazards Identification	
Potential Acute Health Effects: Hazardous in case of skin contact (irritant), of eye contact (irritant), of ingestion, of inhalation. Prolonged exposure may result in skin burns and ulcerations. Over-exposure by inhalation may cause respiratory irritation. Severe over-exposure can result in death.	
Potential Chronic Health Effects: The substance may be toxic to kidneys, the nervous system, central nervous system (CNS). Repeated or prolonged exposure to the substance can produce target organs damage. Repeated exposure to a highly toxic material may produce general deterioration of health by an accumulation in one or many human organs.	
Section 3: First Aid Measures	
Eye Contact: Check for and remove any contact lenses. In case of contact, immediately flush eyes with plenty of water for at least 15 minutes. Cold water may be used. Get medical attention.	
Skin Contact: In case of contact, immediately flush skin with plenty of water for at least 15 minutes while removing contaminated clothing and shoes. Cover the irritated skin with an emollient. Cold water may be used. Wash clothing before reuse. Thoroughly clean shoes before reuse. Get medical attention immediately.	
Serious Skin Contact: Wash with a disinfectant soap and cover the contaminated skin with an anti-bacterial cream. Seek immediate medical attention.	
Inhalation: If inhaled, remove to fresh air. If not breathing, give artificial respiration. If breathing is difficult, give oxygen. Get medical attention immediately.	
Serious Inhalation: Evacuate the victim to a safe area as soon as possible. Loosen tight clothing such as a collar, tie, belt or waistband. If breathing is difficult, administer oxygen. If the victim is not breathing, perform mouth-to-mouth resuscitation. WARNING: It may be hazardous to the person providing aid to give mouth-to-mouth resuscitation when the inhaled material is toxic, infectious or corrosive. Seek immediate medical attention.	
Ingestion: If swallowed, do not induce vomiting unless directed to do so by medical personnel. Never give anything by mouth to an unconscious person. Loosen tight clothing such as a collar, tie, belt or waistband. Get medical attention immediately.	
Section 4: Fire and Explosion Data	
Flammability of the Product: Non-flammable.	
Products of Combustion: Some metallic oxides.	

Fire Hazards in Presence of Various Substances: combustible materials, organic materials.

Fire Fighting Media and Instructions: Oxidizing material. Do not use water jet. Use flooding quantities of water. Avoid contact with organic materials.

Special Remarks on Fire Hazards: Contact with combustible or organic materials may cause fire.

Section 5: Accidental Release Measures

Small Spill: Use appropriate tools to put the spilled solid in a convenient waste disposal container.

Large Spill: Oxidizing material. Poisonous solid. Stop leak if without risk. Do not get water inside container. Avoid contact with a combustible material (wood, paper, oil, and clothing). Do not touch spilled material. Use water spray to reduce vapours. Prevent entry into sewers, basements or confined areas; dike if needed. Eliminate all ignition sources.

Section 6: Handling and Storage

Precautions:

Keep away from heat. Keep away from sources of ignition. Keep away from combustible material. Do not ingest. Do not breathe dust. Wear suitable protective clothing. In case of insufficient ventilation, wear suitable respiratory equipment. If ingested, seek medical advice immediately and show the container or the label. Avoid contact with skin and eyes. Keep away from incompatibles such as reducing agents, combustible materials, organic materials.

Storage:

Keep container tightly closed. Keep container in a cool, well-ventilated area. Separate from acids, alkalies, reducing agents and combustibles.

Section 7: Physical and Chemical Properties

Physical state and appearance: Solid. (Crystals solid. Deliquescent crystals solid.)

Odour: Odourless.

Molecular Weight: 336.27 g/mole

Colour: White.

Dispersion Properties: See solubility in water, acetone.

Solubility: Soluble in cold water, hot water, acetone, alcohol.

Table E- 2: Material Safety Data Sheet - Isopropyl Alcohol

Section 1: Chemical Product
Product Name: Isopropyl alcohol Synonym: 2-Propanol Chemical Name: Isopropanol Chemical Formula: C3-H8-O
Section 2: Hazards Identification
<p>Potential Acute Health Effects: Hazardous in case of eye contact (irritant), of ingestion, of inhalation. Slightly hazardous in case of skin contact (irritant, sensitizer, permeator).</p> <p>Potential Chronic Health Effects: Slightly hazardous in case of skin contact (sensitizer). DEVELOPMENTAL TOXICITY: Classified Reproductive system/toxin/female, Development toxin [POSSIBLE]. The substance may be toxic to kidneys, liver, skin, central nervous system (CNS). Repeated or prolonged exposure to the substance can produce target organs damage.</p>
Section 3: First Aid Measures
<p>Eye Contact: Check for and remove any contact lenses. In case of contact, immediately flush eyes with plenty of water for at least 15 minutes. Cold water may be used. Get medical attention</p> <p>Skin Contact: Wash with soap and water. Cover the irritated skin with an emollient. Get medical attention if irritation develops. Cold water may be used.</p> <p>Inhalation: If inhaled, remove to fresh air. If not breathing, give artificial respiration. If breathing is difficult, give oxygen. Get medical attention if symptoms appear.</p> <p>Serious Inhalation: Evacuate the victim to a safe area as soon as possible. Loosen tight clothing such as a collar, tie, belt or waistband. If breathing is difficult, administer oxygen. If the victim is not breathing, perform mouth-to-mouth resuscitation. Seek medical attention.</p> <p>Ingestion: Do NOT induce vomiting unless directed to do so by medical personnel. Never give anything by mouth to an unconscious person. Loosen tight clothing such as a collar, tie, belt or waistband. Get medical attention if symptoms appear.</p>
Section 4: Fire and Explosion Data
<p>Flammability of the Product: Flammable.</p> <p>Auto-Ignition Temperature: 399°C (750.2°F)</p> <p>Flash Points: 11.667°C (53°F) - 12.778 deg. C (55 deg. F)</p> <p>Flammable Limits: LOWER: 2% UPPER: 12.7%</p> <p>Products of Combustion: These products are carbon oxides (CO, CO2).</p>
<p>Fire Hazards in Presence of Various Substances: Highly flammable in presence of open flames and sparks, of heat. Flammable in presence of oxidizing materials. Non-flammable in presence of shocks.</p> <p>Explosion Hazards in Presence of Various Substances: Explosive in presence of open flames and sparks, of heat.</p> <p>Fire Fighting Media and Instructions: Flammable liquid, soluble or dispersed in water. SMALL FIRE: Use DRY chemical powder. LARGE FIRE: Use alcohol foam, water spray or fog.</p>

Special Remarks on Fire Hazards:

Vapour may travel considerable distance to source of ignition and flash back. CAUTION: MAY BURN WITH NEAR INVISIBLE FLAME. Hydrogen peroxide sharply reduces the auto ignition temperature of Isopropyl alcohol. After a delay, Isopropyl alcohol ignites on contact with dioxigenyl tetrafluorborate, chromium trioxide, and potassium tert-butoxide. When heated to decomposition it emits acrid smoke and fumes.

Special Remarks on Explosion Hazards:

Secondary alcohols are readily autoxidized in contact with oxygen or air, forming ketones and hydrogen peroxide. It can become potentially explosive. It reacts with oxygen to form dangerously unstable peroxides which can concentrate and explode during distillation or evaporation.

Section 5: Accidental Release Measures

Small Spill: Dilute with water and mop up, or absorb with an inert dry material and place in an appropriate waste disposal container.

Large Spill: Flammable liquid. Keep away from heat. Keep away from sources of ignition. Stop leak if without risk. Absorb with DRY earth, sand or other non-combustible material. Do not touch spilled material. Prevent entry into sewers, basements or confined areas; dike if needed

Section 6: Handling and Storage**Precautions:**

Keep away from heat. Keep away from sources of ignition. Ground all equipment containing material. Do not ingest. Do not breathe gas/fumes/ vapor/spray. Avoid contact with eyes. Wear suitable protective clothing. In case of insufficient ventilation, wear suitable respiratory equipment. If ingested, seek medical advice immediately and show the container or the label. Keep away from incompatibles such as oxidizing agents, acids.

Storage:

Store in a segregated and approved area. Keep container in a cool, well-ventilated area. Keep container tightly closed and sealed until ready for use. Avoid all possible sources of ignition (spark or flame).

Section 7: Physical and Chemical Properties

Physical state and appearance: Liquid.

Odour: Pleasant. Odor resembling that of a mixture of ethanol and acetone.

Taste: Bitter. (Slight.)

Molecular Weight: 60.1 g/mole

Colour: Colorless.

Dispersion Properties: solubility in water, methanol, diethyl ether, n-octanol, acetone.

Solubility: Easily soluble in cold water, hot water, methanol, diethyl ether, n-octanol, acetone.

Insoluble in salt solution. Soluble in benzene. Miscible with most organic solvents including alcohol, ethyl alcohol, chloroform.

Table E- 3: Material Safety Data Sheet - Helium

Section 1: Chemical Product
Product Name: Helium Synonym: Helium-4 Chemical Name: Helium Chemical Formula: He
Section 2: Hazards Identification
<p>Potential Acute Health Effects: Hazardous in case of eye contact (irritant), of ingestion, of inhalation. Slightly hazardous in case of skin contact (irritant, sensitizer, permeator).</p> <p>Potential Chronic Health Effects: Slightly hazardous in case of skin contact (sensitizer). DEVELOPMENTAL TOXICITY: Classified Reproductive system/toxin/female, Development toxin [POSSIBLE]. The substance may be toxic to kidneys, liver, skin, central nervous system (CNS). Repeated or prolonged exposure to the substance can produce target organs damage.</p>
Section 3: First Aid Measures
<p>Eye Contact: Immediately flush eyes with plenty of water, occasionally lifting the upper and lower eyelids. Check for and remove any contact lenses. Continue to rinse for at least 10 minutes. Get medical attention if irritation occurs.</p> <p>Skin Contact: Flush contaminated skin with plenty of water. Remove contaminated clothing and shoes. Get medical attention if symptoms occur. Wash clothing before reuse. Clean shoes thoroughly before reuse.</p> <p>Inhalation: Remove victim to fresh air and keep at rest in a position comfortable for breathing. If not breathing, if breathing is irregular or if respiratory arrest occurs, provide artificial respiration or oxygen by trained personnel. It may be dangerous to the person providing aid to give mouth-to-mouth resuscitation. Get medical attention if adverse health effects persist or are severe. If unconscious, place in recovery position and get medical attention immediately. Maintain an open airway. Loosen tight clothing such as a collar,</p> <p>Ingestion: As this product is a gas, refer to the inhalation section.</p>
Section 4: Fire and Explosion Data
<p>Flammability of the Product: Non-Flammable. Products of Combustion: None</p> <p>Fire Hazards in Presence of Various Substances: Use an extinguishing agent suitable for the surrounding fire. Non-flammable in presence of shocks.</p> <p>Special Remarks on Fire Hazards: Promptly isolate the scene by removing all persons from the vicinity of the incident if there is a fire. No action shall be taken involving any personal risk or without suitable training. Contact supplier immediately for specialist advice. Move containers from fire area if this can be done without risk. Use water spray to keep fire-exposed containers cool.</p> <p>Special Remarks on Explosion Hazards: None.</p>

Section 5: Accidental Release Measures

Small Spill: Immediately contact emergency personnel. Stop leak if without risk.

Large Spill: Immediately contact emergency personnel. Stop leak if without risk.

Section 6: Handling and Storage

Precautions:

Eating, drinking and smoking should be prohibited in areas where this material is handled, stored and processed. Workers should wash hands and face before eating, drinking and smoking. Remove contaminated clothing and protective equipment before entering eating areas

Storage:

Store in accordance with local regulations. Store in a segregated and approved area.

Store away from direct sunlight in a dry, cool and well-ventilated area, away from incompatible materials. Keep container tightly closed and sealed until ready for use. Cylinders should be stored upright, with valve protection cap in place, and firmly secured to prevent falling or being knocked over. Cylinder temperatures should not exceed 52 °C (125 °F).

Section 7: Physical and Chemical Properties

Physical state and appearance: Gas

Odour: Odourless

Molecular Weight: 4 g/mole

Colour: Colourless.

Solubility: None.

Table E- 4: Material Safety Data Sheet - Thoron Indicator

Section 1: Chemical Product
Product Name: Thorin Synonym: N/A Chemical Name: N/A Chemical Formula: C ₁₆ H ₁₃ AsN ₂ O ₁₀ S ₂
Section 2: Hazards Identification
<p>Potential Acute Health Effects: Extremely hazardous in case of ingestion, of inhalation. Hazardous in case of skin contact (irritant, permeator), of eye contact (irritant)</p> <p>Potential Chronic Health Effects: Extremely hazardous in case of ingestion, of inhalation. Hazardous in case of skin contact (irritant, permeator), of eye contact (irritant). CARCINOGENIC EFFECTS: Not available. MUTAGENIC EFFECTS: Not available. TERATOGENIC EFFECTS: Not available. DEVELOPMENTAL TOXICITY: Not available.</p>
Section 3: First Aid Measures
<p>Eye Contact: Check for and remove any contact lenses. Do not use an eye ointment. Seek medical attention</p> <p>Skin Contact: After contact with skin, wash immediately with plenty of water. Gently and thoroughly wash the contaminated skin with running water and non-abrasive soap. Be particularly careful to clean folds, crevices, creases and groin. Cover the irritated skin with an emollient. If irritation persists, seek medical attention. Wash contaminated clothing before reusing.</p> <p>Inhalation: Allow the victim to rest in a well ventilated area. Seek immediate medical attention.</p> <p>Serious Skin Contact: Wash with a disinfectant soap and cover the contaminated skin with an anti-bacterial cream. Seek medical attention</p> <p>Ingestion: Do not induce vomiting. Loosen tight clothing such as a collar, tie, belt or waistband. If the victim is not breathing, perform mouth-to-mouth resuscitation. Seek immediate medical attention.</p>
Section 4: Fire and Explosion Data
<p>Flammability of the Product: May be combustible at high temperature.</p> <p>Products of Combustion: These products are carbon oxides (CO, CO₂), nitrogen oxides (NO, NO₂.), sulphur oxides (SO₂, SO₃). Some metallic oxides.</p>
<p>Fire Fighting Media and Instructions: SMALL FIRE: Use DRY chemical powder. LARGE FIRE: Use water spray, fog or foam. Do not use water jet.</p>
<p>Special Remarks on Explosion Hazards: Not available</p>
Section 5: Accidental Release Measures
<p>Small Spill: Use appropriate tools to put the spilled solid in a convenient waste disposal container. Finish cleaning by spreading water on the contaminated surface and dispose of according to local and regional authority requirements.</p>

Large Spill: Use a shovel to put the material into a convenient waste disposal container. Finish cleaning by spreading water on the contaminated surface and allow to evacuate through the sanitary system.

Section 6: Handling and Storage

Precautions:

Keep away from heat. Keep away from sources of ignition. Empty containers pose a fire risk, evaporate the residue under a fume hood. Ground all equipment containing material. Do not breathe dust. Wear suitable protective clothing In case of insufficient ventilation, wear suitable respiratory equipment If you feel unwell, seek medical attention and show the label when possible. Avoid contact with skin and eyes

Storage:

Keep container dry. Keep in a cool place. Ground all equipment containing material. Keep container tightly closed. Keep in a cool, well-ventilated place. Combustible materials should be stored away from extreme heat and away from strong oxidizing agents.

Section 7: Physical and Chemical Properties

Physical state and appearance: Solid.

Odour: Odourless.

Taste: Tasteless

Molecular Weight: 576.3 g/mole

Colour: Orange

Table E- 5: Material Safety Data Sheet - Calcium Carbonate

Section 1: Chemical Product
Product Name: Calcium carbonate Synonym: Limestone Chemical Name: Calcium Carbonate Chemical Formula: CaCO ₃
Section 2: Hazards Identification
<p>Potential Acute Health Effects: Hazardous in case of eye contact (irritant). Slightly hazardous in case of skin contact (irritant), of ingestion, of inhalation.</p> <p>Potential Chronic Health Effects: CARCINOGENIC EFFECTS: Not available. MUTAGENIC EFFECTS: Not available. TERATOGENIC EFFECTS: Not available. DEVELOPMENTAL TOXICITY: Not available. The substance may be toxic to kidneys. Repeated or prolonged exposure to the substance can produce target organs damage</p>
Section 3: First Aid Measures
<p>Eye Contact: Check for and remove any contact lenses. In case of contact, immediately flush eyes with plenty of water for at least 15 minutes. Cold water may be used. WARM water MUST be used. Get medical attention.</p> <p>Skin Contact: Wash with soap and water. Cover the irritated skin with an emollient. Get medical attention if irritation develops.</p> <p>Inhalation: If inhaled, remove to fresh air. If not breathing, give artificial respiration. If breathing is difficult, give oxygen. Get medical attention.</p> <p>Ingestion: Do NOT induce vomiting unless directed to do so by medical personnel. Never give anything by mouth to an unconscious person. Loosen tight clothing such as a collar, tie, belt or waistband. Get medical attention if symptoms appear.</p>
Section 4: Fire and Explosion Data
<p>Flammability of the Product: Non-Flammable.</p> <p>Explosion Hazards in Presence of Various Substances: Risks of explosion of the product in presence of mechanical impact: Not available. Risks of explosion of the product in presence of static discharge: Not available.</p> <p>Special Remarks on Fire Hazards: Will ignite and burn fiercely in contact with fluorine</p> <p>Special Remarks on Explosion Hazards: When a mixture of calcium carbonate and magnesium is heated in a current of hydrogen, a violent explosion occurs.</p>
Section 5: Accidental Release Measures
<p>Small Spill: Use appropriate tools to put the spilled solid in a convenient waste disposal container. Finish cleaning by spreading water on the contaminated surface and dispose of according to local and regional authority requirements.</p> <p>Large Spill: Use a shovel to put the material into a convenient waste disposal container. Finish cleaning by spreading water on the contaminated surface and allow to evacuate through the sanitary system.</p>

Section 6: Handling and Storage

Precautions:

Do not ingest. Do not breathe dust. Avoid contact with eyes. Wear suitable protective clothing. If ingested, seek medical advice immediately and show the container or the label. Keep away from incompatibles such as oxidizing agents, acids.

Storage:

Keep container tightly closed. Keep container in a cool, well-ventilated area. Hygroscopic

Section 7: Physical and Chemical Properties

Physical state and appearance: Solid. (Powdered solid.)

Odour: Odourless

Taste: Chalky

Molecular Weight: 100.09 g/mole

Colour: White

Melting Point: 825°C (1517°F)

Specific Gravity: 2.8 (Water = 1)

Solubility: Very slightly soluble in cold water. Soluble in dilute acid. Insoluble in alcohol.

Table E- 6: Material Safety Data Sheet - Sulfuric Acid

Section 1: Chemical Product
Product Name: Sulfuric acid Synonym: Oil of Vitrio Chemical Name: Hydrogen sulfate Chemical Formula: H ₂ -SO ₄
Section 2: Hazards Identification
<p>Potential Acute Health Effects: Very hazardous in case of skin contact (corrosive, irritant, permeator), of eye contact (irritant, corrosive), of ingestion, of inhalation. Liquid or spray mist may produce tissue damage particularly on mucous membranes of eyes, mouth and respiratory tract. Skin contact may produce burns. Inhalation of the spray mist may produce severe irritation of respiratory tract, characterized by coughing, choking, or shortness of breath. Severe over-exposure can result in death. Inflammation of the eye is characterized by redness, watering, and itching. Skin inflammation is characterized by itching, scaling, reddening, or, occasionally, blistering.</p> <p>Potential Chronic Health Effects: CARCINOGENIC EFFECTS: Classified 1 (Proven for human.) by IARC, + (Proven.) by OSHA. Classified A2 (Suspected for human.) by ACGIH. MUTAGENIC EFFECTS: Not available. TERATOGENIC EFFECTS: Not available. DEVELOPMENTAL TOXICITY: Not available. The substance may be toxic to kidneys, lungs, heart, cardiovascular system, upper respiratory tract, eyes, and teeth. Repeated or prolonged exposure to the substance can produce target organs damage. Repeated or prolonged p. 2 contact with spray mist may produce chronic eye irritation and severe skin irritation. Repeated or prolonged exposure to spray mist may produce respiratory tract irritation leading to frequent attacks of bronchial infection. Repeated exposure to a highly toxic material may produce general deterioration of health by an accumulation in one or many human organs.</p>
Section 3: First Aid Measures
<p>Eye Contact: Check for and remove any contact lenses. In case of contact, immediately flush eyes with plenty of water for at least 15 minutes. Cold water may be used. Get medical attention immediately. Skin Contact: In case of contact, immediately flush skin with plenty of water for at least 15 minutes while removing contaminated clothing and shoes. Cover the irritated skin with an emollient. Cold water may be used. Wash clothing before reuse. Thoroughly clean shoes before reuse. Get medical attention immediately.</p> <p>Inhalation: Evacuate the victim to a safe area as soon as possible. Loosen tight clothing such as a collar, tie, belt or waistband. If breathing is difficult, administer oxygen. If the victim is not breathing, perform mouth-to-mouth resuscitation. WARNING: It may be hazardous to the person providing aid to give mouth-to-mouth resuscitation when the inhaled material is toxic, infectious or corrosive. Seek immediate medical attention</p> <p>Ingestion: Do NOT induce vomiting unless directed to do so by medical personnel. Never give anything by mouth to an unconscious person. Loosen tight clothing such as a collar, tie, belt or waistband. Get medical attention if symptoms appear.</p>
Section 4: Fire and Explosion Data
Flammability of the Product: Non-Flammable.

Fire Hazards in Presence of Various Substances:

Combustible materials

Explosion Hazards in Presence of Various Substances:

Risks of explosion of the product in presence of mechanical impact: Not available. Risks of explosion of the product in presence of static discharge: Not available. Slightly explosive in presence of oxidizing materials.

Special Remarks on Fire Hazards:

Metal acetylides (Monocesium and Monorubidium), and carbides ignite with concentrated sulfuric acid. White Phosphorous + boiling Sulfuric acid or its vapor ignites on contact. May ignite other combustible materials. May cause fire when sulfuric acid is mixed with Cyclopentadiene, cyclopentanone oxime, nitroaryl amines, hexolithium disilicide, phosphorous (III) oxide, and oxidizing agents such as chlorates, halogens, permanganates.

Section 5: Accidental Release Measures

Small Spill: Dilute with water and mop up, or absorb with an inert dry material and place in an appropriate waste disposal container. If necessary: Neutralize the residue with a dilute solution of sodium carbonate.

Large Spill: Corrosive liquid. Poisonous liquid. Stop leak if without risk. Absorb with DRY earth, sand or other non-combustible material. Do not get water inside container. Do not touch spilled material. Use water spray curtain to divert vapour drift. Use water spray to reduce vapours. Prevent entry into sewers, basements or confined areas; dike if needed. Call for assistance on disposal. Neutralize the residue with a dilute solution of sodium carbonate

Section 6: Handling and Storage**Precautions:**

Keep locked up. Keep container dry. Do not ingest. Do not breathe gas/fumes/ vapour/spray. Never add water to this product. In case of insufficient ventilation, wear suitable respiratory equipment. If ingested, seek medical advice immediately and show the container or the label. Avoid contact with skin and eyes. Keep away from incompatibles such as oxidizing agents, reducing agents, combustible materials, organic materials, metals, acids, alkalis, moisture. May corrode metallic surfaces. Store in a metallic or coated fibreboard drum using a strong polyethylene inner package. **Storage:**

Hygroscopic. Reacts. violently with water. Keep container tightly closed. Keep container in a cool, well-ventilated area. Do not store above 23°C (73.4°F).

Section 7: Physical and Chemical Properties

Physical state and appearance: Liquid. (Thick oily liquid.)

Odour: Odourless, but has a choking odour when hot.

Taste: Marked acid taste. (Strong.)

Molecular Weight: 98.09 g/mole

Colour: Colourless

Melting Point: -35°C (-31°F) to 10.36 deg. C (93% to 100% purity)

Specific Gravity: 1.84 (Water = 1)

Solubility: Easily soluble in cold water. Sulfuric is soluble in water with liberation of much heat. Soluble in ethyl alcohol.